INVESTIGATION OF PRE-CLINICAL AND CLINICAL RESULTS AGAINST SARS-COV-2 WILD-TYPE AND ALPHA VARIANTS COMBINATION OF VLP-58-1023-AL-K3 VACCINE

A THESIS SUBMITTED TO

THE GRADUATE SCHOOL OF ENGINEERING AND SCIENCE

OF BILKENT UNIVERSITY

IN PARTIAL FULFILLMENT OF THE REQUIREMENTS FOR

THE DEGREE OF

MASTER OF SCIENCE

IN

MOLECULAR BIOLOGY AND GENETICS

By

Aslı Gülce Bartan

August, 2022

Invcstig:ition of Prc-clinical ant! Clinical Rcsults Against SARS-CoV-2 Wild-Typc and Alplıa Varianls Combinatiorı for V LP -58-1023-AL -K3 Vaccirıc

By Aslı Gülce Barıaıı

Augusı, 2022

Wc ccrtiCyıhat wc havcread this dissertaıionand ıhaı in mır opinionit is fully adequatc in scopcandin quality, as a thcsis for thedegreeof Masterof Science.

Prof. Dr. ihsanGürsel
(Advisor)

Assist. Prof. Serkan İsmail Göktuna

Prof. Dr. GünnurDeniz

Approvcdfor GraduateSchoolof EngineeringandScience

OrhanArıkan
DirecıorofthcGraduaıeSchoobf Engiıiecriiigand Sciencc

ABSTRACT

The SARS-CoV-2 virus, which first appeared in Wuhan, China and had a pandemic effect at the end of 2019, has urgently created need of suitable vaccine candidates' development with its quick spread. Scientists in different laboratories from all over the world, including Turkey, have started the studies of vaccine development with different methods based on the basic proteins of the SARS-CoV-2 virus. Most of these vaccines are based on the Spike protein, which allows the virus to enter the host and survive. Although the Spike protein, which has high antigenic properties and contains the RBD region to bind ACE2 receptor in the host, is effective in the formation of neutralizing antibodies in the person, the virus essentially has 4 structural proteins, not only spike. Our vaccine strategy containing virus-like particles (VLP) was based on the self-assembly property of Spike, Membrane, Envelope and Nucleocapsid proteins, and these protein structures were transformed into plasmids with his-tag labels, and the products were collected in mammalian cells in vitro by the transfection method. VLPs were purified by affinity chromatography and formulated with 2 different adjuvants which are Alum and CpG. Since the virus, which has changed rapidly in the last 2 years, is open to new mutations over spreading, it is very important that our vaccine should be editable and adaptable to new virus variants. Due to the alpha variant effect in the world, which was first seen in the UK and has become widespread all over the world recent years, WT VLP formed with a more stable Spike protein containing a thermostable sub-proline (6p; HexaPro) mutation was used in the first dose of our vaccine, but UK VLP containing alpha variant mutations was used in the second dose. Alum and CpG adjuvants were used together for both injection formulations. Our vaccine has successfully completed Phase 2 studies. As a result of these studies, approximately 115 vaccinated volunteers were followed up for 90 days and immunological analyzes were performed with samples taken at certain day intervals (Day 21, Day 35, Day49 and Day90). As a result of these analyzes, moderate and high levels of neutralizing and non-neutralizing antibody responses were observed in many patients, and a humoral immune response was induced until day 90. In addition, it was observed that the cellular responses of the volunteers are progressed in tendency with the Th1 cell response.

Keywords: COVID-19, SARS-CoV-2, VLP, Vaccine, CpG ODN, Alum

ÖZET

İlk olarak Çin'in Wuhan kentinde ortaya çıkan ve 2019 yılının sonlarında ise pandemik etkisi görülen SARS-CoV-2 virüsü daha önce karşılaşmadığımız etkileri ve hızlı yayılması ile acil olarak uygun aşı adaylarının geliştirilmesine ihtiyaç doğurmuştur. Türkiye de dahil olmak üzere dünyanın dört bir yanından farklı laboratuvarlarda bilim insanları SARS-CoV-2 virüsünün temel proteinlerini baz alarak farklı yöntemler içeren aşı adaylarının çalışmalarını başlatmıştır. Bu aşı adaylarından çoğu virüsün konağa giriş yapmasını ve yaşamasını sağlayan Spike proteini üzerine olmuştur. Antijenik özelliği yüksek olan ve içerdiği RBD bölgesi ile konakta bulunan ACE2 reseptörü ile virüsün vücuda alınmasını sağlayan Spike proteini kişide nötralizan antikor oluşumu konusunda efektif olsa da virüsün esasen 4 yapısal proteini bulunmaktadır. Virüs benzeri partiküller (VLP) içeren aşı stratejimizde Spike, Membran, Zarf ve Nükleokapsid proteinlerinin kendi kendine bir araya gelme özelliği baz alınmış ve bu protein yapıları ile entegre his-tag ile etiketlenmiş bir plasmide kopyalanmıs ve tranfeksiyon yöntemi ile in vitro olarak memeli hücresinde ürünler toplanmıştır. Afinite kromatografisi ile ayrıştırılan ve daha sonra saflaştırma işlemleriyle hazır hale getirilen VLPler 2 farklı adjuvan ile formule edilmiştir. Son 2 yıldır hızla değişime uğrayan virüsün yeni varyantlara da açık olması sebebiyle aşımızın düzenlenebilir olması ve yeni virus koşullarına uyarlanabilmesi çok önemlidir. İlk olarak UK'de görülen ve son bir yıldır tüm dünyada yaygınlaşan alpha varyantı sebebiyle, aşımızın ilk dozunda termostabil altı prolin (6p; HexaPro) mutasyonu içeren daha stabil bir Spike proteini ile oluşturulmuş WT VLP kullanılmış fakat ikinci dozunda alpha variant mutasyonlarını içeren UK VLP kullanılmıştır. Her iki enjeksiyon formulasyonu için de Alum ve CpG adjuvanları birlikte kullanılmıştır. Aşımız Faz2 çalışmalarını başarı ile tamamlamıştır. Bu çalışmalar sonucunda, aşılanan yaklaşık 115 gönüllünün 90 gün boyunca takibi yapılmış ve belirli gün aralıklarında (21.gün, 35.gün, 49.gün ve 90.gün) alınan örneklerle imünolojik analizler yapılmıştır. Bu analizler sonucunda çoğu hastada orta ve yüksek seviyelerde nötralizan ve nötralizan olmayan antikor yanıtları gözlemlenmiş ve 90.güne kadar korunan humoral immün yanıt gözlemlenmiştir. Ayrıca hücresel yanıtları kontrol edilen gönüllülerin Th1 hücre yanıtına uygun olarak ilerlediği görülmüştür.

Anahtar Kelimeler: COVID-19, SARS-CoV-2, VBP, Aşı, CpG ODN, Alum

ACKNOWLEDGEMENTS

In the first instance, I would like to express my great gratitude to Prof. Ihsan Gursel who is not only my advisor but also an inspirer. He has always tried to show me the right way with a patience and support me through the whole way I walked in my master studies. Another heartfelt thanks to Prof. Mayda Gursel for her courage and guidance for everything about life and science. I am really thankful that they gave me the chance to work with them.

I wish to extend my special thanks to my thesis jury: Assist. Prof. Serkan Ismail Goktuna and Prof. Dr. Gunnur Deniz, for their help throughout my master studies. Additional thanks to TÜBİTAK to support our studies financially by the T1004 (18AG020) grant and the team members of Bilkent University, Middle East Technical University and Hacettepe University for their collaboration all the time.

I wish to show my appreciation to all past and current THORLAB members: Artun Bülbül, Tuğçe Yıldırım, Muzaffer Yıldırım, Pınar Gür, Fatma İrem Abraş, Yasemin Ceylan, Yasemin Özsürekçi, Tamer Kahraman and Fuat Cem Yağcı. A special thanks to Emre Mert Ipekoğlu from Troll Lab for his friendship. I especially would like to thank Oguzhan Tarman, Pelin Ersan, Ünal Metin Tokat, Ege Dedeoğlu and Barış Küçükkaraduman for allowing me to have many perfect memories together even every limited time during the laboratory hours. I also want to thank to my beloved friends Irem Evcili, Nilsu Turay, Naz Bozbeyoğlu and Bilgehan Ibibik for their incredible kindness, support and cheer everytime. I would like to say one more special and the biggest thanks to my lovely friends Tuğçe Bildik and Berfu Saraydar for their priceless friendships. I cannot survive without them during the long-lasting laboratory hours, and I will definitely miss so much to work together with 90's Turkish pop music. You are the greatest things that my master years gave me. I am also grateful to Damla Aksoy Kızılkoca, Doğacan Kızılkoca, Nurcan Aksoy and Ergün Aksoy for their intimate support for last 7 years. I would like to express my deepest thanks to my dearest friends Ege Sirkovalı, Şendağ Duru, Serden Ece Ballı and Melis Atbinek for their everlasting friendship. We solved every crisis together twenty-four seven with cheer.

From the bottom of my heart, I would like to say a big thank you for Furkan Aksoy. He has always been my mentor, best friend, love and supporter. He always encouraged me to do my best in every part of the life. I am so grateful for his invaluable love.

My last and greatest thanks are for my lovely family; Rüya Bartan, Ahmet Yüksel Bartan and Ahmet Çağrı Bartan for their reliance, infinite help and love. I am deeply lucky and thankful to have them in my life. Every achievement that I got are made possible by them.

TEŞEKKÜRLER

Öncelikle sadece danışmanım değil, aynı zamanda ilham kaynağım olan Prof. Dr. İhsan Gürsel'e çok teşekkür ediyorum. Bana her zaman sabırla doğru yolu göstermeye çalıştı ve yüksek lisans eğitimimde yürüdüğüm tüm yolda bana destek oldu. Hayata ve bilime dair her konuda cesareti ve rehberliği için Prof. Mayda Gürsel'e de ayrıca yürekten teşekkürlerimi sunuyorum. Bana onlarla çalışma şansı verdikleri için gerçekten minnettarım.

Tez jürisi tarafından yüksek lisans eğitimim boyunca yardımları için Assist. Prof. Serkan Ismail Göktuna ve Prof. Dr. Günnur Deniz'e özel teşekkürlerimi sunarım. Çalışmalarımızı T1004 (18AG020) hibesi ile finansal olarak destekleyen TÜBİTAK'a ve Bilkent Üniversitesi, ODTÜ ve Hacettepe Üniversitesi ekibimiz üyelerine yardımları için ayrıca teşekkür ederim.

Tüm geçmiş ve şimdiki THORLAB üyelerine teşekkürlerimi sunarım: Artun Bülbül, Tuğçe Yıldırım, Muzaffer Yıldırım, Pınar Gür, Fatma İrem Abraş, Yasemin Ceylan, Yasemin Özsürekçi, Tamer Kahraman ve Fuat Cem Yağcı. Troll Lab üyesi olan Emre Mert İpekoğlu'na dostluğu ve anlayışı için özel teşekkürler. Özellikle Oğuzhan Tarman'a, Pelin Ersan'a, Ünal Metin Tokat'a, Ege Dedeoğlu'na ve Barış Küçükkaraduman'a laboratuvarda her kısıtlı zamanımda bile birlikte çok güzel anılar yaşattıkları için teşekkür ederim. Ayrıca her zaman gösterdikleri inanılmaz nezaket, destek ve neşeleri için sevgili arkadaşlarım Irem Evcili, Nilsu Turay, Naz Bozbeyoğlu ve Bilgehan İbibik'e de teşekkür etmek istiyorum. Biricik dostlarım Tuğçe Bildik ve Berfu Saraydar'a paha biçilmez arkadaşlıkları için özel ve büyük teşekkürü borç bilirim. Uzun süren laboratuvar saatlerinde onlarsız hayatta kalamam mümkün olmazdı. Sizinle 90'lar pop müzikleri eşliğinde çalışmayı çok özleyeceğim. Siz yüksek lisans yıllarımın bana verdiği en harika şeysiniz. Damla Aksoy Kızılkoca'ya, Doğacan Kızılkoca'ya, Nurcan Aksoy'a ve Ergün Aksoy'a son 7 yıldır verdikleri olağanüstü destek için çok minnettarım. Sevgili arkadaşlarım Ege Sirkovalı, Şendağ Duru, Serden Ece Ballı ve Melis Atbinek'e sonsuz dostlukları için en derin teşekkürlerimi sunuyorum. Her krizi birlikte 7/24 neşeyle çözdük.

Furkan Aksoy'a kalbimin en derinliklerinden kocaman bir teşekkür etmek istiyorum. Her zaman akıl hocam, en iyi arkadaşım, sevgilim ve destekçim oldu. Hayatımın her alanında elimden gelenin en iyisini yapmam için beni her zaman teşvik etti. Onun paha biçilmez sevgisi için minnettarım.

Son ve en büyük teşekkürüm güzel aileme; Güvenleri, sonsuz yardımları ve sınırsız sevgileri için Rüya Bartan, Ahmet Yüksel Bartan ve Ahmet Çağrı Bartan'a çok teşekkür ederim. Hayatımda oldukları için çok şanslı ve minnettarım. Elde ettiğim her başarı onlar sayesinde mümkün olmuştur.

TABLE OF CONTENTS

ABSTRACT ii
ÖZET iii
ACKNOWLEDGEMENTS iv
TEŞEKKÜRLER vi
TABLE OF CONTENTS viii
LIST OF FIGURES xi
LIST OF TABLES xiii
ABBREVIATIONS xiv
INTRODUCTION 1
1.1. Immune System 1
1.1.1. Innate Immunity 3
1.1.2. Adaptive Immunity 4
1.1.2.1. T-cell Mediated Immunity 5
1.1.2.2. B-cell Mediated Immunity 6
1.1.2.3. Antibodies 7
1.2. COVID-19 9
1.2.1. SARS-CoV-2 9
1.2.2. Life cycle, Pathway and Pathogenesis 10
1.2.3. Variants and Mutations 13
1.3. SARS-CoV-2 Vaccines 15
1.3.1. VLP Vaccines 17
1.4. Adjuvants 19
1.4.1. ALUM 20
1.4.2. CpG ODNs 21
1.5. Clinical Phase Trial Stages of a Vaccine Candidate 23
1.5.1. Phase I Clinical Trial 24

1.5.2. Phase II Clinical Trial 24
1.6. Aims and Outline of the Study 24
MATERIALS AND METHODS 26
2.1. Materials 26
2.1.1. Cell Culture Reagents 26
2.1.2. ELISA Reagents 26
2.1.3. Kits 26
2.2. Methods 28
2.2.1. Volunteers and Controls 28
2.2.2. Peripheric Blood Mononuclear Cells (PBMCs) Isolation from Whole Blood 29
2.2.3. Cell Counting 30
2.2.4. Serum Sample Separation 30
2.2.5. Recombinant Protein Production 30
2.2.6. Preparation of SARS-C0V-2 VLP vaccine for animals 31
2.2.7. Bleeding of Animals 32
2.2.8. Enzyme Linked Immunosorbent Assay (ELISA) 32
2.2.8.1. Human IgG ELISA 32
2.2.8.2. Animal IgG ELISA 33
2.2.9. Cytometric Bead Array (CBA) 33
2.2.10. Chemiluminescent Microparticle Immunoassay (CMIA) 34
2.2.11. CoronaHunter IgG ELISA Kit (Matriks Biotek, Turkey) 35
2.2.12. Statistical Analyses 36
RESULTS 37
3.1. Pre-Clinical Studies 37
3.1.1. Humoral Immune Response in Animals against Wild-Type and Alpha Variants Combined VLP-58-1023-AL-K3 SARS-COV-2 Vaccine Formulations 37
3.2. Clinical Studies 50
3.2.1. Humoral Immune Response in Phase-2 Clinical Trial Volunteers against Wild-Type and Alpha Combined VLP-58-1023-AL-K3 SARS-COV-2 Vaccine 50

3.2.2. Cellular Immune Response in Phase-2 Clinical Trial Volunteers against Wild-Type and Alpha Combined VLP-58-1023-AL-K3 SARS-COV-2 Vaccine 60

DISCUSSION 66

FUTURE PERSPECTIVES 73

BIBLIOGRAPHY 74

APPENDIX 81

LIST OF FIGURES

Figure 1.1. Classification of immune cells.....2
Figure 1.2. Diversification of T helper cell subsets 3
Figure 1.3. SARS-CoV-2 Structure 10
Figure 1.4. Life cycle of SARS-CoV-2.....11
Figure 1.5. Pathogenesis of SARS-CoV-2.....12
Figure 1.6. SARS-CoV2 Vaccine Platforms.....17
Figure 1.7. Mechanism of VLP vaccines.....18
Figure 1.8. Action mechanism of alum-based vaccines.....20
Figure 1.9. Immunomodulatory action of CpG ODN.....21
Figure 1.10. Innate and adaptive responses of CpG ODN stimulation.....22
Figure 1.11. PRR pathway of CpG ODN.....23
Figure 3.1. Antibody Production of female Balb/c mice against in house recombinant trimeric Spike Protein.....40
Figure 3.2. Antibody Production of female Balb/c mice against in house recombinant Nucleocapsid Protein. 42
Figure 3.3. Antibody Production of female Balb/c mice against in house recombinant WT RBD Protein.....44
Figure 3.4. Antibody Production of female Balb/c mice against commercial recombinant UK RBD Protein.....46
Figure 3.5. Antibody Production of female Balb/c mice against commercial recombinant Delta RBD Protein.....49
Figure 3.6. Antibody Production of Phase 2 volunteers against in house recombinant trimeric Spike Protein.....52
Figure 3.7. Antibody Production of Phase 2 volunteers against in house recombinant Nucleocapsid Protein. 54
Figure 3.8. Antibody production of Phase 2 volunteers against in house recombinant proteins of RBD variants.....56
Figure 3.9. Neutralizing antibody levels of Phase 2 volunteers against RBD protein by Abbott Kit (Deren Laboratory, Ankara, Turkey). 58
Figure 3.10 Antibody Production of Phase 2 volunteers against trimeric Spike protein by CoronaHunter Kit (Matriks Biotek, Ankara, Turkey).....59
Figure 3.11. Th1 responses of Phase 2 volunteers before and after stimulation of S, N, M, O peptide pool.....61

Figure 3.12. Th2 responses of Phase 2 volunteers before and after stimulation of S, N, M, O peptide pool 62
Figure 3.13. IL-6 production and Treg response of Phase 2 volunteers before and after stimulation of S, N, M, O peptide pool 63
Figure 3.14. Th17 responses of Phase 2 volunteers before and after stimulation of S, N, M, O peptide pool 64
Figure 3.15. T response pie chart of Phase 2 volunteers 65

LIST OF TABLES

Table 2.1. Recombinant and Secondary Proteins used in ELISA 27
Table 2.2 Formulation of VLP vaccine for Phase 2 study. 28
Table 2.3 Necessities to be a volunteer 29
Table 2.4 Formulation of VLP vaccine for pre-clinic animal study. 31
Table 3.1. Codes of COVID-19 Infected Phase2 volunteers and their infection dates after the first injection 51

ABBREVIATIONS

Angiotensin-Converting Enzyme 2	ACE2
Alkaline phosphatase	ALP
Aluminum hydroxide	Alum
Antigen presenting cell	APC
Activating protein 1	AP1
Area under the curve	AUC
Bicinchoninic acid	BCA
B cell receptors	BCR
Bovine serum albumin	BSA
Biological Safety Level 3	BSL3
Cytometric Bead Array	CBA
Cluster of differentiation	CD
CCAAT/enhancer binding protein	CEBP
Chemiluminescent Microparticle Immunoassay	CMIA
Coronavirus disease 2019	COVID-19
Cytosine poly guanine	CpG
CpG oligodeoxynucleotide	CpG ODN
cAMP-responsive element binding protein	CREB
Cytotoxic T lymphocyte	CTL
Dendritic cell	DC
Dimethyl sulfoxide	DMSO

Deoxyribonucleic acid	DNA
Dulbecco’s Phosphate Saline Buffer	DPBS
Envelope protein	E
Enzyme Linked Immunosorbent Assay	ELISA
Endoplasmic reticulum	ER
Fetal bovine serum	FBS
Follicular T cells	Tfh
Forward scattered	FSC
Global Initiative on Sharing All Influenza Data	GISAID
Human embryonic kidney-293 fast-transfection	HEK293-FT
Interferon	IFN
Immunoglobulin	Ig
Interleukin	IL
Interferon-gamma inducible protein	IP
Interleukin-1 receptor-activated kinase	IRAK
Membrane protein	M
Monocyte chemoattractant protein	MCP
Middle East respiratory syndrome	MERS
Major histocompatibility complex	MHC
Messenger ribonucleic acid	mRNA
Myeloid differentiation primary response gene 88	MYD88
Nucleocapsid protein	N
Nuclear factor-κB	NF-κB
National Institute for Biological Standards and Control	NIBSC

Natural killer	NK
Natural killer cells	NKC
Optical density	OD
Pathogen-associated structural patterns	PASP
Peripheral blood mononuclear cell	PBMC
Pattern recognition receptors	PRR
PE-conjugated streptavidin	SA-PE
Polymerase chain reaction	PCR
Plasmacytoid dendritic cells	pDC
Phosphatidylinositol 3-kinases	PI3K
p-Nitrophenyl Phosphate	PNPP
Red blood cells	RBC
Receptor-binding domain	RBD
Ribonucleic acid	RNA
Reactive oxygen species	ROS
Room temperature	RT
Replication/transcription complex	RTC
R-phycoerythrin	PE
Spike protein	S
Streptavidin	SA
Severe acute respiratory syndrome coronavirus	SARS-CoV
Severe Acute Respiratory Syndrome Coronavirus 2	SARS-CoV-2
Sodium Dodecyl Sulfate Polyacrylamide Gel Electrophoresis	SDS-PAGE
Size scattered	SSC

Serum separating tubes	SST
T cell receptors	TCR
T helper cells	Th
T helper cells class 1	Th1
T helper cells class 2	Th2
T helper cells class 9	Th9
T helper cells class 17	Th17
T helper cells class 22	Th22
Toll-like receptors	TLR
Transmembrane serine protease 2	TMPRSS2
Tumour Necrosis Factor	TNF
Tumour-necrosis factor receptor-associated factor 6	TRAF6
Regulatory T cells	Treg
Virus-like-particle	VLP
Wild-type	WT
World Health Organization	WHO

CHAPTER 1

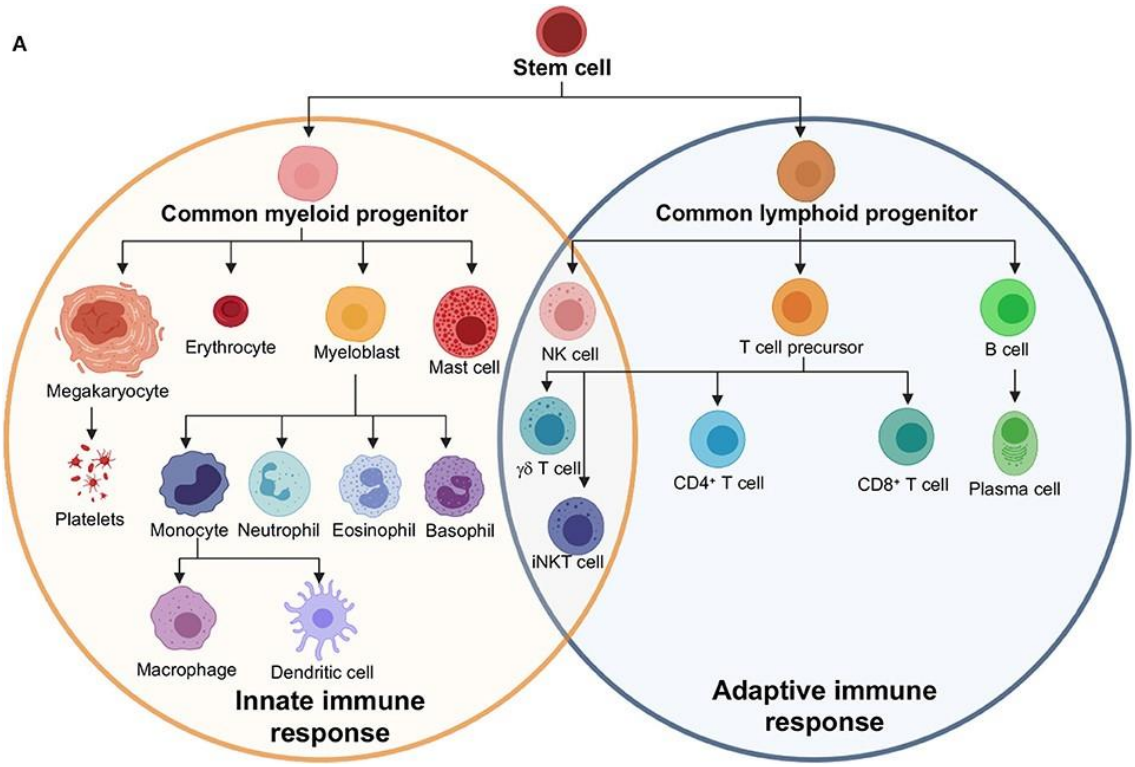
INTRODUCTION

1.1. Immune System

The immune system is a collection of molecules, cells and tissues that provide resistance to infections. The coordinated reaction of this system against foreign molecules such as microorganisms, is called the immune response. The task of the immune system is to recognize molecules that are foreign to the body and destroy them. There are two separate immune response mechanisms that work in harmony with each other: the innate and the adaptive immune response. Innate immune response elements are important in inducing adaptive immune responses. All immune responses are self-limiting and disappear once the infectious agent is destroyed.

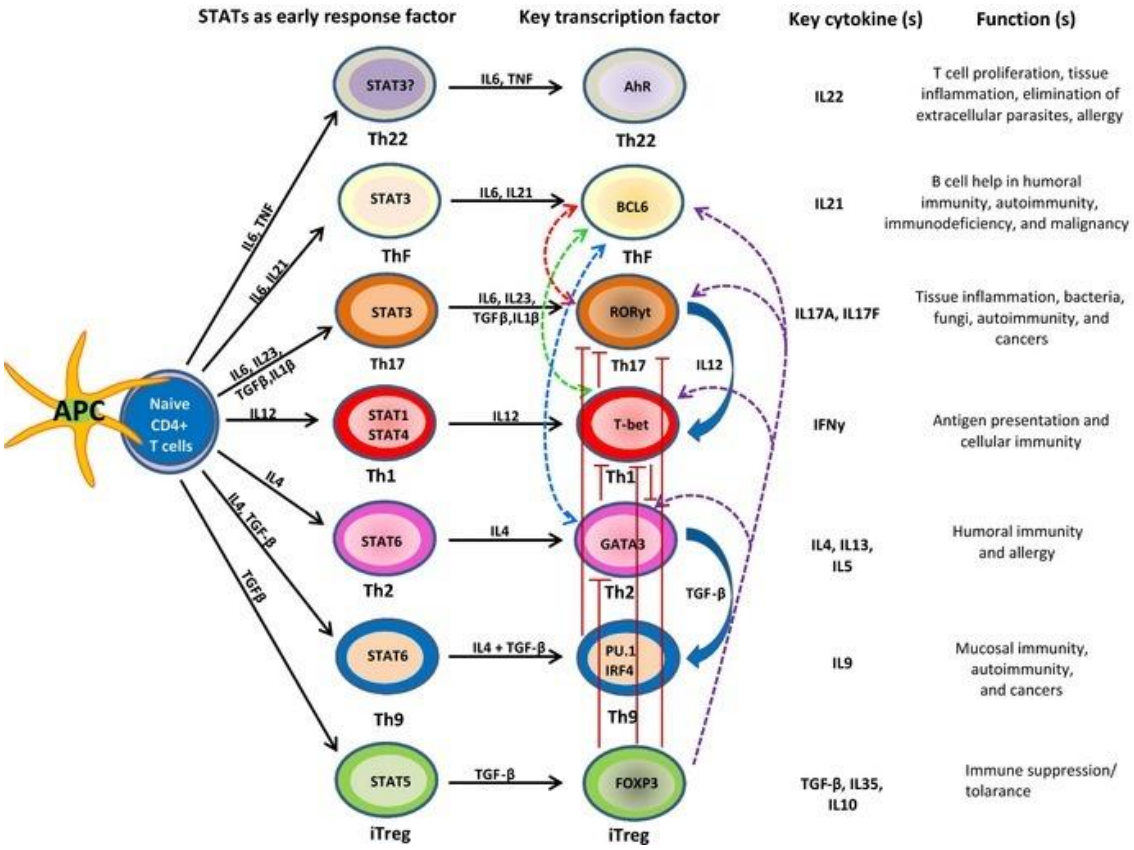
As a cellular immune system component, leukocytes have a big role to play. By applying different immunological and histological assays, subsets of several leukocytes can be differentiated. For this, antigens found in their cell membranes are distinctive which are called cluster of differentiation (CD) numbers. These antigens can be selected by specific monoclonal antibodies. Before circulation of leukocytes in the body, differentiation starts in hematopoietic stem cells (Figure 1.1). Second differentiation occurs in common myeloid progenitor cell and myeloid stem cell. Myeloid progenitor cell gives rise to major lymphocytes called B cells, T cells and natural killer (NK) cells. For all of these lymphocytes and NK cell subsets, distinguishing surface phenotypes can be found such as T cell receptors (TCRs) and B cell receptors (BCRs) to bind the processed antigen presented by antigen presenting cells (APCs). These TCRs have different surface phenotype by having CD4 marker or CD8 marker. CD4+ T cells are known as helper T cells which have a big role in balance in immunity and communication between other cells such as B cells and innate immunity cells like macrophages. CD8+ T cells are known as cytotoxic T cells which are effective against direct action of immune response to pathogens. After action of T cells, B cells and innate immunity cells against pathogens, different chemokines and cytokines release and these cytokines and chemokines also cause differentiation of T helper cells to small subsets like Th1, Th2, Th17 and Treg (Figure 1.2) and also diversification of B cells into plasma cells which are

a big source of immunoglobulin production. NK cells can be distinguished by their granulocyted structure phenotypically. Also, myeloid stem cells become granulocytes, megakaryocytes and platelets, and erythrocytes. Granulocyte lineage is important to give function as neutrophils, monocytes, macrophages, eosinophils, basophils, and mast cells. Neutrophiles have ability to produce big amount of reactive oxygen species (ROS) to fight with the bacterial pathogens in the first defense of the body. Monocytes found in the blood and macrophages found in the tissue have high phagocytic capacity to clear microbes and they have a big interaction with lymphocytes as a bridge between innate immunity and adaptive immunity by binding to other complement proteins and immunoglobulins that are produced by and found in B cells. Eosinophiles have also phagocytic capacity and they also provide effective defense against parasites. Basophiles are the rarest molecules found in the blood and they have no ability to phagocyte. Lastly, mast cells carry IgE in their surfaces which is the key marker for hypersensitive responses against parasites and they release sufficient amount of IL-4 to start allergic immune response [1].



Murin, CD. "Considerations of Antibody Geometric Constraints on NK Cell Antibody Dependent Cellular Cytotoxicity." Frontiers. 2020

Figure 1.1. Classification of immune cells



Tripathi SK, Lahesmaa R. Transcriptional and epigenetic regulation of T-helper lineage specification. Immunol Rev. 2014;261(1):62-83.

Figure 1.2. Diversification of T helper cell subsets

1.1.1. Innate Immunity

Innate Immunity defines the immune response mechanisms that only create the first response against infectious agents, exist from birth in healthy individuals, and are activated within hours after exposure to the agent. This response recognizes specific molecules carried by microorganisms but is not specific to the agent. It provides stimulation of the most effective acquired immune response (cellular/secretory) mechanisms in eliminating the causative microorganism. Epithelial barriers, phagocytes (monocytes/macrophages, neutrophils, etc.), natural killer cells (NKC) and complement system constitute the elements of this type of immune response. It has no memory, exhibits the same response in every encounter. During the action, it is important to distinguish between self and non-self. Although adaptive immunity can do it specifically, innate immunity has a way to discriminate between the cells of our body and microbes. Most of the pathogens have common molecules that host body have not. These molecules

are called pathogen-associated immunostimulants. For example, peptidoglycan wall found in bacteria, LPS found in gram-negative bacteria, glycosylphosphatidylinositol found in Plasmodium and CpG motif found in short bacterial DNA sequences as a effective stimulator of macrophages and big initiator of inflammatory response for antibody production from B cells. All of these and more pathogen-associated immunostimulants are recognized by the host with the help of pattern recognition receptors (PRRs) in the surface and soluble receptors mostly found in complement system of innate immunity in order to activate phagocytosis, initiate innate immunity and direct killing of pathogens [2].

1.1.2. Adaptive Immunity

Adaptive Immunity is the response of a late (within days) and slow onset, but specific and strong immune response against microorganisms and other foreign antigens that invade tissues by passing epithelial barriers and reaching lymphoid organs. Defines the mechanisms by which it occurs. The cells responsible for the emergence of the adaptive immune response are lymphocytes. B lymphocytes and their antibodies with its products eliminate extracellular pathogens, while effector T-lymphocytes destroy intracellular pathogens. It has memory, a faster and more effective immune response occurs in repeated encounters.

There are two types of adaptive immune response mechanisms:

a. Humoral Immune Response: It is manifested by proteins called antibodies formed by B-lymphocytes removed and is effective in eliminating extracellular pathogens. Antibodies circulate freely and are found in mucosal secretions of the gastrointestinal tract/respiratory/genitourinary tract to fight the microorganisms and their products (toxins, etc.) in the circulation and prevents them from colonizing and invading tissues. Since it cannot enter the cell, it cannot eliminate intracellular microorganisms. Among the antigens it recognizes are molecules such as proteins, carbohydrates, lipids, nucleic acids, etc.

b. Cellular Immune Response: It is elicited by T-lymphocytes. Helper T-lymphocytes (Th) strengthen the natural immune response mechanisms by activating phagocytes on the one hand and enable humoral immune response mechanisms to work by activating B

lymphocytes on the other hand. Cytotoxic T lymphocytes (CTL) kill cells containing foreign protein in their cytoplasm. T lymphocytes only recognize antigens in protein structure and form a response against them [1].

There are 5 main stages of an adaptive immune response [3]. First one is antigen recognition. An antigen is recognized by immature lymphocytes. Naive lymphocytes carry antigen receptors, but they are inexperienced and cannot perform effector functions to destroy the antigen. They are found in the lymph nodes or circulate between the lymph nodes and blood, searching for the appropriate antigen to recognize and bind throughout their lives. When they encounter the appropriate antigen, they differentiate into effector cells or memory cells, enabling the antigen-specific immune response mechanism to come into play. The second stage is lymphocyte activation. It is characterized by clonal enlargement. Some of the naive lymphocytes such as B and T lymphocytes transform into effector lymphocytes such as plasma cells and effector T cells, respectively. The third step of the adaptive immune response is antigen destruction. Effector lymphocytes and their products together with natural immune response elements destroy the microorganism. Plasma cells secrete antibodies, helper T cells secrete cytokines and cytotoxic T cells destroy infected host cells with cytotoxic effect. The fourth stage is called decreased immune response. Following the elimination of the agent, most of the effector cells activated by the antigen die by "apoptosis". Dying cells are eliminated by phagocytes. The remaining cells form memory cells and migrate to bone marrow. Finally, the last stage is completed by the memory development. Although there is no antigen in the body, memory lymphocytes remain in the resting phase for months/years, or even lifelong, and quickly form an immune response (secondary immune response) after re-exposure with the same antigen.

1.1.2.1. T-cell Mediated Immunity

Categorization of T cells depending on their expressions of TCRs can be done in two ways; Tα/β and Tγ/δ cells. The rare ones are Tγ/δ cells which can be found in a peripheral blood of murine only about 1-10% but more common in epidermis. Common Tα/β cells can be identified in three different subsets as helper CD4+T cells and cytotoxic CD8+ T cells and regulatory CD4+ CD25+ T cells.

CD4+ T helper cells are classified in 6 main cell subsets: Th1, Th2, Th17, T follicular helper cells (Tfh), Th9, and Th22 cells. The common feature of all of these T helper cell subsets is recognition of antigens is presented with the help of class II MHC molecules on APCs (dendritic cells, macrophages, and B lymphocytes). Activation of macrophages is provided by Th1 cells which is also required for cell-mediated immunity in fighting with pathogens intracellularly. Th2 cells are important for communication with B cells for production of antibody and class switching. Th17, Th9 and Th22 are crucial for mucosal immunity activation and protection. T cell subsets can be defined according to their capacity to detect and produce different inductive cytokines from different transcription factors. As shown in Figure 1.2, substantial amount of IFN-γ secretion and T-bet transcription factor expression is made by Th1 cell subset while Th2 cells are key players for secretion of IL-4, IL-5, and IL-13 and expression of GATA-3 transcription factor. Th17 cells are important for IL-17A, IL-17F, and IL-22 secretion and transcription factor of RORγt expression. Treg cell subset produces TGF-β and IL-10 and express Foxp3. Last but not least, Th22 cells secretes adequate amount of IL-22.

Expression of CD8 marker is specific to cytotoxic CD8+ T cells which is known with specific lytic capacity by using different mechanisms such as production and secretion of granules which are cytotoxic and initiation of apoptosis by using Fas and Fas ligand communications. Their common feature is that their presentation from APCs are carried out by class I MHCs [4].

1.1.2.2. B-cell Mediated Immunity

A big part of the humoral immunity is generated by antibodies released from B cells. Antibodies bind to extracellular antigens and undertake the task of neutralizing or eliminating them. Humoral immunity constitutes the primary immune defense mechanism against extracellular microorganisms containing polysaccharides and lipid antigens and their toxins. B lymphocytes constitute 5-15% of the lymphocytes in the blood. These cells are also found in the spleen, lymph nodes, tonsils, and mucosa-associated lymphoid tissue. Its primary functions are antibody production and secretion. Mature naive B cells can recognize antigen but fail to secrete antibodies. For antibody secretion, they must first be activated, since B cell activation is a process consisting of sequential complex steps [5]. B cell activation can occur in 2 ways: T cell-dependent and

T cell-independent. B cells can recognize antigens of different natures such as polysaccharides, lipids, glycolipids, nucleic acids and small soluble molecules. These are generally polyvalent/multivalent (antigens containing many of the same epitope on the surface) type antigens and can activate B cells directly. These are T cell-independent antigens for B cells. However, CD4+ T cell assistance is required for B cell activation by protein antigens. Therefore, proteins are T cell-dependent antigens for B cells. The antigen-binding part of the BCR cannot bind to the entire antigen, but only to a small part (epitope). In order for the BCR to send activation signals, at least 2 BCR molecules must be noncovalently cross-linked with the polyvalent antigen and the cytoplasmic tails of the BCR molecules must converge. The cytoplasmic tails of the BCR of naïve mature B cells are short. This tail lacks signal transduction capability. BCR-associated signals are sent by 2 molecules called Igα and Igβ (CD79a and CD79b). Membrane IgM or IgD (BCR) and Igα and Igβ together form the BCR complex. Transcription factors such as Fos, Jun, and NF-kB initiate the expression of genes that ensure B cell proliferation and differentiation. However, the signal of the antigen-BCR complex is not the only one for B cell activation. Cytokine and chemokine receptor expression increases in activated B cells. B cells can be activated also by Toll-like receptors (TLR) which is a component of the innate immune system. TLR expression increases with BCR stimulation in memory B cells. TLR stimulation leads to polyclonal proliferation, memory B-plasma cell transformation and polyclonal production of IgM/IgG and cytokines (IL-6 and 12) in memory B cells. B cells express TLRs that can recognize many ligands such as proteins, polysaccharides, lipids and nucleic acids, the best known of which are TLR-2, TLR-3, TLR-4, TLR-5, TLR-7 and TLR-9 [6].

1.1.2.3. Antibodies

Firstly, a blood agent has been found to neutralize a toxin specific to diphtheria in 1890. This agent has named as ‘Antikörper’, or antibodies, produced by plasma B cells, which can bind and neutralize its opposite called antigen. According to sizing columns done after electrophoresis by Tiselius and Kabat in 1939, antibodies were classified as their gamma globulin fractions called immunoglobulin (Ig) based on “heavy” (IgM), “regular” (IgA, IgE, IgD, IgG), and “light” (light chain) dimers [7]. Immunoglobulins have two big main roles to play in the body: 1) They are the receptors of B cell surfaces to

allow the antigen binding for activation of cell signaling 2) They are the soluble molecules which are effective to bind and neutralize free antigens far away.

Primary immune response is performed by IgM because of its first place in expression during B cell development. Detection of IgM is mostly collaborated in diagnosis of acute exposure to a pathogen. IgM is firstly expressed as monomeric in the surface of naïve B cells but upon stimulation with an antigen and maturation, it is found as pentameric (rarely hexameric) form and secreted. This pentameric form functions in opsonization and destruction of pathogen and if antigen has multiple repeating epitopes, IgM will easily have multimeric interactions with it [8]. As a result, IgM antibodies are more likely to be poly-reactive rather than other immunoglobulin types and this feature allows IgM antibodies to be faster defenders against pathogens.

IgD antibody is found rarely in human serum. Although unclear function of circulating IgD antibodies, it is known that they can react with specific bacterial proteins like Moraxella catarrhalis [9]. B cell stimulation will occur after binding of bacterial epitopes to circulating IgD. More studied form of immunoglobulin D is membrane-bound form, and it functions as cooperator of IgM and they both are associated with CD79a and CD79b for signaling. Also, it is stated that B cell fate can be regulated by membrane bound IgD in developmental stages [10].

IgG is found mostly (75%) in human serum. Among other immunoglobulin isotypes, longest half-life in serum is belong to IgG. Well-studied IgG has four identified sub-classes in human: IgG1, IgG2, IgG3 and IgG4. Respectively, IgG1 is the mostly found subclass in serum and IgG4 is the rarest one. Each subclass has different plasticity and affinity which can affect antigen interactions. Even though the biggest role of IgG antibodies is direct contribution to immune response by their neutralizing capacity against pathogens and viruses, there are other mechanisms of IgG antibodies in action: 1) Immobilization of pathogens by opsonization and elimination by phagocytosis by other phagocytic immune cells 2) Activation of classical complement pathway 3) Type II and type III hypersensitivity reactions. IgG expressed as small and monomeric and secreted easily to tissues with this structure. Class switching of IgG antibodies are very common and due to this high-capacity response and available maturation, they are included in secondary immune responses [11].

High levels of IgA can be found in mucosal areas such as saliva [12]. In serum, it is found as monomeric but in mucosal surfaces it can form dimer, trimer or tetramer. IgA has two identified sub-classes in human: IgA1 and IgA2. In mucosal areas IgA antibodies performs as direct neutralizer against bacteria, toxins and viruses. In intracellular areas, IgA has polymeric form and defined pathogens may be caught by IgA glycans [13].

IgE has the shortest half-life in serum. It is very potent to fight with parasites, hypersensitivity, and allergic reactions. IgE mostly works with mast cells, basophils, Langerhans cells and eosinophils. It is a big candidate for therapies against allergy and asthma as development of anti-IgE antibodies [14].

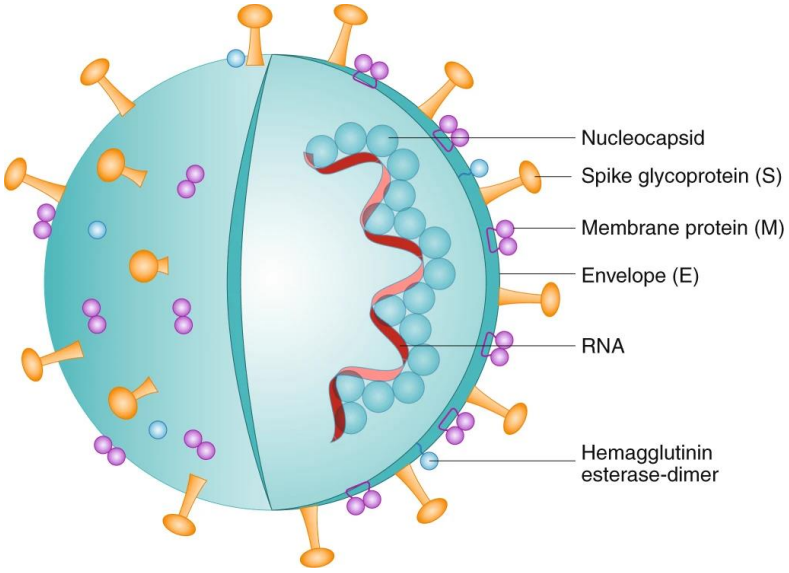
1.2. COVID-19

Coronavirus disease 2019 (COVID-19) is a zoonotic infection caused by Severe Acute Respiratory Syndrome Coronavirus 2 (SARS-CoV-2), which was first identified in the city of Wuhan, China, in late 2019 with a very high pathogenicity and contagiousness. COVID-19 has a broad clinical spectrum, including asymptomatic infection, mild upper respiratory disease, respiratory failure from severe viral pneumonia, and even death [15].

1.2.1. SARS-CoV-2

The origin of SARS-CoV-2 comes from Beta coronaviruses which is a group of RNA viruses which can lead fatal respiratory infections. Recently in this group, Severe Acute Respiratory Syndrome Coronavirus (SARS-CoV), Middle East respiratory syndrome (MERS) and SARS-CoV-2 are found [16]. The closest relation of SARS-CoV-2 originates from bats, the RaTG13 virus, sharing almost 96% sequence homology [17]. SARS-CoV-2 is an enveloped virus packed by nucleocapsid phosphoproteins includes inside a positive-sense single-stranded RNA genome (29.8 to 29.9 kb), several micro molecules and proteins [18,19]. SARS-CoV-2 has four main structural proteins: membrane (M), envelope (E), spike (S) and nucleocapsid (N) proteins. In Spike, there are two subunits: 1) S1 which is connected with the receptor-binding domain (RBD) that functions as binding to a receptor (ACE2) on the cell surface of the host 2) S2 which is required to fuse with cell membrane of the host and cleaved after binding for stabilization of the virus [20]. Envelope

surrounds the RNA genome and molecules needed for virus life cycle and in the inner part of the envelope, nucleocapsids can be found as connected with RNA genome [21]. Lastly, membrane encloses viral structures (Figure 1.3)



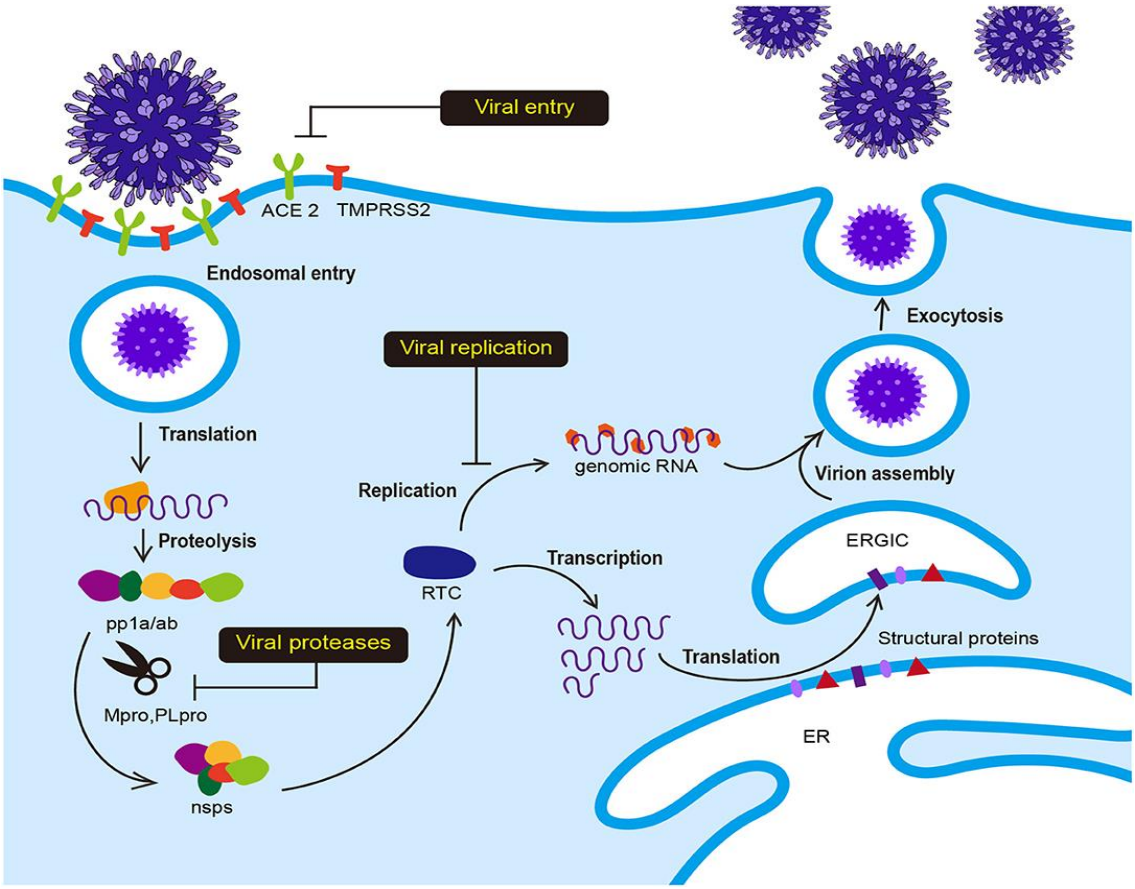
Florindo, HF., Kleiner, R., Vaskovich-Koubi, D., Acúrcio, R. C., Carreira, B., Yeini, E. et al. Immune-mediated approaches against COVID-19. 2020. Nature News.

Figure 1.3. SARS-CoV-2 Structure

1.2.2. Life cycle, Pathway and Pathogenesis

Life cycle of SARS-CoV-2 begins with the binding of glycoproteins in transmembrane Spike to its receptor in the host which is angiotensin-converting enzyme 2 (ACE2) [22]. After binding of glycoproteins in Spike, ACE2 binding unit of Spike which is S1 unit interacts ACE2 with its peptide domain. Then, S1/S2 junction is affected with this ACE2-S1 interaction and transmembrane serine protease 2 (TMPRSS2) is triggered to cleave the secondary site (S2) and causes an irreversible conformational change in both subunits. Afterwards, S2 moves forward to host membrane to affect intracellularly. Inserted S2 in host cell leads to connect cellular and viral membranes [20]. After the endocytosis, viral genomic RNA which is uncoated is transported into the cytosol and ORF1a and 1b translations are triggered. Replication/transcription complex (RTC) is initiated by the help of viral proteases [23] and ER-related extracellular vesicles helps the viral assembly for virus secretion into host cells [24]. Lastly, exocytosis of viruses inside

secretory vesicles occurs along the host cell [25]. The summary of SARS-CoV-2 life cycle can be seen in Figure 1.4.

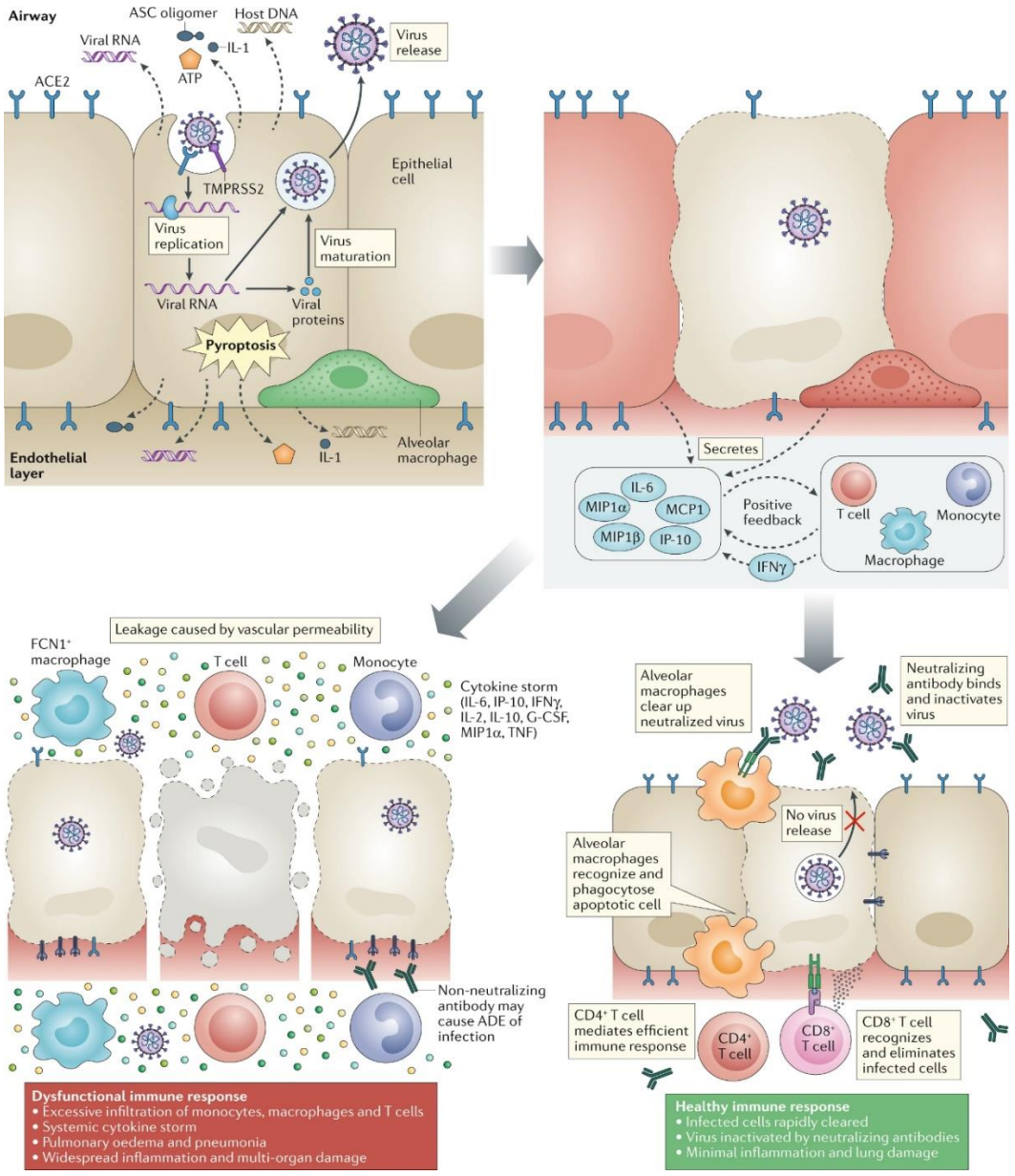


Jeong, GU., Song, H., Yoon, GY., Kim, D., Kwon, YC. Therapeutic strategies against covid-19 and structural characterization of SARS-COV-2.2020.

Figure 1.4. Life cycle of SARS-CoV-2

SARS-CoV-2 pathophysiology resembles to SARS-CoV that acts upon respiratory system mainly, but SARS-CoV-2 can affect multiple organs such as heart, liver and kidney. Most common symptoms are cough, headache, joint and muscle pains, fatigue and fever [26]. SARS-CoV-2 also has similar symptoms with Kawasaki disease like dysfunction in cardiac system, shock and abdominal pain [27]. Big part of transmission from human to human which causes COVID-19 disease occurs by respiratory droplets [28] and incubation period, before symptoms cannot be seen, can change between 4-6 days. However, this period can change according to delayed peak of the viral load [29]. Symptomatic patients have more risk as a potential transmitter of SARS-CoV-2 unlike

asymptomatic patients [30]. ACE2, which is first promoter of SARS-CoV-2 entry to the host, is found mostly in the surface of alveolar epithelial type II cells which is essential for gas exchange in lungs [31]. However, ACE2 can also be found in extrapulmonary tissues, including heart, intestine, blood vessels, kidneys, and urinary bladder [32]. After viral infection, epithelial cell death occurs and cause apoptosis and/or pyroptosis which leads to secretion of pro-inflammatory cytokines such as IL-1β, IL-6, IL-8, TNF-α, IP10, MCP-1 (Figure 1.5) [33,34].



Tay, MZ., Poh, CM., Rénia, L., MacAry, PA. The Trinity of COVID-19: Immunity, inflammation and intervention. 2020. Nature News.

Figure 1.5. Pathogenesis of SARS-CoV-2

After triggering primary immune system by various cytokines and chemokines, macrophages are recruited to the infection site and by the help of monocyte interaction, additional cytokines, such as IFN-γ, are released to trigger secondary immune response regulated mainly by T cells and B cells. If the patient has dysfunctional immune response, it will cause excessive infiltration of immune cells which leads systemic cytokine storm, extended inflammation and multiple damaged organs. These patients can be identified with increased serum level of IL-6, IL-10, IP-10, MCP-1, IFN-γ, IL-2, TNF-α (Figure 1.5). However, if the patient has a healthy immune response, neutralizing antibodies will inactivate/neutralize viruses and macrophages will eliminate neutralized viruses, CD4+ T cells will provide an efficient immune response by cytokines and CD8+ T cells will kill infected cells (Figure 1.5). Additionally, antigen-presenting cells (APC)s, play a big role in induction of T cells. DCs recognize the virus and presents the epitope of viral antigens to T cells by using MHCs. MHCI is used for presentation of antigen by APCs to CD8+ T cells and MHCII is used for presentation of antigen by APCs to CD4+ T helper cells (Th cells). While CD8+ T cells are directly affective in elimination of infected cells, Th cells are important to trigger B cells for production of antibodies specific to viruses. Increased T cell against S, N, and M proteins are detected in PBMCs from SARS-CoV-2 convalescent serum samples [35].

1.2.3. Variants and Mutations

Characterization of SARS-CoV-2 showed a low mutation rate than that of influenza. Several different viral clades are defined with specific mutations by Global Initiative on Sharing All Influenza Data (GISAID) after RNA sequences' phylogenetic analysis [36]. First novel virus variant is emerged in early 2020 which is D614G mutation in spike protein, the substitution at 614th position of aspartic acid with glycine, is mostly seen in Europe. D614G mutation showed its effect in the population around 100% by mid-2020 [37,38]. In addition to D614G mutation, different mutations occurred to cause different variants to spread.

Primarily, in late 2020, B.1.1.7 mutation is emerged in UK which is growing widely in early 2021. This mutation led various genetic changes in the viral genome. One of the critical mutations in this variant is mutation N501Y which leads increased affinity for ACE2 receptor in the host to bind altered spike protein of virus and made infectivity

increased. Other important mutation in UK variant is P681H which occurs very close to furin cleavage site and leads more stable viral structure and increases transmission. Also, several amino acid deletions in spike proteins, such as 69-70del and Y144 deletion, and deletions in Orf8, ORF1ab and nucleocapsid protein are found in UK B.1.1.7 variant [39]. UK variant is also called as Alpha variant.

Following after 1 month, two new variants were observed in South Africa and Brazil. South Africa variant has named as B.1.351 and Brazil variant has named as P.1 variant. Characterization of B.1.351 variant showed that five important substitutions additional to D614G and N501Y among eight mutations in spike has emerged which are K417N, E484K, D80A, D215G and A701V. Also new deletions occurred in spike protein. South Africa variant overall showed increased transmissibility and capability for immune escape [40]. P.1 variant developed 17 additional mutations and various deletions in spike proteins and viral genome. Among these 17 mutations, a trio structure formed by K417T, E484K, and N501Y in RBD of spike protein causes increased affinity to the host ACE2 receptor which is associated with high mortality in the population [41].

In early 2021, a dominant lineage, called B.1.617 which includes Delta (B.1.617.2) and Kappa (B.1.617.1), in Maharashtra-India has emerged [42]. Although it is thought that they are coming from a common ancestor, Kappa variant has a mutation in RBD site which is a substitution from E484 to Q484 which showed increased effect in evading antibody neutralization [43] while Delta variant, named as T478K mutation in RBD of spike protein, showed higher transmissibility and spread over countries by replacing dominant SARS-CoV-2 variant as Delta from Alpha [44]. Delta variant showed higher stability in the host and caused more severe cases in the populations over the world [45].

The last identified variant up today is called Omicron variant (B.1.1.529), showed first in Botswana and South Africa. Omicron variant is hard to fight with because in addition to higher transmissibility by mutations in S2 fusion domain, there are about 15 mutations in spike protein which is important for vaccine-elicited immunity [46]. These mutations include G339D, S371L, S373P, S375F, K417N, N440K, G446S, S477N, T478K, E484A, Q493R, G496S, Q498R, N501Y, Y505H (https://covdb.stanford.edu/page/mutation-viewer/#omicron).

1.3. SARS-CoV-2 Vaccines

SARS-CoV-2 vaccine development achieved in very short time than most of other vaccines developed over centuries because there has no ready-to-use treatment for COVID-19 disease and severity became threatening for populations from the beginning of the disease. SARS-CoV-2 vaccines were able to be ready in 10 months thanks to availability in huge resources of information and funding to reach the goal by pharmaceutical companies, biotechnology companies and research laboratories in universities [47]. Many companies used spike protein-based strategy to develop vaccines against SARS-CoV-2 by using it as an antigen. However, there are other several strategies developed over time which includes some other structural and non-structural proteins as antigens in order to take advantage of triggering additional T cell and B cell responses [48]. Here are four main vaccination strategies for SARS-CoV-2 (Figure 1.6):

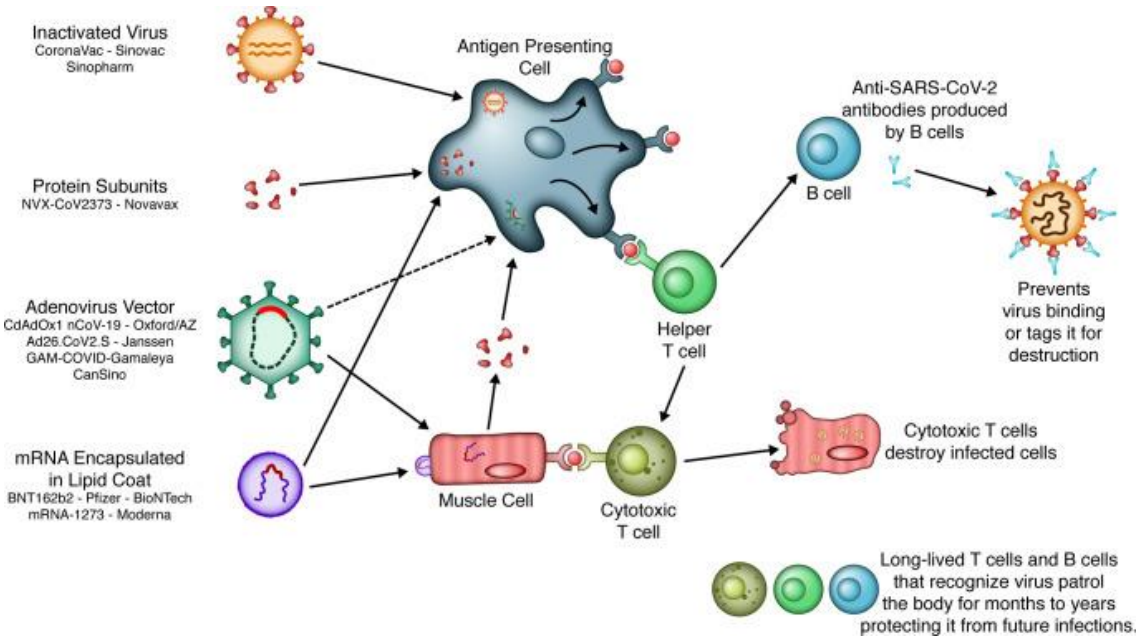
mRNA Vaccines: It can be defined as lipid nanoparticles which contains encapsulated and genetically engineered mRNA encodes for spike protein of the virus in the host to be endocytosed and translated into protein for prompting anti-viral immune response [49]. Moderna (mRNA-1273) and BioNTech/Pfizer (BNT162b1& BNT162b2) are two companies among others that use mRNA strategy for SARS-CoV-2 vaccine development. For both vaccine strategies, intramuscular injection has been applying to volunteers. The most common side effects are headache, fatigue, myalgia, chills and pain [50] at the injection site which are transient that starts after 15 hours of injection and end in 2 days [51]. Side effects were more common after the booster dose. Good antibody responses developed in all groups according to high neutralizing antibody titers and tendency to Th1 response [52].

Viral vector (adenovirus) vaccines: They are produced by Astrazeneca, Johnson & Johnson and Sputnik. As a recent technology, viruses are altered to eliminate their replication capability and virulence but not too much to lose their capability to infect human cells. By using adenoviruses, they deliver the genetic material of the virus to the host and antigenic proteins inside the host are produced to be presented to immune cells following the lymphocyte activation [53]. Astrazeneca and Oxford University revealed AZD1222 vaccine which uses engineered chimpanzee adenovirus (ChAdOx1) to encode for the wild-type SARS-CoV-2 S protein. Th1-skewed T cells responses were observed, and 90% efficacy has seen after ‘prime-boost’ immunization [54]. Johnson & Johnson uses

replicating-defective adenovirus 26 (Ad26.COV) to encode for stabilized SARS-CoV-2 pre-fusion Spike. SARS-CoV-2 pseudo virus assay was performed and virus neutralizing antibodies was reported after two-dose regimen. Also, antibodies against RBD production and increased Th-1 skewed T-cell responses were documented. Sputnik V uses heterogenous regimen with injection of replication-defective Ad26 firstly and boosting of replication-defective Ad5 secondly. 91.4% effective humoral immune responses and effective CD4+ and CD8+ T cell responses was reported [53].

Inactivated virus vaccines: It is one of the old and reliable method over the vaccine groups. The virus is inactivated in a Biological Safety Level 3 (BSL3) laboratory to not cause any disease but supported with an adjuvant for an effective immune triggering because during inactivation process antigens can be damaged. CoronaVac, which is developed by Sinovac Research and Development Co., is an alum-adjuvanted vaccine and uses CN2 strain of SARS-CoV-2 by the activation of β-propiolactone. High antibody levels against S and RBD proteins and low levels of anti-nucleocapsid antibodies were observed. For this vaccine, no T cell responses were documented and 90% seropositivity was recorded [53].

Protein subunit vaccines: It is on trial by Novavax with the name of NVX-CoV2373 from the USA. They used protein fragments of the virus which are innocuous to human body. These protein subunits are nanoparticles expressed in baculovirus and produced in insect cells that mimic SARS-CoV2 full-length Spike protein and provide a humoral and cellular immune response in the human body by the help of an adjuvant called Matrix-M1, saponin-based material [55]. Besides the vaccine platforms mimic only the spike proteins, other structural proteins can be added to the vaccine formulation by forming virus-like-particle (VLP) (WHO, 2022).

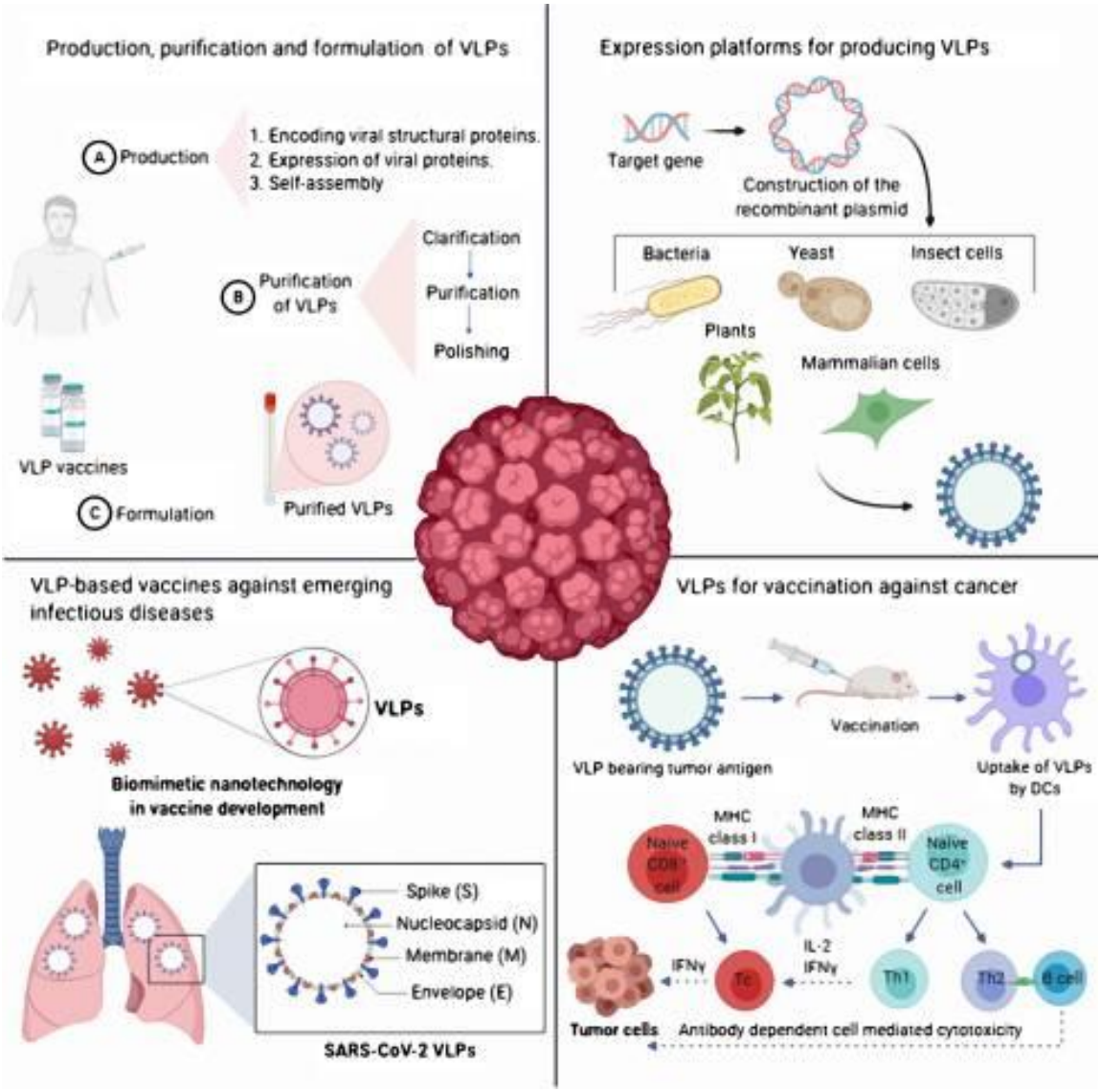


Golob, JL., Lugogo, N., Lauring, AS., & Lok, AS. SARS-CoV-2 vaccines: a triumph of science and collaboration. JCI insight, 2021; 6(9).

Figure 1.6. SARS-CoV2 Vaccine Platforms

1.3.1. VLP Vaccines

VLP vaccine platform brings simple storage, administration, safety and effectiveness. Although many SARS-CoV2 vaccine strategies are based on spike protein found in the virus, VLPs contain one or more nanoparticles of main structural proteins in SARS-CoV2 virus such as Spike (S), membrane (M), nucleocapsid (N) and envelope (N). VLPs mimic the shape and size of the virus but lacks replication capability to infect a cell because they do not have genetic material. In vitro, prokaryotic cells and mammalian cell lines can be used as expression systems to generate VLPs [56]. Thanks to organized structure, self-assembly and geometrical suitability, VLPs are similar to pathogen-associated structural patterns (PASP) which helps for identification of antigenic molecules by immune system [57,58]. In production of VLP vaccines, structural proteins are encoded, viral proteins are expressed in cell cultures and self-assembly occurs. Then, clarification and purification steps are carried out. Lastly, formulation of the vaccine is generated with appropriate adjuvants and doses of VLPs produced (See Figure 1.7).



Nooraei, S., Bahrulolum, H., Hoseini, ZS., Katalani, C., Hajizade, A., Easton, AJ., Ahmadian, G. Virus-like particles: Preparation, immunogenicity and their roles as nanovaccines and Drug Nanocarriers. 2021. Journal of nanobiotechnology.

Figure 1.7. Mechanism of VLP vaccines

In response of VLP-based vaccines, dendritic cells and other antigen-presenting cells uptake VLPs and present the epitopes with the help of MHC complexes. MHC I complex present the epitopes taken from APCs to CD8+ T cells and MHC II complex present the epitopes to naïve CD4+ T cells. Viral structural proteins trigger TCR of helper T cells and induced Th cells to secrete cytokines for cellular immunity. Also, these cytokines induce B cells to differentiate into plasma cells for production of efficient neutralizing antibodies [59].

VLP vaccines have a big potential for both neutralizing antibody production and cell mediated immune triggering compared to the results in conventional vaccination strategies like inactivated virus vaccines [60].

One of the advantages of VLPs is adaptation and effectiveness of the vaccine formulation against newly formed variants such as Alpha (B.1.1.7), Beta (B.1.351), Gamma (P.1), Delta (B.1.617.1 and B.1.617.2) and Omicron (B.1.1.529). Because most of the mutations occur in sequences of spike protein, the variants of concern have big potential of escaping from neutralizing antibodies produced by Spike-based vaccines. Presence of other structural proteins would allow triggering strong immunity contributing cellular protective mechanism of virus clearance. Additional proteins to spike, especially M and N, support T cell dependent epitopes to be presented that allow spreading along cellular and humoral immune system. Also, antibodies produced against N protein has a hypothetical potential to harbor cross-immunity for world-wide spreading variants [61].

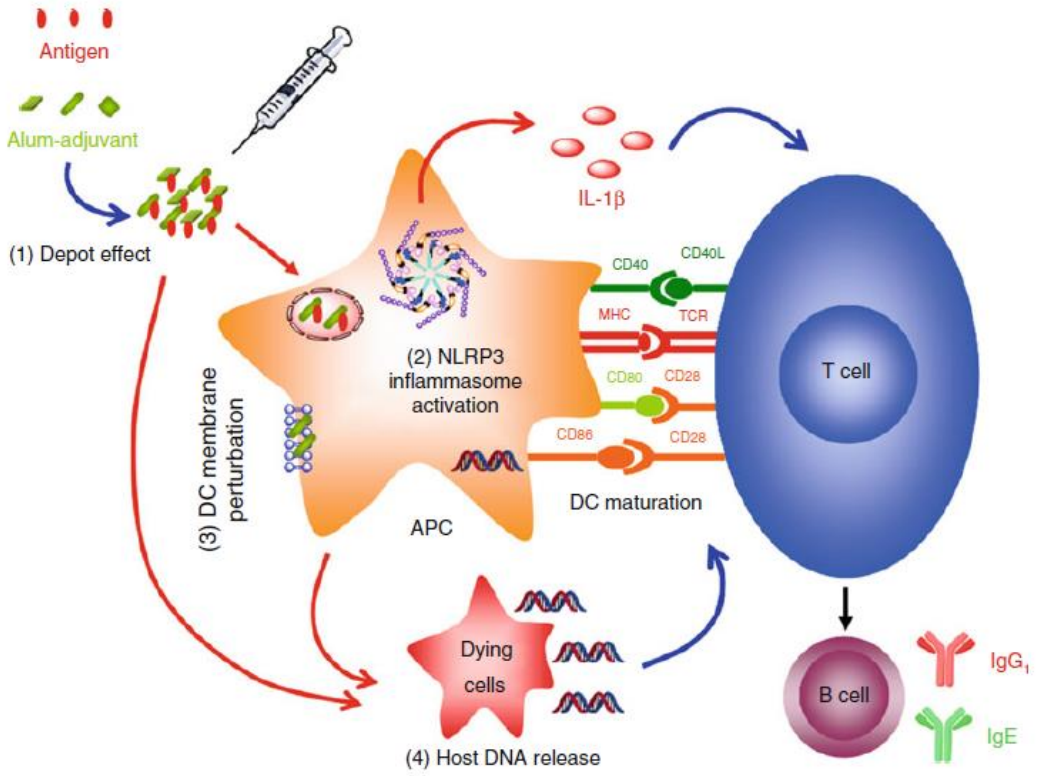
1.4. Adjuvants

Novel vaccines have superiority over conventional vaccines in terms of being pure and safe, but their protective properties need to be improved. This improvement can be achieved by the use of substances or carriers that enhance the humoral and cellular immune response to an antigen, called adjuvants. They are used to increase the early and long-term immune response in vaccines. Subunit vaccines produced by modern biotechnological methods are more pure, safer and have less side effects. Adjuvants have different mechanisms of action at the cellular and molecular level: 1) Storage effect for slow release of antigen 2) Targeting to and activation of antigen-presenting cells 3) Stimulation of cytokines 4) Conformational changes of antigen molecules 5) Change of net polar charges of molecules. According to one mode of action, some adjuvants denature antigen molecules and convert them into particulate compounds. Thus, their recognition by macrophages becomes easier. Antigens with the help of adjuvants stimulate B or T cell response, resulting in the production of memory and effector cells. Here are some examples of mostly used adjuvants in vaccine platforms: aluminum salt-based (Alum) adjuvant, liposome/virosomes, pattern recognition receptors (PRRs) agonist adjuvant (Poly I:C, double-stranded RNA analog), CpG oligodeoxynucleotide

(CpG ODN), flagellin, Toll like receptors 7 (TLR7), and TLR7/8 agonists), chitosan, emulation adjuvant, IL-12 and bacterial toxin [62].

1.4.1. ALUM

The most commonly used insoluble aluminum salts in humans are aluminum hydroxide, aluminum phosphate and aluminum hydroxyl-phosphate [63]. Their mechanism of action is explained as the storage of antigen in the injection site and its long-term release from there and as these adjuvants induce a local inflammatory reaction and stimulate macrophages and other immune system cells. Antigen uptake into APCs is facilitated and both humoral and cellular immune responses are stimulated (Figure 1.8). Especially in combination with VLPs, aluminum salts are preferrable such as Engerix-B (HBV vaccine), Gardasil (HPV vaccine), Cervarix (HPV vaccine), and Hecolin (HEV vaccine) [64].

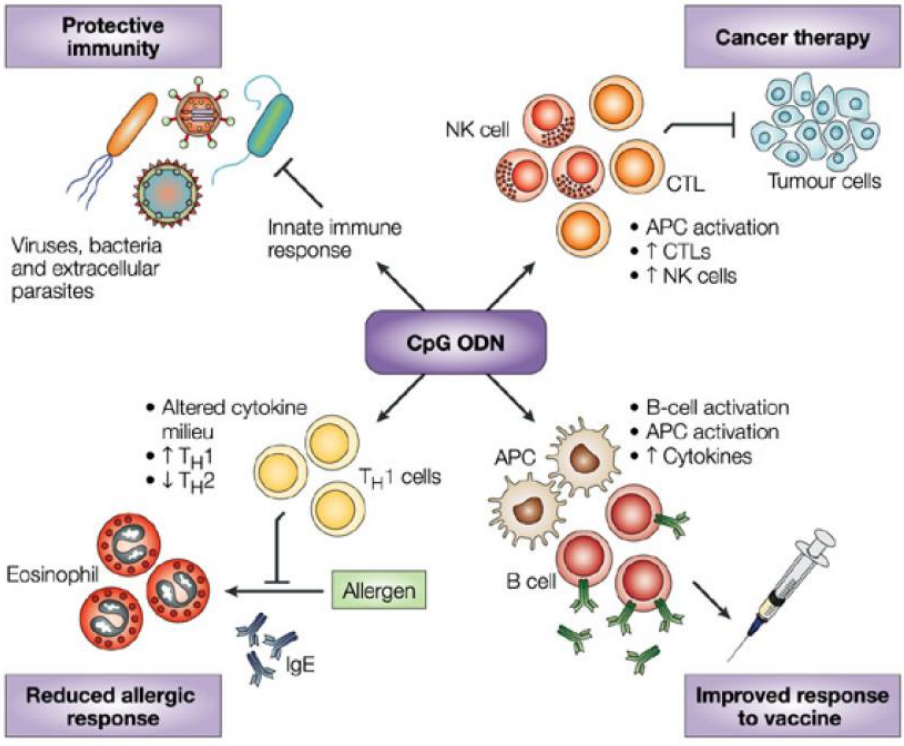


Xia T., Sun B. and Ji Z. Aluminum Based Nano-Adjuvants. 2015. Encyclopedia of Nanotechnology.

Figure 1.8. Action mechanism of alum-based vaccines

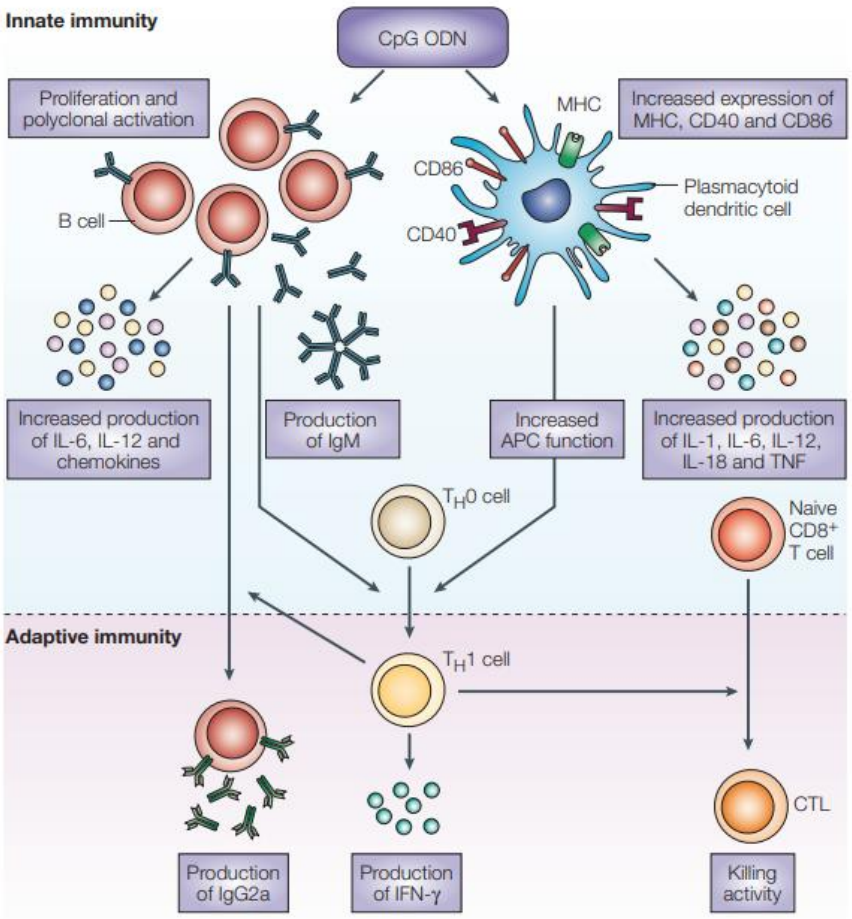
1.4.2. CpG ODNs

With the discovery of the immunostimulant effect of DNA, DNA-based adjuvant research began. A six-deoxynucleotide long DNA molecule with a CpG dinucleotide in the middle is called a CpG motif. It is 20 times more abundant in bacterial DNA than in mammalian DNA. This repetitive CpG motif in bacterial cells is immediately recognized as foreign and dangerous by TLRs (innate immunity) in mammalian cells, and interferons (α and β) and IL-12 are secreted by immune system cells. There are two types of CpG ODNs: 1) D-type (Class A) 2) K-type (Class B). D-type ODNs are strong inducers of type I interferons such as IFNα and activators of NK cells [65] while K-type ODNs are strong inducers of B cell stimulation and monocyte maturation. Because K-type ODNs are strong activators of humoral immune milieu, they are the perfect match as a vaccine adjuvant [66]. Thus, while the cellular immune response is stimulated in benefit of Th1 response, the allergic response is also suppressed because Th2 response is reduced (See Figure 1.9). This is an indication that DNA molecules containing CpG motifs can be used as adjuvants in therapeutic applications and vaccines [67] (See Figure 1.10).



Klinman, D. M. Immunotherapeutic uses of CPG oligodeoxynucleotides. 2004. Nature News.

Figure 1.9. Immunomodulatory action of CpG ODN

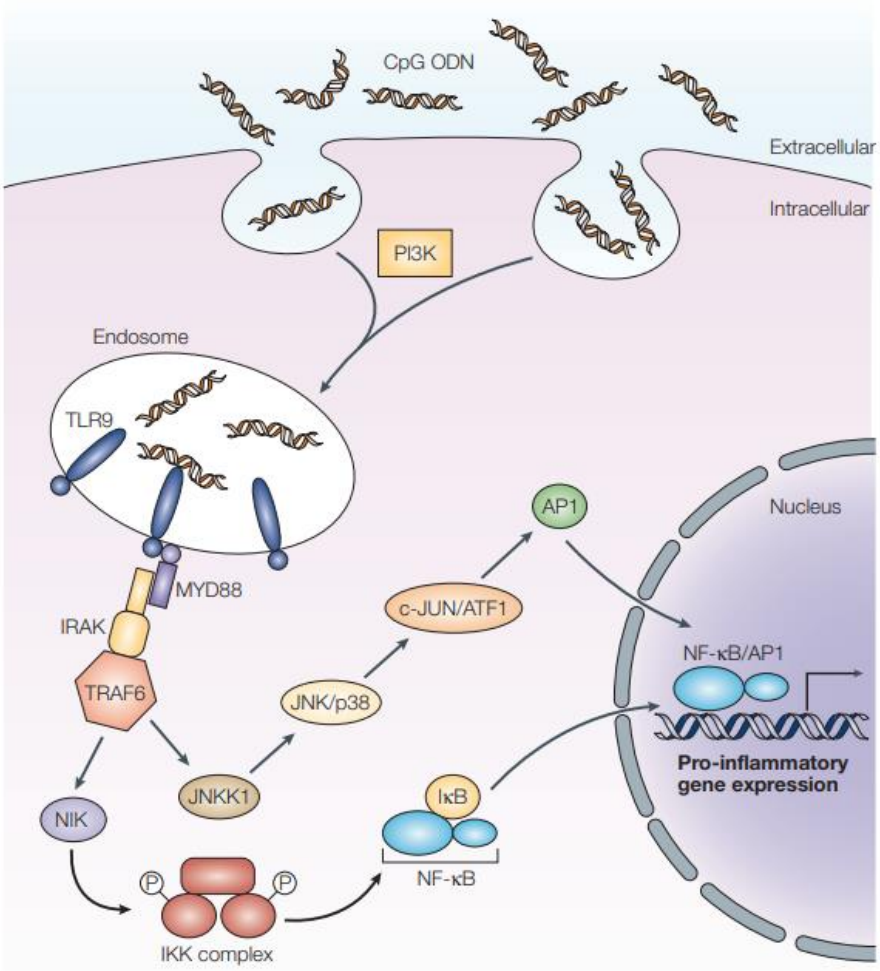


Klinman, D. M. Immunotherapeutic uses of CPG oligodeoxynucleotides. 2004. Nature News.

Figure 1.10. Innate and adaptive responses of CpG ODN stimulation

CpG ODN is one of the PRR agonist adjuvant which is a pathogen-associated molecular patterns and trigger Toll-like family of receptors (TLRs). TLR9 is the member which detects synthetic oligodeoxynucleotides (ODNs) with CpG motifs and stimulate innate immune system by increasing function of APCs and inducing antigen-specific adaptive immunity [67]. Immune cells, that has TLR9 such as B cells and plasmacytoid dendritic cells (pDCs), uptake CpG ODN intracellularly and through phosphatidylinositol 3-kinases (PI3Ks), endosomal TLR9 interacts with CpG ODNs [68]. After this highly specific interaction, signalling cascade through myeloid differentiation primary response gene 88 (MYD88), interleukin-1 (IL-1) receptor-activated kinase (IRAK) and tumour-necrosis factor receptor (TNFR)-associated factor 6 (TRAF6) is started. Thanks to this signalling pathway, nuclear factor-κB (NF-κB), activating protein 1 (AP1), CCAAT/enhancer binding protein (CEBP) and cAMP-responsive element binding

protein (CREB) are triggered and end up with activation of transcription factors necessary for upregulation of pro-inflammatory cytokines genes (See Figure 1.11). Also, interaction of these activated immune cells by CpG ODNs, causes differentiation and maturation of natural killer (NK) cells, T cells and monocytes/macrophages. All of these cell groups secrete Th1-skewed immune milieu [69].



Klinman, D. M. Immunotherapeutic uses of CPG oligodeoxynucleotides. 2004. Nature News.

Figure 1.11. PRR pathway of CpG ODN

1.5. Clinical Phase Trial Stages of a Vaccine Candidate

Features expected from an ideal vaccine; It is effective and safe, provides immunity for a long time, does not have side and toxic effects, does not cause infection, is durable for a long time, can be preserved and is cheap. It should also be easy to administer and suitable for combination with other vaccines [70]. Pre-clinical studies include in vitro and

in vivo studies in animals prior to human studies. It uses tissue, cell culture systems, or animal testing to evaluate the safety and immunogenicity of the candidate vaccine. An idea of a safe starting dose is obtained for the next stage of the study. Many candidate vaccines do not pass this stage as they do not produce the expected immune response. The preclinical stages usually last at least 1-2 years [71].

1.5.1. Phase I Clinical Trial

In this phase, pharmacokinetics and side effects of the vaccine are investigated in a small number of (20-100) healthy volunteers. The main purpose is to obtain 'safety data' and to determine the type and extent of immune response triggered by the vaccine and adjusting the optimal dosage for human health. Studies are completed in an average of 1-1.5 years [71].

1.5.2. Phase II Clinical Trial

A group of 100-200 people participate, and it is done in a center like university hospitals. Studies are generally planned as single or double blind and placebo controlled. The main aim of this phase is efficacy and safety. In this phase, the optimal dose, initial schedule and safety profile of the candidate vaccine should be defined. The studies take an average of 2 years to complete [71].

1.6. Aims and Outline of the Study

SARS-CoV-2, which first appeared in Wuhan, China in late 2019 and spread rapidly all over the world, still strongly continues its pandemic effect all over the world. Although there was no definitive treatment and vaccine study in the first moments of the pandemic, successful vaccine candidates and treatment combinations have started to be applied today. The reality of other epidemics and pandemics that are likely to be seen all over the world today and in the future is completely obvious, and the most important thing is to create appropriate editable vaccine platforms as well as appropriate treatments. SARS-CoV-2 vaccines generally target the Spike protein found in the virus, but rapid changes and mutations in the virus lead to the formation of new variants. It is observed that the

effectiveness and formation of neutralizing antibodies against viral compounds of many vaccine candidates is decreased due to mutations in the spike protein on these variants, and this necessitates the development of new vaccines for these variants.

With our VLP-58-1023-Al-K3 SARS-CoV-2 vaccine, we aimed to strongly stimulate cellular and humoral immunity by supporting 4 main structural proteins (S, N, M and E) of the virus with 2 different and effective adjuvants (Alum and K-type CpG ODN). We aimed to show that the biggest advantage of our vaccine compared to other vaccines is that it can be adapted quickly against new variants and to prove that two different combinations (Wild Type and Alpha variant) give more effective results for inducing Th1-skewed T cell response and production of neutralizing antibodies when combined. In this context, prefusion stabilized six proline (HexaPro) mutated Wild Type VLP products are combined with Allhydrogel (Alum) and K-type (Class B) CpG ODN and formulated as mentioned in Section 2.2.1 for Phase 2 clinical trials as a first dose of injection. Then, UK VLP products which includes specific mutations seen in Alpha variant are combined with Allhydrogel (Alum) and K-type CpG ODN and formulated as same as mentioned in Section 2.2.1 for Phase 2 clinical trials as a booster (second) dose of injection after 21 days of first dose. In regular time intervals (Day0, Day21, Day35, Day49 and Day90), sera and blood samples from the volunteers were collected and immunogenicity assays like Enzyme Linked Immunosorbent Assay (ELISA), Chemiluminescent Microparticle Immunoassay (CMIA) and Cytometric Bead Array (CBA) were applied to all volunteers. These assays showed that neutralizing antibody production and cellular and humoral response against WT+UK formulation works well in most of the patients.

CHAPTER 2

MATERIALS AND METHODS

2.1. Materials

2.1.1. Cell Culture Reagents

2% wash medium was prepared by using heat-inactivated Fetal Bovine Serum (Biological Industries, Israel), RPMI 1640 (Biological Industries, Israel), Penicillin-Streptomycin (Biological Industries, Israel) and HEPES Buffer (Biological Industries, Israel). 10% resting medium was prepared by using same reagents mentioned in the last sentence and Sodium Pyruvate (G Biological Industries, Israel) and Non-Essential Amino Acids (Biological Industries, Israel). Recipes of the media is attached in Appendix 1. Lymphocyte separation media was purchased from Capricorn Scientific, Germany. 1X Dulbecco's Phosphate Saline Buffer (DPBS) were purchased from (Biological Industries, Israel). Dimethyl sulfoxide (DMSO) was purchased from Applichem, Germany.

2.1.2. ELISA Reagents

Details of recombinant proteins and secondary antibodies used for ELISA procedure were showed in Table 2.1. Recipes of washing buffer, blocking buffer and p-Nitrophenyl Phosphate (PNPP) substrate (Thermo Fisher Scientific, USA) were attached in Appendix 1. As ELISA control reagents, NIBSC First WHO International Reference Panel for anti-SARS-CoV-2 Immunoglobulin (20/268), NIBSC Anti-SARS-CoV-2 Verification Panel for Serology Assays (20/B770) and 35 Convalescent serum samples received from Marmara University, Department of Infectious Diseases, Istanbul, Turkey.

2.1.3. Kits

Corona Hunter Q-CORS IgG ELISA Kit was purchased from Matriks Biotek, Turkey with catalog number of COR-QNS-IGG-STRIM. LEGENDplex™ HU Th Cytokine

Panel (12-plex) w/ VbP V02 Kit was purchased from Biolegend, USA with catalog number of 741028. SARS-CoV-2 SMNO Defined Peptide Pool was purchased from Mabtech, Nacka, Sweden with catalog number of 3622-1.

Table 2.1. **Recombinant and Secondary Proteins used in ELISA**

Recombinant Antibody	**Brand Name/Country**	**Catalogue Number**	**Working Concent.**
Recombinant Spike	Turkey	Homemade	6 ug/ml for human
Recombinant Spike	Turkey	Homemade	4 ug/ml for animal
Recombinant Nucleocapsid	Turkey	Homemade	4 ug/ml for human
Recombinant Nucleocapsid	Turkey	Homemade	1 ug/ml for animal
SARS-CoV-2 Wild-Type RBD	Turkey	Homemade	4 ug/ml for animal
SARS-CoV-2 RBD (Wild Type)	ProteoGenix, France	PX-COVP046-100	1 ug/ml
SARS-CoV-2 RBD (UK Alpha Variant)	ProteoGenix, France	PX-COVP052-100	1 ug/ml
SARS-CoV-2 RBD (Indian Delta Variant)	ProteoGenix, France	PX-COVP061-100	1 ug/ml
Goat Anti-Human IgG-AP	Southern Biotech, USA	2040-04	1:1000
Goat Anti-Mouse IgG-AP	Southern Biotech, USA	1030-04	1:1000

2.2. Methods

2.2.1. Volunteers and Controls

In this study, 117 volunteers to be vaccinated with SARS-COV-2 VLP vaccine (VLP-58-1023-Al-K3) are involved. Cohort of volunteers were selected before the vaccination according to the features listed in Table 2.3. Their bloods are collected in both serum separating tubes (SST) and K2 EDTA blood collection tubes by Ankara Dr. Abdurrahman Yurtaslan Oncology Training and Research Hospital (Ankara,Turkey), Kocaeli Medical Faculty Hospital (Kocaeli, Turkey) and Yedikule Chest Diseases and Thoracic Surgery Training and Research Hospital (Istanbul, Turkey). Blood collection have been done for 5 different time points which were Day 0 (before vaccination), Day 21 (before second dose of vaccine), Day 35 (after 1 week of two doses vaccination), Day 49 (After 2 weeks of two doses vaccination) and Day 90 (3 months after first injection of vaccine). Moreover, PCR tests against SARS-COV-2 were done for regular intervals showed that some volunteers exposed to virus infection over time (See Table 3.1). As positive control groups 35 convalescent sera which were recruited from Marmara University (Department of Infectious Diseases, Istanbul, Turkey), 37 NIBSC First WHO International Reference Panel for anti-SARS-CoV-2 Immunoglobulin and 5 NIBSC Anti-SARSCoV-2 Verification Panel for Serology Assays were used. Phase2 Clinical Study was carried out with an approval of Dr. Abdurrahman Yurtaslan Ankara Oncology Training and Research Hospital ethics committee. (Approval no: 2021-06/1231).

Table 2.2 Formulation of VLP vaccine for Phase 2 study.

1ml injection	**40 µg VLP + 600 µg Alum + 300 µg CpG ODN-K3**	**1st injection WT VLP (Day0)**	**2nd injection UK VLP (Day21)**

Table 2.3 Necessities to be a volunteer

Inclusions	Exclusions
Female and/or Male	-
Ages between 18-59	Ages under 18, above 59
Negative for SARS-COV2 PCR test	Positive for SARS-COV2 PCR test
Willingness	Reluctance
Body Mass Index (BMI) between 18-35 kg/m2.	Body Mass Index (BMI) under 18 or above 35 kg/m2.
Physical and psychological health	Unhealthiness

2.2.2. Peripheric Blood Mononuclear Cells (PBMCs) Isolation from Whole Blood

In K2 EDTA blood collection tubes (BD Biosciences, USA), averagely 5 ml of peripheral blood samples were collected from all volunteers. The blood samples were diluted with room temperature (RT) 1X DPBS (Biological Industries, Israel) at the same volume of blood (1:1 v/v). Into a separate 15 ml falcon tubes, 3:2 ratio of lymphocyte separation media (Capricorn Scientific, Germany) were prepared and 1:1 diluted blood sample were layered on top of it. Tightened falcons were centrifuged at 540xg for 30 minutes at which the deacceleration is zero to not damage the layer that will be formed by different cell types in the blood. 5 layers in the tube that was obtained were containing plasma, PBMCs, lymphocyte separation media, neutrophiles and red blood cells (RBCs) from upper to bottom, respectively. For this study, plasma samples were collected first with sterile Pasteur pipette and then PBMCs were taken from a blurred layer just above the lymphocyte seperation media into different 15 ml falcon tubes. Washing step have been performed to PBMC tubes by completing the tube volume using complete RPMI-1640 medium containing 2% FBS and centrifuge the tubes at 540xg for 10 minutes for twice. Afterwards, the cell pellets were resuspended in 1 ml of FBS and by using flow cytometry, the cell count has calculated. The cells were frozen as 1 ml in 2 ml cryovials at which maximum cell count should be 10M/ml into %10 DMSO/FBS solution. Frozen PBMC samples were collected at liquid nitrogen tanks. For plasma tubes, to get rid of exosomes and other small proteins, the tightened tubes were centrifuged at 1500xg for 10 min and the suspension formed in the tubes were collecting into a clean falcon tube

without touching the pellet formed at the bottom. For clean plasma suspension, snap freezing was performed by using liquid nitrogen and the frozen plasma samples were collected at -80 °C.

2.2.3. Cell Counting

10 µl of aliquot from 500 µl PBMC cell suspension was taken into 1.5 ml eppendorf tube that is filled with 990 µl RPMI 1640 medium to dilute the cells. From the cuvette 50 µl of diluted cells were analysed in Novocyte 3000 flow cytometer and gating was done to remove debris from living cells according to FSC and SSC positions in x and y axes, respectively. Then, dilution factor was calculated to reach the total number of living cells in 1 ml media cell suspension and multiplied by counted cell number in flow cytometry.

2.2.4. Serum Sample Separation

In SST blood collection tubes (BD Biosciences, USA), approximately 5 ml of blood samples were centrifuged at 2500xg for 10 min to separate serum samples thanks to the special gel structure at the bottom of the tube that causes a clear separation of blood cells and the related particles that can cause blood clotting in the bottom and remain a clear serum sample of the volunteer. Serum samples were aliquoted as maximum 500 µl in sterile 1.5 ml eppendorf tubes and stored at -80 °C.

2.2.5. Recombinant Protein Production

HEK293-FT human embryonic kidney cell line (Thermo, USA) was used for transfection of his-tagged pVitro2 S and pVitro1 N plasmids. After transfection, cells were incubated for 96-120 hours for protein secretion. Next, cell medium was collected and collected medium was centrifuged, filtered with 0.22 µm membrane and stored. For purification of his-tagged proteins. affinity chromatography method was used by the help of ÄKTA go fast protein liquid chromatography system (Cytiva, USA). The column that will be used was equilibrated and sample was applied and washed along His-Trap 1 mL pre-packed IMAC column (Cytiva, USA). By using imizadole buffer, elution step was

performed at fraction tubes to collect wanted his-tagged recombinant spike and nucleocapsid proteins. Further, desalting step was performed by using desalting column (Cytiva, U.S.A.) in order to remove imizadole buffer. Last buffer exchange was done by using D-PBS. Finally, protein presence was checked by recording A280 values and quantification of proteins was done by using BCA assay and protein presence was proved by SDS-PAGE Western Blotting and Silver Staining (See detailed information from Ipekoglu, E.M. 2021).

2.2.6. Preparation of SARS-C0V-2 VLP vaccine for animals

For animal experiments 6-8 weeks of female Balb/c mice were used in 3 different groups totally. These groups include 3 different forms of VLP (Wuhan, Alpha and Delta variants), 2 different doses (2.5 μg and 5 μg) with combination of two different doses of adjuvant (120 μg, 60 μg and 30 μg) formulation (Table 2.4).

Table 2.4 Formulation of VLP vaccine for pre-clinic animal study.

<table>
<tr><td>G1</td><td>Placebo</td><td></td><td></td><td></td></tr>
<tr><td rowspan="3">G2</td><td>2.5 μg VLP + 120 μg Alum + 60 μg CpG</td><td rowspan="3">1st injection WT VLP</td><td rowspan="3">2nd injection UK VLP</td><td rowspan="3">3rd injection UK VLP</td></tr>
<tr><td>5 μg VLP + 120 μg Alum + 60 μg CpG</td></tr>
<tr><td>5 μg VLP + 60 μg Alum + 30 μg CpG</td></tr>
</table>

For each group, 100 μl responsible formulation was injected subcutaneously as 7 replicates of mice and in total 28 mice were used in this experiment and placebo group had no injection as a control group. Each cage contained 7 mice that were vaccinated with same formulation. No mortality, difference in general posture, body weight changes and hyperthermia and/or hypothermia were observed in any animal during the study period.

2.2.7. Bleeding of Animals

After 2 weeks (Day14), first bleeding was performed. Next, second injection was applied to 3 groups of animals subcutaneously and at Day30 second bleeding was performed. Then, third bleeding was done at Day60. Afterwards, a third injection was applied to 3 groups of animals subcutaneously and two weeks after third injection, fourth bleeding was performed. All these bleeding procedures were done from the tail of the vein and the averagely 300 µl blood was collected in BD microtainer SST blood collection tubes. In order to separate clean sera from the tubes, samples were centrifuged at 2500xg for 10 minutes. Fresh sera were collected at 0.6 ml eppendorf tubes and stored at -20°C.

2.2.8. Enzyme Linked Immunosorbent Assay (ELISA)

2.2.8.1. Human IgG ELISA

Recombinant proteins were prepared in 1X DPBS as coating antibodies and each well of 2HB 96-well immunoplates were coated with 50 µl of coating antibodies. These antibodies and their working concentrations were listed in Table 2.1. Coated immunoplates were incubated for overnight at 4°C. Next day, 200 µl of blocking buffer that contains BSA (Capricorn, USA) to prevent adherence between plate and antibodies were filled to each well and the plates were incubated at room temperature for 2 hours. After blocking step, plates were washed with wash buffer for 4 times and distilled water for 2 times then dried. Serum samples of volunteers that will be studied for the ELISA procedure were collected and 6X serial dilution was followed for recombinant spike and nucleocapsid proteins and 4X serial dilution was followed for different variants of RBD proteins which were specific to wilt type, alpha and delta, in the plates starting from 1:100 up to 1:3600 and 1:6400, respectively as 50 µl for each well. The plates were incubated at 4°C for overnight. After incubation of serum samples, the plates were washed again as the same and dried. ALP-conjugated human-IgG solution (Southern Biotech, ABD) is diluted with blocking buffer up to 1:1000 and each well were filled with 50 µl of IgG solution and the incubation was started at room temperature for 2 hours. Afterwards, the plates were washed again as the same and dried. Lastly, p-nitrophenyl phosphate (PNPP) substrate (Thermo, ABD) was added as 50 µl to each well and the development of the

plates were recorded and in ten-minute intervals OD values were read at 405 nanometers in the ELISA reader (Molecular Devices, ABD) continuously.

2.2.8.2. Animal IgG ELISA

The initial steps of the procedure (coating, blocking and washing steps) were the same with human IgG ELISA and the differences in the concentrations were indicated in Table 2.1. Only blocking incubation time for animal IgG ELISA was 5 hours. For animal sera collected from the vein of the mice, 4X serial dilution was followed in the plates starting from 1:50 up to 1:819200 as 50 µl for each well. Incubation temperature and time were the same as human IgG ELISA. Next, the plate was washed like the same procedure mentioned above and dried. ALP-conjugated mouse-IgG solution (Southern Biotech, ABD) is diluted with blocking buffer up to 1:1000 and each well were filled with 50 µl of IgG solution and the incubation was started at room temperature for 2 hours. Afterwards, the plates were washed and dried again samely. Finally, PNPP substrate (Thermo, ABD) was added as 50 µl to each well and the development of the plates were recorded and in one hour intervals OD values were read at 405 nanometers in the ELISA reader (Molecular Devices, ABD) continuously.

2.2.9. Cytometric Bead Array (CBA)

In order to check T helper cytokine expression which is essential in immune response regulation, LEGENDplex™ Multi-Analyte Flow Assay Kit (BioLegend, USA) which is a bead-based immunoassay was used. This kit requires prior preparation of samples which was cell thawing of PBMC samples collected from Phase 2 volunteers regarding to 35th day after first vaccination and peptide layering. For this, previously freezed cells were thawed and they were rested in 2 ml 20% RPMI medium at CO_2 incubator in 37°C for 1 hour. Then, the cells were counted to reach the precise amount needed for assay by the help of Novocyte 3000 flow cytometer (ACEA Biosciences, USA) (See Section 2.2.3). Next, the V-bottom plate was layered by 2 ug/ml SMNO peptide pool (Mabtech, Sweden), rested cells were added (1M/well) and incubated at 37°C for 48 hours. After incubation period, supernatant was collected and centrifuged at 300 g for 5 minutes and according to manufacturer's instructions T helper cell responses were determined thanks to 12 different cytokines' (IL-2, IL4, IL5, IL6, IL9, IL10, IL13,

IL17A, IL17F, IL22, IFN-γ and TNF-α) quantification by LEGENDplex™ HU Th Cytokine Panel (12-plex) w/ VbP kit (Biolegend, USA). Firstly, reagent preparation was followed for beads, wash buffer and standards according to kit guideline and 25 µl assay buffer for each well of 96-well V bottom plate was filled. Then, into corresponding wells, 25 µl supernatant samples or 25 µl standard samples were added. Afterwards, mixed beads were vortexed well and added to each well as 25 µl. Aluminum foil covered into the plate to avoid light and incubation started for 2 hours on a plate shaker at 800 rpm. Following the incubation, V-bottom plate was centrifuged at 1050 rpm for 5 minutes and the plate was inverted to remove the supernatant immediately. The plate was washed twice with 200 µl/well 1X wash buffer provided by manufacturer. The plate was gently dried, then centrifuged at the same speed and time applied in previously. Detection antibody was added to the wells as 25 µl and after covering the plate with aluminum foil, incubation period started for 1 hour on plate shaker at 800 rpm. PE-conjugated streptavidin (SA-PE) was added to each well as 25 µl and incubated for 30 minutes with aluminum foil cover on top on a plate shaker at 800 rpm. Washing step was re-applied to the plate twice like previously. Finally, resuspension of beads was provided by 150 µl 1X wash buffer and reading was carried out on NovoCyte 3000 flow cytometer (ACEA Biosciences, USA). The results was analysed with LEGENDplex™ Data Analysis Software (Biolegend, USA).

2.2.10. Chemiluminescent Microparticle Immunoassay (CMIA)

Chemiluminescent microparticle immunoassay (CMIA) (Abbott, USA) was performed to detect neutralizing antibody levels found in the collected serum samples from the volunteers regarding to 0th, 21st, 35th, 49th, 90th day after first injection of vaccine against receptor binding domain (RBD) of S1 subunit. Quantification and qualification were provided by AdviseDx SARS-CoV-2 IgG II Quant assay by the help of ARCHITECT i System. Thanks to collaboration with DEREN Laboratory (Ankara, Turkey), the procedure was performed according to manufacturer's protocol. This automated and two-step immunoassay started with the incubation of serum samples from the volunteers (500 µl sera/person), SARS-CoV-2 antigen coated paramagnetic microparticles and assay diluent together to carry out binding of IgG antibodies found in sera with SARS-CoV-2 antigen coated microparticles. After a washing step, incubation

of anti-human IgG acridinium-labeled conjugate was performed and one more washing step followed. Pre-Trigger and Trigger Solutions are added for a reaction to record resulting chemiluminescent in a direct relationship between the amount of IgG to SARS-CoV-2 in sera. Positive values were determined based on 50.0 AU/ml cut off means that recordings above 50.0 AU/ml were accepted as positive in antibody production.

2.2.11. CoronaHunter IgG ELISA Kit (Matriks Biotek, Turkey)

IgG antibody production for determination of neutralizing capacity was provided by CoronaHunter Anti-SARS-CoV-2 Trimeric Spike IgG ELISA Kit (Matriks Biotek, Turkey). According to manufacturer's protocol, the following steps were performed. First of all, in a 96-well round bottom plate (Sarstedt, Germany), sera collected from volunteers were diluted in 1:100 ratio with the Assay Diluent provided by the kit. Next, 100 µl of Assay Diluent were distributed into all wells of spike protein coated 96-well plate provided by the kit and 20 µl of 1:100 diluted serum samples were distributed in the necessary wells of the previously coated plate in order to get a final concentration of 1:600 with the serum samples. Then, 20 µl of standard samples, low level controls and high-level controls were added into respective wells and the plate was covered with a adhesive foil and left for incubation at room temperature for 60 minutes. The microtiter plate was washed with 300 µl 1X Washing buffer for three times and dried. Afterwards, 100 µl of Conjugate provided by the kit was pipetted onto each well and after covering the plate with a foil, it was incubated for 30 minutes at room temperature. The plate was washed and dried as the same and 100 µl of Substrate solution was distributed to each well. The plate was left for incubation for 20 minutes at dark and room temperature. Lastly, the enzymatic reaction between conjugate and substrate was stopped by pipetting 100 µl of Stop solution into each well of the plate and by using ThermoMax microplate reader (Molecular Devices, USA), optical density (OD) values were recorded at 450 nm.

2.2.12. Statistical Analyses

To analyze statistical differences, GraphPad Prism 9 statistical software was used. Clinical human studies and pre-clinical animal studies were compared thanks to one-way ANOVA with Dunnett's multiple comparisons tests. The statistically significant values were determined as P value below 0.5.

CHAPTER 3

RESULTS

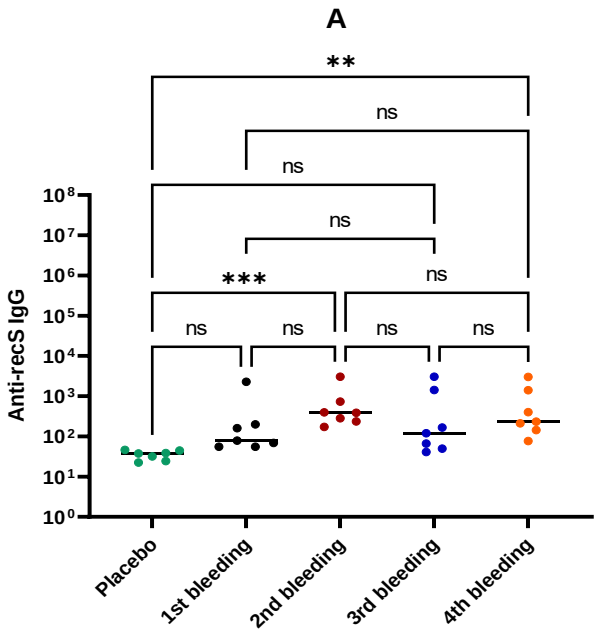
3.1. Pre-Clinical Studies

3.1.1. Humoral Immune Response in Animals against Wild-Type and Alpha Variants Combined VLP-58-1023-AL-K3 SARS-COV-2 Vaccine Formulations

Pre-clinical study is a major step to carry a vaccine candidate from laboratory to clinic with regard to approval of product safety and effectiveness in inducing immune response applying necessary immunological assays in animals (WHO, 2022). *In vivo* tests to determine doses of main product and adjuvants of vaccine candidate should be done before applying the vaccine to humans. At this point, we aimed to analyze 3 different combinations of our vaccine with different variant type of VLPs (WT and UK) and different doses of adjuvants in the formulation (See Table 2.4). We used 4 different cages that contain 7 replicas of female Balb/c mice which are placebo group with no injection as negative control group, group A with low dose (2.5 ug) VLP and high dose adjuvants, group B with high dose (5 ug) VLP and high dose adjuvants and group C with high dose (5 ug) VLP and low dose adjuvants. First doses are injected as WT VLP and second doses are injected as UK VLP for three cages (A, B, C). Additionally, all 3 groups with injections received a third dose (a second booster) which is formulated with UK VLP. Here we aimed to show that adapting our VLP product for last emerging variants over time, the efficacy of the vaccine can be improved. UK variant has many mutations which causes enhanced transmissibility and promoted virus entry, so that many vaccines have lost their efficacy against alpha variant [72]. In our vaccine we tried to reveal that having both WT and UK VLP variants will increase the protective immunity.

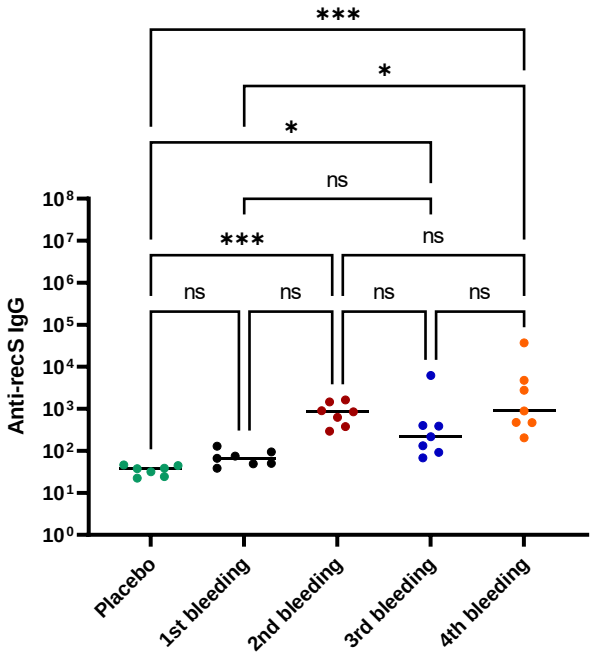
First of all, we would like to see is there any induced humoral immune response in the mice and bleeding from the mice tails was performed at regular time intervals after each injection. First bleeding was done after 2 weeks of first WT VLP formulated injections, second bleeding was done after 2 weeks of second UK VLP formulated injections, third bleeding was done after 2 months of second injection and lastly, fourth bleeding was done after 2 weeks of third UK VLP formulated injections.

We decided to check antibody levels against 5 recombinant proteins of SARS-CoV-2 which are different RBD variants, Spike and Nucleocapsid because of their highly antigenic capacity. In figure 3.1A and figure 3.1B, after the first booster (second bleeding) with a UK VLP formulation, high antibody production level against spike protein was observed when compared to first bleeding. After 2 months of first injection (3rd bleeding), humoral immune response decreased for most of the mice which is almost very close to negative placebo control group and a second booster was applied with UK VLP formulation. Lastly, antibody levels got well similar to seen in second bleeding. Surprisingly, in figure 3.1C, high dose VLP and low dose adjuvant showed a long term and efficient immune response against spike protein and even in 3rd bleeding high antibody levels were observed without any decrease. Over the three groups of animal vaccination, the formulation with high dose VLP and low dose adjuvant in group C is the most effective one.



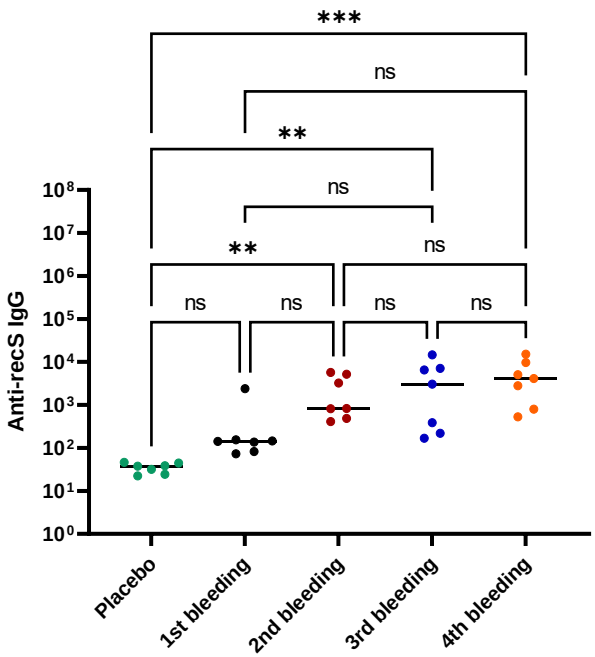
	Placebo	1st bleeding	2nd bleeding	3rd bleeding	4th bleeding
Geometric mean	1.531	2.153	2.656	2.294	2.567

B



	Placebo	1st bleeding	2nd bleeding	3rd bleeding	4th bleeding
Geometric mean	1.531	1.821	2.871	2.462	3.184

C

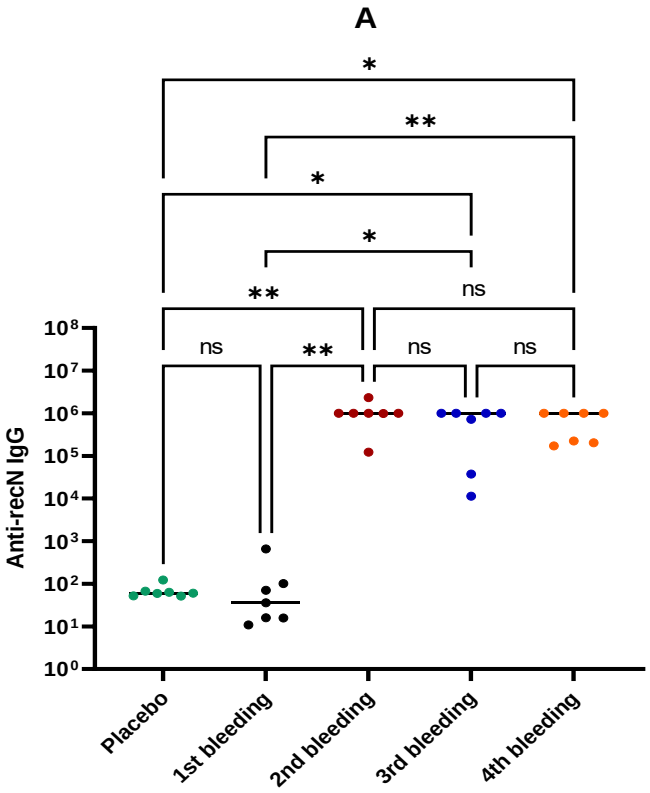


	Placebo	1st bleeding	2nd bleeding	3rd bleeding	4th bleeding
Geometric mean	1.531	2.257	3.158	3.210	3.508

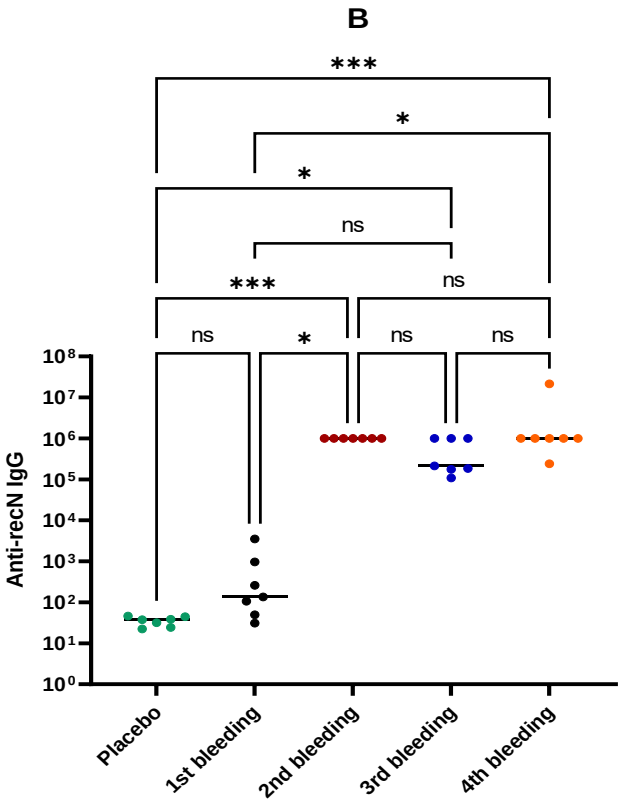
Figure 3.1. Antibody Production of female Balb/c mice against in house recombinant trimeric Spike Protein.

Titer dot graphs of animals in regular day intervals after injections of VLP-58-1023-AL-K3 vaccine (First bleeding is done after 2 weeks of first injection, second bleeding is done after 2 weeks of second injection, third bleeding is done after 2 months of second injection and fourth bleeding is done after 2 weeks of third injection) against Spike; 96-well 2HB maxi-binding ELISA plates were coated with 4 μg/ml in-house recombinant spike protein and plates were blocked. After the serial dilutions of volunteers' sera, ALP-tagged anti-mouse IgG secondary antibody were filled into wells and finally PNPP substrate was added into plate and optical density values were recorded. A) represents Group A which received low dose (2.5 μg) VLP but high dose adjuvants (2.5:120:60, VLP:Alum:CpG) B) represents Group B which received high dose (5 μg) VLP and high dose adjuvants (5:120:60, VLP:Alum:CpG) and C) represents Group C which received high dose (5 μg) VLP but low dose adjuvants (5:60:30, VLP:Alum:CpG), with the comparison of placebo negative control group without any injection. Geometric means of each group were indicated in the table below the figure. The comparison was done by one-way ANOVA with Dunnett's multiple comparisons test. P < .05, **P < .01, *P < .001, ***P < .0001.

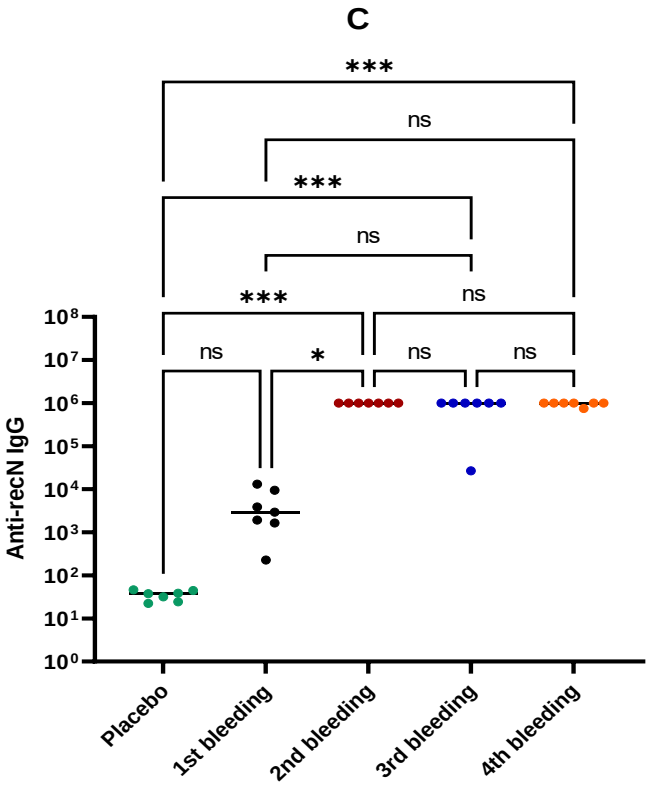
Overall, in figure 3.2, thanks to high binding affinity of recombinant nucleocapsid protein produced as a last batch in our laboratory, used in last two bleedings, high levels of non-neutralizing antibody levels were detected in animal IgG ELISA against nucleocapsid protein. As the same pattern in anti-spike animal IgG ELISA, in all groups (A, B and C) high levels of antibody titer showed in second bleeding and there was almost no decrease in third bleeding results. Beginning from second bleeding results, there was a non-significant change between the further bleedings. As the same as all animal results, after a second booster, fourth bleeding results were at the top.



	Placebo	1st bleeding	2nd bleeding	3rd bleeding	4th bleeding
Geometric mean	1.815	1.666	5.922	5.499	5.699



	Placebo	1st bleeding	2nd bleeding	3rd bleeding	4th bleeding
Geometric mean	1.531	2.327	6.000	5.553	6.102



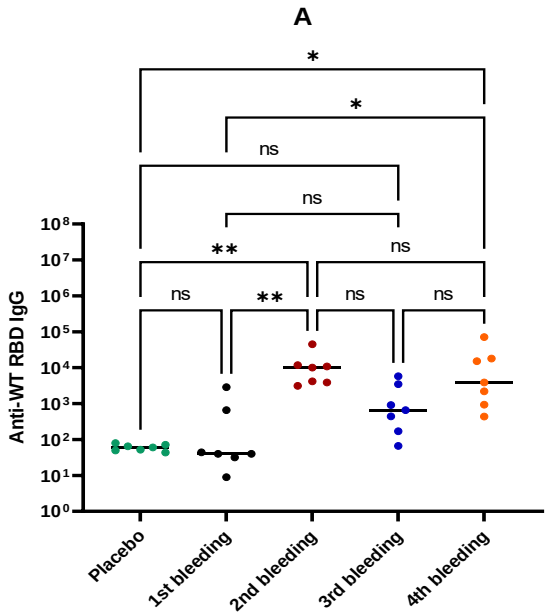
	Placebo	1st bleeding	2nd bleeding	3rd bleeding	4th bleeding
Geometric mean	1.531	3.429	6.000	5.775	5.982

Figure 3.2. Antibody Production of female Balb/c mice against in house recombinant Nucleocapsid Protein.

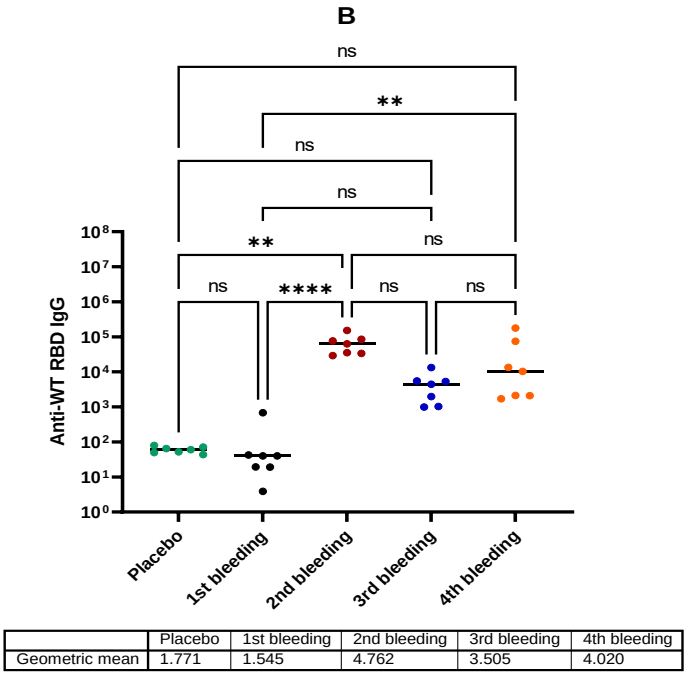
Titer dot graphs of animals in regular day intervals after injections of VLP-58-1023-AL-K3 vaccine (First bleeding is after 2 weeks of first injection, second bleeding is after 2 weeks of second injection, third bleeding is after 2 months of second injection and fourth bleeding is after 2 weeks of third injection) against Nucleocapsid; 96-well 2HB maxi-binding ELISA plates were coated with 1 µg/ml in-house recombinant nucleocapsid protein and plates were blocked. After the serial dilutions of volunteers' sera, ALP-tagged anti-mouse IgG secondary antibody were filled into wells and finally PNPP substrate was added into plate and optical density values were recorded. A) represents Group A which received low dose (2.5 µg) VLP but high dose adjuvants (2.5:120:60, VLP:Alum:CpG) B) represents Group B which received high dose (5 µg) VLP and high dose adjuvants (5:120:60, VLP:Alum:CpG) and C) represents Group C which received high dose (5 µg) VLP but low dose adjuvants (5:60:30, VLP:Alum:CpG), with the comparison of placebo negative control group without any injection. Geometric means of each group were indicated in the table below the figure. The comparison was done by one-way ANOVA with Dunnett's multiple comparisons test. P < .05, **P < .01, *P < .001, ***P < .0001.

After the investigation of neutralizing antibody levels by anti-spike IgG ELISA and non-neutralizing antibody levels by anti-nucleocapsid IgG ELISA, we want to further discover the neutralizing antibody titer levels with three different variant type of RBD proteins which includes the changes seen in alpha and delta variants in addition to authentic one. Because we included both WT and UK VLPs in our vaccine formulation, we checked antibodies against WT RBD and UK RBD. However, because of the potential of new variant emergences every day, and Delta variant is on the carpet lastly, we also want to check the efficacy of the vaccine against RBD protein includes delta mutations.

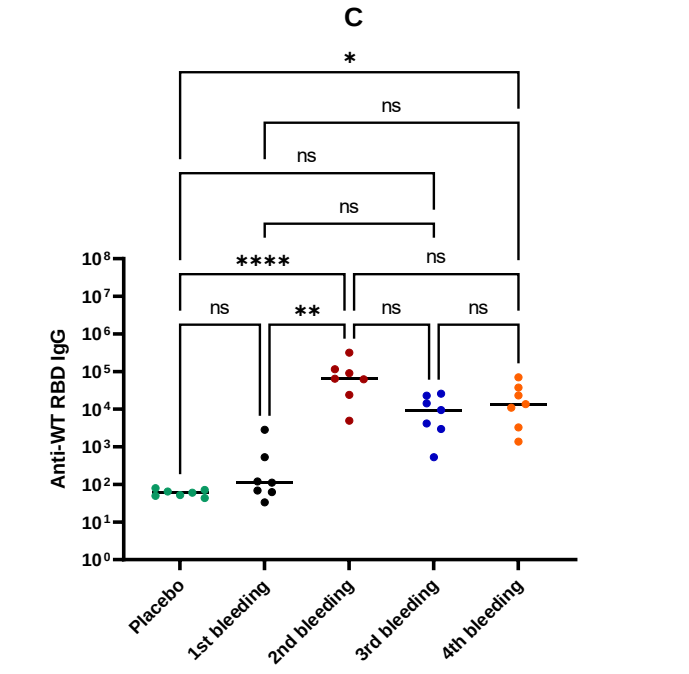
In figure 3.3, for all three A, B and C groups, second bleeding results were the maximum among all bleedings and there is a small decrease after 2 months of injection which indicates that there is a need for a third dose as the same as previous animal IgG ELISA results. After a second booster, antibody titers against WT RBD protein are getting higher, and reach very close levels of second bleeding results. Overall, it can be said that group C is the most effective formulation against WT RBD response.



	Placebo	1st bleeding	2nd bleeding	3rd bleeding	4th bleeding
Geometric mean	1.771	1.939	3.924	2.825	3.690



	Placebo	1st bleeding	2nd bleeding	3rd bleeding	4th bleeding
Geometric mean	1.771	1.545	4.762	3.505	4.020



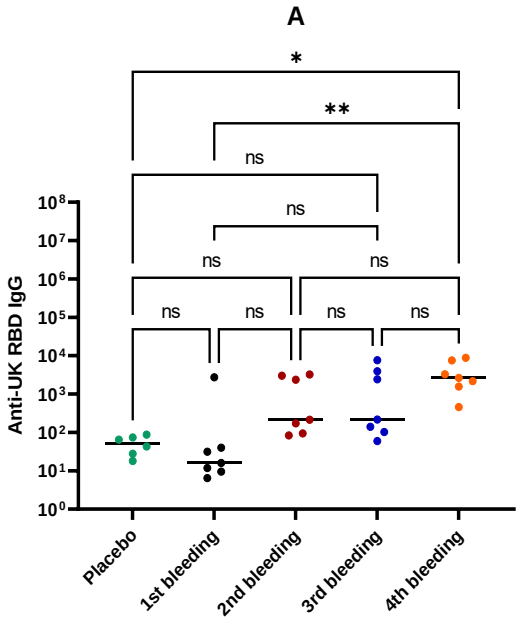
	Placebo	1st bleeding	2nd bleeding	3rd bleeding	4th bleeding
Geometric mean	1.771	2.209	4.743	3.817	4.086

Figure 3.3. Antibody Production of female Balb/c mice against in house recombinant WT RBD Protein

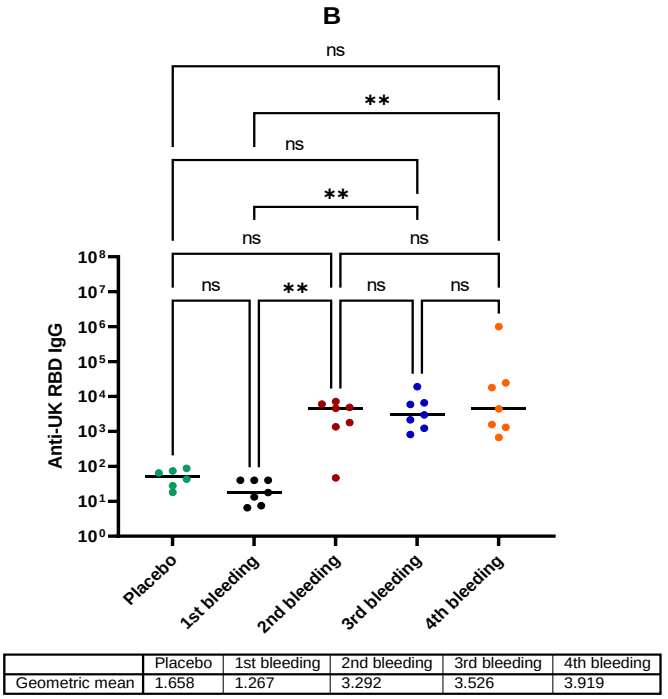
Titer dot graphs of animals in regular day intervals after injections of VLP-58-1023-AL-K3 vaccine (First bleeding is after 2 weeks of first injection, second bleeding is after 2 weeks of second injection, third bleeding is after 2 months of second injection and fourth bleeding is after 2 weeks of third injection) against WT RBD; 96-well 2HB maxi-binding ELISA plates were coated with 4 µg/ml in-house recombinant WT RBD protein and plates were blocked. After the serial dilutions of volunteers' sera, ALP-tagged anti-mouse IgG secondary antibody were filled

into wells and finally PNPP substrate was added into plate and optical density values were recorded. A) represents Group A which received low dose (2.5 µg) VLP but high dose adjuvants (2.5:120:60, VLP:Alum:CpG) B) represents Group B which received high dose (5 µg) VLP and high dose adjuvants (5:120:60, VLP:Alum:CpG) and C) represents Group C which received high dose (5 µg) VLP but low dose adjuvants (5:60:30, VLP:Alum:CpG), with the comparison of placebo negative control group without any injection. Geometric means of each group were indicated in the table below the figure. The comparison was done by one-way ANOVA with Dunnett's multiple comparisons test. P < .05, **P < .01, *P < .001, ***P < .0001.

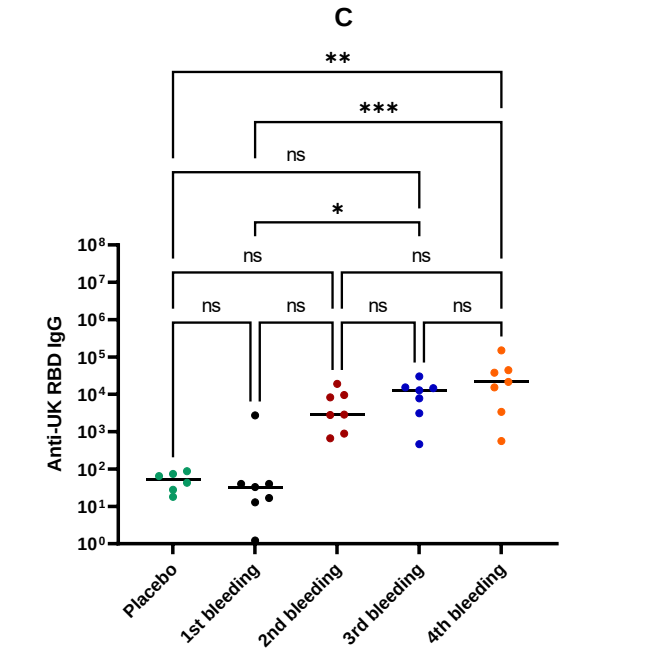
In figure 3.4A and 3.4B, antibody titers after first bleeding are as low as placebo group as expected. However, there is an increase after a first booster dose which is belong to second bleeding. Third bleeding and second bleeding levels were very similar. Lastly, the highest humoral immune response is belonged to fourth bleeding after a second booster dose in group A and group B. In figure 3.4C, the maximum effect in antibody production is seen after a third dose however high dose VLP and low dose adjuvant formulation indicated that longer term production before a third dose is showed. Thanks to this data we revealed that using UK VLP as a third dose, we obtained effective and long-term antibody production against UK RBD.



	Placebo	1st bleeding	2nd bleeding	3rd bleeding	4th bleeding
Geometric mean	1.658	1.515	2.689	2.732	3.422



	Placebo	1st bleeding	2nd bleeding	3rd bleeding	4th bleeding
Geometric mean	1.658	1.267	3.292	3.526	3.919



	Placebo	1st bleeding	2nd bleeding	3rd bleeding	4th bleeding
Geometric mean	1.658	1.511	3.551	3.857	4.171

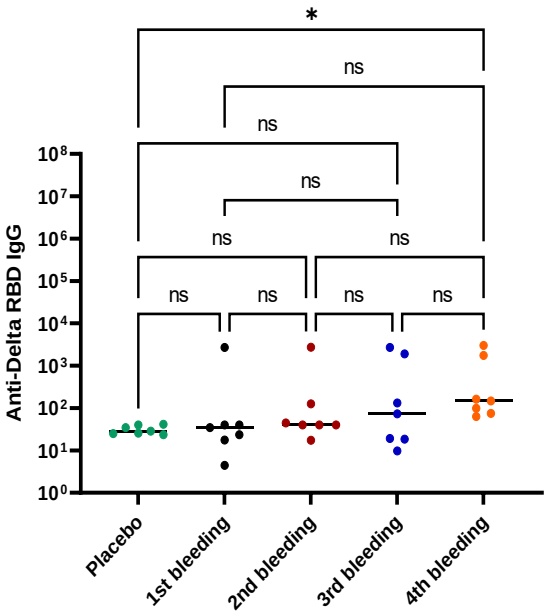
Figure 3.4. Antibody Production of female Balb/c mice against commercial recombinant UK RBD Protein

Titer dot graphs of animals in regular day intervals after injections of VLP-58-1023-AL-K3 vaccine (First bleeding is after 2 weeks of first injection, second bleeding is after 2 weeks of second injection, third bleeding is after 2 months of second injection and fourth bleeding is after 2 weeks of third injection) against UK RBD; 96-well 2HB maxi-binding ELISA plates were

coated with 1 μg/ml commercial recombinant UK RBD protein and plates were blocked. After the serial dilutions of volunteers' sera, ALP-tagged anti-mouse IgG secondary antibody were filled into wells and finally PNPP substrate was added into plate and optical density values were recorded. A) represents Group A which received low dose (2.5 μg) VLP but high dose adjuvants (2.5:120:60, VLP:Alum:CpG) B) represents Group B which received high dose (5 μg) VLP and high dose adjuvants (5:120:60, VLP:Alum:CpG) and C) represents Group C which received high dose (5 μg) VLP but low dose adjuvants (5:60:30, VLP:Alum:CpG), with the comparison of placebo negative control group without any injection. Geometric means of each group were indicated in the table below the figure. The comparison was done by one-way ANOVA with Dunnett's multiple comparisons test. P < .05, **P < .01, *P < .001, ***P < .0001.

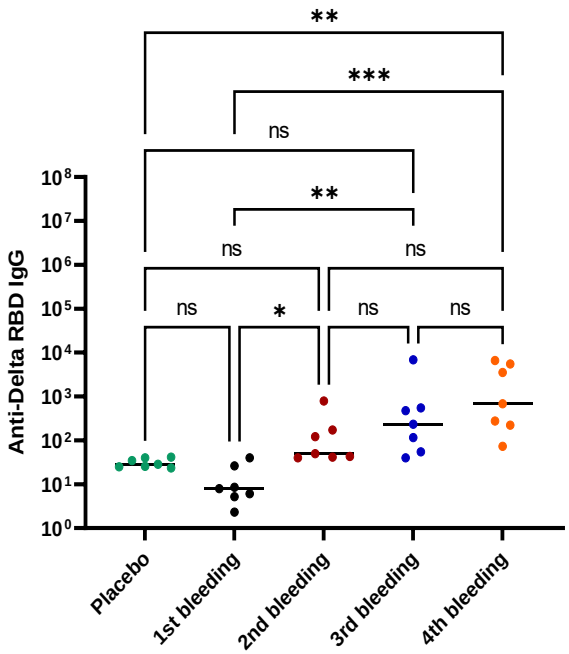
In figure 3.5, no significant decrease was observed after two months of first injection (3rd bleeding) for all three A, B and C groups which made us believe that including UK VLP in our vaccine formulation can be more effective and long-term against other potential variants just like the Delta variant. Nevertheless, the highest antibody levels against Delta RBD protein are belonged to fourth bleeding which proves the effect of third dose similar to other pre-clinical data. The importance of the true dosage and the formulation has well-seen from this result. The lowest antibody production is observed from all bleeding results with the low dose VLP and low dose adjuvant formulation of group A which indicates it is the less effective combination. Also, highest antibody titer levels are seen from all bleeding results with the high dose VLP and low dose adjuvant combination of group C which shows it is the most effective formulation. Figure 3.5 also proves that there is a significant protection against Delta RBD which says our vaccine formulation of group C can be even protective for B.1.1.7 mutation emerged in UK and very common all over the world in these days.

A

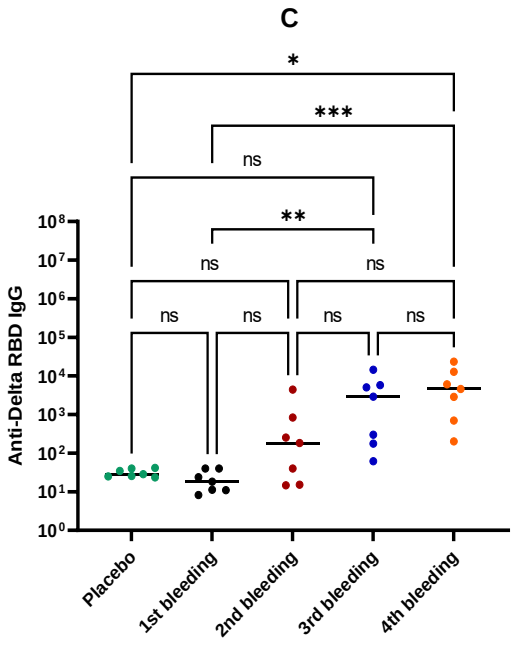


	Placebo	1st bleeding	2nd bleeding	3rd bleeding	4th bleeding
Geometric mean	1.484	1.634	1.889	2.033	2.396

B



	Placebo	1st bleeding	2nd bleeding	3rd bleeding	4th bleeding
Geometric mean	1.484	0.9586	1.967	2.430	2.941



	Placebo	1st bleeding	2nd bleeding	3rd bleeding	4th bleeding
Geometric mean	1.484	1.263	2.170	3.086	3.505

Figure 3.5. Antibody Production of female Balb/c mice against commercial recombinant Delta RBD Protein

Titer dot graphs of animals in regular day intervals after injections of VLP-58-1023-AL-K3 vaccine (First bleeding is after 2 weeks of first injection, second bleeding is after 2 weeks of second injection, third bleeding is after 2 months of second injection and fourth bleeding is after 2 weeks of third injection) against Delta RBD; 96-well 2HB maxi-binding ELISA plates were coated with 1 µg/ml commercial recombinant Delta RBD protein and plates were blocked. After the serial dilutions of volunteers' sera, ALP-tagged anti-mouse IgG secondary antibody were filled into wells and finally PNPP substrate was added into plate and optical density values were recorded. A) represents Group A which received low dose (2.5 µg) VLP but high dose adjuvants (2.5:120:60, VLP:Alum:CpG) B) represents Group B which received high dose (5 µg) VLP and high dose adjuvants (5:120:60, VLP:Alum:CpG) and C) represents Group C which received high dose (5 µg) VLP but low dose adjuvants (5:60:30, VLP:Alum:CpG), with the comparison of placebo negative control group without any injection. Geometric means of each group were indicated in the table below the figure. The comparison was done by one-way ANOVA with Dunnett's multiple comparisons test. P < .05, **P < .01, *P < .001, ***P < .0001.

Overall, pre-clinical studies elucidated us with regard to most effective doses of VLP and adjuvant combination to use it in clinical studies at humans. These data proved that high dose VLP combination with low doses of adjuvants (Group C) showed longer term production after the first dose of vaccine injection and overall highest antibody titers in most of the bleedings were observed in group C.

3.2. Clinical Studies

3.2.1. Humoral Immune Response in Phase-2 Clinical Trial Volunteers against Wild-Type and Alpha Combined VLP-58-1023-AL-K3 SARS-COV-2 Vaccine

In novel VLP vaccine strategy, rather than targeting only spike protein, more than one structural and non-structural proteins are targeted in the same formulation. In our VLP-58-1023-AL-K3 vaccine, 4 main structural proteins of SARS-CoV2 are in the main goal that includes S, N, M and E proteins. Moreover, there are several different variants emerging over time which decreases efficacy in most of the current vaccine candidates. In our previous pre-clinical studies (Section 3.1.1.), we tried to show boosting with a different variant (WT and UK) of SARS-CoV2 VLP is going to trigger immune system strongly and provide an efficient and long-term immunity against the virus by the help of right formulation. At that point, we formulated our vaccine with almost ten times more amount of VLP, Alum and CpG for human injections. The formulation can be seen from Table 2.2. However, as seen in every vaccine formulation, even though the complete protection is expected after the vaccination, it is possible to become infected even after two doses of vaccine injection. In this case it is expected to see asymptomatic and mild cases. After our vaccination, there is no mortality in the infected volunteers and the symptoms are mild. The list of the infected volunteers was showed in Table 3.1.

Because spike and nucleocapsid proteins have antigenic property in the viral structure of SARS-CoV-2 to produce a humoral immune response in the body, we decided to check antibody production at regular time intervals (Day0, Day21, Day35, Day49 and Day90) of Phase 2 volunteers against in house recombinant trimeric Spike (Figure 3.6), in house recombinant Nucleocapsid (Figure 3.7) and different commercial RBD variant (Wild-Type RBD (Figure 3.8A), Alpha RBD (Figure 3.8B) and Delta RBD (Figure 3.8C)) proteins by using Enzyme Linked Immunosorbent Assay (ELISA) (See 2.2.8). Because we run out of RBD recombinant proteins, we were not able to run Day0 samples for RBD variants in ELISA procedures. In Figure 3.6, recombinant spike protein that we produced (Section 2.2.5) was used as coating antibody in order to see humoral response against spike viral protein in volunteers. Figure 3.6A includes all the volunteers even he had COVID-19 infection once and Figure 3.6B excludes these infected volunteers. In here we aimed to prove a concept that including COVID-19 infected volunteer in our data does

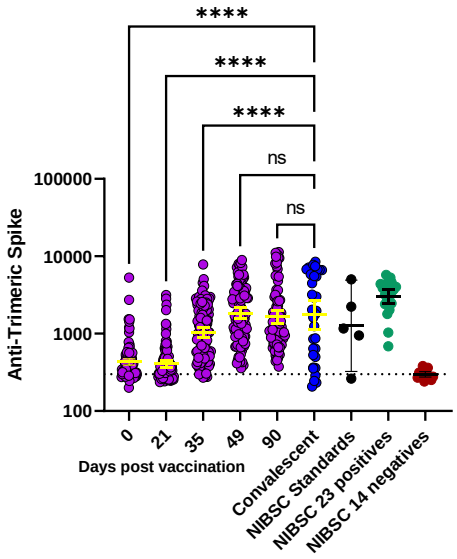
not affect our vaccine efficacy and very close geometric means are obtained in antibody production.

Overall, in Figure 3.6, NIBSC standards and convalescent samples were added to the ELISA plates for comparison. 5 NIBSC standards include 20/150 (high), 20/148 (mid), 20/144 (low anti-S, high anti-N), 20/140 (low) and 20/142 (negative) human plasma. 37 NIBSC convalescent plasma include 23 positive and 14 negative samples. Additionally, 35 convalescent sera (Marmara University, Istanbul, Turkey) were included. When viewed averagely, 21 days after first (wild type) injection, area under the curve (AUC) results are only in the above of negative threshold. However, after 2 weeks (Day35) of booster injection with alpha variant, AUC results are highly increased. Even in Day49 and Day90, average antibody production is almost reached the average level obtained in the 35 convalescent sera and no negative values obtained in both Day35, Day49 and Day90. Individual OD value graphs were indicated in Appendix 2.

Table 3.1. Codes of COVID-19 Infected Phase2 volunteers and their infection dates after the first injection

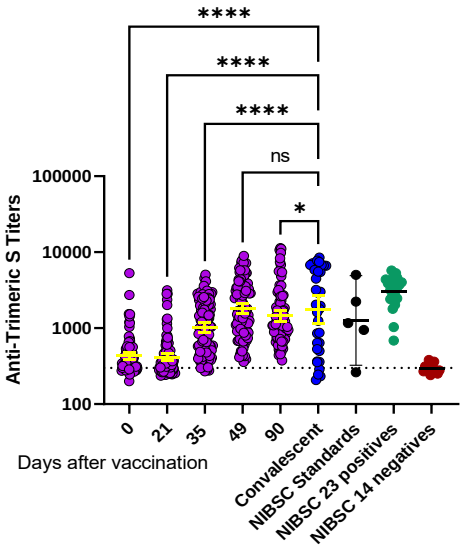
Volunteer Code	Infection Day after first injection
1010061	Day79
1010099	Day68
1010223	Day98
1010235	Day53
1010274	Day57
1020023	Day91
1030023	Day8
1030063	Day92
1030070	Day84
1030098	Day56

A



	0	21	35	49	90	Convalescent	NIBSC Standards	NIBSC 23 positives	NIBSC 14 negatives
Number of values	114	112	112	106	99	35	5	23	14
Geometric mean	430.7	411.0	1046	1843	1643	1756	1264	3015	297.4
Geometric SD factor	1.649	1.722	2.235	2.329	2.507	3.485	2.987	1.663	1.146
Lower 95% CI of geo. mean	392.5	371.3	899.8	1566	1368	1143	324.8	2420	274.9
Upper 95% CI of geo. mean	472.6	455.1	1216	2169	1973	2696	4919	3756	321.8

B



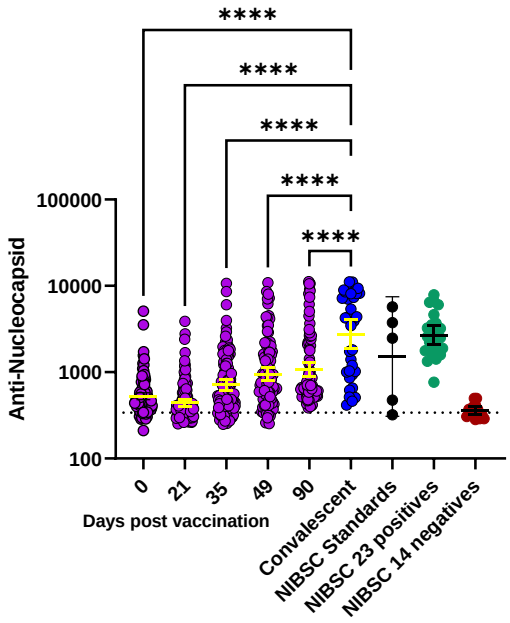
	0	21	35	49	90	Convalescent	NIBSC Standards	NIBSC 23 positives
Number of values	114	111	111	106	93	35	5	23
Geometric mean	430.7	412.7	1027	1804	1466	1756	1264	3015
Geometric SD factor	1.649	1.723	2.192	2.307	2.284	3.485	2.987	1.663
Lower 95% CI of geo. mean	392.5	372.6	886.3	1536	1237	1143	324.8	2420
Upper 95% CI of geo. mean	472.6	457.2	1191	2120	1737	2696	4919	3756

Figure 3.6. Antibody Production of Phase 2 volunteers against in house recombinant trimeric Spike Protein.

Collective dot graphs of A) all Phase2 volunteers and B) excluded volunteers who have COVID-19 infected, in regular day intervals after first injection of VLP-58-1023-AL-K3 vaccine (0,21,35,49,90) against spike with the comparison of convalescents sera, NIBSC Standards and

NIBSC convalescent plasma samples (positive and negative plasma); 96-well 2HB maxi-binding ELISA plates were coated with 6 µg/ml in-house recombinant spike protein and plates were blocked. After the serial dilutions of volunteers' sera, ALP-tagged anti-human IgG secondary antibody were filled into wells and finally PNPP substrate was added into plate and optical density values were recorded at 405 nm. Number of values and statistical values were indicated in the table below the figure. The comparison was done by one-way ANOVA with Dunnett's multiple comparisons test. P < .05, **P < .01, *P < .001, ***P < .0001.

In Figure 3.7, recombinant nucleocapsid, produced (Section 2.2.5) in house, was used as coating antibody to detect non-neutralizing antibody production in volunteers against nucleocapsid structural protein. As the same as Spike ELISA (Figure 3.6), 5 NIBSC standards, 35 convalescent serum samples and 37 NIBSC convalescent plasma were added to the ELISA plates. In average, Day21 AUC results were closely related with negative threshold. Successfully, in Day35 after booster injection with alpha variant, AUC results are increased but not as much as spike protein because nucleocapsid detection is highly sensitive [73] and the batch that was produced was impure when compared to pre-clinical studies. Even in Day49 and Day90, average antibody production levels are getting increased but stayed moderate. Individual OD value graphs were indicated in Appendix 2.



	0	21	35	49	90	Convalescent	NIBSC Standards	NIBSC 23 positives	NIBSC 14 negatives
Number of values	114	112	112	106	99	35	5	23	14
Geometric mean	526.4	439.2	716.4	948.5	1069	2770	1519	2668	357.5
Geometric SD factor	1.636	1.665	2.198	2.396	2.584	3.054	3.610	1.793	1.200
Lower 95% CI of geo. mean	480.5	399.2	618.2	801.6	884.3	1887	308.5	2073	321.8
Upper 95% CI of geo. mean	576.8	483.2	830.2	1122	1291	4064	7476	3434	397.2

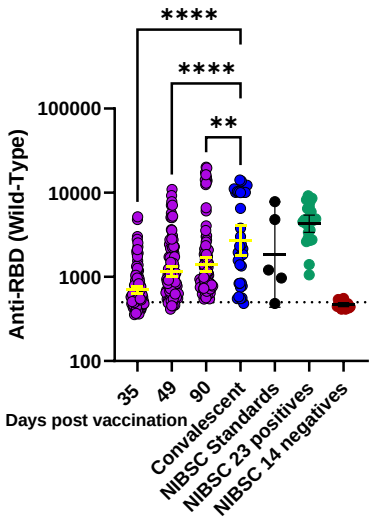
Figure 3.7. Antibody Production of Phase 2 volunteers against in house recombinant Nucleocapsid Protein.

Collective dot graphs of Phase2 volunteers in regular day intervals after first injection of VLP-58-1023-AL-K3 vaccine (0,21,35,49,90) against nucleocapsid with the comparison of convalescents sera, NIBSC Standards and NIBSC convalescent plasma samples (positive and negative plasma). 96-well 2HB maxi-binding ELISA plates were coated with 4 µg/ml in-house recombinant nucleocapsid protein and plates were blocked. After the serial dilutions of volunteers' sera, ALP-tagged anti-human IgG secondary antibody were filled into wells and finally PNPP substrate was added into plate and optical density values were recorded at 405 nm. Number of values and statistical values were indicated in the table below the figure. The comparison was done by one-way ANOVA with Dunnett's multiple comparisons test. P < .05, **P < .01, *P < .001, ***P < .0001.

In Figure 3.8, all the same comparative samples were used as same as Figure 3.6 and 3.7. Overall, commercial wild-type RBD recombinant protein (Figure 3.8A), commercial alpha RBD recombinant protein (Figure 3.8B) and commercial delta RBD recombinant protein (Figure 3.8C) were used to detect antibodies against them produced in Phase 2 volunteers.

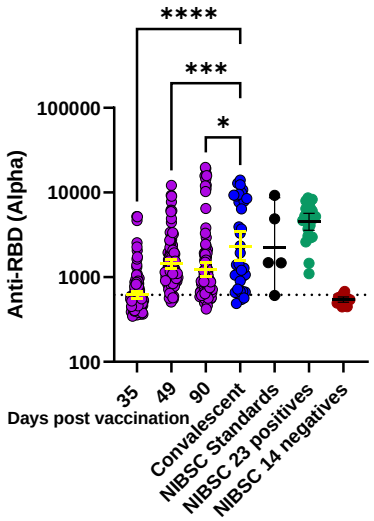
In figure 3.8A, in all time intervals moderate levels of antibody production is observed. Especially at Day90, there is even no negative values for volunteers. In antibody titer levels against RBD UK protein (Figure 3.8B), the average levels got closer to positive control convalescent group thanks to effect of UK VLP used in our vaccine formulation. Additionally, even delta variant mutations have differences when compared to alpha variant, non-significant differences are observed between positive control group and Day90 samples (Figure 3.8.C). It reveals that using two different combinations of VLP variants showed an efficacy against Delta variant. Overall, of anti-RBD data, starting from Day35, activation of humoral immunity increased against each type of RBD recombinant proteins, and AUC results reached the maximum at Day90. Individual OD value graphs were indicated in Appendix 2.

A



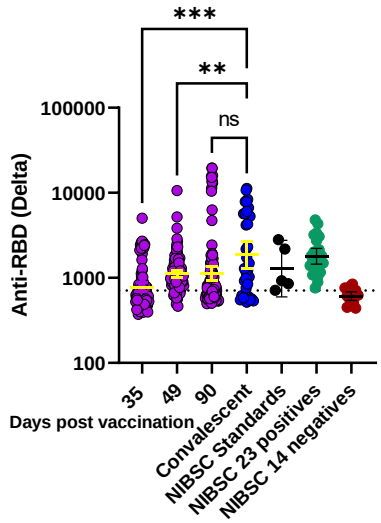
	35	49	90	Convalescent	NIBSC Standards	NIBSC 23 positives	NIBSC 14 negatives
Number of values	112	106	99	35	5	23	14
Geometric mean	704.3	1152	1418	2719	1843	4282	466.8
Geometric SD factor	1.728	2.139	2.606	3.235	3.198	1.726	1.099
Lower 95% CI of geo. mean	635.7	994.8	1171	1817	435.2	3382	441.9
Upper 95% CI of geo. mean	780.2	1333	1716	4070	7807	5421	493.1

B



	35	49	90	Convalescent	NIBSC Standards	NIBSC 23 positives	NIBSC 14 negatives
Number of values	112	106	99	35	5	23	14
Geometric mean	619.8	1436	1236	2325	2270	4514	542.4
Geometric SD factor	1.717	1.990	2.625	3.193	2.940	1.700	1.135
Lower 95% CI of geo. mean	560.2	1258	1020	1560	594.9	3589	504.3
Upper 95% CI of geo. mean	685.8	1640	1498	3465	8661	5677	583.5

C



	35	49	90	Convalescent	NIBSC Standards	NIBSC 23 positives	NIBSC 14 negatives
Number of values	112	106	99	35	5	23	14
Geometric mean	777.8	1116	1125	1874	1283	1795	609.6
Geometric SD factor	1.859	1.631	2.684	2.884	1.852	1.636	1.231
Lower 95% CI of geo. mean	692.5	1016	924.3	1303	596.6	1451	540.6
Upper 95% CI of geo. mean	873.6	1226	1370	2697	2758	2221	687.4

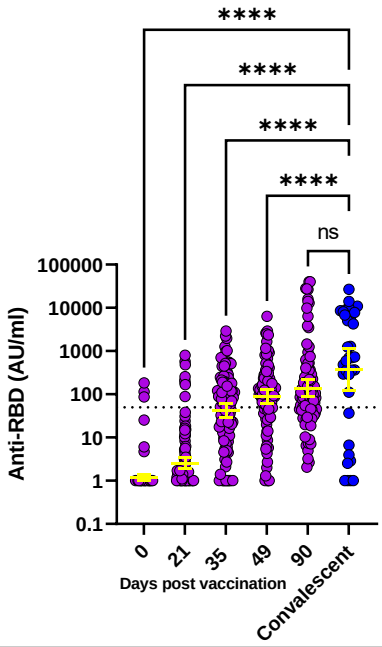
Figure 3.8. Antibody production of Phase 2 volunteers against commercial recombinant proteins of RBD variants.

Collective dot graphs of Phase2 volunteers in regular day intervals after first injection of VLP-58-1023-AL-K3 vaccine (35,49,90) against A) wild-type RBD, B) alpha RBD and C) delta RBD with the comparison of convalescents sera, NIBSC Standards and NIBSC convalescent plasma

samples (positive and negative plasma); Each 96-well 2HB maxi-binding ELISA plate was coated with 1 μg/ml commercial recombinant RBD variant proteins and plates were blocked. After the serial dilutions of volunteers' sera, ALP-tagged anti-human IgG secondary antibody were filled into wells and finally PNPP substrate was added into plate and optical density values were recorded at 405nm. Number of values and statistical values were indicated in the table below the figure. The comparison was done by one-way ANOVA with Dunnett's multiple comparisons test. P < .05, **P < .01, *P < .001, ***P < .0001.

In collaboration with an accredited laboratory (Deren Laboratory, Ankara, Turkey) for further validation, neutralizing antibody levels were recorded by using Abbott Kit with ARCHITECT i System (See Section 2.2.10) and antibody levels against trimeric spike recombinant protein were additionally checked by using CoronaHunter Spike-IgG ELISA Kit (See Section 2.2.11). In Figure 3.9, AU/ml results obtained from Abbott Kit were showed. According to manufacturer's protocol, results under the value of 50 are counted as negative. Based on this value, positive averages are belonged to Day49 and Day90. When compared to Day0 results of the Abbott Kit, antibody titer values increased significantly. In Figure 3.10, ng/ml results were obtained from CoronaHunter Spike-IgG ELISA Kit and it is seen that after the second injection, there is no significant difference between average values of Day35, Day49 and Day90 when compared to average of convalescent sera. Almost all of the volunteers, positive antibody productions were observed above the threshold.

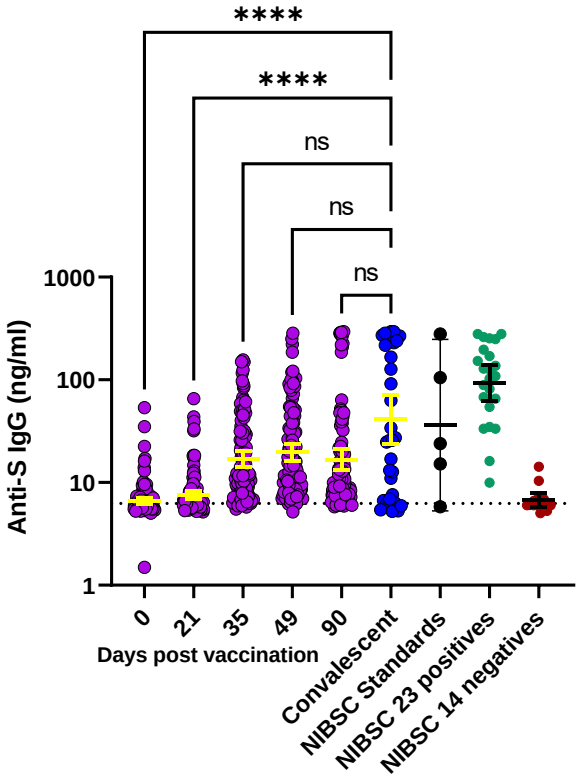
In conclusion, all of these data, that indicate antibody levels against Spike, Nucleocapsid and three different RBD variants with further investigations of two different kits for neutralization, showed a positive antibody production against SARS-CoV-2 essential structural proteins. We hypothesized that positive humoral response will successfully activate innate immune compartment and will help to induce cellular immunity.



	0	21	35	49	90	Convalescent
Number of values	112	113	114	102	99	35
Geometric mean	1.206	2.540	41.77	87.99	138.9	367.4
Geometric SD factor	2.357	5.025	7.556	6.603	8.730	26.71
Lower 95% CI of geo. mean	1.027	1.880	28.70	60.73	90.18	118.9
Upper 95% CI of geo. mean	1.416	3.432	60.79	127.5	214.0	1136

Figure 3.9. Neutralizing antibody levels of Phase 2 volunteers against RBD protein by Abbott Kit (Deren Laboratory, Ankara, Turkey).

Collective dot graphs of Phase2 volunteers in regular day intervals after first injection of VLP-58-1023-AL-K3 vaccine (21,35,49,90) against RBD recombinant protein with the comparison of convalescents sera; 500 µl from each volunteer sera were incubated with RBD-specific paramagnetic coating microparticle and assay diluent. Next, incubation of anti-human IgG acridinium-labeled conjugate and Pre-Trigger and Trigger solutions were applied. Lastly, chemiluminescent results were recorded. Number of values and statistical values were indicated in the table below the figure. The comparison was done by one-way ANOVA with Dunnett's multiple comparisons test. P < .05, **P < .01, *P < .001, ***P < .0001.



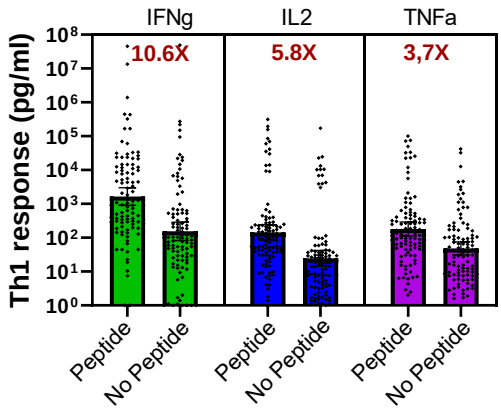
	0	21	35	49	90	Convalescent	NIBSC Standards	NIBSC23 positives	NIBSC 14 negatives
Geometric mean	6.651	7.623	16.98	19.68	16.73	41.35	36.15	92.78	6.768
Geometric SD factor	1.468	1.589	2.533	2.658	3.211	4.945	4.700	2.511	1.316
Lower 95% CI of geo. mean	6.198	6.995	14.29	16.29	13.29	23.88	5.293	62.31	5.775
Upper 95% CI of geo. mean	7.138	8.307	20.17	23.78	21.06	71.61	247.0	138.1	7.931

Figure 3.10 Antibody Production of Phase 2 volunteers against trimeric Spike protein by CoronaHunter Kit (Matriks Biotek, Ankara, Turkey).

Collective dot graphs of Phase2 volunteers in regular day intervals after first injection of VLP-58-1023-AL-K3 vaccine (0,21,35,49,90) against spike with the comparison of convalescents sera, NIBSC Standards and NIBSC convalescent plasma samples (positive and negative plasma); Pre-coated plates with recombinant trimeric Spike protein were filled with 1:600 diluted sera of volunteers. HRP-tagged anti-human IgG conjugate was filled into wells and finally TMB substrate was added into plate and optical density values were recorded at 450 nm. Number of values and statistical values were indicated in the table below the figure. The comparison was done by one-way ANOVA with Dunnett's multiple comparisons test. P < .05, **P < .01, *P < .001, ***P < .0001.

3.2.2. Cellular Immune Response in Phase-2 Clinical Trial Volunteers against Wild-Type and Alpha Combined VLP-58-1023-AL-K3 SARS-COV-2 Vaccine

Targeting strong cellular immunity is a key point for a vaccine design and long-term efficacy of humoral response. Almost 30% of CD4+ T cell response and activation of some non-structural proteins against SARS-CoV2, as showed in convalescent serum samples from recovered SARS-CoV2 patients, occurred by M and N proteins of the virus. Additionally, SARS-CoV2 CD8+ T cell response accounts for almost 30% of spike protein, 15% of nucleocapsid protein and 20% of membrane protein [74]. Because our vaccine contains both S, N, M and E proteins of the virus, we expected to see strong T cell response. Additional to this, adjuvants used in our formulation provide a tendency to produce Th1-skewed cellular immune milieu (See Figure 1.10), we aimed to show that strong Th1 response is produced additional to Th2, Th17 and Treg responses. A wide-range peptide pool (S, N, M, O) was used to trigger T helper cell responses in the Phase 2 volunteers PBMCs and the results were compared between with and without peptide pool stimulation by using 12 different cytokines which are IL-2, IL4, IL5, IL6, IL9, IL10, IL13, IL17A, IL17F, IL22, IFN-γ and TNF-α (See Section 2.2.9). Day35 samples of the volunteers were studied in whole assay. In Figure 3.11, IFN-γ secretion from PBMCs of Phase 2 volunteers showed a significant increase about 10.6-fold after peptide stimulation. And so on, IL-2 and TNF-α showed almost 6-fold and 4-fold increases, respectively. The increase in three of them showed strong Th1 response to S, N, M, O peptide pool.



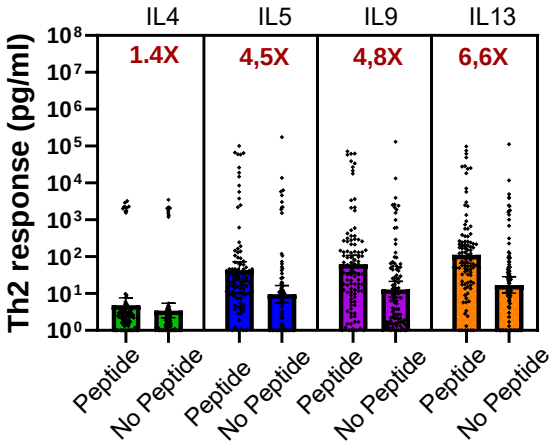
	IFNg		IL2		TNFa	
	A:1	A:2	B:1	B:2	C:1	C:2
Number of values	101	101	101	101	101	101
Geometric mean	1649	154.4	143.7	24.67	179.7	48.37
Geometric SD factor	20.70	23.27	13.50	14.30	11.08	9.531
Lower 95% CI of geo. mean	906.9	82.93	85.94	14.59	111.8	30.99
Upper 95% CI of geo. mean	3000	287.3	240.2	41.72	288.9	75.48

Figure 3.11. Th1 responses of Phase 2 volunteers before and after stimulation of S, N, M, O peptide pool

Column graphs of Phase2 volunteers to show cytokine production of IFN-γ, IL-2 and TNF-α in Th1 response. Half of the V-bottom plate was layered by 2 µg/ml SMNO peptide pool (Mabtech, Sweden) and into all wells 1 M/well PBMCs of the Phase 2 volunteers were added for an incubation step at 37°C for 48 hours. Collected supernatant was further studied according to manufacturer's instructions (LEGENDplex™ HU Th Cytokine Panel (12-plex) w/ VbP kit, Biolegend, USA). The results were analysed with LEGENDplex™ Data Analysis Software (Biolegend, USA). 'Peptide' indicates values after stimulation of PBMCs with SNMO peptide pool and 'No Peptide' indicates values with no stimulation but only resting of PBMCs. X values above each group of columns indicates ratio of increase after peptide pool stimulation. Number of values and statistical values were indicated in the table below the figure.

In Figure 3.12, IL-5, IL-9 and IL-13 production in PBMCs of Phase 2 volunteers showed a significant increase about 4.5-fold, 4.8-fold and 6,6-fold, respectively after peptide stimulation. Additionally, IL-4 showed a low increase about 1.5-fold. The increase in four of them showed an additional support of Th2 response to S, N, M, O peptide pool but not as much as Th1 response in total.

In Figure 3.13A, IL-6 production is almost remained the same before and after peptide stimulation. Furthermore, Figure 3.13B showed that there is almost no induction of Treg response as understood from unchanged IL-10 secretion after peptide stimulation.

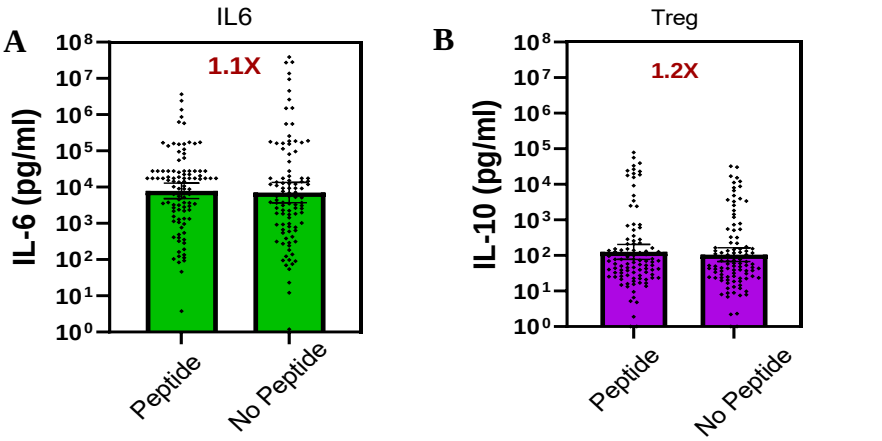


	IL4		IL5		IL9		IL13	
	A:1	A:2	B:1	B:2	C:1	C:2	D:1	D:2
Number of values	101	101	101	101	101	101	101	101
Geometric mean	4.798	3.462	43.16	9.670	62.47	12.91	111.6	17.03
Geometric SD factor	10.27	9.626	14.49	15.19	16.70	12.48	14.06	13.66
Lower 95% CI of geo. mean	3.030	2.214	25.46	5.652	35.83	7.844	66.23	10.16
Upper 95% CI of geo. mean	7.599	5.413	73.16	16.55	108.9	21.25	188.1	28.53

Figure 3.12. Th2 responses of Phase 2 volunteers before and after stimulation of S, N, M, O peptide pool

Column graphs of Phase2 volunteers to show cytokine production of IL-4, IL-5, IL-9 and IL-13 in Th2 response. Half of the V-bottom plate was layered by 2 µg/ml SMNO peptide pool (Mabtech, Sweden) and into all wells 1 M/well PBMCs of the Phase 2 volunteers were added for an incubation step at 37°C for 48 hours. Collected supernatant was further studied according to manufacturer's instructions (LEGENDplex™ HU Th Cytokine Panel (12-plex) w/ VbP kit, Biolegend, USA). The results were analysed with LEGENDplex™ Data Analysis Software (Biolegend, USA). 'Peptide' indicates values after stimulation of PBMCs with SNMO peptide pool and 'No Peptide' indicates values with no stimulation but only resting of PBMCs. X values above each group of columns indicates ratio of increase after peptide pool stimulation. Number of values and statistical values were indicated in the table below the figure.

In our novel SARS-CoV-2 vaccine strategy, additional to complete protection against the virus, it is important to minimize the symptoms and have a quick recovery in case of an infection. In Figure 3.14, another Th subset, Th17 cytokines, were studied because Th17 subset is important for induction of macrophages, neutrophiles and some microbials and have a role in phagocytic killing of microbes [75]. 2-fold increases are showed in IL-17A and IL-17F cytokines while IL-22 secretion has almost twice increase about 5-fold after peptide stimulation.



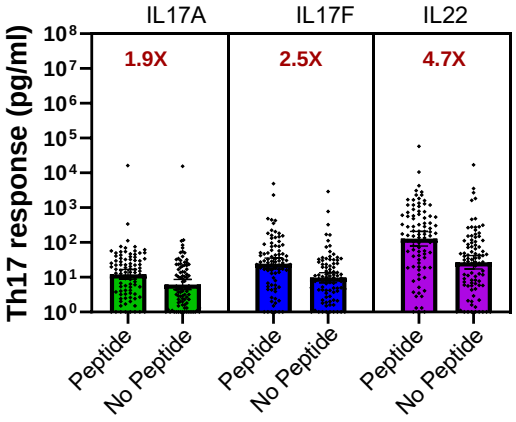
	IL6	
	A:1	A:2
Number of values	101	101
Geometric mean	7830	7056
Geometric SD factor	12.04	26.62
Lower 95% CI of geo. mean	4791	3692
Upper 95% CI of geo. mean	12797	13487

	IL10	
	A:1	A:2
Number of values	101	101
Geometric mean	126.7	105.5
Geometric SD factor	11.53	9.830
Lower 95% CI of geo. mean	78.20	67.22
Upper 95% CI of geo. mean	205.3	165.7

Figure 3.13. IL-6 production and Treg response of Phase 2 volunteers before and after stimulation of S, N, M, O peptide pool

Column graphs of Phase2 volunteers to show cytokine production of A) IL-6 and B) IL-10. Half of the V-bottom plate was layered by 2 µg/ml SMNO peptide pool (Mabtech, Sweden) and into all wells 1 M/well PBMCs of the Phase 2 volunteers were added for an incubation step at 37°C for 48 hours. Collected supernatant was further studied according to manufacturer's instructions (LEGENDplex™ HU Th Cytokine Panel (12-plex) w/ VbP kit, Biolegend, USA). The results were analysed with LEGENDplex™ Data Analysis Software (Biolegend, USA). 'Peptide' indicates values after stimulation of PBMCs with SNMO peptide pool and 'No Peptide' indicates values with no stimulation but only resting of PBMCs. X values above each group of columns indicates ratio of increase after peptide pool stimulation. Number of values and statistical values were indicated in the table below the figure.

In Figure 3.15, each class of T helper subsets are shown in percentages among total T cell response after 2 weeks of booster injection of VLP-58-1023-Al-K3 SARS-COV-2 vaccine in Phase 2 volunteers. 30.5% percentage of T cell response is belonged to Th1 cytokines, 21,5% is belong to Th17 cytokines, 22% is belong to Th2 response, IL-6 cytokine made up about 18% of total T cell response and finally Treg induction is about 8% of total T cell response.



	IL17A		IL17F		IL22	
	A:1	A:2	B:1	B:2	C:1	C:2
Number of values	89	89	89	89	89	89
Geometric mean	12.10	6.157	24.69	9.707	128.0	26.92
Geometric SD factor	4.751	4.959	5.526	4.711	9.718	8.239
Lower 95% CI of geo. mean	8.713	4.394	17.23	7.003	79.30	17.26
Upper 95% CI of geo. mean	16.80	8.627	35.40	13.45	206.7	41.97

Figure 3.14. Th17 responses of Phase 2 volunteers before and after stimulation of S, N, M, O peptide pool

Column graphs of Phase2 volunteers to show cytokine production of IL-17A, IL-17F and IL-22 in Th17 response. Half of the V-bottom plate was layered by 2 µg/ml SMNO peptide pool (Mabtech, Sweden) and into all wells 1 M/well PBMCs of the Phase 2 volunteers were added for an incubation step at 37°C for 48 hours. Collected supernatant was further studied according to manufacturer's instructions (LEGENDplex™ HU Th Cytokine Panel (12-plex) w/ VbP kit, Biolegend, USA). The results were analysed with LEGENDplex™ Data Analysis Software (Biolegend, USA). 'Peptide' indicates values after stimulation of PBMCs with SNMO peptide pool and 'No Peptide' indicates values with no stimulation but only resting of PBMCs. X values above each group of columns indicates ratio of increase after peptide pool stimulation. Number of values and statistical values were indicated in the table below the figure.

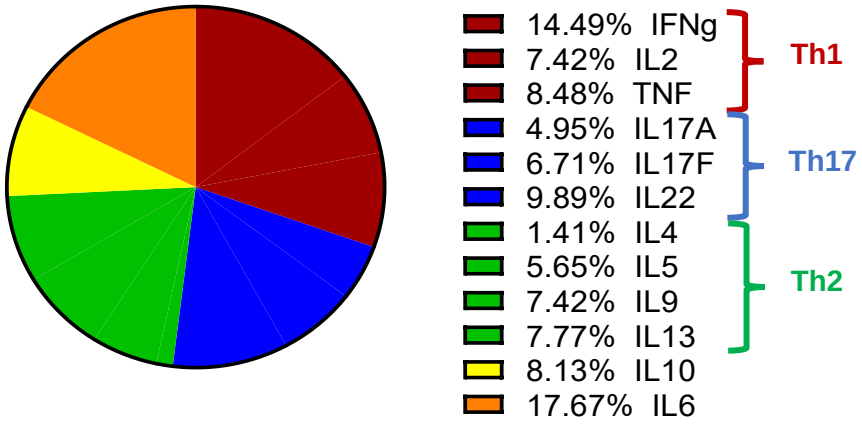


Figure 3.15. T response pie chart of Phase 2 volunteers

Collective pie chart of Phase2 volunteers to show cytokine production belong to all T responses after stimulation of PBMCs with S, N, M, O peptide pool. Red part shows Th1 responses with indicated percentages of IFN-γ, IL-2 and TNF-α. Blue part shows Th17 responses with indicated percentages of IL-17A, IL-17F and IL-22. Green part shows Th2 responses with indicated percentages of IL-4, IL-5, IL-9 and IL-13. Yellow part shows Treg response with indicated percentage of IL-10. Orange part shows IL-6 production.

Overall, it can be seen that Th1-skewed cellular immunity is induced after VLP-58-1023-Al-K3 SARS-COV-2 vaccine, but there is a significant induction in all other Th cell subsets which is very important in support of humoral immunity and clearance of pathogens.

CHAPTER 4

DISCUSSION

In late 2019, most threatening challenge for humanity has emerged which is COVID-19 pandemic. It was not possible to turn the normal life conditions back until an effective and free-of-risk vaccine candidate is found. All over the world, many scientists have started to study on a safe COVID-19 vaccine. Because this pandemic has caused by SARS-CoV-2, structural proteins are based on the vaccine design for all vaccine candidates. This protein has become only Spike protein mostly, because it is the first effecting protein with an ACE-2 receptor in the body mostly on bronchial and alveolar epithelial cells [76] with its receptor-binding domain by the help of an induction of TMPRSS2 for an entry. For the design of an effective vaccine, nature of cellular and humoral protective immunity should be understood, and a vaccine strategy should be developed. In this case, this is not only the spike protein that has an immunoprotective effect but also 3 other main structural proteins are in the pie which are N, M and E proteins. Additionally, there are many other variants emerged in COVID-19 pandemic which causes more severe causes and harden to fight with the virus. The vaccines that would be produced according to wild spike protein at the first step might lose the efficacy against these variants. That's why we designed the spike protein with the conformations suited for alpha (UK) variant which is on the carpet mostly in these days. Additional to this, in order to see the combinations of different vaccination combination with both Wild-Type spike containing VLP and UK-adapted spike containing VLP, we used both of them as first and second injections, respectively. Also, in order to obtain more stable spike structure to avoid degradation during the formulation and entry inside the body, we created six-proline mutated HexaPro spike protein in Wild-Type VLP. The effect of other mutations is excluded in the formulation for this thesis study.

In all pre-clinical and clinical studies, we included four proteins in our VLP-58-1023-Al-K3 SARS-COV-2 vaccine; E, N and M proteins originated from the wild-type virus and HexaPro prefusion stabilized S protein produced by a substitution on its six-proline amino acid. The produced VLP is combined with 2 adjuvants which are Alum and K-type CpG ODN. The first start should be done pre-clinically in order to determine the dosage and toxicity effects to prove safety of the vaccine. Pre-clinical studies are completed with total of 28 mice which includes 21 mice with 2 different VLP dosage and 2 different adjuvant dosage and an additional negative control placebo group of 7 mice (See Table 2.2.3). It is seen that group C, which includes high dose antigen but low dose adjuvant, is the most effective group in antibody production and long-term immune response. The behaviour of aluminum hydroxide is different from some other adjuvants such as squalene-based oil-in-water emulsions (SE) in a way that antigen given with SE acts rapidly in an antibody response because its movement through follicular B cells is faster, but antigen given with Alum stays the local injection site for a while as a depot and absorbed slowly [77]. In that case, giving the optimal but not the highest amount of adjuvants is preferred and in the usage of high concentration of adjuvants, adsorption of antigen will be limited so less effective antibody response will provided [78]. This study reveals successful humoral response in vaccinated mice. After the second injections, in all formulations there are positive antibody production levels in all groups, but the most effective formulation was belonged to group C, because in the response against all recombinant proteins group C showed long-term effect in the third bleeding which is after 2 months of the injection. It is thought to because of the depot effect of Alum as discussed above.

In recent studies, it has been shown that, a third dose of a protein subunit vaccine showed higher immunogenicity in both pre-clinical and clinical studies. The third dose of a protein subunit vaccine increased the humoral protection from 76% to 97% in a way that the neutralizing antibody production is increased [79]. Also, not only after applying a three doses of protein subunit injections, as a booster vaccination, a third dose of protein subunit vaccine after two doses of inactivated vaccines are showed similar results [80]. Our pre-clinical studies revealed that very similar to protein subunit vaccines, three doses of VLP vaccination are very effective for a long-lasting humoral immunity against most antigenic structural proteins which are spike, nucleocapsid and different type of RBD variants of the SARS-CoV-2.

Because we reached the highest efficacy with 5 μg VLP + 60 μg Alum + 30 μg CpG ODN-K3 as a result of pre-clinical studies and there is almost about 1/10 ratio for dosage [81] between animal and human studies, clinical studies were performed by 40 μg VLP + 600 μg Alum + 300 μg CpG ODN-K3 on Phase 2 volunteers. Phase 2 volunteers were selected clinically by the approval of them and 5 main time intervals (Day0, Day21, Day35, Day49 and Day90) was determined for immunogenicity assays of their serum samples. The target of neutralizing antibodies for SARS-CoV-2 is mostly S protein because it contains S2 and S1 domains for detection and cleavage to enter in the body. S1 domain also contains RBD which is specific to ACE2 for host. In that case we utilized in-house trimeric structure of recombinant S protein, and three different variants of recombinant RBD proteins for detection of neutralizing antibody production in both pre-clinical and clinical studies by using IgG ELISA procedure. Including pre-clinical and clinical results, positive antibody production levels against Spike protein are observed after the booster dose. Especially antibody levels in Phase 2 volunteers of clinical study against recombinant trimeric HexaPro Spike protein are very close to our positive control group (Convalescent serum samples) at Day49 and Day90. Positive but moderate levels of neutralizing antibody production are observed against three different variants of recombinant RBD proteins (WT, UK and Delta) for both pre-clinical and clinical results. The only exception among them is WT RBD recombinant protein that was used in pre-clinical studies which is homemade. All other recombinant RBD protein types used in pre-clinical and clinical studies were commercial, and the recommended usage was 1 μg/ml per coating although homemade WT RBD was recommended as 4 μg/ml per coating. Animal experiments revealed that positive but lower production of antibodies against RBD proteins when compared to titers against Spike protein were seen similar to Phase 2 volunteers. These results can be explained in a way that because we do not target only the spike protein in our vaccine, the specificity for detection of RBD domain might be lower when compared to whole spike protein structure. Very similar results were showed by applying two accredited kits which are Abbott Kit (Deren Laboratory, Ankara, Turkey) and CoronaHunter Kit (Matriks Biotek, Ankara, Turkey). Abbott uses recombinant RBD protein and CoronaHunter uses recombinant trimeric Spike protein as coating antibodies. The results were similar and positive but low-moderate levels of antibody production is obtained from Abbott Kit result. Recently it is showed that, it is not a must that very high levels of detectable neutralizing antibody levels must be proven because even with the natural infection of SARS-CoV-2, only 10% of the population

shows high levels of neutralizing antibody production. Almost 70% of the exposures with the virus in the population generates low detectable amount of neutralizing antibodies [82]. However, starting from Day35, high levels of antibody production, which are close to positive control convalescent group, against trimeric S protein is obtained from CoronaHunter Kit.

Anti-N antibodies have no direct neutralizing effect for the body. However, it follows protection through providing interactions with Fc regions resulting complement-dependent cytotoxicity and phagocytosis effect [76]. Besides this innate function of N-antibodies, they provide undeniable cellular immunity due to increased dendritic cell function. Furthermore, nucleocapsid is a mostly found structure for many common viruses and having non-neutralizing N antibodies might provide cross-protective immunity against multiple subtypes of influenza virus [83]. In our study we aimed to show that having non-neutralizing nucleocapsid antibodies will provide benefit in the enhancement of cellular immunity because non-neutralizing nucleocapsid antibodies causes formation of immune complexes which can trigger generation of mature dendritic cells, formation of Th1 cytokines and CTL responses [83]. Even though no mechanistic details are included in this study, besides having a medical understanding behind nucleocapsid protein in many viral infections, mechanism of immune response is not clear. However, James LC et al. showed that a mechanism against enveloped viruses that prove effect of non-neutralizing antibodies. It says antibody-dependent intracellular neutralization is triggered by N protein via the TRIM mechanism [84]. In our study, the sensitivity of nucleocapsid capturing antibodies used in pre-clinical and clinical studies were differed. Two different batches of recombinant nucleocapsid protein were used. The recombinant nucleocapsid protein that we used in clinical studies were produced in adherent HEK-293T cells in an FBS-containing culture media. So that, degradation product was a lot, and the product cannot be purified in a clear form. Overall, anti-N production was tested in clinical studies with a low quality and high impurity conditions. The recombinant nucleocapsid protein that we used in pre-clinical studies were produced in suspension HEK-293 cells with a serum-free media. So that there were very low levels of degradation product formed and recombinant protein purification was more stable and purer. Besides having high levels of anti-N antibodies in pre-clinical studies, we had moderate levels of humoral response against nucleocapsid in clinical studies because difference of the batches causes signal to background ratio difference between the capturing antibodies. However, we had still moderate-positive levels of antibody production occurred in the Phase 2 volunteers starting

from Day35. AUC levels against N protein continued to increase in Day49 and reached the top at Day90. Overall, having humoral responses against two highly antigenic viral structures of SARS-CoV-2 which are N and S proteins including three different RBD variant proteins, showed that an effective antibody response is produced with our vaccine.

The aim behind using 2 different adjuvants is to reach a strong Th1-skewed cellular immunity and inducing the strength of CTLs with this formulation. Also, it is expected to be seen that although Alum has Th2 tendency to produce a cellular immunity in the body, in the combination of CpG will have additional and high Th1-skewed immunity [85]. Th1 response is critical for fighting intracellular pathogens such as viruses while Th2 response is mostly needed for parasitic infections [86]. In COVID-19, Th polarization is very critical. Imbalance of Th2/Th1 can cause severe effects in the patients with natural infections. So that, it is important to have a balanced cellular immune response after a vaccination. Th2/Th1 imbalance causes Th2 cytokine storm and showed higher mortality risk in natural infection [87]. Serrano A. et al. showed that Th1-skewed immunity plays an important role in quick recovery and mild symptoms. Mechanistically in a natural infection, after SARS-CoV-2 was sensed by APCs such as DCs, MHCs present the antigen epitopes to Th0 cells. After this point, Th2 polarization causes delay in virus clearance because of the cytokines produced such as IL-5 by eosinophil accumulation, IL-4 with inhibition of antiviral clearance and IL-13 with eosinophil infiltration which causes overall antiviral response suppression against SARS-CoV-2 and this polarization causes severe cases with the domination of Th17 and Th2 cytokine storm. If Th0 cells polarized toward Th1 immune milieu, virus clearance occurs thanks to production of IFN-γ which triggers CTLs to kill the viral protein structures, induction of macrophages for phagocytic activity and activation of B cells to present antigens for other T-cell interactions. So, Th1 polarization shows antiviral immune responses against SARS-CoV-2 and natural infections toward Th1 immune milieu show mild symptoms [86]. In our vaccine it is observed that most of the T cell response is occurred by Th1 immune milieu which is about 32% is followed by Th17 and Th2 responses with 21% of the overall cellular response. Our vaccine provided a favorable balance between T cell polarizations. Although Th1-skewed immunity is important in the defense against COVID-19, extreme levels of Th1 activation is not favorable because of the side effects like rheumatoid arthritis. So that, it is important to have a balance between Th1/Th2/Th17 responses.

Least percentage is belonged to Treg response with 8% followed by IL-6 response with 18%. It is good to have less Treg (IL-10) response against the vaccine because it is a potential suppressor of Th1 response. Even, IL-10 production is suggested as discriminator of COVID-19 progression in the patients due to this property [87]. As in IL-10 property, IL-6 has the similar effect in severity of the natural infections. Enhancement of IL-10 and IL-6 levels are observed in the severe cases of the patients of COVID-19 [88]. Carstens and Noronha et. al (2020) suggested that increased levels of IL-6 production can lead to lymphopenia. Our study reveals that our vaccine induces lesser IL-6 and IL-10 compared to other cytokines. This feature of our vaccine provides quick recovery in case of an infection and mild symptoms in addition to favorable antiviral clearance.

The role of Th17 in COVID-19 has been showed as not only suppression of Th1 immune milieu but also induction of Th2 cytokine storm. During natural infections, it has been proved that having increased IL-17, IL-10 and IL-6 responses caused hospitalization of COVID-19 patients with severe symptoms and high mortality [89]. Th17 has also provided some part of IFN-γ production for CD8+ T cell activation and virus clearance, that's why having a balanced Th17 response is favorable. In Th17 cell subset, IL-17 and IL-22 shows distinct general functions even though they are related to each other. Although IL-17 triggers inflammatory response by inducing pro-inflammatory cytokines, IL-22 is mainly protective and regulatory. IL-17 mechanism performed through NF-κB and MAP kinases in order to induce pro-inflammatory cytokines and chemokines like IL-6, granulocyte-macrophage colony-stimulating factor (GM-CSF) and CXCL10. Unlike IL-17, IL-22 works through JAK-STAT pathway in order to trigger homeostasis, tissue defense and it also provide enhanced function of epithelial protection [90]. Another foundation of our study was that S, N, M, O peptide stimulated PBMC's of the Phase2 volunteers indicated moderate levels of IL-22 compared to low IL-17A and IL-17F cytokine production. This reveals that regulatory function of the CD4+ T cells were triggered by IL-22 but not IL-10. We hypothesized that low levels of IL-17 will less often induce Th2 pro-inflammatory cytokines and Th1-skewed cellular immunity will be protected.

Taken together, we utilized two different variant sequences in our VLPs and combined them with 2 different adjuvants in order to provide Th1-skewed cellular immunity in the volunteers. In our recent studies, we performed Phase 1 studies of the VLP-58-1023-Al-K3 SARS-COV-2 vaccine including placebo, low doses and high doses VLP formulations in three different groups of volunteers. At this study, both first and second injections are done with the formulations including HexaPro WT + HexaPro WT VLP injections combining with 600 μg Alum + 300 μg K3-CpG. At the end of Phase 1 studies, we observed better positive humoral response and induced cellular immunity with the volunteers injected with high dose VLP (40 ug) so that we included high dose VLP formulation in our Phase 2 studies. Because of the variants of concerns emerged in late 2020s, we decided to design different sequences of the VLP. On these days, Alpha variant firstly seen in UK was popular among the patients and spread widely and quickly. When these variant emergences taken into consideration, we hypothesized that adding a alpha variant sequence in our vaccine will improve the antibody response against the new variant and strengthen cellular immunity, so we adapted a new UK VLP including the alpha variant mutations in it and combined HexaPro WT VLP in the first injection and UK VLP in the second injection. As a result, positive antibody production against S and N proteins of the virus in pre-clinical and clinical studies were observed. Also, antibody production against three different variants of RBD protein was checked to see the effect of the vaccine in other mutations and positive results were obtained even against Delta RBD protein in both pre-clinical and clinical studies. Furthermore, cellular immunity was checked in Phase 2 volunteers against S, N, M and O protein stimulation, and it is showed that VLP-58-1023-Al-K3 SARS-COV-2 vaccine induces mostly Th1 response which is favorable against viral clearance and there is a balanced Th1/Th2 response among all T cell immune milieu. There is also IL-6, IL-10 and IL-17 responses which are low but not negative regarding to overall T cell response. Lastly, IL-22 was the regulatory cytokine in our vaccine to inhibit overactivation of cytokine storm. In addition to this master study, there are ongoing studies in our laboratory which are trying to determine the most effective vaccine formulation against new variants to be potentially form. This VLP vaccine is completely safe, effective and favorable because it is easy and fast to design against new variant formations.

CHAPTER 5

FUTURE PERSPECTIVES

VLP-58-1023-Al-K3 SARS-COV-2 vaccine revealed that humoral response against S, N and RBD variant proteins are positive in most of the Phase 2 volunteers and strong cellular immune response has been formed in most of the patients after the stimulation of S, N, M and O peptide pools. Our study did not include the participant cell types of the immune system in that humoral and cellular response. In a short-term interval after the vaccine injections are completed, innate cell responses can be identified specifically which can also help in characterization of T cell responses. In that case, dendritic cells can play role which can help CTL activation with the changes in cytokine production. Additional to this, we hypothesized that nucleocapsid protein that our vaccine included in the formulation has an effect in cross-reactive T cell formation and increasing the T cell response by the help of M protein. The contribution of each S, N and M proteins to the overall T cell response can be identified. So, the effect of including all four proteins in our vaccine could be proved practically. Furthermore, there is no study of our vaccine has been showed in children and older people. Because the T cell responses of older people and children can vary, the effect of the vaccine should be proved in all age ranges. Last but not least, we hypothesized that a third dose of VLP-58-1023-Al-K3 vaccine will improve the humoral and cellular immune response better than other vaccine candidates. As in study of Gao et. al (2021), Phase 2 studies of protein subunit similar to our protein design-based vaccine showed that third dose vaccination (prime, boost, boost) increased significantly the levels of IgG titers and believed to be longer-term in efficacy. Also, we believed that homologous injection of three doses of VLP vaccination rather than a heterologous vaccination will be more effective for inducing immune response.

BIBLIOGRAPHY

1. Abbas AK, Lichtman AH, Pillai S. Basic Immunology - 6th Edition. Accessed March 17, 2022. https://www.elsevier.com/books/basic-immunology/abbas/978-0-323-54943-1

2. Alberts B, Johnson A, Lewis J, Raff M, Roberts K, Walter P. Innate Immunity. *Molecular Biology of the Cell 4th edition*. Published online 2002. Accessed March 17, 2022. https://www.ncbi.nlm.nih.gov/books/NBK26846/

3. Murphy K Travers, Paul, Walport M, Janeway C. *Janeway's Immunobiology.* Garland Science; 2008.

4. Varadé J, Magadán S, González-Fernández Á. Human immunology and immunotherapy: main achievements and challenges. *Cell Mol Immunol*. 2021;18(4):805-828. doi:10.1038/s41423-020-00530-6

5. Abbas A, Lichtman AH, Pillai S. Cellular and Molecular Immunology - 9th Edition. Accessed March 17, 2022. https://www.elsevier.com/books/cellular-and-molecular-immunology/abbas/978-0-323-47978-3

6. Delves PJ, Roitt IM. The immune system. First of two parts. *N Engl J Med*. 2000;343(1):37-49. doi:10.1056/NEJM200007063430107

7. Schroeder HW, Cavacini L. Structure and function of immunoglobulins. *J Allergy Clin Immunol*. 2010;125(2 Suppl 2):S41-52. doi:10.1016/j.jaci.2009.09.046

8. Boes M. Role of natural and immune IgM antibodies in immune responses. *Mol Immunol*. 2000;37(18):1141-1149. doi:10.1016/s0161-5890(01)00025-6

9. Riesbeck K, Nordstrom T. Structure and immunological action of the human pathogen Moraxella catarrhalis IgD-binding protein. *Crit Rev Immunol*. 2006;26(4):353-376. doi:10.1615/critrevimmunol.v26.i4.40

10. Geisberger R, Lamers M, Achatz G. The riddle of the dual expression of IgM and IgD. *Immunology*. 2006;118(4):429-437. doi:10.1111/j.1365-2567.2006.02386.x

11. Vidarsson G, Dekkers G, Rispens T. IgG subclasses and allotypes: from structure to effector functions. *Front Immunol*. 2014;5:520. doi:10.3389/fimmu.2014.00520

12. Woof JM, Mestecky J. Mucosal immunoglobulins. *Immunol Rev*. 2005;206:64-82. doi:10.1111/j.0105-2896.2005.00290.x

13. Corthésy B. Roundtrip ticket for secretory IgA: role in mucosal homeostasis? *J Immunol*. 2007;178(1):27-32. doi:10.4049/jimmunol.178.1.27

14. Chang TW, Wu PC, Hsu CL, Hung AF. Anti-IgE antibodies for the treatment of IgE-mediated allergic diseases. *Adv Immunol*. 2007;93:63-119. doi:10.1016/S0065-2776(06)93002-8

15. Zhou F, Yu T, Du R, et al. Clinical course and risk factors for mortality of adult inpatients with COVID-19 in Wuhan, China: a retrospective cohort study. *Lancet*. 2020;395(10229):1054-1062. doi:10.1016/S0140-6736(20)30566-3

16. Munster VJ, Koopmans M, van Doremalen N, van Riel D, de Wit E. A Novel Coronavirus Emerging in China - Key Questions for Impact Assessment. *N Engl J Med*. 2020;382(8):692-694. doi:10.1056/NEJMp2000929

17. Zhou P, Yang XL, Wang XG, et al. A pneumonia outbreak associated with a new coronavirus of probable bat origin. *Nature*. 2020;579(7798):270-273. doi:10.1038/s41586-020-2012-7

18. Orhan IE, Senol Deniz FS. Natural Products as Potential Leads Against Coronaviruses: Could They be Encouraging Structural Models Against SARS-CoV-2? *Nat Prod Bioprospect*. 2020;10(4):171-186. doi:10.1007/s13659-020-00250-4

19. Lu R, Zhao X, Li J, et al. Genomic characterisation and epidemiology of 2019 novel coronavirus: implications for virus origins and receptor binding. *Lancet*. 2020;395(10224):565-574. doi:10.1016/S0140-6736(20)30251-8

20. Hoffmann M, Kleine-Weber H, Schroeder S, et al. SARS-CoV-2 Cell Entry Depends on ACE2 and TMPRSS2 and Is Blocked by a Clinically Proven Protease Inhibitor. *Cell*. 2020;181(2):271-280.e8. doi:10.1016/j.cell.2020.02.052

21. Chang C ke, Hou MH, Chang CF, Hsiao CD, Huang T huang. The SARS coronavirus nucleocapsid protein--forms and functions. *Antiviral Res*. 2014;103:39-50. doi:10.1016/j.antiviral.2013.12.009

22. Zhuang MW, Cheng Y, Zhang J, et al. Increasing host cellular receptor-angiotensin-converting enzyme 2 expression by coronavirus may facilitate 2019-nCoV (or SARS-CoV-2) infection. *J Med Virol*. 2020;92(11):2693-2701. doi:10.1002/jmv.26139

23. Zhang L, Lin D, Sun X, et al. Crystal structure of SARS-CoV-2 main protease provides a basis for design of improved α-ketoamide inhibitors - PubMed. Accessed March 17, 2022. https://pubmed.ncbi.nlm.nih.gov/32198291/

24. Knoops K, Kikkert M, Worm SHE van den, et al. SARS-coronavirus replication is supported by a reticulovesicular network of modified endoplasmic reticulum. *PLoS Biol*. 2008;6(9):e226. doi:10.1371/journal.pbio.0060226

25. Fehr AR, Perlman S. Coronaviruses: an overview of their replication and pathogenesis. *Methods Mol Biol*. 2015;1282:1-23. doi:10.1007/978-1-4939-2438-7_1

26. Huang C, Wang Y, Li X, et al. Clinical features of patients infected with 2019 novel coronavirus in Wuhan, China. *Lancet*. 2020;395(10223):497-506. doi:10.1016/S0140-6736(20)30183-5

27. Rowley AH. Understanding SARS-CoV-2-related multisystem inflammatory syndrome in children. *Nat Rev Immunol*. 2020;20(8):453-454. doi:10.1038/s41577-020-0367-5

28. Eastin C, Eastin T. Clinical Characteristics of Coronavirus Disease 2019 in China. *J Emerg Med*. 2020;58(4):711-712. doi:10.1016/j.jemermed.2020.04.004

29. He X, Lau EHY, Wu P, et al. Temporal dynamics in viral shedding and transmissibility of COVID-19. *Nat Med*. 2020;26(5):672-675. doi:10.1038/s41591-020-0869-5

30. Peiris JSM, Chu CM, Cheng VCC, et al. Clinical progression and viral load in a community outbreak of coronavirus-associated SARS pneumonia: a prospective study. *Lancet*. 2003;361(9371):1767-1772. doi:10.1016/s0140-6736(03)13412-5

31. Zou X, Chen K, Zou J, Han P, Hao J, Han Z. Single-cell RNA-seq data analysis on the receptor ACE2 expression reveals the potential risk of different human organs vulnerable to 2019-nCoV infection. *Front Med*. 2020;14(2):185-192. doi:10.1007/s11684-020-0754-0

32. Monteil V, Kwon H, Prado P, et al. Inhibition of SARS-CoV-2 Infections in Engineered Human Tissues Using Clinical-Grade Soluble Human ACE2. *Cell*. 2020;181(4):905-913.e7. doi:10.1016/j.cell.2020.04.004

33. Li S, Jiang L, Li X, et al. Clinical and pathological investigation of patients with severe COVID-19. *JCI Insight*. 2020;5(12):138070. doi:10.1172/jci.insight.138070

34. Yap JKY, Moriyama M, Iwasaki A. Inflammasomes and Pyroptosis as Therapeutic Targets for COVID-19. *J Immunol*. 2020;205(2):307-312. doi:10.4049/jimmunol.2000513

35. Ni L, Ye F, Cheng ML, et al. Detection of SARS-CoV-2-Specific Humoral and Cellular Immunity in COVID-19 Convalescent Individuals. *Immunity*. 2020;52(6):971-977.e3. doi:10.1016/j.immuni.2020.04.023

36. Bakhiet M, Taurin S. SARS-CoV-2: Targeted managements and vaccine development. *Cytokine Growth Factor Rev*. 2021;58:16-29. doi:10.1016/j.cytogfr.2020.11.001

37. Mercatelli D, Giorgi FM. Geographic and Genomic Distribution of SARS-CoV-2 Mutations. *Front Microbiol*. 2020;11:1800. doi:10.3389/fmicb.2020.01800

38. Dearlove B, Lewitus E, Bai H, et al. A SARS-CoV-2 vaccine candidate would likely match all currently circulating variants | PNAS. Accessed March 17, 2022. https://www.pnas.org/doi/10.1073/pnas.2008281117

39. Rambaut A, Loman N, Pybus O, et al. Preliminary genomic characterisation of an emergent SARS-CoV-2 lineage in the UK defined by a novel set of spike mutations - SARS-CoV-2 coronavirus / nCoV-2019 Genomic Epidemiology. Virological. Published December 18, 2020. Accessed March 17, 2022. https://virological.org/t/preliminary-genomic-characterisation-of-an-emergent-sars-cov-2-lineage-in-the-uk-defined-by-a-novel-set-of-spike-mutations/563

40. Tegally H, Wilkinson E, Giovanetti M, et al. Detection of a SARS-CoV-2 variant of concern in South Africa. *Nature*. 2021;592(7854):438-443. doi:10.1038/s41586-021-03402-9

41. Faria NR, Mellan TA, Whittaker C, et al. Genomics and epidemiology of a novel SARS-CoV-2 lineage in Manaus, Brazil. *medRxiv*. Published online March 3, 2021:2021.02.26.21252554. doi:10.1101/2021.02.26.21252554

42. Cherian S, Potdar V, Jadhav S, et al. Convergent evolution of SARS-CoV-2 spike mutations, L452R, E484Q and P681R, in the second wave of COVID-19 in Maharashtra, India. Published online May 3, 2021:2021.04.22.440932. doi:10.1101/2021.04.22.440932

43. Weisblum Y, Schmidt F, Zhang F, et al. Escape from neutralizing antibodies by SARS-CoV-2 spike protein variants. *Elife*. 2020;9:e61312. doi:10.7554/eLife.61312

44. Challen R, Dyson L, Overton CE, et al. Early epidemiological signatures of novel SARS-CoV-2 variants: establishment of B.1.617.2 in England. Published online June 7, 2021:2021.06.05.21258365. doi:10.1101/2021.06.05.21258365

45. Riley S, Wang H, Eales O, et al. REACT-1 round 12 report: resurgence of SARS-CoV-2 infections in England associated with increased frequency of the Delta variant. Published online June 21, 2021:2021.06.17.21259103. doi:10.1101/2021.06.17.21259103

46. Cele S, Jackson L, Khoury DS, et al. Omicron extensively but incompletely escapes Pfizer BNT162b2 neutralization. *Nature*. 2022;602(7898):654-656. doi:10.1038/s41586-021-04387-1

47. Ball P. The lightning-fast quest for COVID vaccines - and what it means for other diseases. *Nature*. 2021;589(7840):16-18. doi:10.1038/d41586-020-03626-1

48. Ho D, Tsuji M. Infectious diseases: breakthroughs in developing vaccines, immune protective monitoring and measuring toxicity with functional proteomics. Accessed March 17, 2022. https://www.nxtbook.com/nxtbooks/gen/isoplexis_infectdis_ebook/index.php#/p/1

49. Wang MY, Zhao R, Gao LJ, Gao XF, Wang DP, Cao JM. SARS-CoV-2: Structure, Biology, and Structure-Based Therapeutics Development. *Front Cell Infect Microbiol*. 2020;10:587269. doi:10.3389/fcimb.2020.587269

50. Anderson EJ, Rouphael NG, Widge AT, et al. Safety and Immunogenicity of SARS-CoV-2 mRNA-1273 Vaccine in Older Adults. *N Engl J Med*. 2020;383(25):2427-2438. doi:10.1056/NEJMoa2028436

51. Baden LR, El Sahly HM, Essink B, et al. Efficacy and Safety of the mRNA-1273 SARS-CoV-2 Vaccine. *N Engl J Med*. 2021;384(5):403-416. doi:10.1056/NEJMoa2035389

52. Polack FP, Thomas SJ, Kitchin N, et al. Safety and Efficacy of the BNT162b2 mRNA Covid-19 Vaccine. *New England Journal of Medicine*. 2020;383(27):2603-2615. doi:10.1056/NEJMoa2034577

53. Kyriakidis NC, López-Cortés A, González EV, Grimaldos AB, Prado EO. SARS-CoV-2 vaccines strategies: a comprehensive review of phase 3 candidates. *NPJ Vaccines*. 2021;6(1):28. doi:10.1038/s41541-021-00292-w

54. Graham SP, McLean RK, Spencer AJ, et al. Evaluation of the immunogenicity of prime-boost vaccination with the replication-deficient viral vectored COVID-19 vaccine candidate ChAdOx1 nCoV-19. Published online June 20, 2020:2020.06.20.159715. doi:10.1101/2020.06.20.159715

55. Golob JL, Lugogo N, Lauring AS, Lok AS. SARS-CoV-2 vaccines: a triumph of science and collaboration. *JCI Insight*. 6(9):e149187. doi:10.1172/jci.insight.149187

56. Latham T, Galarza JM. Formation of Wild-Type and Chimeric Influenza Virus-Like Particles following Simultaneous Expression of Only Four Structural Proteins. *J Virol*. 2001;75(13):6154-6165. doi:10.1128/JVI.75.13.6154-6165.2001

57. Mohsen MO, Gomes AC, Vogel M, Bachmann MF. Interaction of Viral Capsid-Derived Virus-Like Particles (VLPs) with the Innate Immune System. *Vaccines (Basel)*. 2018;6(3):37. doi:10.3390/vaccines6030037

58. Silva AL, Peres C, Conniot J, et al. Nanoparticle impact on innate immune cell pattern-recognition receptors and inflammasomes activation. *Seminars in Immunology*. 2017;34:3-24. doi:10.1016/j.smim.2017.09.003

59. Florindo HF, Kleiner R, Vaskovich-Koubi D, et al. Immune-mediated approaches against COVID-19. *Nat Nanotechnol*. 2020;15(8):630-645. doi:10.1038/s41565-020-0732-3

60. Nooraei S, Bahrulolum H, Hoseini ZS, et al. Virus-like particles: preparation, immunogenicity and their roles as nanovaccines and drug nanocarriers. *J Nanobiotechnology*. 2021;19:59. doi:10.1186/s12951-021-00806-7

61. Yılmaz IC, Ipekoglu EM, Bülbül A, et al. Development and preclinical evaluation of virus-like particle vaccine against COVID-19 infection - Yilmaz - 2022 - Allergy - Wiley Online Library. Accessed March 17, 2022. https://onlinelibrary.wiley.com/doi/10.1111/all.15091

62. Cimica V, Galarza JM. Adjuvant Formulations for Virus-Like Particle (VLP) Based Vaccines. *Clin Immunol*. 2017;183:99-108. doi:10.1016/j.clim.2017.08.004

63. Lua LHL, Connors NK, Sainsbury F, Chuan YP, Wibowo N, Middelberg APJ. Bioengineering virus-like particles as vaccines. *Biotechnology and Bioengineering*. 2014;111(3):425-440. doi:10.1002/bit.25159

64. Hutchins B, Sajjadi N, Seaver S, et al. Working toward an adenoviral vector testing standard. *Mol Ther*. 2000;2(6):532-534. doi:10.1006/mthe.2000.0217

65. Krug A, Rothenfusser S, Hornung V, et al. Identification of CpG oligonucleotide sequences with high induction of IFN-alpha/beta in plasmacytoid dendritic cells. *Eur J Immunol*. 2001;31(7):2154-2163. doi:10.1002/1521-4141(200107)31:7<2154::aid-immu2154>3.0.co;2-u

66. Krieg AM, Yi AK, Matson S, et al. CpG motifs in bacterial DNA trigger direct B-cell activation. *Nature*. 1995;374(6522):546-549. doi:10.1038/374546a0

67. Klinman DM. Immunotherapeutic uses of CpG oligodeoxynucleotides. *Nat Rev Immunol*. 2004;4(4):249-259. doi:10.1038/nri1329

68. Hemmi H, Takeuchi O, Kawai T, et al. A Toll-like receptor recognizes bacterial DNA. *Nature*. 2000;408(6813):740-745. doi:10.1038/35047123

69. Klinman DM, Yi AK, Beaucage SL, Conover J, Krieg AM. CpG motifs present in bacteria DNA rapidly induce lymphocytes to secrete interleukin 6, interleukin 12, and interferon gamma. *Proc Natl Acad Sci U S A*. 1996;93(7):2879-2883.

70. Levine MM, Sztein MB. Vaccine development strategies for improving immunization: the role of modern immunology. *Nat Immunol*. 2004;5(5):460-464. doi:10.1038/ni0504-460

71. Vaccine Development, Testing, and Regulation | History of Vaccines. Accessed March 19, 2022. https://www.historyofvaccines.org/multilanguage/content/articles/vaccine-development-testing-and-regulation

72. Hirabara SM, Serdan TDA, Gorjao R, et al. SARS-COV-2 Variants: Differences and Potential of Immune Evasion. *Frontiers in Cellular and Infection Microbiology*. 2022;11. Accessed April 14, 2022. https://www.frontiersin.org/article/10.3389/fcimb.2021.781429

73. Burbelo PD, Riedo FX, Morishima C, et al. Detection of Nucleocapsid Antibody to SARS-CoV-2 is More Sensitive than Antibody to Spike Protein in COVID-19 Patients. *medRxiv*. Published online April 24, 2020:2020.04.20.20071423. doi:10.1101/2020.04.20.20071423

74. Grifoni A, Weiskopf D, Ramirez SI, et al. Targets of T Cell Responses to SARS-CoV-2 Coronavirus in Humans with COVID-19 Disease and Unexposed Individuals. *Cell*. 2020;181(7):1489-1501.e15. doi:10.1016/j.cell.2020.05.015

75. Lin Y, Slight SR, Khader SA. Th17 cytokines and Vaccine Induced Immunity. *Semin Immunopathol*. 2010;32(1):79-90. doi:10.1007/s00281-009-0191-2

76. Jeyanathan M, Afkhami S, Smaill F, Miller MS, Lichty BD, Xing Z. Immunological considerations for COVID-19 vaccine strategies. *Nat Rev Immunol*. 2020;20(10):615-632. doi:10.1038/s41577-020-00434-6

77. Pedersen GK, Wørzner K, Andersen P, Christensen D. Vaccine Adjuvants Differentially Affect Kinetics of Antibody and Germinal Center Responses. *Frontiers in Immunology*. 2020;11. Accessed April 13, 2022. https://www.frontiersin.org/article/10.3389/fimmu.2020.579761

78. HogenEsch H, O'Hagan DT, Fox CB. Optimizing the utilization of aluminum adjuvants in vaccines: you might just get what you want. *npj Vaccines*. 2018;3(1):1-11. doi:10.1038/s41541-018-0089-x

79. Yang S, Li Y, Dai L, et al. Safety and immunogenicity of a recombinant tandem-repeat dimeric RBD-based protein subunit vaccine (ZF2001) against COVID-19 in adults: two randomised, double-blind, placebo-controlled, phase 1 and 2 trials. *The Lancet Infectious Diseases*. 2021;21(8):1107-1119. doi:10.1016/S1473-3099(21)00127-4

80. Zhang R, Li D, Xu K, et al. A protein subunit vaccine booster following two doses of inactivated SARS-CoV-2 vaccine provides high neutralisation of SARS-CoV-2 and its variants in mice. *The Lancet Microbe*. 2022;3(3):e165-e166. doi:10.1016/S2666-5247(21)00331-1

81. Nair AB, Jacob S. A simple practice guide for dose conversion between animals and human. *J Basic Clin Pharm*. 2016;7(2):27-31. doi:10.4103/0976-0105.177703

82. McDade TW, Sancilio A, D'Aquila R, et al. Low Levels of Neutralizing Antibodies After Natural Infection With Severe Acute Respiratory Syndrome Coronavirus 2 in a Community-Based Serological Study. *Open Forum Infectious Diseases*. 2022;9(3):ofac055. doi:10.1093/ofid/ofac055

83. Carragher DM, Kaminski DA, Moquin A, Hartson L, Randall TD. A Novel Role for Non-Neutralizing Antibodies against Nucleoprotein in Facilitating Resistance to Influenza Virus. *The Journal of Immunology*. 2008;181(6):4168-4176. doi:10.4049/jimmunol.181.6.4168

84. Caddy SL, Vaysburd M, Papa G, et al. Viral nucleoprotein antibodies activate TRIM21 and induce T cell immunity. *EMBO J*. 2021;40(5):e106228. doi:10.15252/embj.2020106228

85. Millan CLB, Weeratna R, Krieg AM, Siegrist CA, Davis HL. CpG DNA can induce strong Th1 humoral and cell-mediated immune responses against hepatitis B surface antigen in young mice. *Proc Natl Acad Sci U S A*. 1998;95(26):15553-15558.

86. Aleebrahim-Dehkordi E, Molavi B, Mokhtari M, et al. T helper type (Th1/Th2) responses to SARS-CoV-2 and influenza A (H1N1) virus: From cytokines produced to immune responses. *Transpl Immunol*. 2022;70:101495. doi:10.1016/j.trim.2021.101495

87. Gil-Etayo FJ, Suàrez-Fernández P, Cabrera-Marante O, et al. T-Helper Cell Subset Response Is a Determining Factor in COVID-19 Progression. *Front Cell Infect Microbiol*. 2021;11:624483. doi:10.3389/fcimb.2021.624483

88. Gong J, Dong H, Xia QS, et al. Correlation analysis between disease severity and inflammation-related parameters in patients with COVID-19: a retrospective study. *BMC Infect Dis*. 2020;20:963. doi:10.1186/s12879-020-05681-5

89. Martonik D, Parfieniuk-Kowerda A, Rogalska M, Flisiak R. The Role of Th17 Response in COVID-19. *Cells*. 2021;10(6):1550. doi:10.3390/cells10061550

90. Valeri M, Raffatellu M. Cytokines IL-17 and IL-22 in the host response to infection. *Pathog Dis*. 2016;74(9):ftw111. doi:10.1093/femspd/ftw111

APPENDIX

Appendix 1

Cell Culture Media Recipe

2% Wash medium

- 500 ml RPMI-1640 Media containing 2mM L-Glutamine at a final
- 10.64 ml heat-inactivated FBS
- 5.32 ml HEPES (10mM) Buffer
- 5.32 ml Penicillin/Streptomycin (50µg/ml)

10% Resting Medium Recipe

- 500 ml RPMI-1640 Media containing 2mM L-Glutamine at a final
- 58.14 ml heat-inactivated FBS
- 5.8 ml HEPES (10mM) Buffer
- 5.8 ml Non-Essential Amino Acids (1X from 100X Stock Solution)
- 5.8 ml Na-Pyruvate (110µg/ml)
- 5.8 ml Penicillin/Streptomycin (50µg/ml)

5% Blocking Buffer Recipe (ELISA)

- 100 grams Bovine Serum Albumin (Capricorn, Germany)
- 1 mL Tween20 (0.025%) (VWR, USA)
- Completed up to 2 mL with 1X handmade PBS

(Remaining medium can be aliquoted at 50 ml falcon and can be stored at –20°C)

Wash Buffer Recipe (ELISA)

- 18 L distilled H2O

- 2 L handmade 10X PBS

- 10 mL Tween20 (VWR, USA)

Handmade 10X Phosphate Buffered Saline (PBS)

- 80 g Sodium Chloride-NaCl (Isolal, Germany)

- 2 g Potassium Chloride-KCl (Merck, Germany)

- 15.2 g Sodium phosphate dibasic dihydrate-$Na_2HPO_4.2H_2O$ (Sigma Aldrich, USA)

- 2 g Potassium Phosphate Monobasic-KH_2PO_4 (Sigma Aldrich, USA)

- Completed up to 1 lt with ddH_2O

(After preparation of 10X PBS, pH was adjusted to 6.8 and autoclave process was done.)

Handmade 1X PBS

10X handmade PBS buffer was diluted with ddH_2O in 1:10 ratio.

(After preparation of 1X PBS, pH was adjusted to 7.2 and autoclave process was done.)

PNPP Substrate (Thermo Fisher Scientific, USA) (ELISA)

For 1 plate;

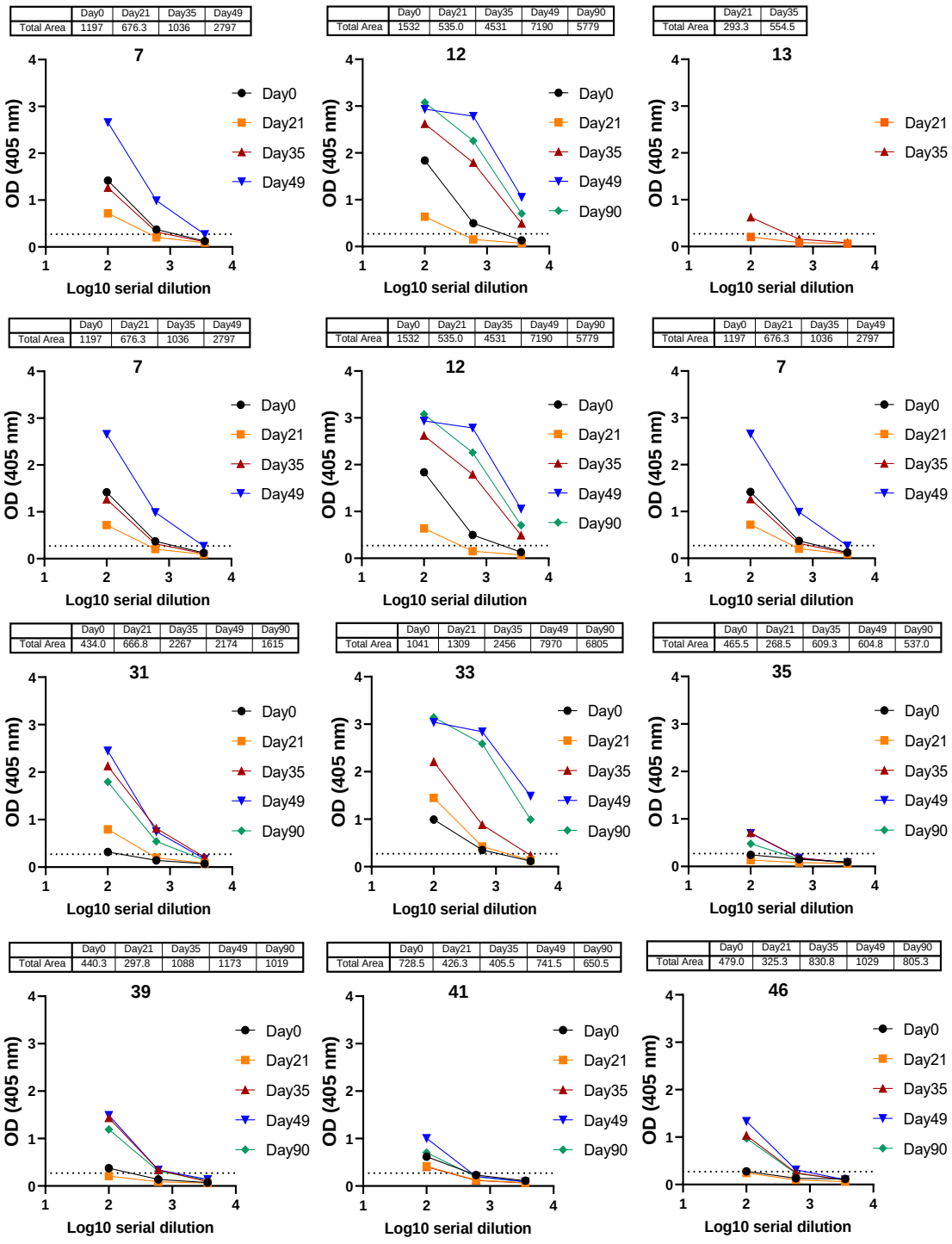
- 4 ml double-distilled H2O

- 1 PNPP tablet

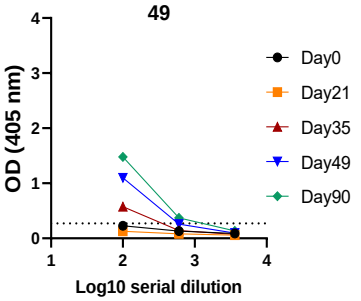
- 1 ml PNPP buffer

Appendix 2

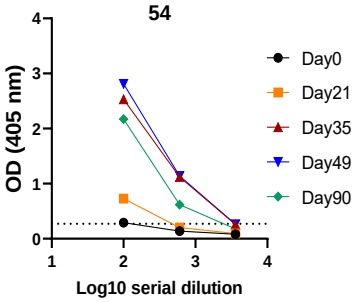
Day by day individual OD graphs after injection of VLP-58-1023-AL-K3 vaccine for each Phase 2 volunteers with 6X serial dilutions of sera from 100X to 3600X against recombinant S protein. 96-well 2HB maxi-binding ELISA plates were coated with 6 ug/ml in-house recombinant spike protein and plates were blocked. After the serial dilutions of volunteers' sera, ALP-tagged anti-human IgG secondary antibody were filled into wells and finally PNPP substrate was added into plate and optical density values were recorded at 405 nm.



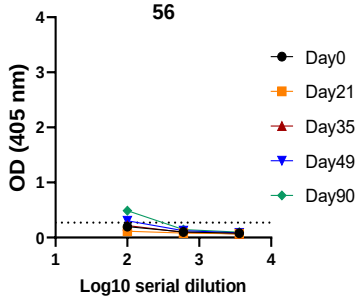
	Day0	Day21	Day35	Day49	Day90
Total Area	423.3	263.8	500.3	865.3	1224



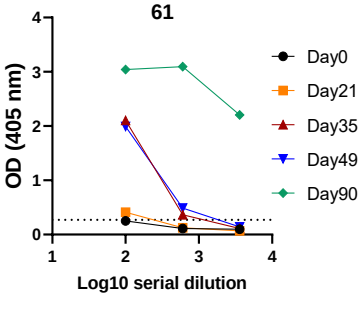
	Day0	Day21	Day35	Day49	Day90
Total Area	434.3	678.0	2982	3084	1890



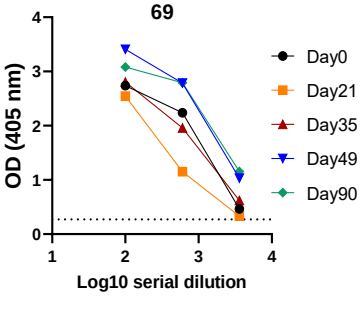
	Day0	Day21	Day35	Day49	Day90
Total Area	343.3	274.3	318.5	422.5	520.8



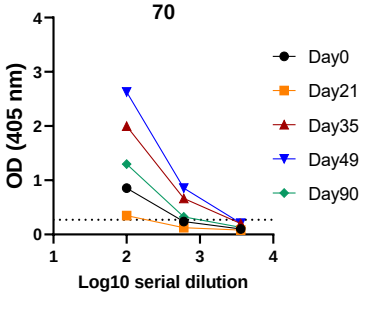
	Day0	Day21	Day35	Day49	Day90
Total Area	407.3	422.3	1331	1562	9481



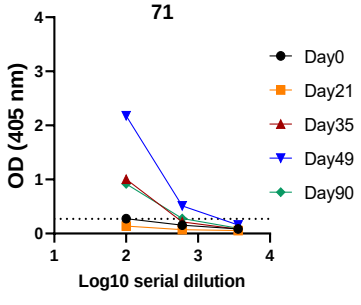
	Day0	Day21	Day35	Day49	Day90
Total Area	5299	3151	5059	7275	7389



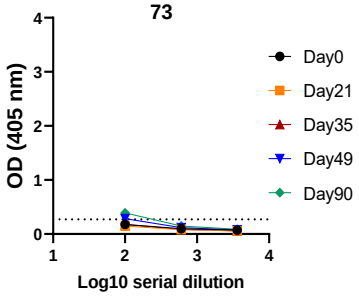
	Day0	Day21	Day35	Day49	Day90
Total Area	778.5	431.0	1968	2470	1086



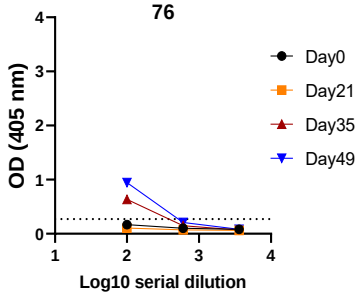
	Day0	Day21	Day35	Day49	Day90
Total Area	465.5	246.0	748.8	1681	864.5



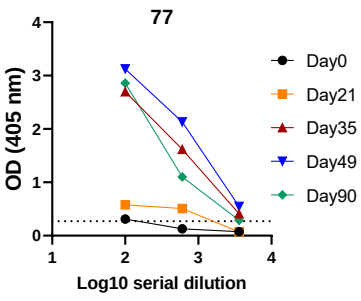
	Day0	Day21	Day35	Day49	Day90
Total Area	319.3	269.0	276.3	389.8	492.3



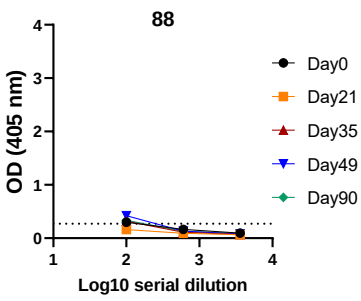
	Day0	Day21	Day35	Day49
Total Area	345.3	242.3	521.5	728.3



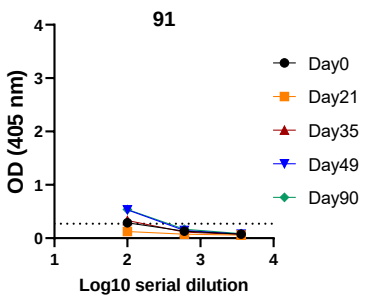
	Day0	Day21	Day35	Day49	Day90
Total Area	416.5	1145	4124	5331	3077



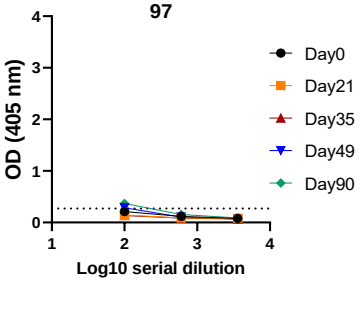
	Day0	Day21	Day35	Day49	Day90
Total Area	504.3	297.0	379.3	453.0	439.5



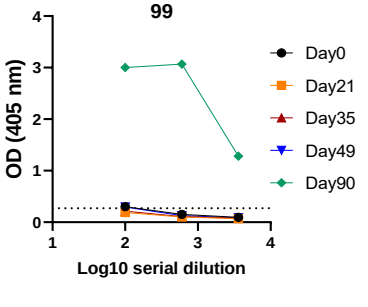
	Day0	Day21	Day35	Day49	Day90
Total Area	415.8	254.5	388.3	500.8	555.8



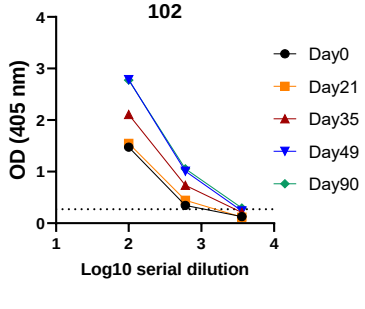
	Day0	Day21	Day35	Day49	Day90
Total Area	376.5	314.0	281.5	358.8	497.3



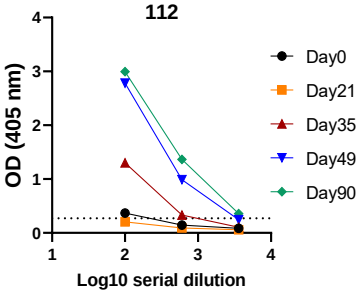
	Day0	Day21	Day35	Day49	Day90
Total Area	484.3	322.8	357.8	427.3	8042



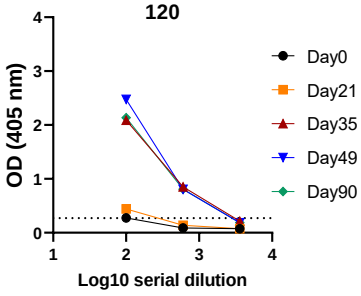
	Day0	Day21	Day35	Day49	Day90
Total Area	1164	1341	2127	2818	2981



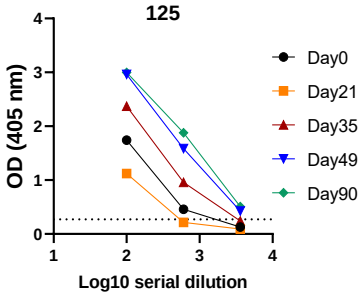
	Day0	Day21	Day35	Day49	Day90
Total Area	471.8	297.8	1064	2794	3675



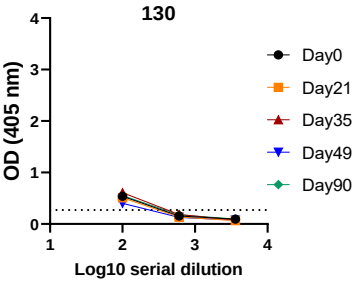
	Day0	Day21	Day35	Day49	Day90
Total Area	340.3	465.0	2338	2305	2230



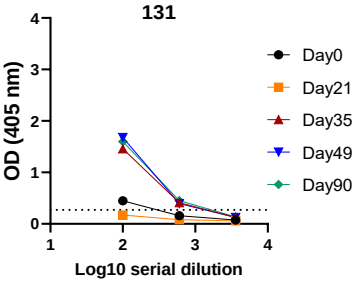
	Day0	Day21	Day35	Day49	Day90
Total Area	1428	791.8	2636	4154	4804



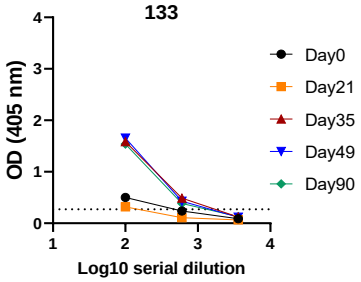
	Day0	Day21	Day35	Day49	Day90
Total Area	548.5	462.0	590.0	433.5	593.5



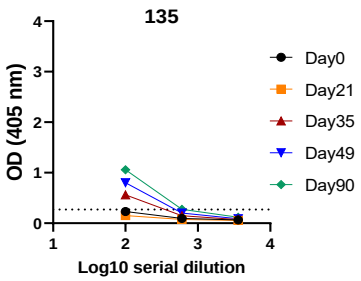
	Day0	Day21	Day35	Day49	Day90
Total Area	499.0	274.5	1275	1300	1393



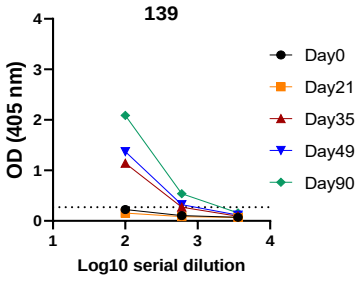
	Day0	Day21	Day35	Day49	Day90
Total Area	672.3	362.8	1431	1338	1250



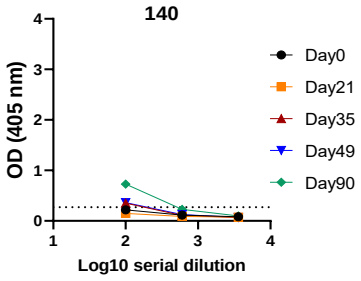
	Day0	Day21	Day35	Day49	Day90
Total Area	321.8	253.5	504.3	682.8	924.5



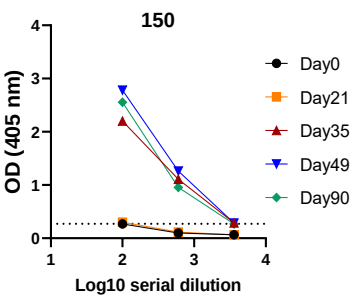
	Day0	Day21	Day35	Day49	Day90
Total Area	343.0	291.3	898.0	1078	1702



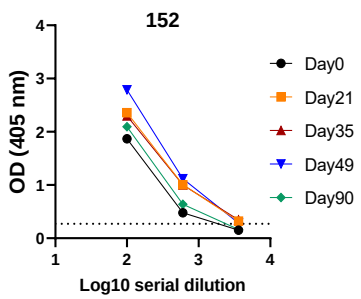
	Day0	Day21	Day35	Day49	Day90
Total Area	375.8	302.5	379.3	412.8	729.8



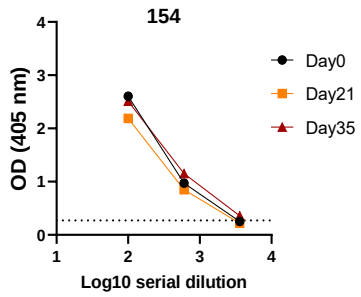
	Day0	Day21	Day35	Day49	Day90
Total Area	334.3	375.5	2922	3335	2710



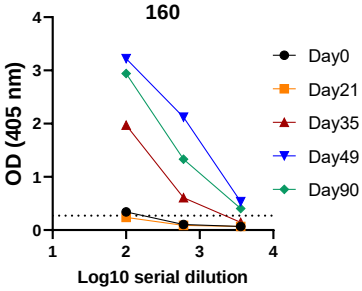
	Day0	Day21	Day35	Day49	Day90
Total Area	1529	2828	2848	3085	1889



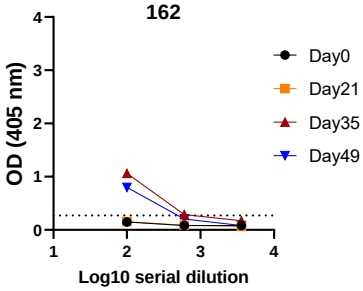
	Day0	Day21	Day35
Total Area	2724	2360	3181



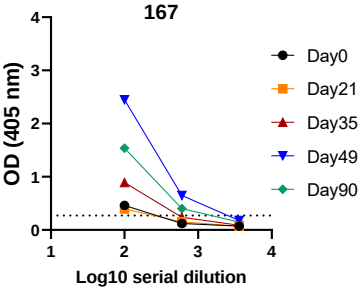
	Day0	Day21	Day35	Day49	Day90
Total Area	368.3	321.0	1776	5318	3671



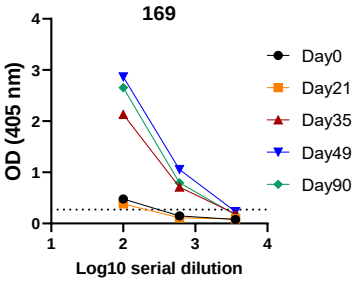
	Day0	Day21	Day35	Day49
Total Area	301.0	292.3	1026	684.3



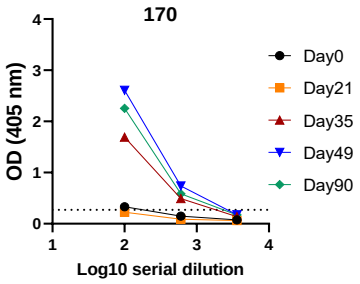
	Day0	Day21	Day35	Day49	Day90
Total Area	439.8	471.3	771.8	2015	1308



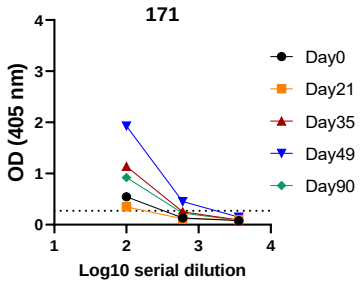
	Day0	Day21	Day35	Day49	Day90
Total Area	495.5	424.0	2055	2911	2304



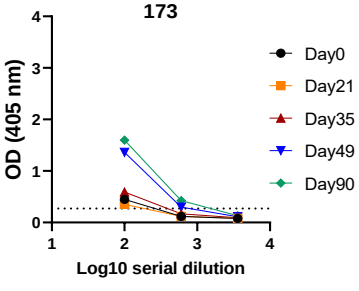
	Day0	Day21	Day35	Day49	Day90
Total Area	456.3	303.8	1489	2208	1847



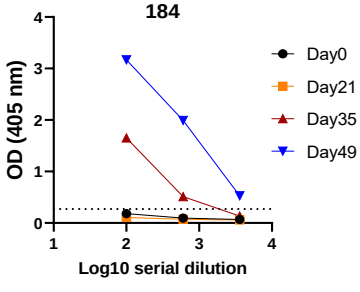
	Day0	Day21	Day35	Day49	Day90
Total Area	479.5	439.5	866.5	1494	754.8



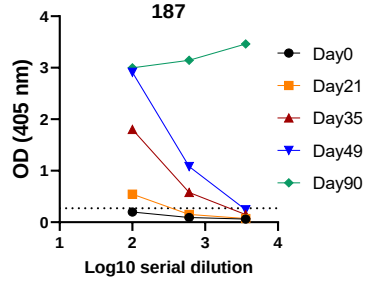
	Day0	Day21	Day35	Day49	Day90
Total Area	437.8	418.3	578.5	1031	1343



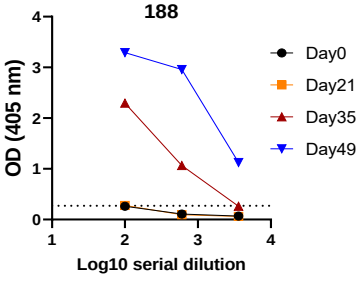
	Day0	Day21	Day35	Day49
Total Area	313.8	236.8	1509	5067



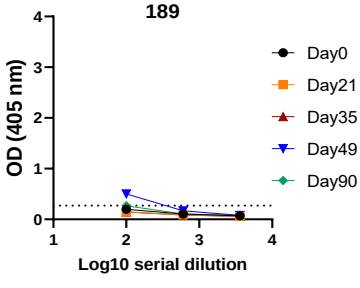
	Day0	Day21	Day35	Day49	Day90
Total Area	305.0	506.8	1684	2985	11445



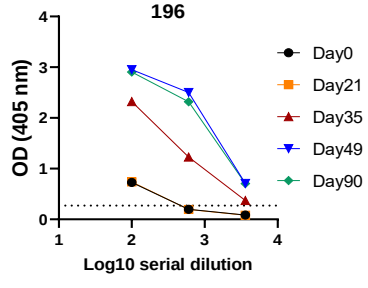
	Day0	Day21	Day35	Day49
Total Area	359.8	329.0	2834	7685



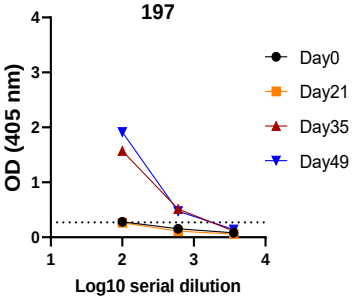
	Day0	Day21	Day35	Day49	Day90
Total Area	333.8	283.3	270.0	538.5	373.8



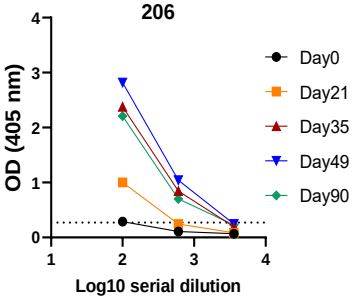
	Day0	Day21	Day35	Day49	Day90
Total Area	656.5	648.5	3287	6175	5842



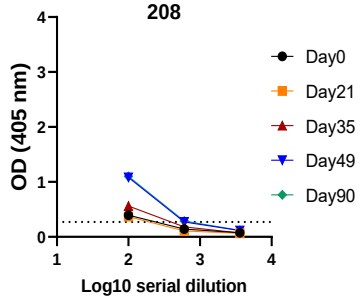
	Day0	Day21	Day35	Day49
Total Area	463.0	348.5	1459	1518



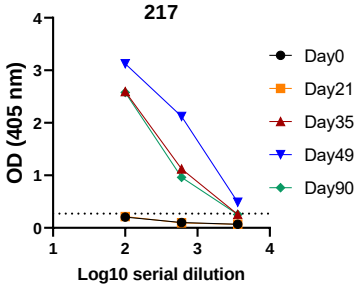
	Day0	Day21	Day35	Day49	Day90
Total Area	362.0	805.3	2364	2894	2126



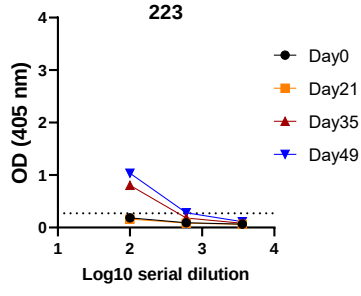
	Day0	Day21	Day35	Day49	Day90
Total Area	457.8	378.8	567.5	918.5	957.5



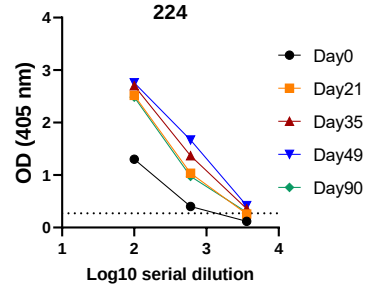
	Day0	Day21	Day35	Day49	Day90
Total Area	329.8	319.0	2995	5222	2710



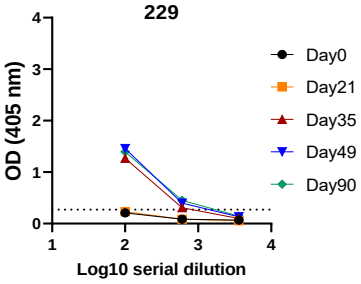
	Day0	Day21	Day35	Day49
Total Area	304.8	282.3	640.8	917.3



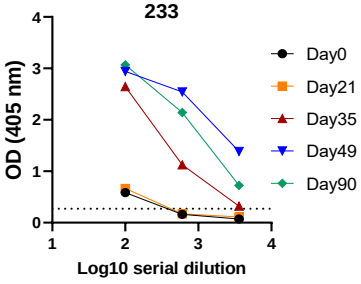
	Day0	Day21	Day35	Day49	Day90
Total Area	1201	2831	3605	4240	2764



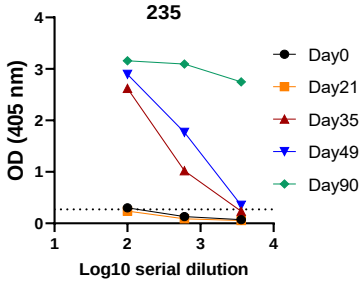
	Day0	Day21	Day35	Day49	Day90
Total Area	304.3	289.3	1003	1258	1354



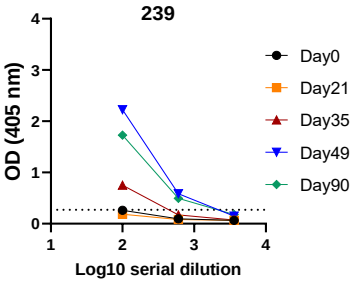
	Day0	Day21	Day35	Day49	Day90
Total Area	534.3	634.3	3109	7259	5605



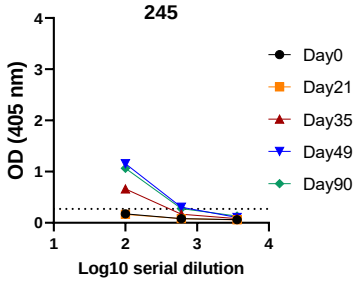
	Day0	Day21	Day35	Day49	Day90
Total Area	410.0	293.0	2794	4344	10326



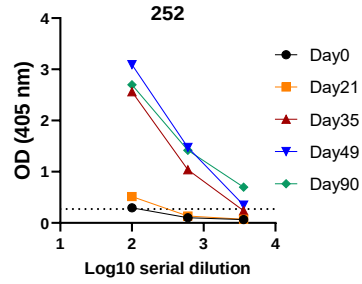
	Day0	Day21	Day35	Day49	Day90
Total Area	329.5	288.5	592.5	1804	1565



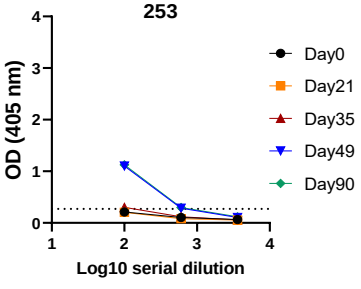
	Day0	Day21	Day35	Day49	Day90
Total Area	279.8	271.5	578.0	977.0	952.3



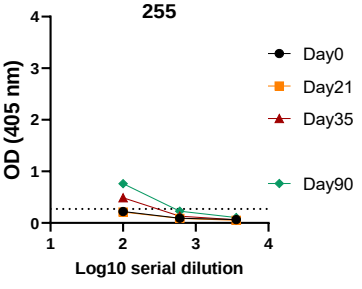
	Day0	Day21	Day35	Day49	Day90
Total Area	345.0	473.0	2813	3877	4204



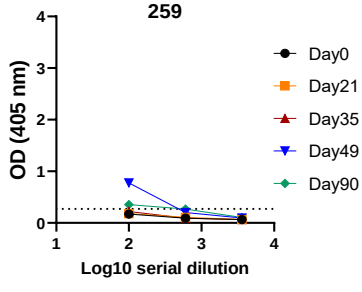
	Day0	Day21	Day35	Day49	Day90
Total Area	332.3	278.8	366.0	933.3	978.0



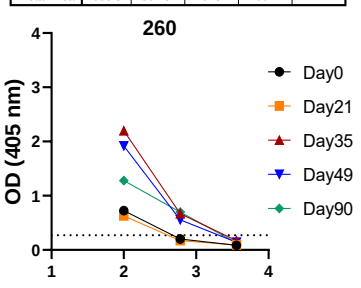
	Day0	Day21	Day35	Day90
Total Area	316.8	283.0	445.8	748.5



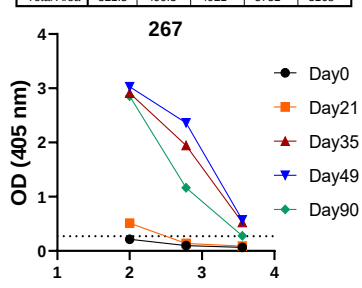
	Day0	Day21	Day35	Day49	Day90
Total Area	299.5	329.0	310.3	691.5	714.0



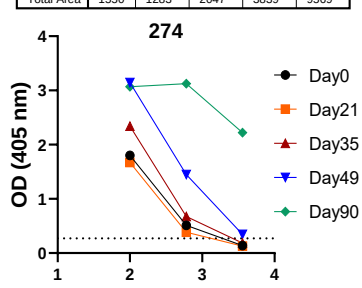
	Day0	Day21	Day35	Day49	Day90
Total Area	663.8	594.3	1978	1664	1744



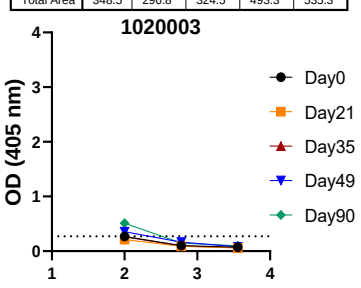
	Day0	Day21	Day35	Day49	Day90
Total Area	321.3	499.3	4921	5751	3168



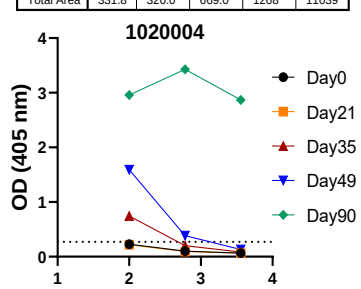
	Day0	Day21	Day35	Day49	Day90
Total Area	1550	1283	2047	3839	9569



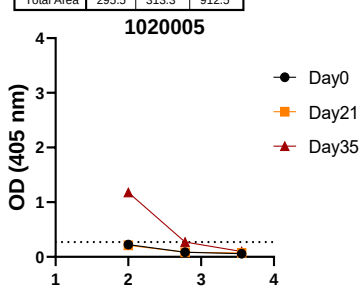
	Day0	Day21	Day35	Day49	Day90
Total Area	348.5	296.8	324.5	493.3	535.3



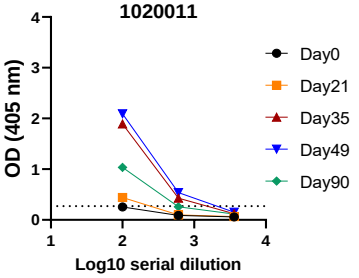
	Day0	Day21	Day35	Day49	Day90
Total Area	331.8	320.0	669.0	1268	11039



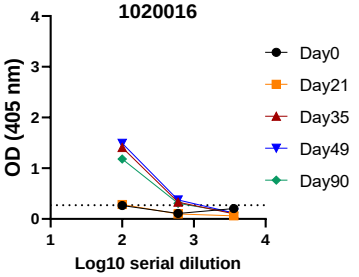
	Day0	Day21	Day35
Total Area	295.5	313.3	912.5



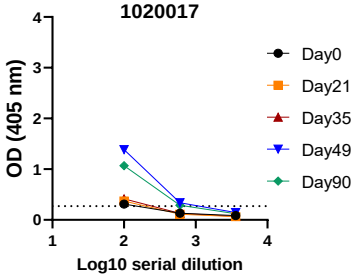
	Day0	Day21	Day35	Day49	Day90
Total Area	306.5	379.3	1407	1694	884.3



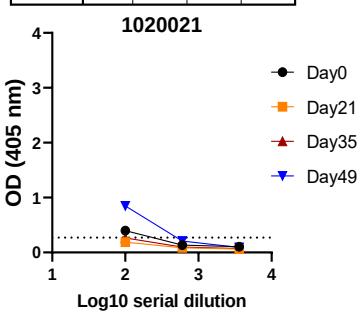
	Day0	Day21	Day35	Day49	Day90
Total Area	562.8	334.3	1084	1205	1016



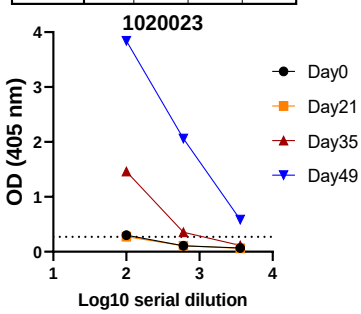
	Day0	Day21	Day35	Day49	Day90
Total Area	433.5	383.3	429.3	1156	955.3



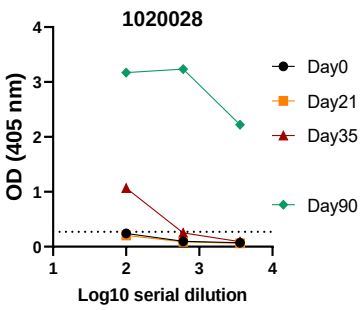
	Day0	Day21	Day35	Day49
Total Area	496.3	290.0	348.8	719.3



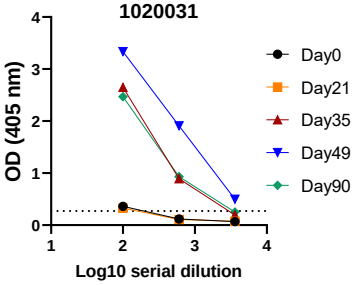
	Day0	Day21	Day35	Day49
Total Area	368.0	352.0	1159	5442



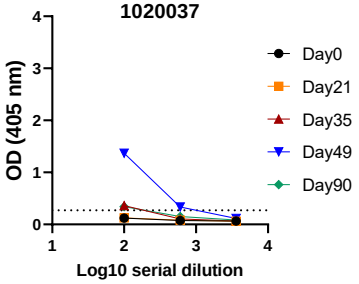
	Day0	Day21	Day35	Day90
Total Area	343.0	300.0	841.3	9786



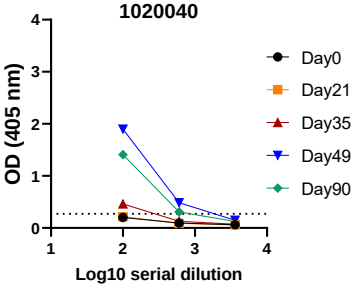
	Day0	Day21	Day35	Day49	Day90
Total Area	404.3	383.5	2512	4916	2623



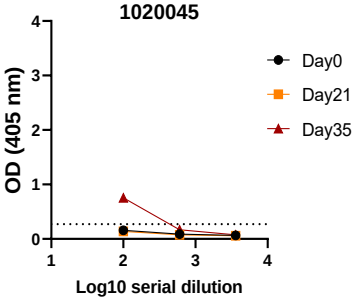
	Day0	Day21	Day35	Day49	Day90
Total Area	259.3	266.0	371.5	1099	482.0



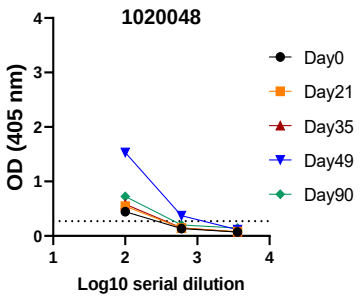
	Day0	Day21	Day35	Day49	Day90
Total Area	313.0	297.8	445.8	1546	1079



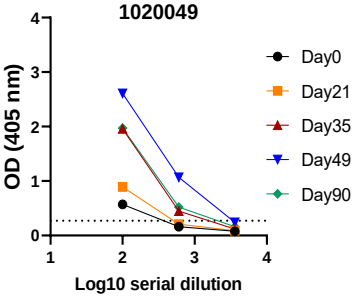
	Day0	Day21	Day35
Total Area	287.8	250.8	593.8



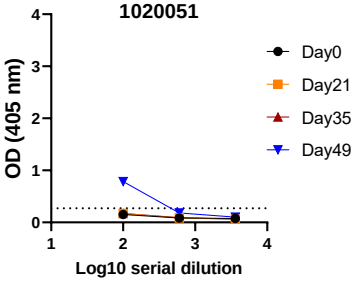
	Day0	Day21	Day35	Day49	Day90
Total Area	457.0	503.5	511.3	1207	750.3



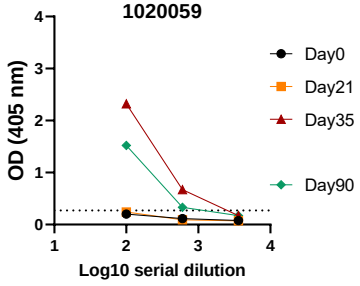
	Day0	Day21	Day35	Day49	Day90
Total Area	539.8	721.0	1451	2883	1648



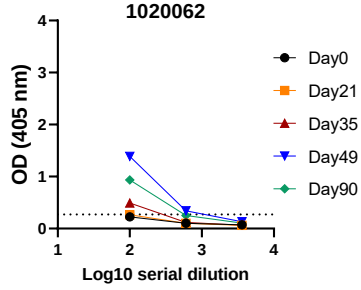
	Day0	Day21	Day35	Day49
Total Area	299.5	284.8	297.0	664.8



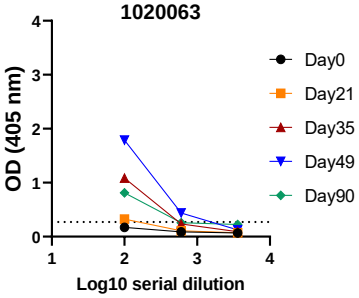
	Day0	Day21	Day35	Day90
Total Area	371.5	331.3	2008	1219



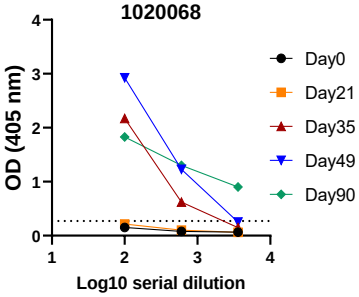
	Day0	Day21	Day35	Day49	Day90
Total Area	341.0	334.5	430.3	1143	834.3



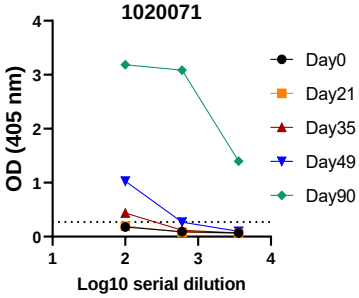
	Day0	Day21	Day35	Day49	Day90
Total Area	295.5	373.5	821.8	1399	989.8



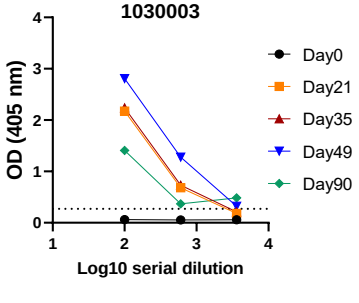
	Day0	Day21	Day35	Day49	Day90
Total Area	274.0	326.8	1853	3260	4082



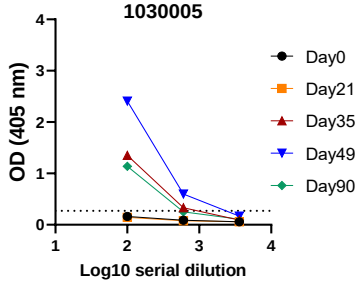
	Day0	Day21	Day35	Day49	Day90
Total Area	309.0	285.8	416.5	873.0	8289



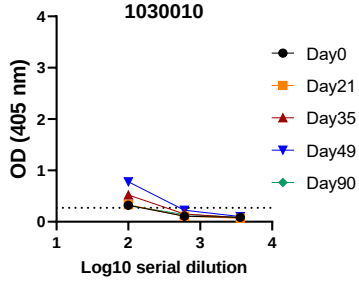
	Day0	Day21	Day35	Day49	Day90
Total Area	200.3	2012	2157	3422	1726



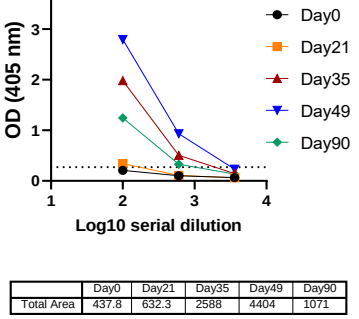
	Day0	Day21	Day35	Day49	Day90
Total Area	284.3	263.0	1059	1902	889.8



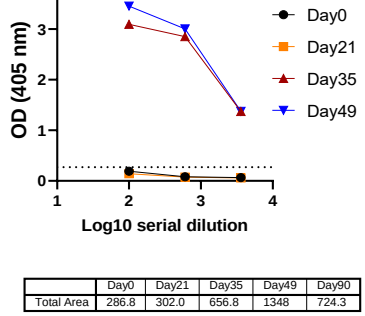
	Day0	Day21	Day35	Day49	Day90
Total Area	396.8	375.3	512.0	740.0	452.5



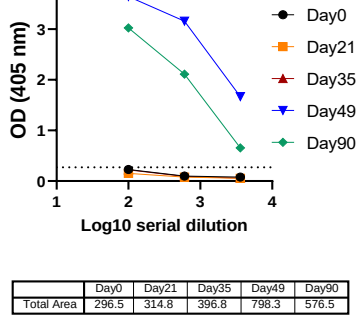
	Day0	Day21	Day35	Day49	Day90
Total Area	330.0	367.5	1593	2675	1088



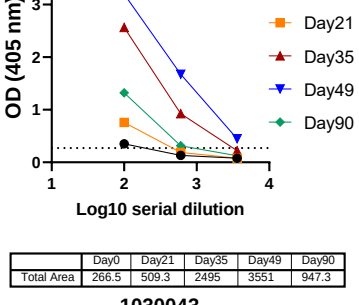
	Day0	Day21	Day35	Day49
Total Area	287.0	258.8	7823	8185



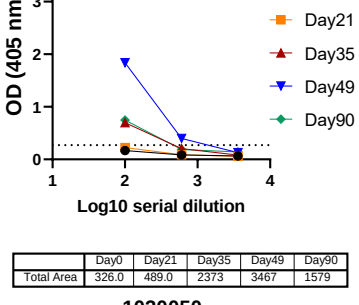
	Day0	Day21	Day35	Day49	Day90
Total Area	345.5	256.8	305.0	8941	5435



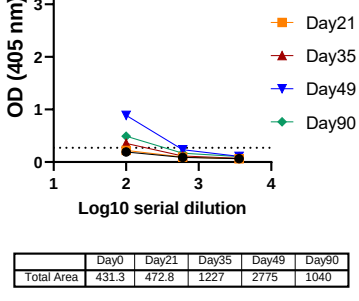
	Day0	Day21	Day35	Day49	Day90
Total Area	437.8	632.3	2588	4404	1071



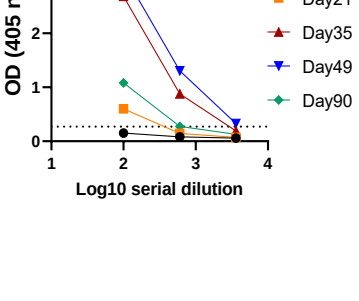
	Day0	Day21	Day35	Day49	Day90
Total Area	286.8	302.0	656.8	1348	724.3



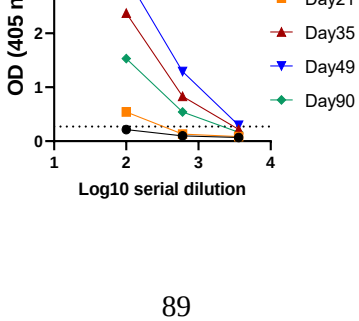
	Day0	Day21	Day35	Day49	Day90
Total Area	296.5	314.8	396.8	798.3	576.5



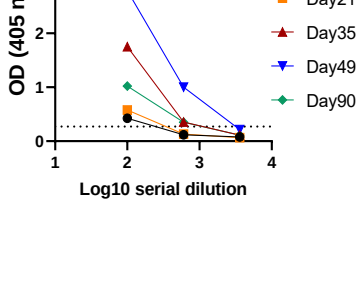
	Day0	Day21	Day35	Day49	Day90
Total Area	266.5	509.3	2495	3551	947.3



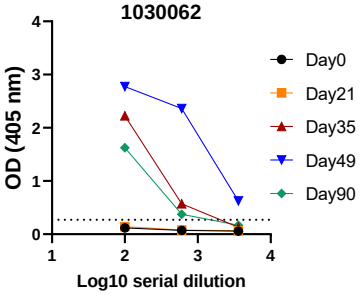
	Day0	Day21	Day35	Day49	Day90
Total Area	326.0	489.0	2373	3467	1579



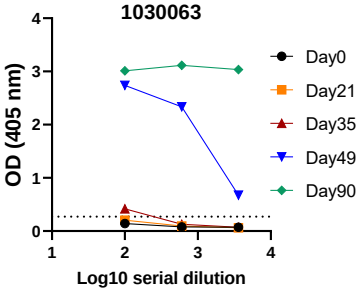
	Day0	Day21	Day35	Day49	Day90
Total Area	431.3	472.8	1227	2775	1040



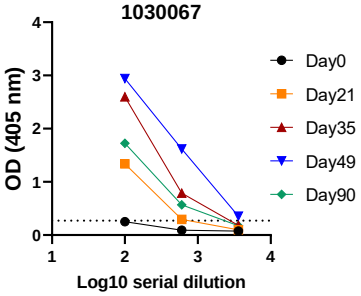
	Day0	Day21	Day35	Day49	Day90
Total Area	244.8	266.3	1754	5765	1316



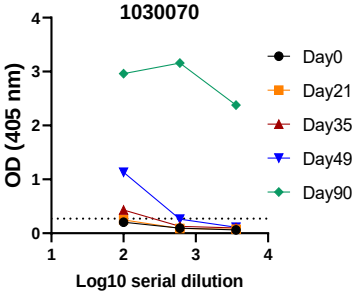
	Day0	Day21	Day35	Day49	Day90
Total Area	278.3	310.5	431.5	5783	10757



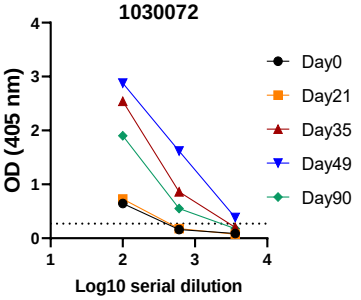
	Day0	Day21	Day35	Day49	Day90
Total Area	339.5	996.0	2302	4101	1686



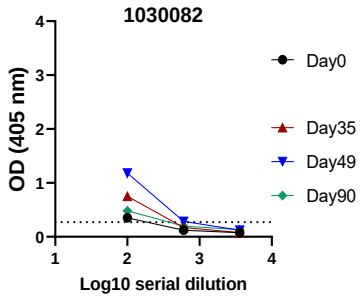
	Day0	Day21	Day35	Day49	Day90
Total Area	310.0	327.3	477.3	908.0	9833



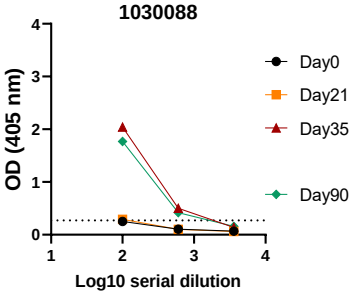
	Day0	Day21	Day35	Day49	Day90
Total Area	576.8	606.0	2447	4128	1710



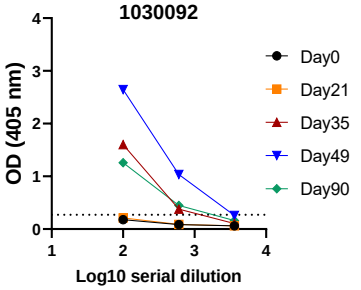
	Day0	Day35	Day49	Day90
Total Area	414.0	609.5	978.8	662.3



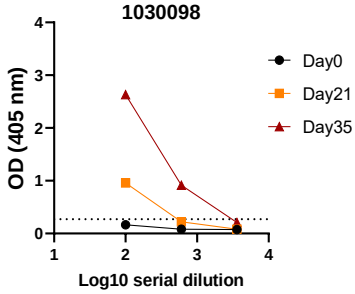
	Day0	Day21	Day35	Day90
Total Area	347.0	341.3	1597	1414



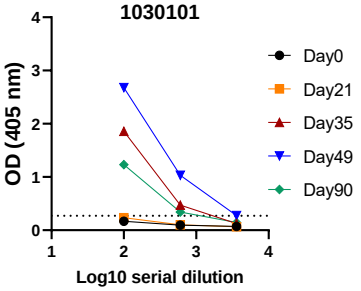
	Day0	Day21	Day35	Day49	Day90
Total Area	287.0	303.3	1216	2858	1342



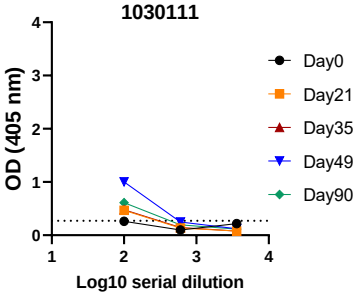
	Day0	Day21	Day35
Total Area	299.0	748.5	2570



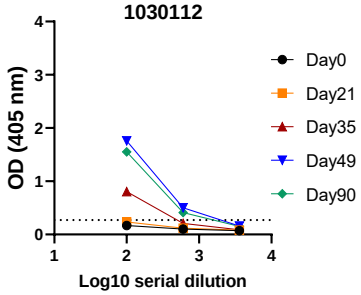
	Day0	Day21	Day35	Day49	Day90
Total Area	318.0	329.5	1475	2885	1125



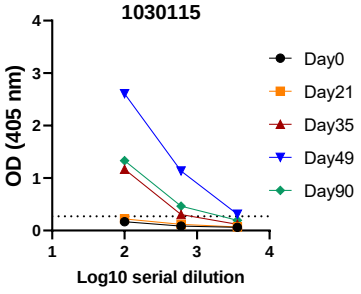
	Day0	Day21	Day35	Day49	Day90
Total Area	565.5	472.3	487.3	867.3	665.3



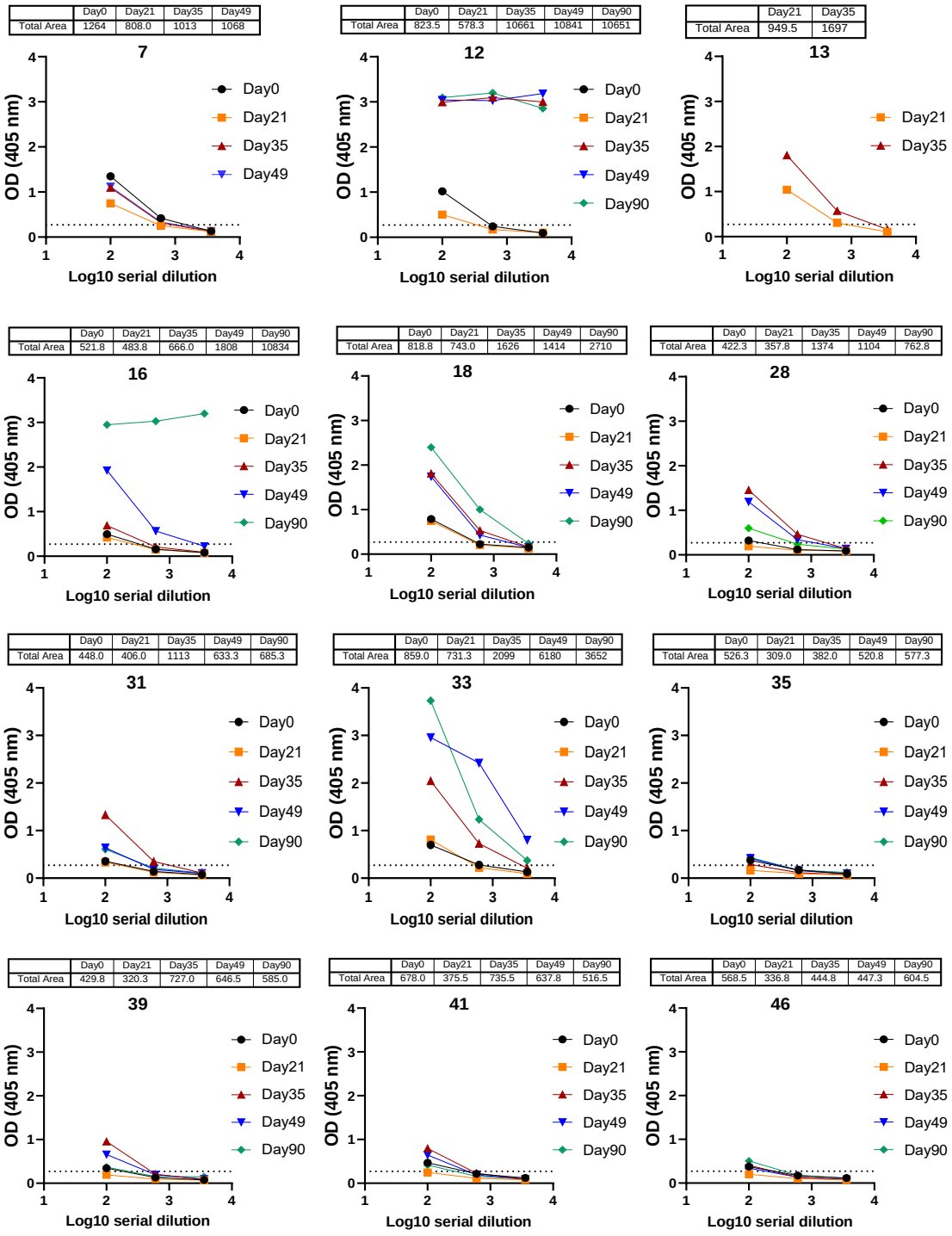
	Day0	Day21	Day35	Day49	Day90
Total Area	331.8	388.3	703.8	1553	1335



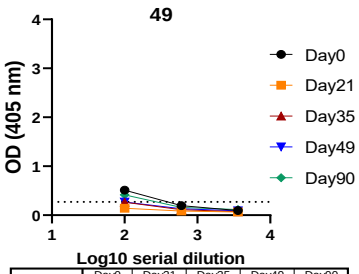
	Day0	Day21	Day35	Day49	Day90
Total Area	285.3	365.5	999.5	3105	1440



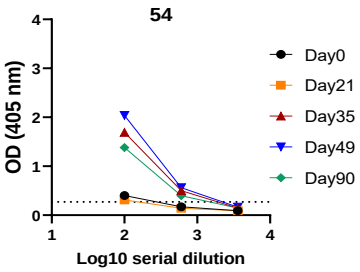
Day by day individual OD graphs after injection of VLP-58-1023-AL-K3 vaccine for each Phase 2 volunteers with 6X serial dilutions of sera from 100X to 3600X against recombinant N protein. 96-well 2HB maxi-binding ELISA plates were coated with 4 ug/ml in-house recombinant nucleocapsid protein and plates were blocked. After serial dilutions of volunteers' sera, ALP-tagged anti-human IgG secondary antibody were filled into wells and finally PNPP substrate was added into plate and optical density values were recorded at 405 nm.



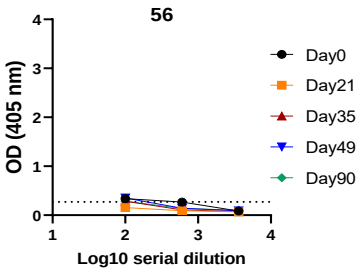
	Day0	Day21	Day35	Day49	Day90
Total Area	608.3	279.5	366.8	430.5	550.8



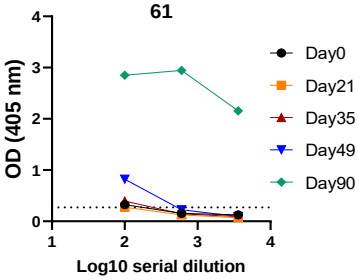
	Day0	Day21	Day35	Day49	Day90
Total Area	537.3	467.3	1517	1737	1260



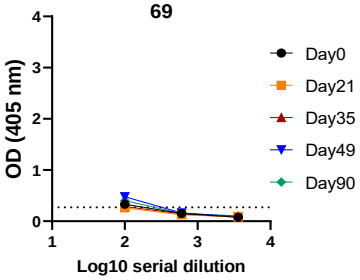
	Day0	Day21	Day35	Day49	Day90
Total Area	679.8	302.0	367.3	467.8	464.5



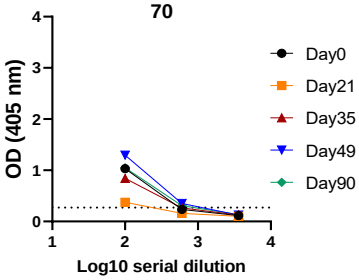
	Day0	Day21	Day35	Day49	Day90
Total Area	538.5	387.5	487.5	741.8	9100



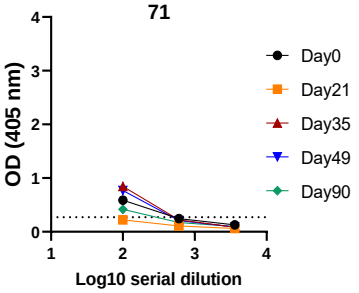
	Day0	Day21	Day35	Day49	Day90
Total Area	465.3	410.3	439.5	539.8	525.3



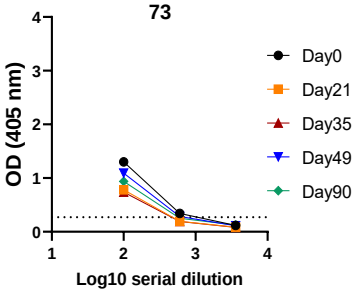
	Day0	Day21	Day35	Day49	Day90
Total Area	843.0	520.0	861.8	1126	1000



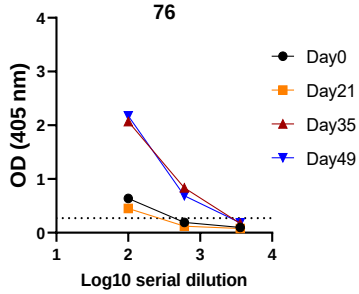
	Day0	Day21	Day35	Day49	Day90
Total Area	768.0	337.0	722.5	688.3	549.3



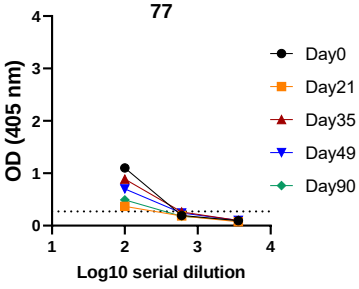
	Day0	Day21	Day35	Day49	Day90
Total Area	1102	664.3	642.3	943.0	857.8



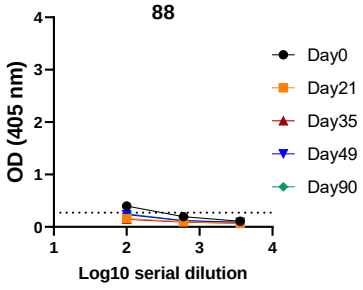
	Day0	Day21	Day35	Day49
Total Area	640.3	444.8	2232	2027



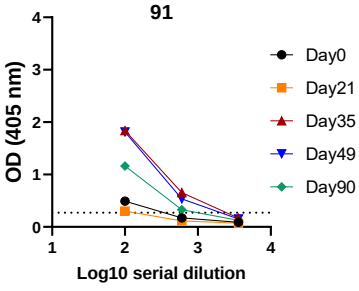
	Day0	Day21	Day35	Day49	Day90
Total Area	757.8	528.5	830.8	750.3	589.5



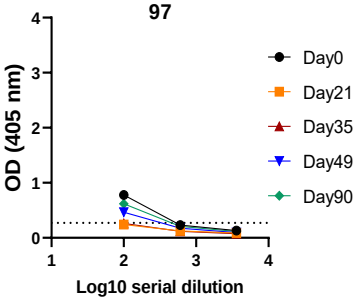
	Day0	Day21	Day35	Day49	Day90
Total Area	601.0	312.8	300.8	400.8	403.0



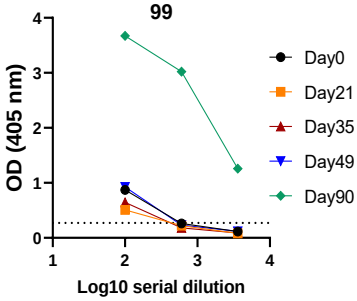
	Day0	Day21	Day35	Day49	Day90
Total Area	561.0	381.8	1858	1617	1052



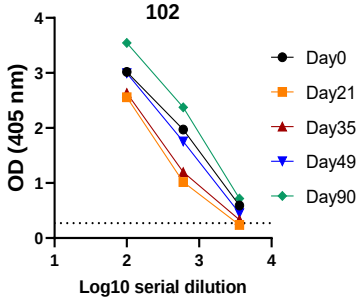
	Day0	Day21	Day35	Day49	Day90
Total Area	791.8	411.3	388.3	563.3	693.3



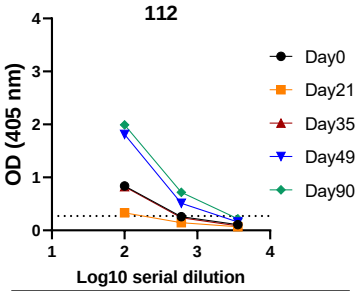
	Day0	Day21	Day35	Day49	Day90
Total Area	844.3	631.8	610.5	814.8	8092



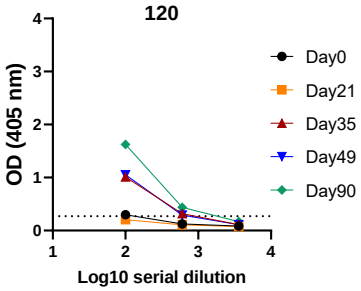
	Day0	Day21	Day35	Day49	Day90
Total Area	5090	2778	3249	4493	6121



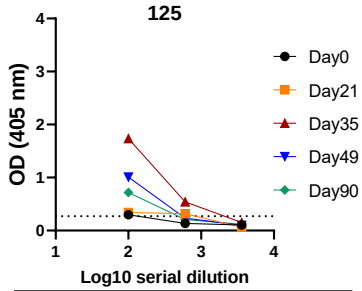
	Day0	Day21	Day35	Day49	Day90
Total Area	823.0	435.8	746.8	1586	2085



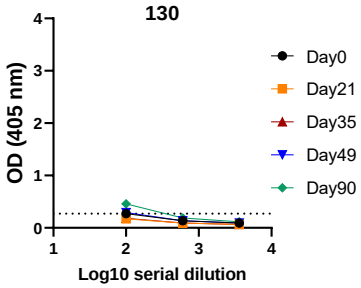
	Day0	Day21	Day35	Day49	Day90
Total Area	420.3	351.0	974.5	941.5	1425



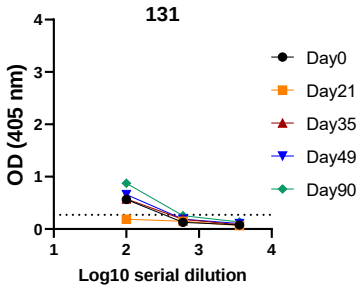
	Day0	Day21	Day35	Day49	Day90
Total Area	465.0	737.8	1610	806.8	722.0



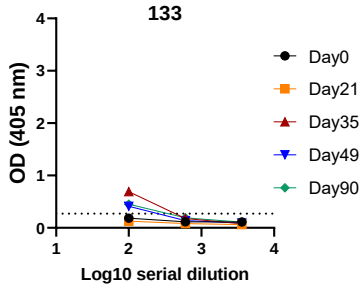
	Day0	Day21	Day35	Day49	Day90
Total Area	440.8	301.0	307.3	447.0	615.8



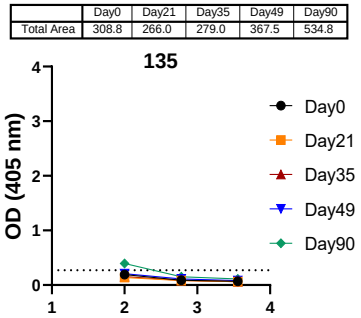
	Day0	Day21	Day35	Day49	Day90
Total Area	480.5	404.8	587.0	648.0	871.0



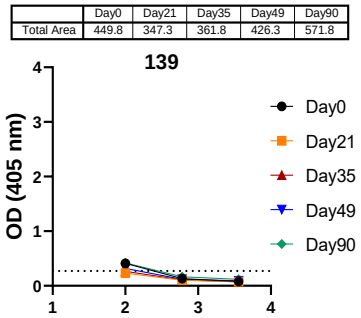
	Day0	Day21	Day35	Day49	Day90
Total Area	415.0	268.5	600.0	486.0	609.8



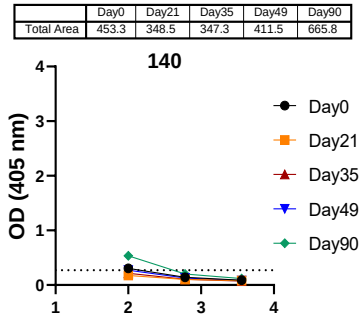
	Day0	Day21	Day35	Day49	Day90
Total Area	308.8	266.0	279.0	367.5	534.8



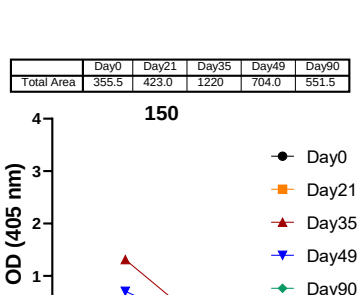
	Day0	Day21	Day35	Day49	Day90
Total Area	449.8	347.3	361.8	426.3	571.8



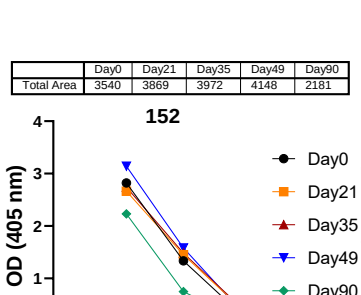
	Day0	Day21	Day35	Day49	Day90
Total Area	453.3	348.5	347.3	411.5	665.8



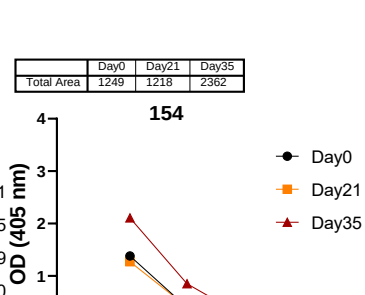
	Day0	Day21	Day35	Day49	Day90
Total Area	355.5	423.0	1220	704.0	551.5



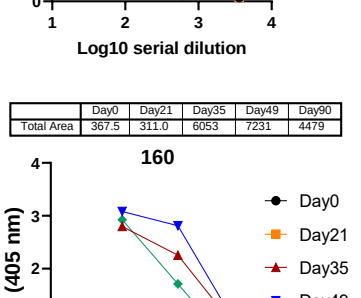
	Day0	Day21	Day35	Day49	Day90
Total Area	3540	3869	3972	4148	2181



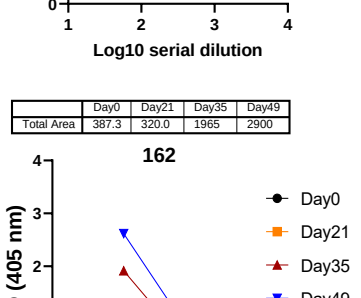
	Day0	Day21	Day35
Total Area	1249	1218	2362



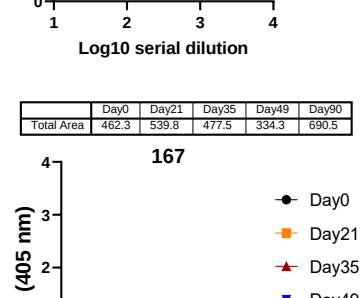
	Day0	Day21	Day35	Day49	Day90
Total Area	367.5	311.0	6053	7231	4479



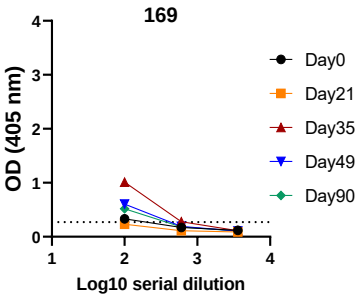
	Day0	Day21	Day35	Day49
Total Area	387.3	320.0	1965	2900



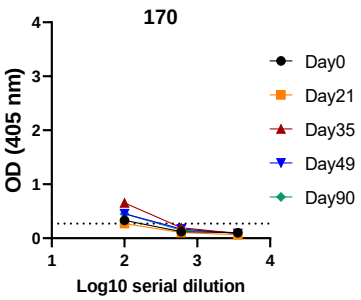
	Day0	Day21	Day35	Day49	Day90
Total Area	462.3	539.8	477.5	334.3	690.5



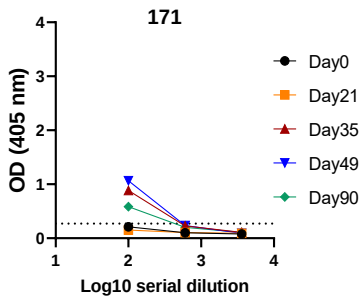
	Day0	Day21	Day35	Day49	Day90
Total Area	563.5	382.3	904.0	643.3	607.3



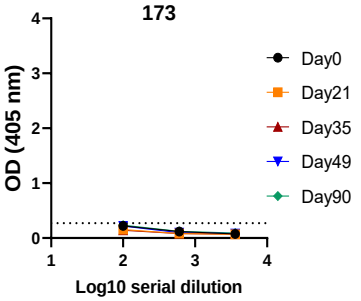
	Day0	Day21	Day35	Day49	Day90
Total Area	447.5	349.0	638.5	547.3	528.3



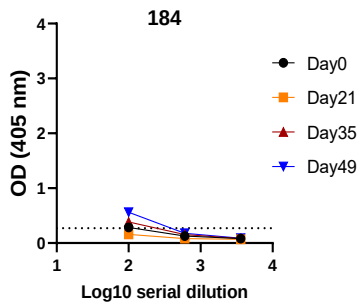
	Day0	Day21	Day35	Day49	Day90
Total Area	351.8	361.3	780.5	818.8	658.3



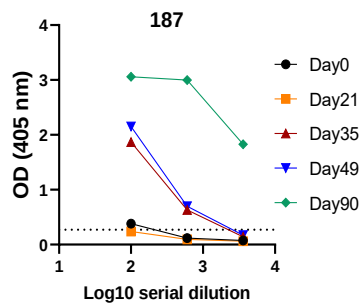
	Day0	Day21	Day35	Day49	Day90
Total Area	377.8	286.0	280.5	347.5	410.0



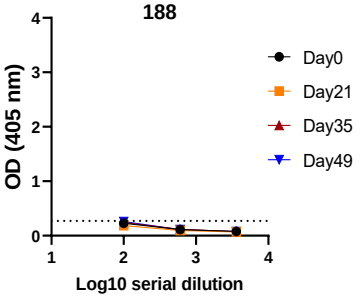
	Day0	Day21	Day35	Day49
Total Area	419.8	281.5	487.5	582.5



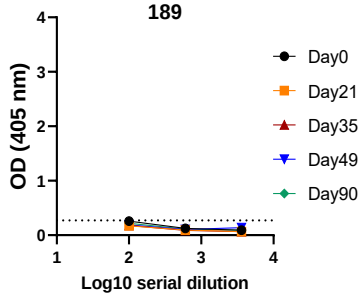
	Day0	Day21	Day35	Day49	Day90
Total Area	419.5	315.5	1786	2019	8751



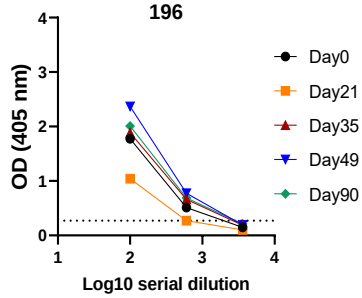
	Day0	Day21	Day35	Day49
Total Area	366.8	312.5	372.8	371.5



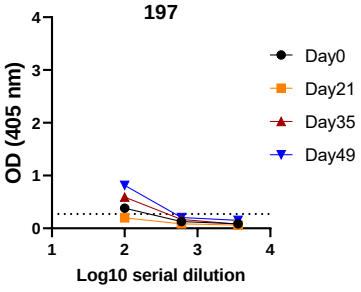
	Day0	Day21	Day35	Day49	Day90
Total Area	423.0	303.0	299.5	437.8	386.8



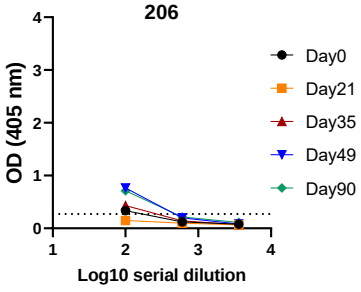
	Day0	Day21	Day35	Day49	Day90
Total Area	1565	888.0	1910	2235	2028



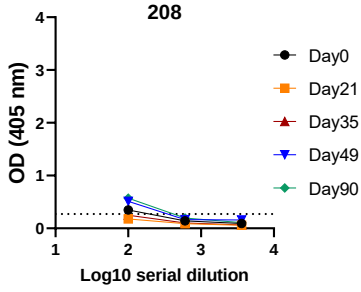
	Day0	Day21	Day35	Day49
Total Area	445.0	289.5	560.5	787.3



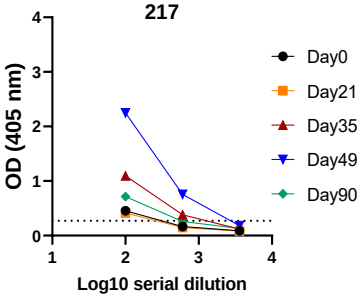
	Day0	Day21	Day35	Day49	Day90
Total Area	412.8	302.5	456.5	662.5	722.0



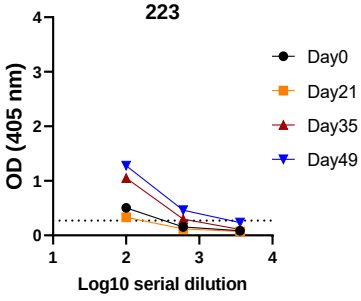
	Day0	Day21	Day35	Day49	Day90
Total Area	472.0	287.8	336.3	652.5	646.5



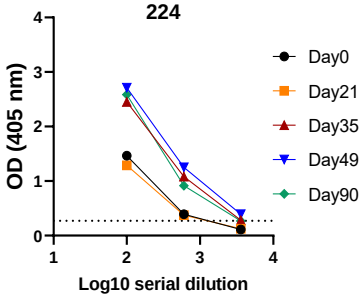
	Day0	Day21	Day35	Day49	Day90
Total Area	539.5	487.3	1118	2157	827.3



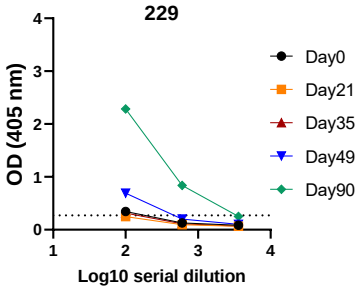
	Day0	Day21	Day35	Day49
Total Area	523.5	394.3	944.5	1481



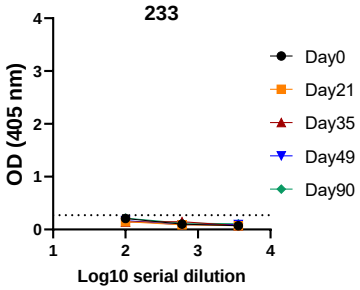
	Day0	Day21	Day35	Day49	Day90
Total Area	1214	1169	2928	3457	2651



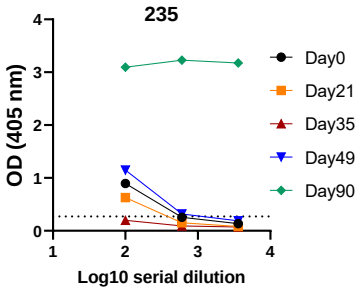
	Day0	Day21	Day35	Day49	Day90
Total Area	437.8	327.3	373.3	676.8	2411



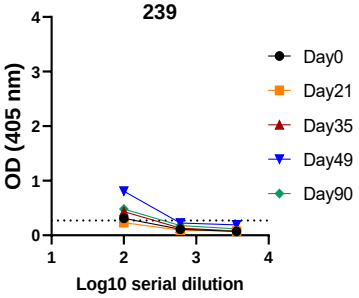
	Day0	Day21	Day35	Day49	Day90
Total Area	335.8	297.3	405.5	337.3	430.8



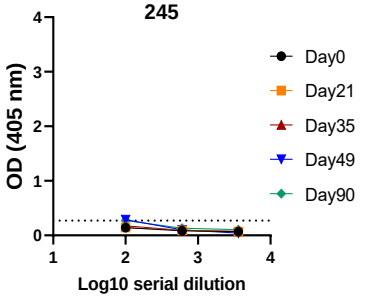
	Day0	Day21	Day35	Day49	Day90
Total Area	874.5	545.0	313.5	1127	11182



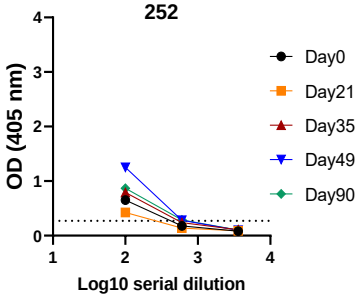
	Day0	Day21	Day35	Day49	Day90
Total Area	383.3	340.0	453.8	880.8	612.8



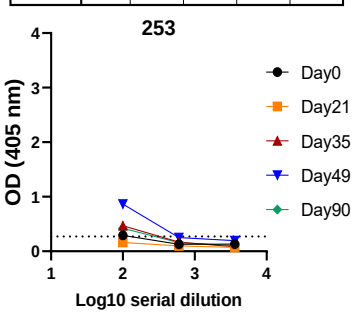
	Day0	Day21	Day35	Day49	Day90
Total Area	285.5	299.8	318.8	310.0	454.8



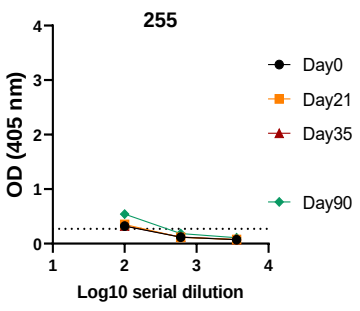
	Day0	Day21	Day35	Day49	Day90
Total Area	598.8	484.8	776.8	956.8	872.8



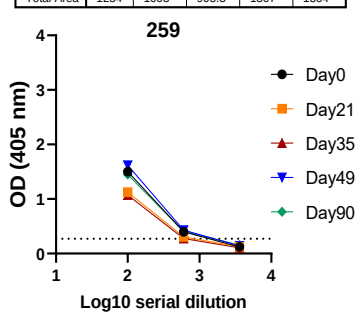
	Day0	Day21	Day35	Day49	Day90
Total Area	498.3	322.0	532.8	946.3	536.8



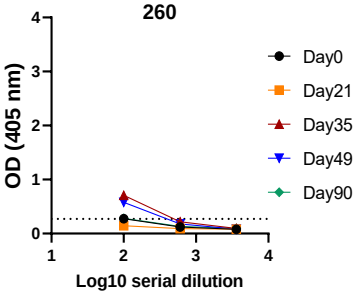
	Day0	Day21	Day35	Day90
Total Area	396.8	405.3	407.3	622.8



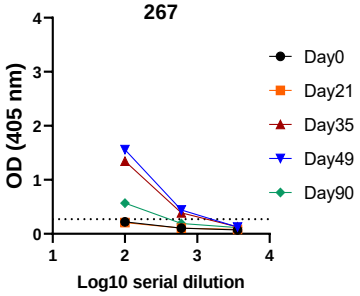
	Day0	Day21	Day35	Day49	Day90
Total Area	1254	1003	905.3	1367	1304



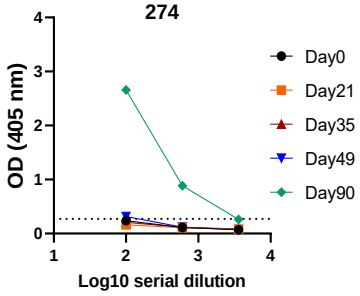
	Day0	Day21	Day35	Day49	Day90
Total Area	400.8	318.8	699.5	584.0	443.5



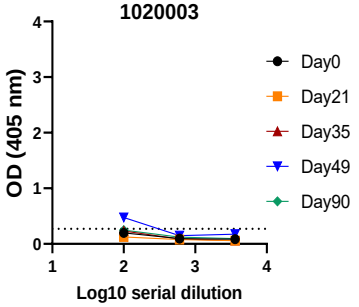
	Day0	Day21	Day35	Day49	Day90
Total Area	347.5	357.5	1206	1349	651.0



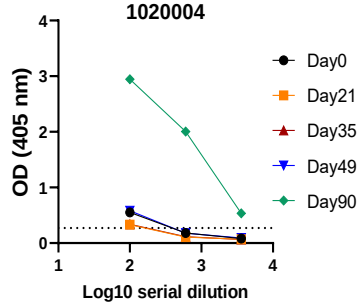
	Day0	Day21	Day35	Day49	Day90
Total Area	360.3	349.3	381.5	392.3	2602



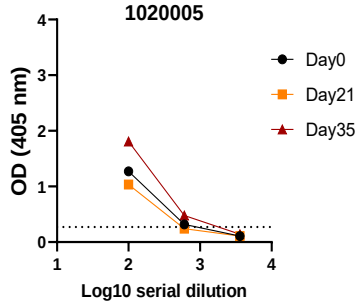
	Day0	Day21	Day35	Day49	Day90
Total Area	340.3	251.5	309.5	643.5	421.5



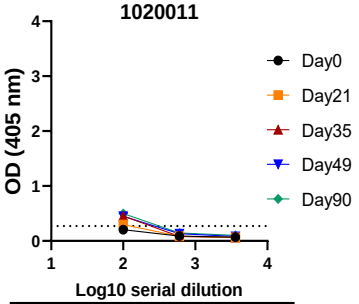
	Day0	Day21	Day35	Day49	Day90
Total Area	581.0	374.0	385.0	595.5	5051



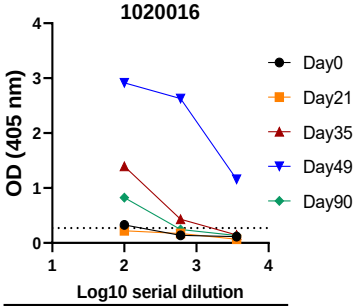
	Day0	Day21	Day35
Total Area	1036	842.8	1498



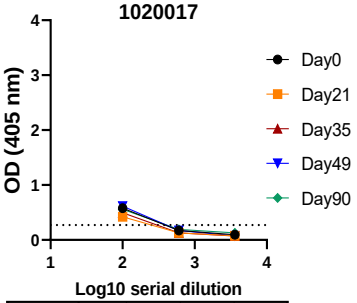
	Day0	Day21	Day35	Day49	Day90
Total Area	304.0	321.0	352.0	464.5	529.8



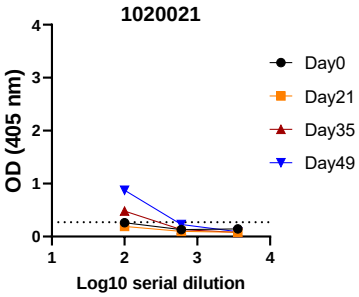
	Day0	Day21	Day35	Day49	Day90
Total Area	495.8	458.5	1321	7065	835.8



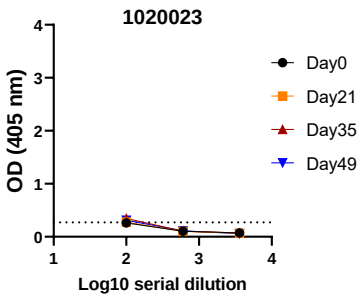
	Day0	Day21	Day35	Day49	Day90
Total Area	588.5	440.8	459.3	568.8	664.0



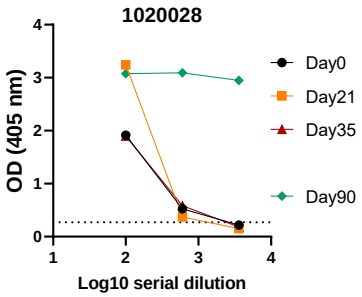
	Day0	Day21	Day35	Day49
Total Area	510.5	342.5	463.8	755.5



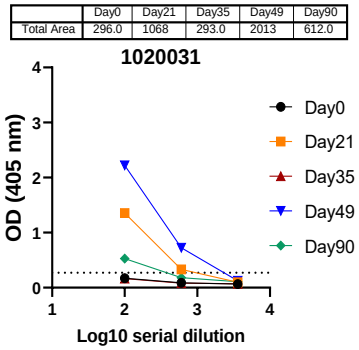
	Day0	Day21	Day35	Day49
Total Area	353.5	344.3	376.8	366.0



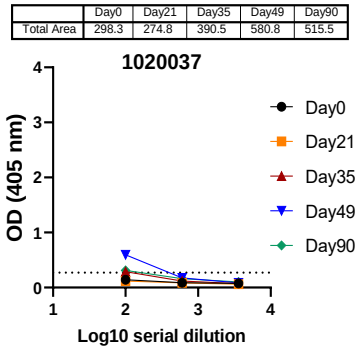
	Day0	Day21	Day35	Day90
Total Area	1725	1688	1768	10601



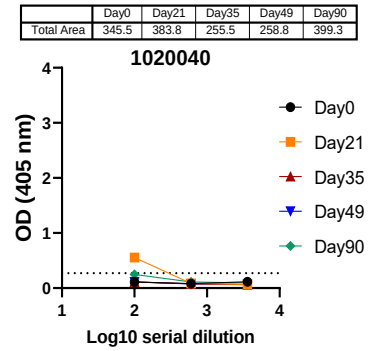
	Day0	Day21	Day35	Day49	Day90
Total Area	296.0	1068	293.0	2013	612.0



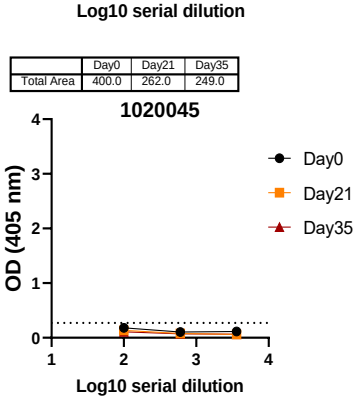
	Day0	Day21	Day35	Day49	Day90
Total Area	298.3	274.8	390.5	580.8	515.5



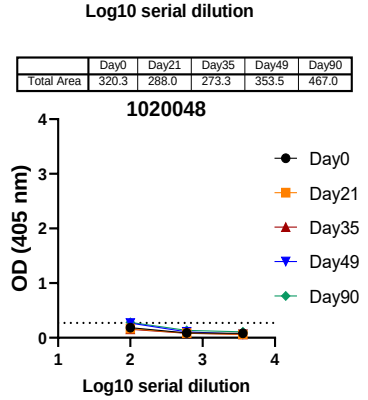
	Day0	Day21	Day35	Day49	Day90
Total Area	345.5	383.8	255.5	258.8	399.3



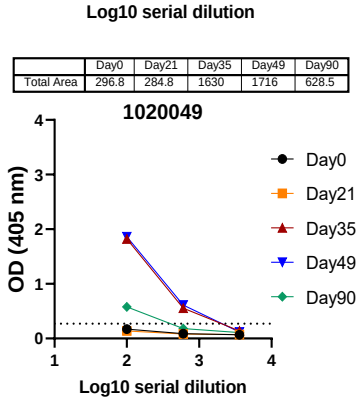
	Day0	Day21	Day35
Total Area	400.0	262.0	249.0



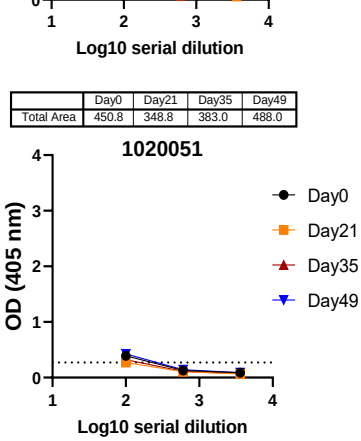
	Day0	Day21	Day35	Day49	Day90
Total Area	320.3	288.0	273.3	353.5	467.0



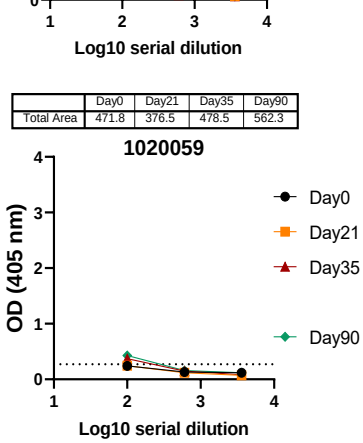
	Day0	Day21	Day35	Day49	Day90
Total Area	296.8	284.8	1630	1716	628.5



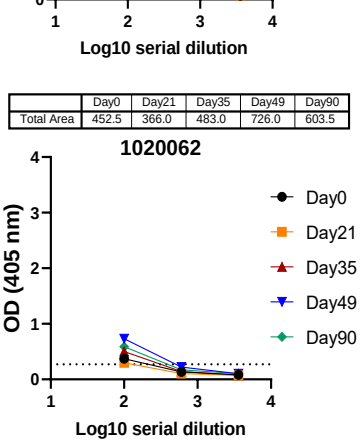
	Day0	Day21	Day35	Day49
Total Area	450.8	348.8	383.0	488.0



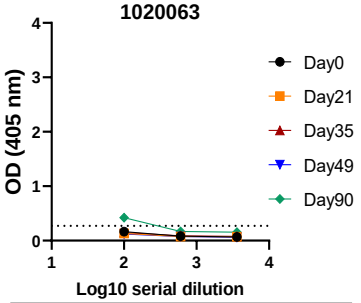
	Day0	Day21	Day35	Day90
Total Area	471.8	376.5	478.5	562.3



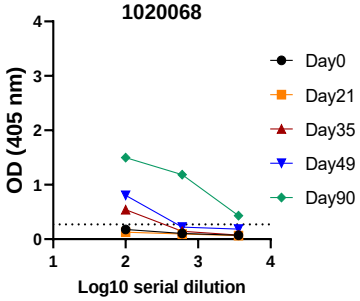
	Day0	Day21	Day35	Day49	Day90
Total Area	452.5	366.0	483.0	726.0	603.5



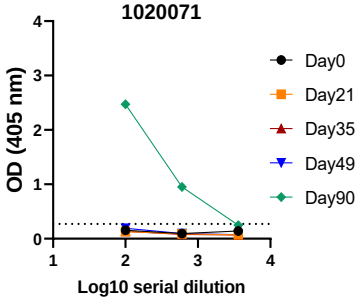
	Day0	Day21	Day35	Day49	Day90
Total Area	286.8	268.8	311.8	253.3	633.8



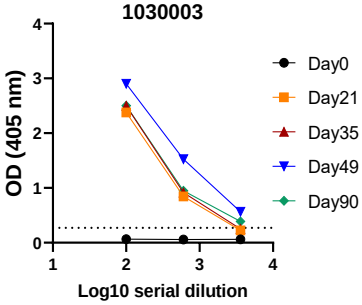
	Day0	Day21	Day35	Day49	Day90
Total Area	333.0	299.3	503.5	862.3	3097



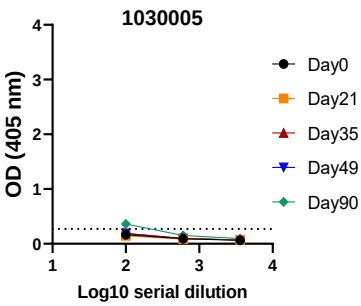
	Day0	Day21	Day35	Day49	Day90
Total Area	418.5	294.0	270.8	328.5	2658



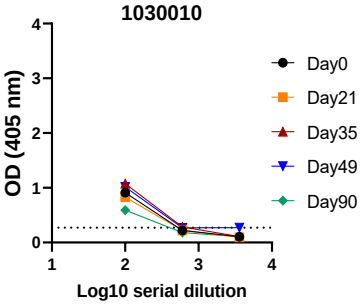
	Day0	Day21	Day35	Day49	Day90
Total Area	210.8	2408	2607	4240	2866



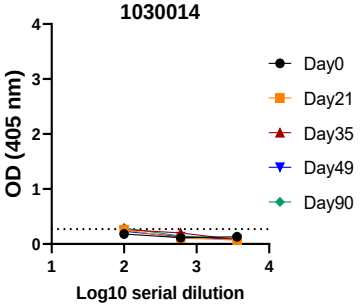
	Day0	Day21	Day35	Day49	Day90
Total Area	301.3	293.0	321.8	315.3	498.8



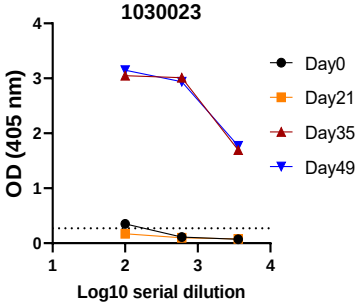
	Day0	Day21	Day35	Day49	Day90
Total Area	770.3	741.0	926.3	1128	628.5



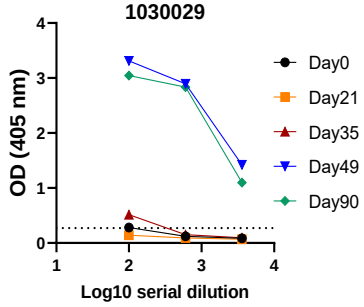
	Day0	Day21	Day35	Day49	Day90
Total Area	441.3	358.8	533.8	410.0	473.8



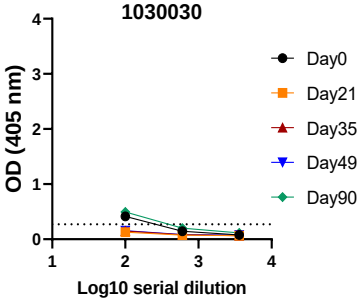
	Day0	Day21	Day35	Day49
Total Area	388.3	332.0	8576	8585



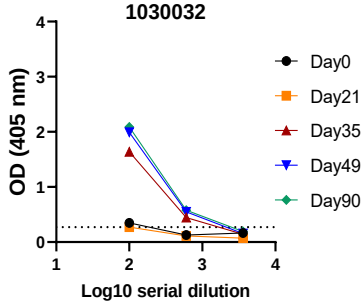
	Day0	Day21	Day35	Day49	Day90
Total Area	411.3	298.5	536.8	8026	7371



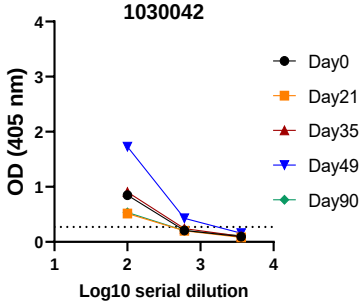
	Day0	Day21	Day35	Day49	Day90
Total Area	475.8	262.8	275.8	296.8	649.5



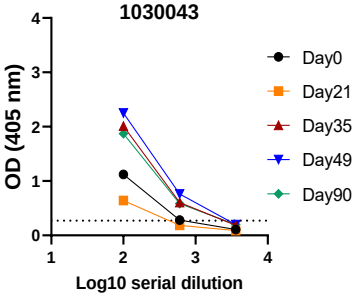
	Day0	Day21	Day35	Day49	Day90
Total Area	560.3	369.0	1399	1691	1826



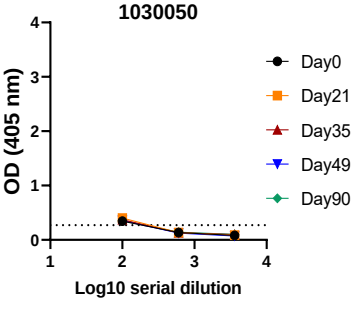
	Day0	Day21	Day35	Day49	Day90
Total Area	718.8	598.8	804.8	1417	663.5



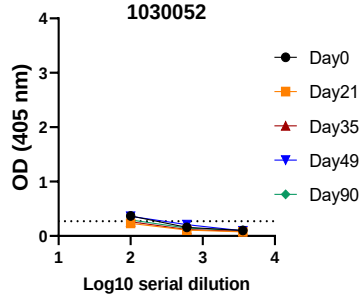
	Day0	Day21	Day35	Day49	Day90
Total Area	935.8	619.3	1843	2197	1787



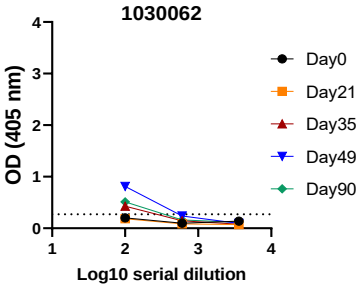
	Day0	Day21	Day35	Day49	Day90
Total Area	443.8	466.5	465.8	413.5	489.8



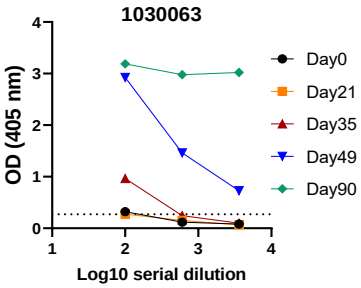
	Day0	Day21	Day35	Day49	Day90
Total Area	523.8	360.8	402.5	599.0	479.0



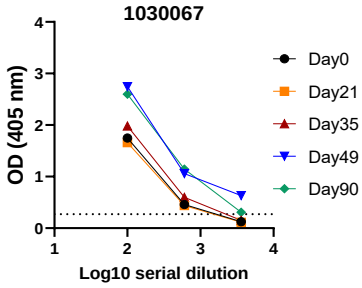
	Day0	Day21	Day35	Day49	Day90
Total Area	425.5	298.0	478.3	765.5	586.8



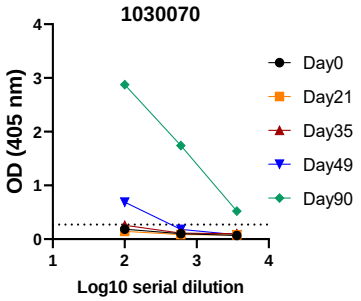
	Day0	Day21	Day35	Day49	Day90
Total Area	413.5	433.5	815.8	4382	10538



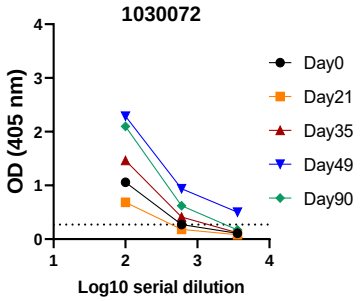
	Day0	Day21	Day35	Day49	Day90
Total Area	1428	1350	1773	3489	3117



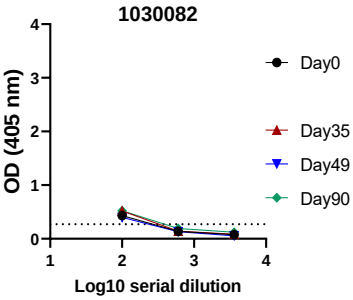
	Day0	Day21	Day35	Day49	Day90
Total Area	328.3	305.5	408.3	612.8	4549



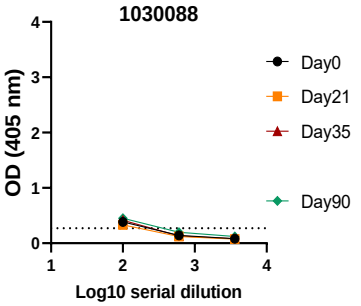
	Day0	Day21	Day35	Day49	Day90
Total Area	906.0	613.3	1266	2964	1873



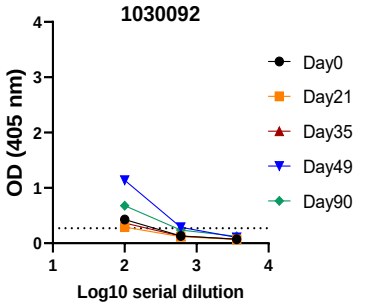
	Day0	Day35	Day49	Day90
Total Area	461.8	505.3	416.3	647.8



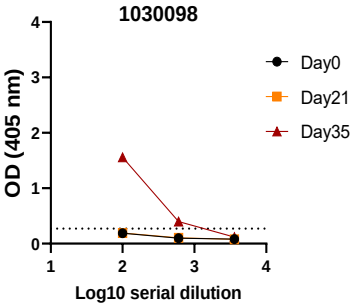
	Day0	Day21	Day35	Day90
Total Area	466.3	407.0	461.0	640.8



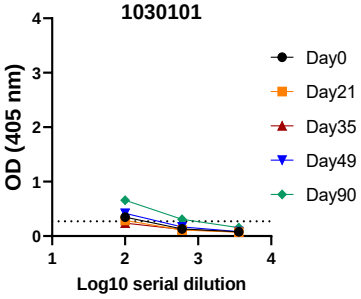
	Day0	Day21	Day35	Day49	Day90
Total Area	445.0	378.0	429.8	944.3	771.8



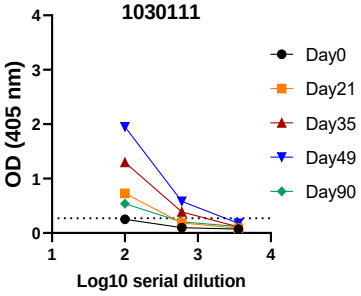
	Day0	Day21	Day35
Total Area	343.5	349.0	1260



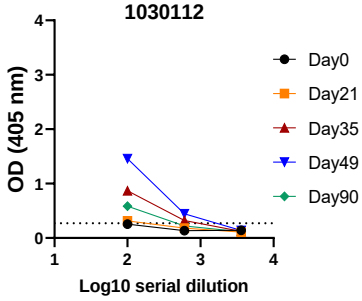
	Day0	Day21	Day35	Day49	Day90
Total Area	436.5	375.5	387.0	521.5	934.5



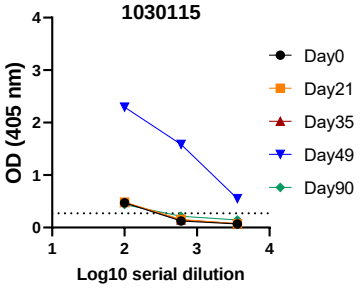
	Day0	Day21	Day35	Day49	Day90
Total Area	341.0	641.0	1175	1776	671.8



	Day0	Day21	Day35	Day49	Day90
Total Area	511.3	559.8	963.8	1354	709.0

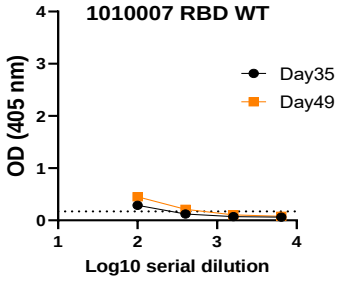


	Day0	Day21	Day35	Day49	Day90
Total Area	438.8	500.5	485.5	4171	701.8

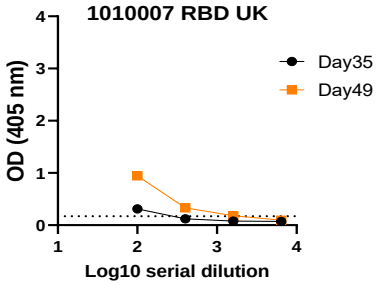


Day by day individual OD graphs after injection of VLP-58-1023-AL-K3 vaccine for each Phase 2 volunteers with 4X serial dilutions of sera from 100X to 6400X against recombinant RBD variants. 96-well 2HB maxi-binding ELISA plates were seperately coated with 1 ug/ml in-house recombinant WT RBD, UK RBD and Delta RBD and plates were blocked. After the serial dilutions of volunteers' sera, ALP-tagged anti-human IgG secondary antibody were filled into wells and finally PNPP substrate was added into plate and optical density values were recorded at 405 nm.

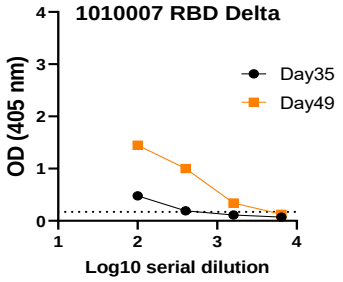
	Day35	Day49
Total Area	501.2	729.5



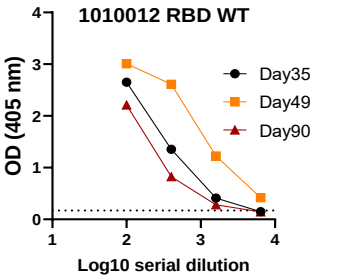
	Day35	Day49
Total Area	541.7	1168



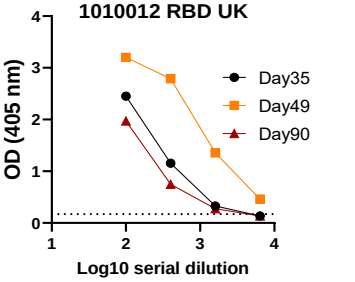
	Day35	Day49
Total Area	722.0	2285



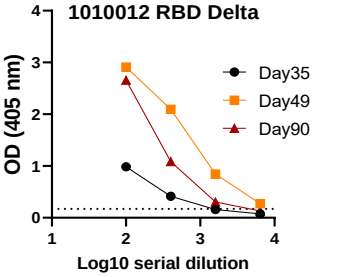
	Day35	Day49	Day90
Total Area	3007	7092	2145



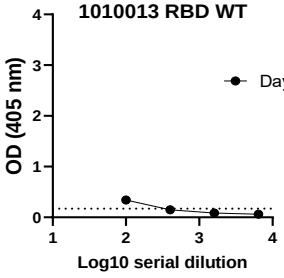
	Day35	Day49	Day90
Total Area	2543	7740	2007



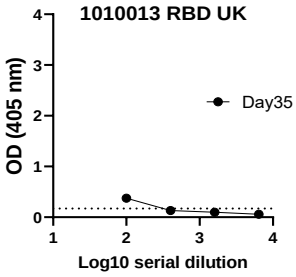
	Day35	Day49	Day90
Total Area	1117	5197	2440



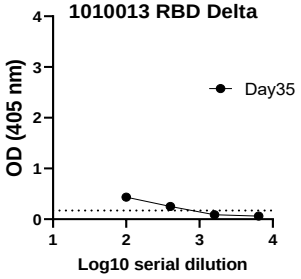
	Day35
Total Area	568.4



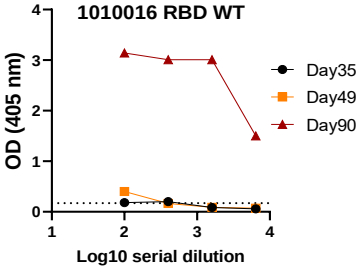
	Day35
Total Area	592.5



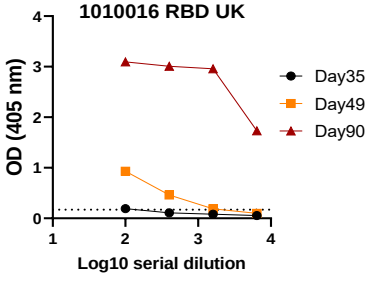
	Day35
Total Area	663.2



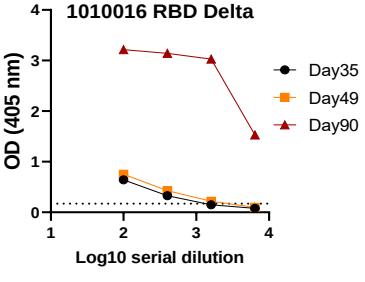
	Day35	Day49	Day90
Total Area	573.0	620.3	15357



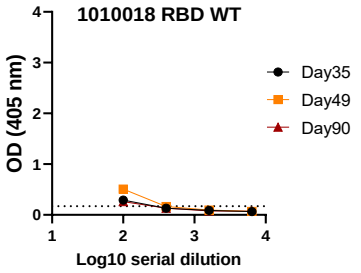
	Day35	Day49	Day90
Total Area	484.7	1283	15744



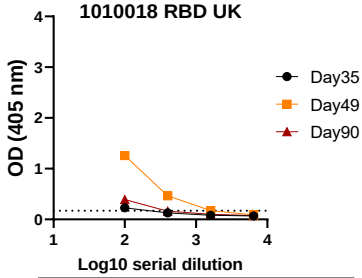
	Day35	Day49	Day90
Total Area	968.1	1323	15594



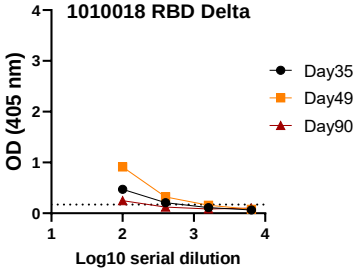
	Day35	Day49	Day90
Total Area	558.2	642.0	547.1



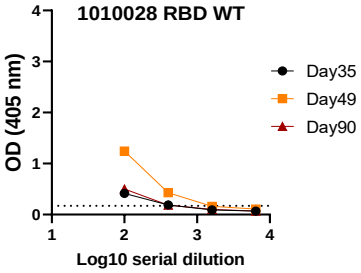
	Day35	Day49	Day90
Total Area	538.8	1276	660.0



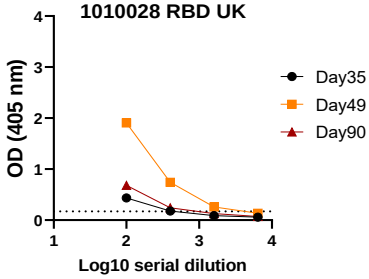
	Day35	Day49	Day90
Total Area	714.5	1038	631.4



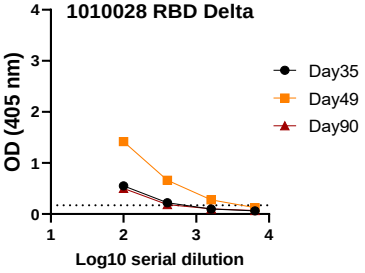
	Day35	Day49	Day90
Total Area	636.9	1257	679.7



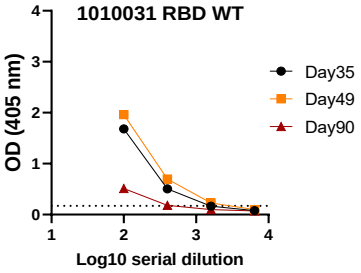
	Day35	Day49	Day90
Total Area	598.4	1942	831.9



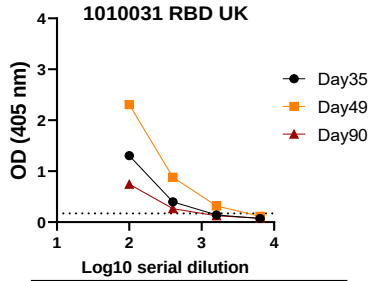
	Day35	Day49	Day90
Total Area	691.8	1838	679.7



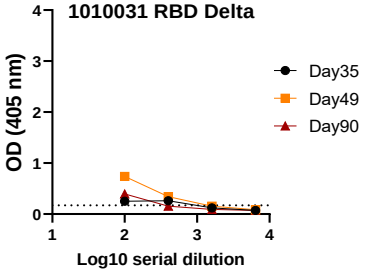
	Day35	Day49	Day90
Total Area	1312	1733	680.9



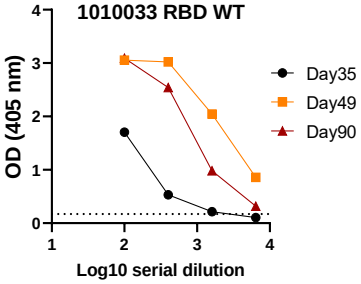
	Day35	Day49	Day90
Total Area	1085	2233	867.2



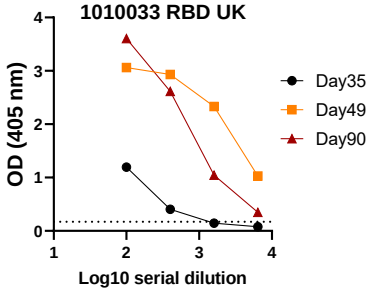
	Day35	Day49	Day90
Total Area	772.2	1035	622.7



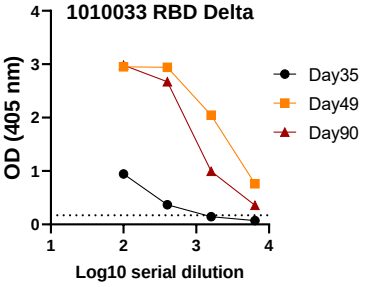
	Day35	Day49	Day90
Total Area	1551	10918	6074



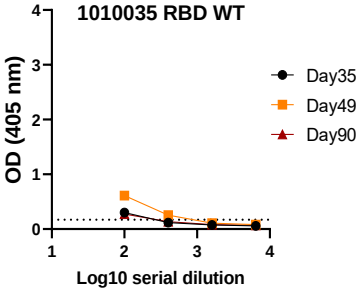
	Day35	Day49	Day90
Total Area	1108	12122	6480



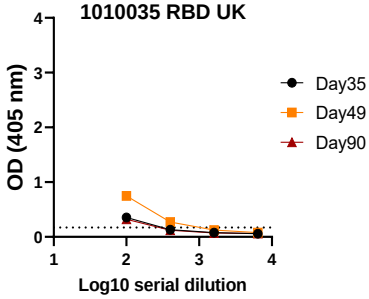
	Day35	Day49	Day90
Total Area	1025	10605	6296



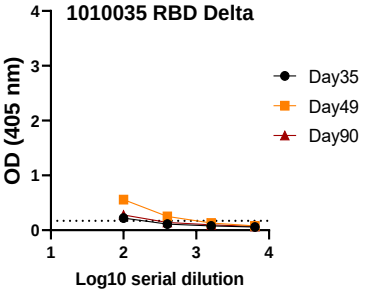
	Day35	Day49	Day90
Total Area	502.5	801.3	545.4



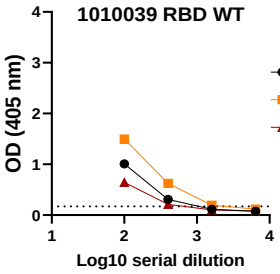
	Day35	Day49	Day90
Total Area	525.5	877.7	504.2



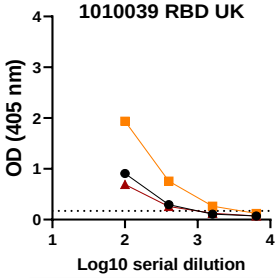
	Day35	Day49	Day90
Total Area	491.9	848.4	604.5



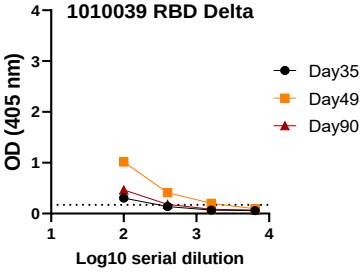
	Day35	Day49	Day90
Total Area	902.4	1564	747.2



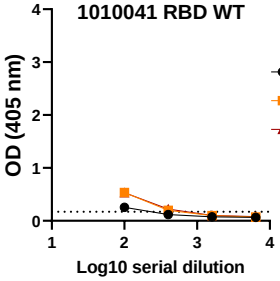
	Day35	Day49	Day90
Total Area	852.5	1947	845.3



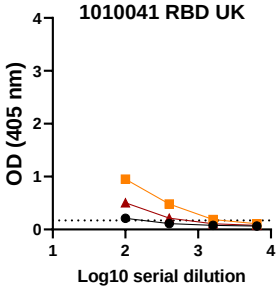
	Day35	Day49	Day90
Total Area	492.3	1298	630.6



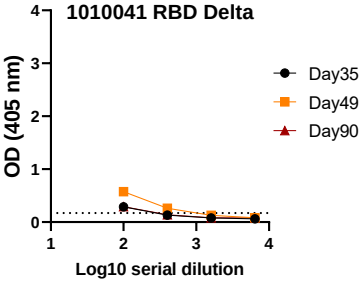
	Day35	Day49	Day90
Total Area	510.3	689.3	734.1



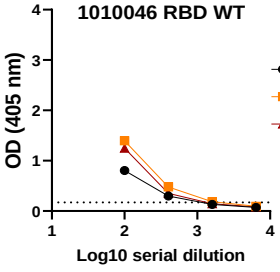
	Day35	Day49	Day90
Total Area	507.3	1325	750.5



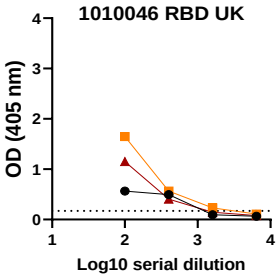
	Day35	Day49	Day90
Total Area	519.2	867.5	575.3



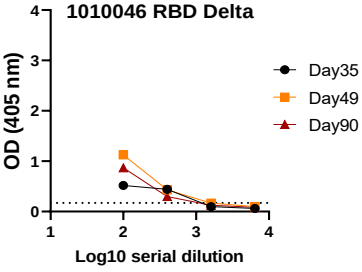
	Day35	Day49	Day90
Total Area	906.0	1347	1080



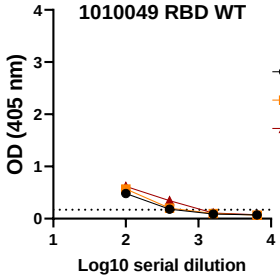
	Day35	Day49	Day90
Total Area	893.1	1627	1101



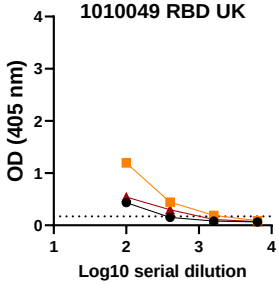
	Day35	Day49	Day90
Total Area	847.5	1229	927.9



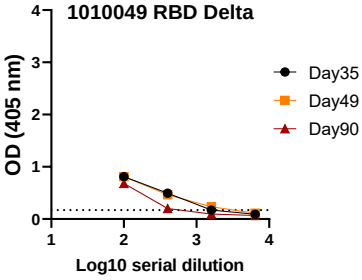
	Day35	Day49	Day90
Total Area	639.9	687.9	852.5



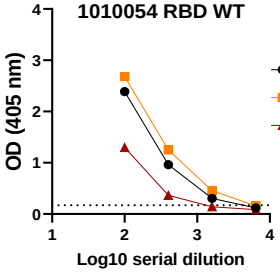
	Day35	Day49	Day90
Total Area	575.1	1298	814.4



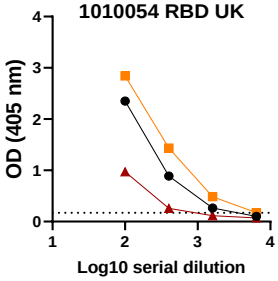
	Day35	Day49	Day90
Total Area	1226	1451	700.2



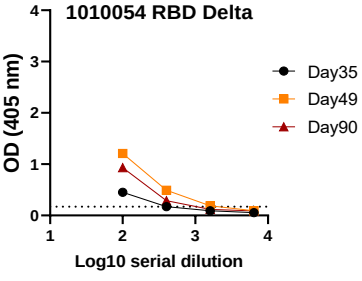
	Day35	Day49	Day90
Total Area	2275	3085	1094



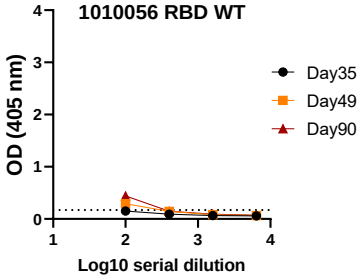
	Day35	Day49	Day90
Total Area	2064	3379	854.6



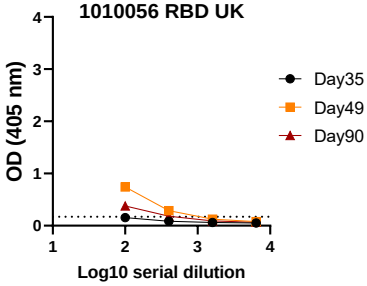
	Day35	Day49	Day90
Total Area	608.1	1337	928.4



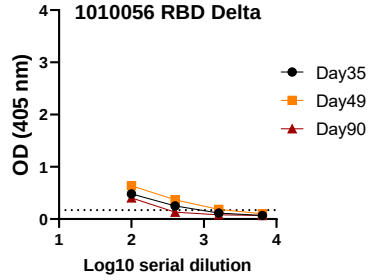
	Day35	Day49	Day90
Total Area	431.3	552.8	625.7



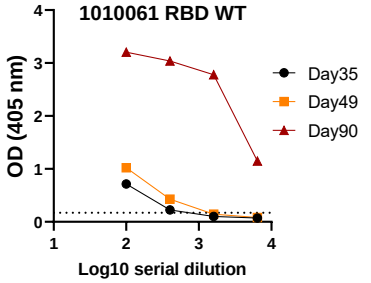
	Day35	Day49	Day90
Total Area	399.5	894.8	622.2



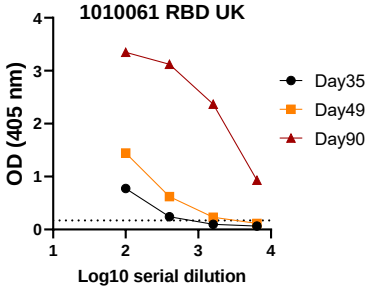
	Day35	Day49	Day90
Total Area	774.2	1164	571.2



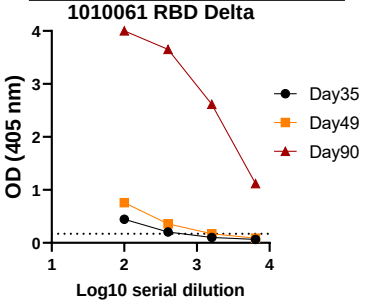
	Day35	Day49	Day90
Total Area	744.0	1104	13853



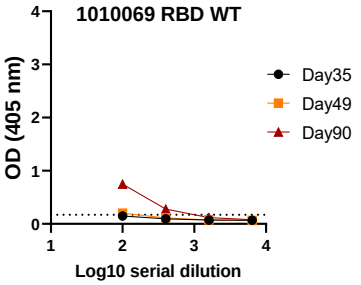
	Day35	Day49	Day90
Total Area	753.0	1658	12182



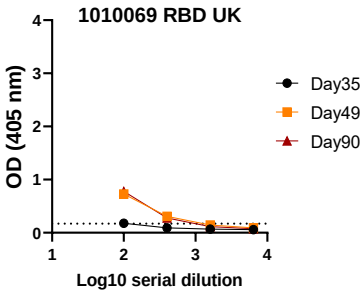
	Day35	Day49	Day90
Total Area	685.5	1111	13869



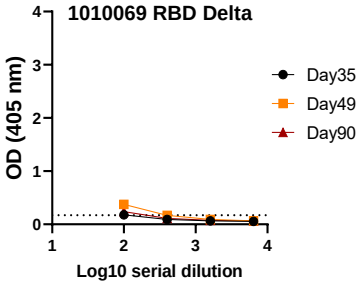
	Day35	Day49	Day90
Total Area	470.0	496.7	858.8



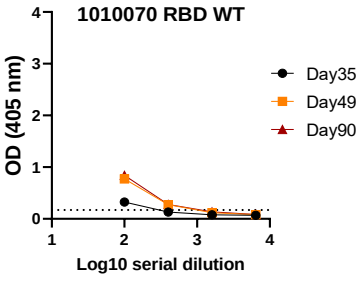
	Day35	Day49	Day90
Total Area	436.1	994.1	846.3



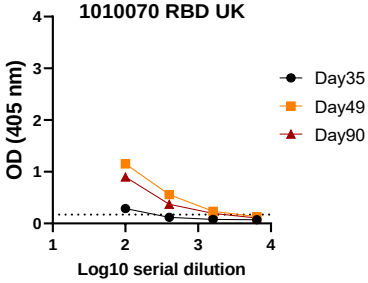
	Day35	Day49	Day90
Total Area	421.7	613.7	497.1



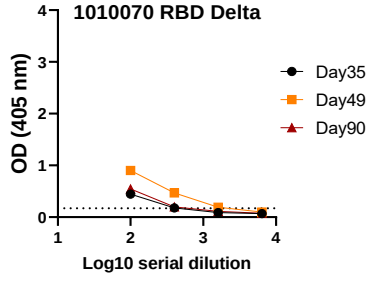
	Day35	Day49	Day90
Total Area	538.2	867.6	937.7



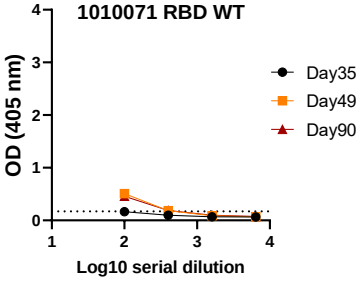
	Day35	Day49	Day90
Total Area	544.5	1616	1252



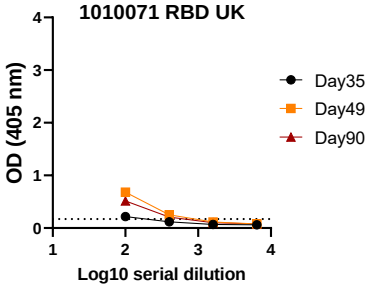
	Day35	Day49	Day90
Total Area	630.3	1290	750.0



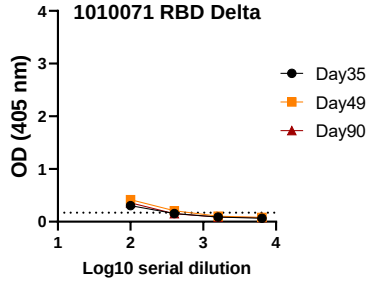
	Day35	Day49	Day90
Total Area	460.1	642.9	689.3



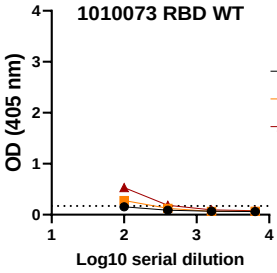
	Day35	Day49	Day90
Total Area	478.8	821.3	724.4



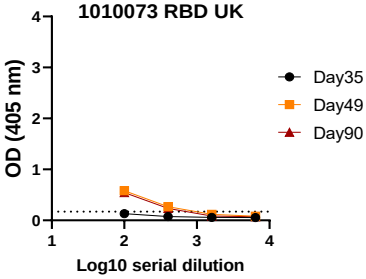
	Day35	Day49	Day90
Total Area	588.2	727.1	620.4



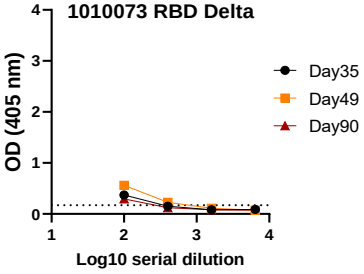
	Day35	Day49	Day90
Total Area	438.2	496.8	687.3



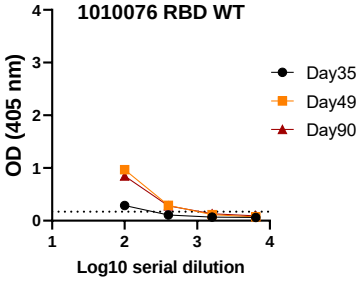
	Day35	Day49	Day90
Total Area	391.1	843.8	682.2



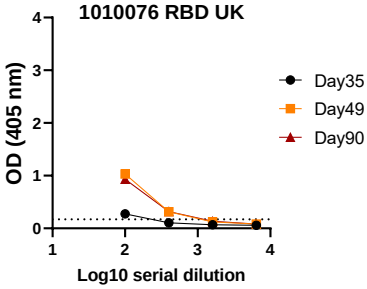
	Day35	Day49	Day90
Total Area	624.3	772.1	548.4



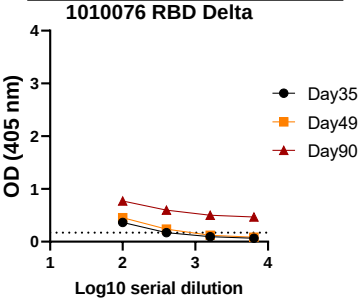
	Day35	Day49	Day90
Total Area	476.1	873.6	951.2



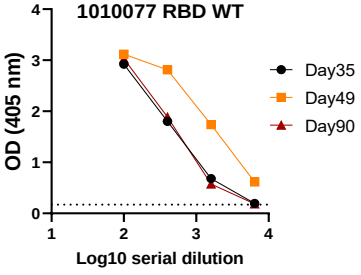
	Day35	Day49	Day90
Total Area	464.4	953.9	978.5



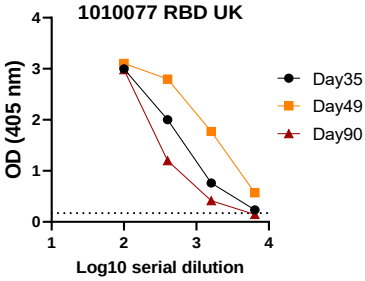
	Day35	Day49	Day90
Total Area	622.4	819.8	3195



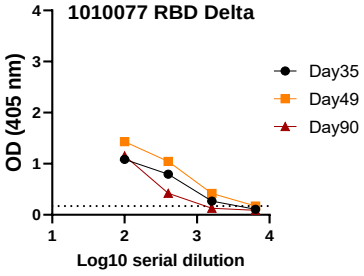
	Day35	Day49	Day90
Total Area	4302	9260	4036



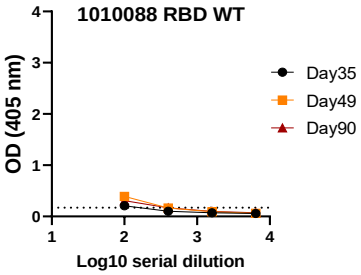
	Day35	Day49	Day90
Total Area	4800	9241	2943



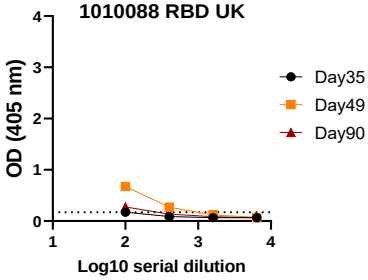
	Day35	Day49	Day90
Total Area	1829	2663	1091



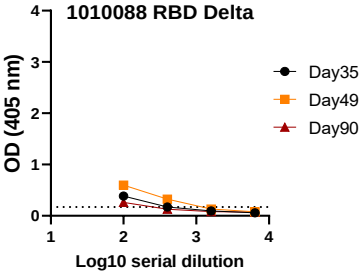
	Day35	Day49	Day90
Total Area	466.7	607.5	644.4



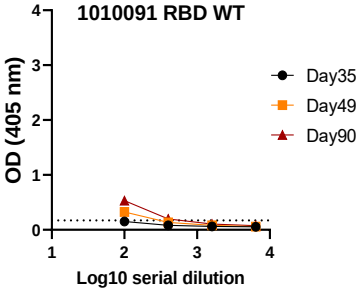
	Day35	Day49	Day90
Total Area	442.2	835.8	557.3



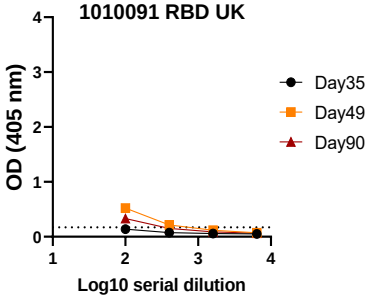
	Day35	Day49	Day90
Total Area	612.0	919.2	542.3



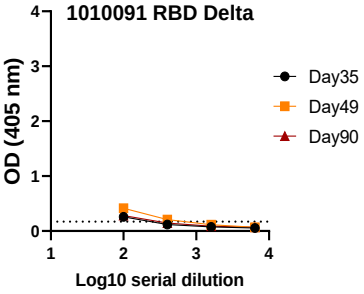
	Day35	Day49	Day90
Total Area	406.2	543.6	723.2



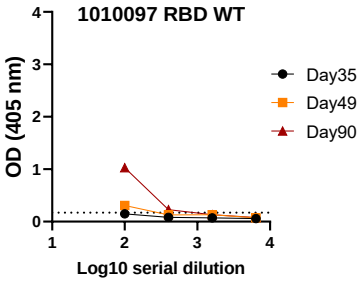
	Day35	Day49	Day90
Total Area	384.8	762.2	583.7



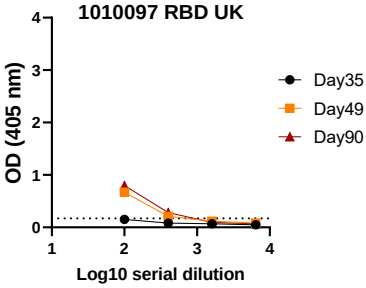
	Day35	Day49	Day90
Total Area	480.2	730.5	572.6



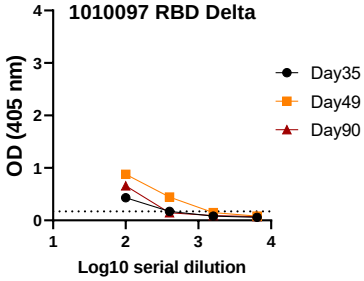
	Day35	Day49	Day90
Total Area	437.6	706.2	911.7



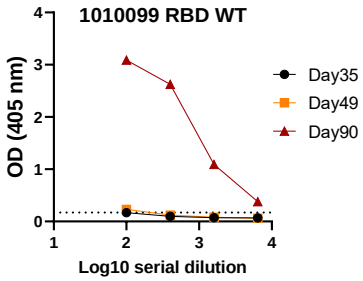
	Day35	Day49	Day90
Total Area	402.6	812.0	781.8



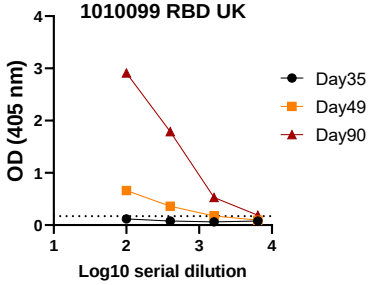
	Day35	Day49	Day90
Total Area	585.3	1112	653.3



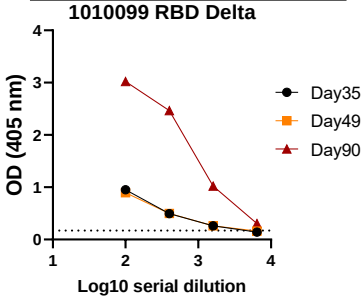
	Day35	Day49	Day90
Total Area	478.2	518.0	6619



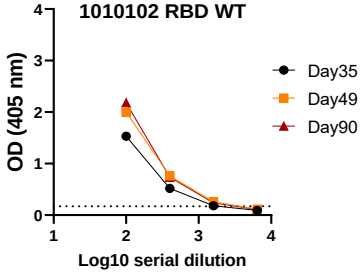
	Day35	Day49	Day90
Total Area	449.9	1122	3813



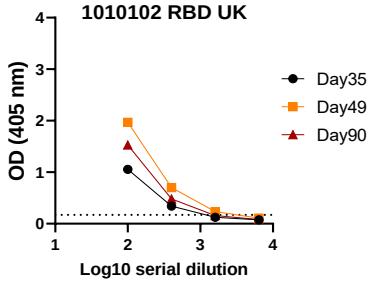
	Day35	Day49	Day90
Total Area	1631	1686	6102



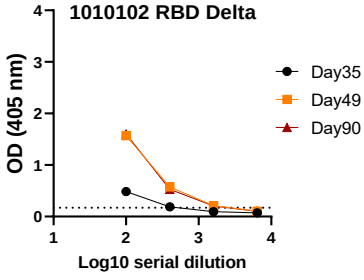
	Day35	Day49	Day90
Total Area	1388	1916	1858



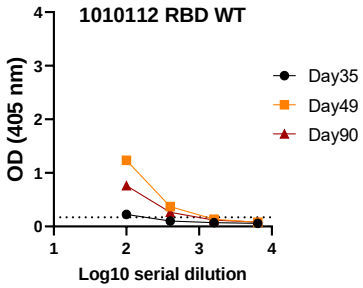
	Day35	Day49	Day90
Total Area	969.9	1783	1254



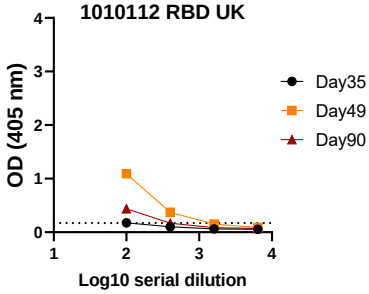
	Day35	Day49	Day90
Total Area	669.3	1553	1491



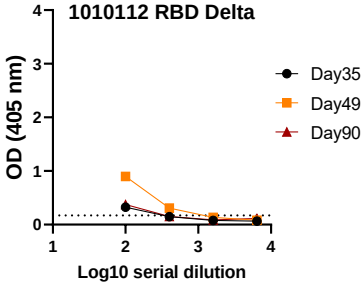
	Day35	Day49	Day90
Total Area	458.1	1060	869.6



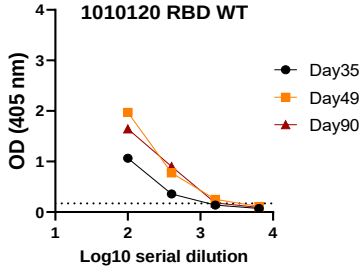
	Day35	Day49	Day90
Total Area	416.7	1115	620.0



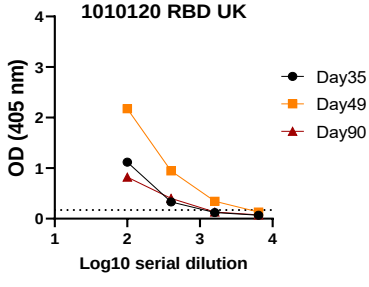
	Day35	Day49	Day90
Total Area	551.7	963.5	708.2



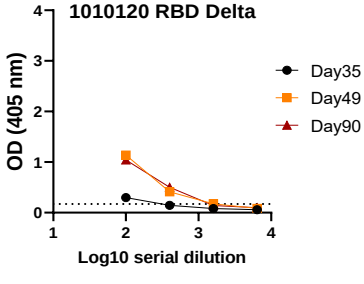
	Day35	Day49	Day90
Total Area	1012	1890	1689



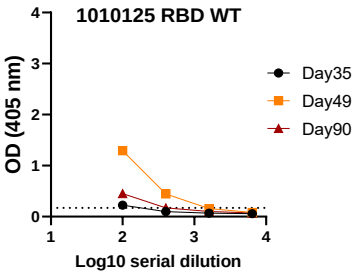
	Day35	Day49	Day90
Total Area	948.9	2388	990.8



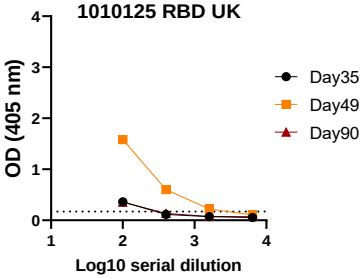
	Day35	Day49	Day90
Total Area	532.5	1206	1196



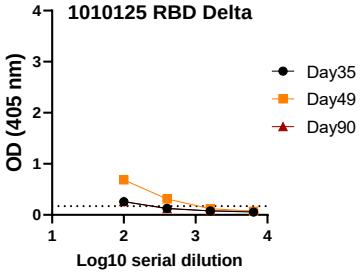
	Day35	Day49	Day90
Total Area	450.5	1196	666.3



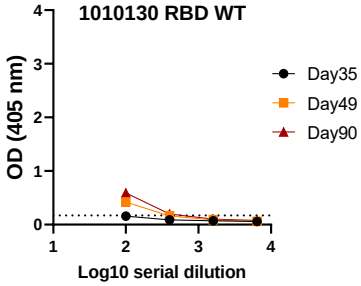
	Day35	Day49	Day90
Total Area	484.7	1607	552.9



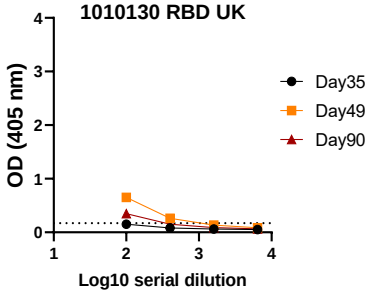
	Day35	Day49	Day90
Total Area	503.7	880.1	532.2



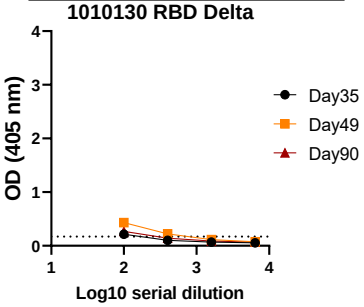
	Day35	Day49	Day90
Total Area	447.3	595.7	732.2



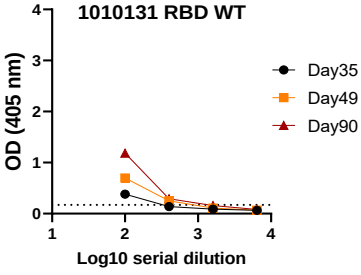
	Day35	Day49	Day90
Total Area	395.4	905.0	589.2



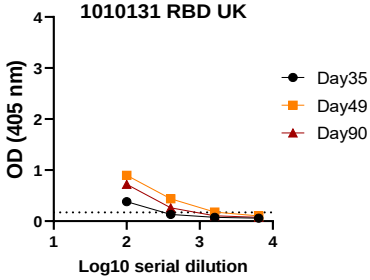
	Day35	Day49	Day90
Total Area	441.2	753.9	574.7



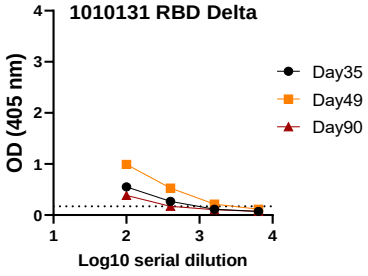
	Day35	Day49	Day90
Total Area	576.0	778.2	1065



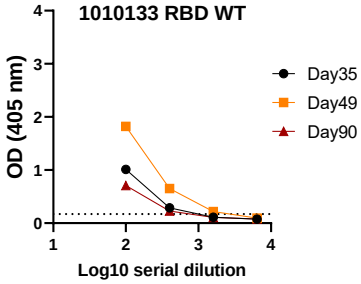
	Day35	Day49	Day90
Total Area	518.4	1251	800.9



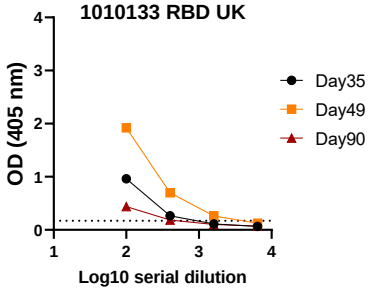
	Day35	Day49	Day90
Total Area	795.5	1472	677.9



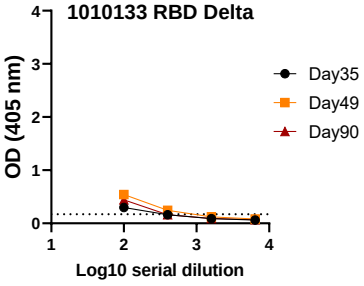
	Day35	Day49	Day90
Total Area	882.8	1648	792.9



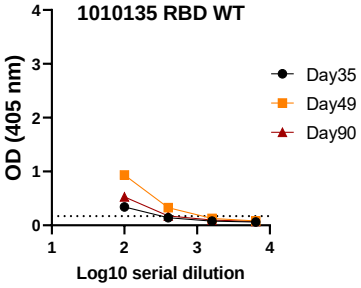
	Day35	Day49	Day90
Total Area	838.1	1893	679.5



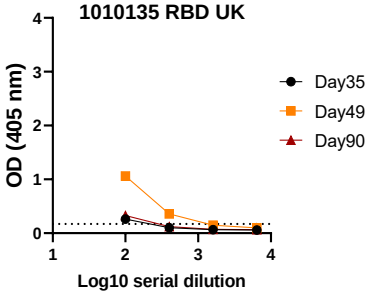
	Day35	Day49	Day90
Total Area	584.0	825.2	625.4



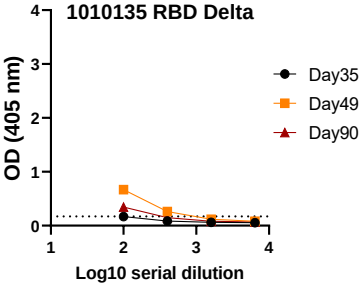
	Day35	Day49	Day90
Total Area	536.0	967.8	677.3



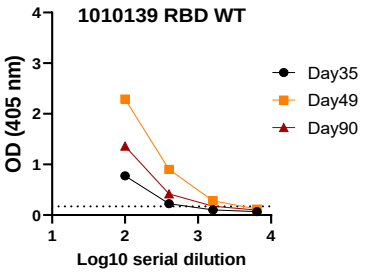
	Day35	Day49	Day90
Total Area	451.4	1108	512.6



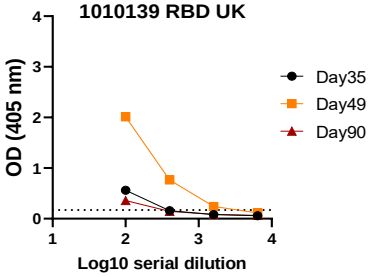
	Day35	Day49	Day90
Total Area	412.4	849.5	572.1



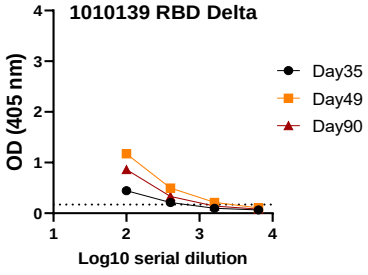
	Day35	Day49	Day90
Total Area	750.6	2142	1273



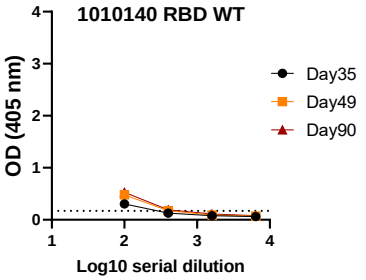
	Day35	Day49	Day90
Total Area	589.2	1878	570.6



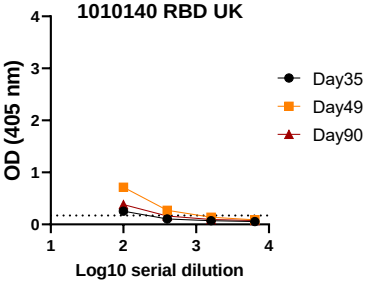
	Day35	Day49	Day90
Total Area	675.8	1449	994.2



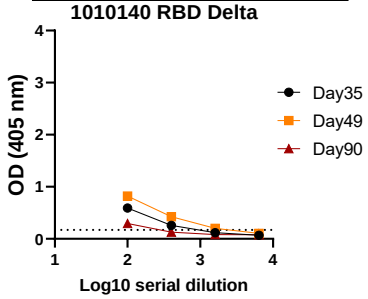
	Day35	Day49	Day90
Total Area	519.3	646.2	748.8



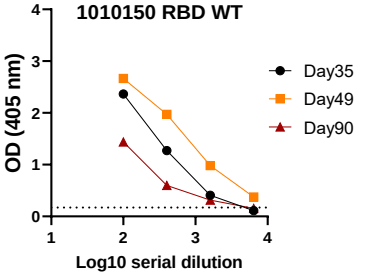
	Day35	Day49	Day90
Total Area	458.9	935.9	642.8



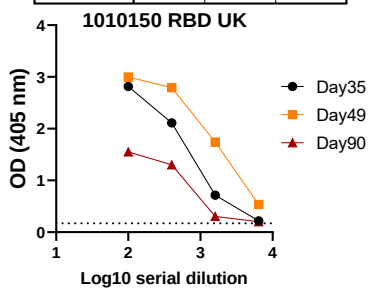
	Day35	Day49	Day90
Total Area	801.9	1293	574.7



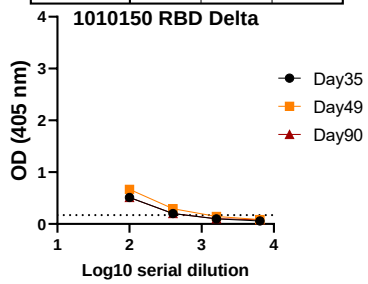
	Day35	Day49	Day90
Total Area	2800	5721	1983



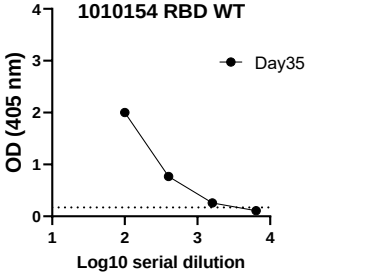
	Day35	Day49	Day90
Total Area	4672	9048	2614



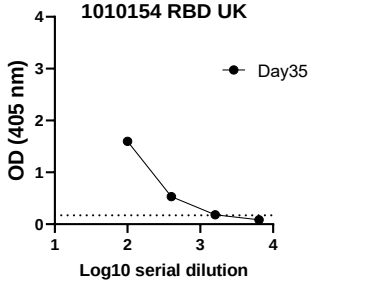
	Day35	Day49	Day90
Total Area	669.2	958.7	722.0



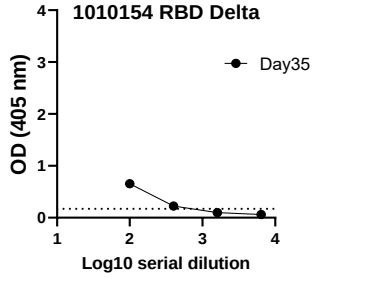
	Day35
Total Area	1913



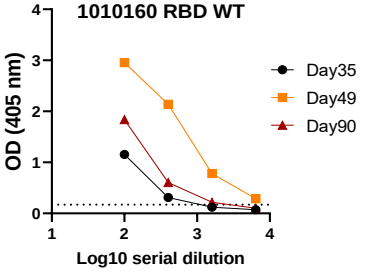
	Day35
Total Area	1392



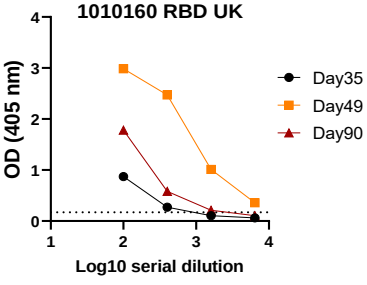
	Day35
Total Area	712.1



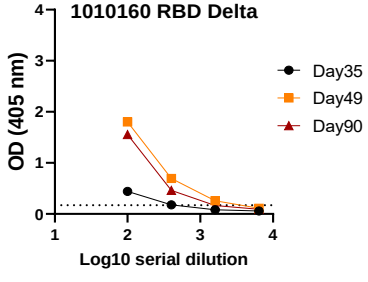
	Day35	Day49	Day90
Total Area	946.2	5084	1620



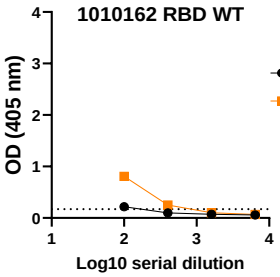
	Day35	Day49	Day90
Total Area	794.6	6200	1596



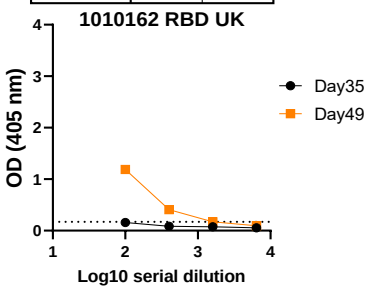
	Day35	Day49	Day90
Total Area	582.8	1827	1295



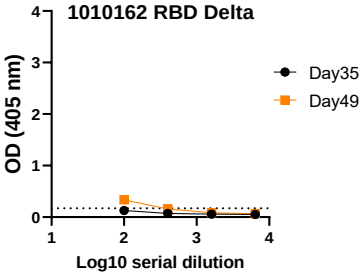
	Day35	Day49
Total Area	456.2	777.9



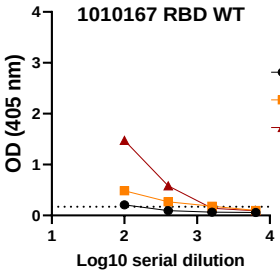
	Day35	Day49
Total Area	441.2	1226



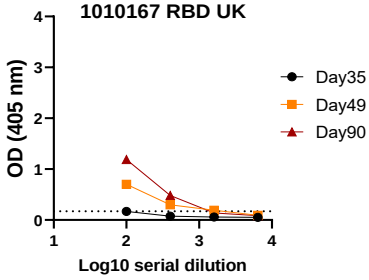
	Day35	Day49
Total Area	372.2	577.4



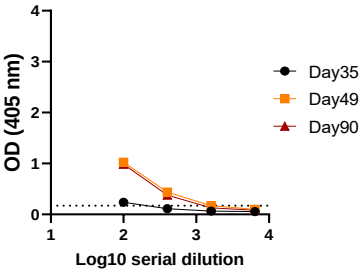
	Day35	Day49	Day90
Total Area	433.7	1054	1302



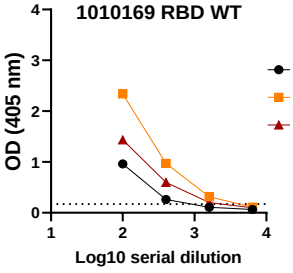
	Day35	Day49	Day90
Total Area	386.4	1129	1159



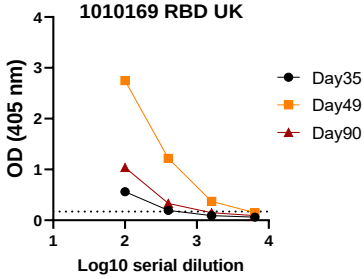
	Day35	Day49	Day90
Total Area	447.6	1224	1011



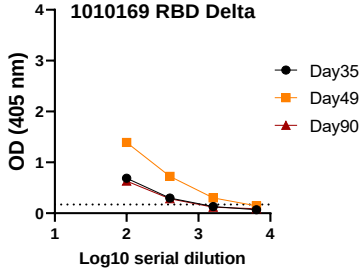
	Day35	Day49	Day90
Total Area	815.4	2289	1508



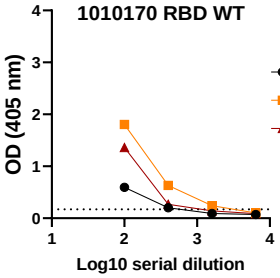
	Day35	Day49	Day90
Total Area	650.7	2796	1062



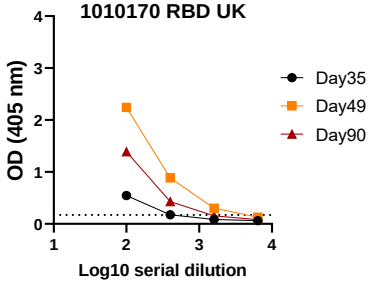
	Day35	Day49	Day90
Total Area	891.6	2006	872.0



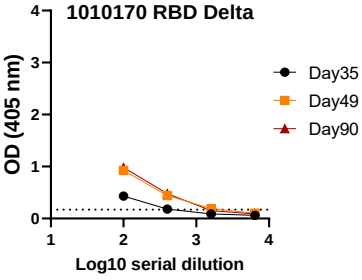
	Day35	Day49	Day90
Total Area	683.1	1719	1043



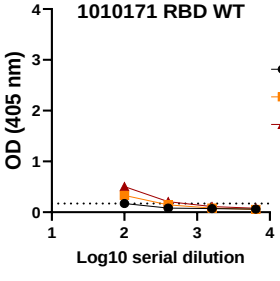
	Day35	Day49	Day90
Total Area	618.9	2211	1191



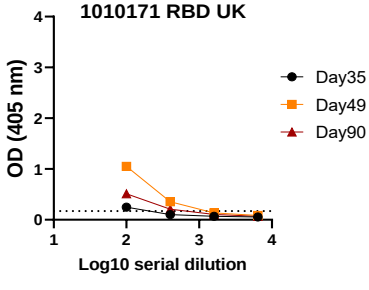
	Day35	Day49	Day90
Total Area	607.7	1290	1180



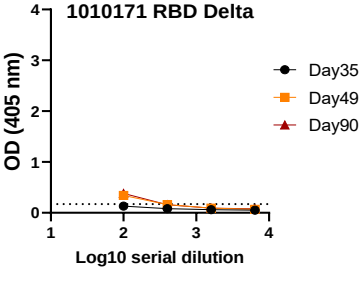
	Day35	Day49	Day90
Total Area	444.5	533.6	753.5



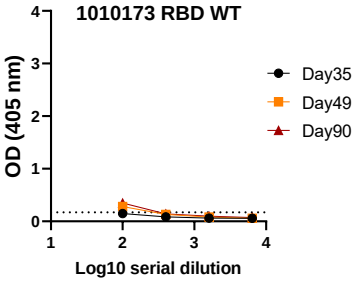
	Day35	Day49	Day90
Total Area	448.2	1036	711.2



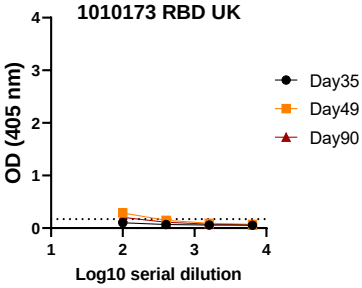
	Day35	Day49	Day90
Total Area	387.9	617.4	638.6



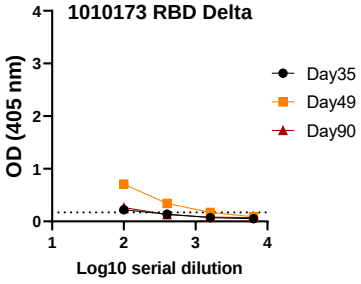
	Day35	Day49	Day90
Total Area	413.4	528.5	627.0



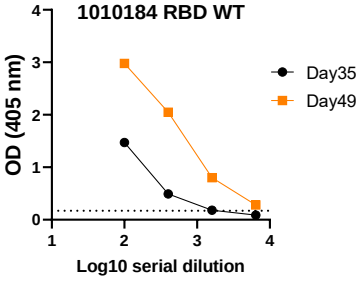
	Day35	Day49	Day90
Total Area	369.9	607.7	497.4



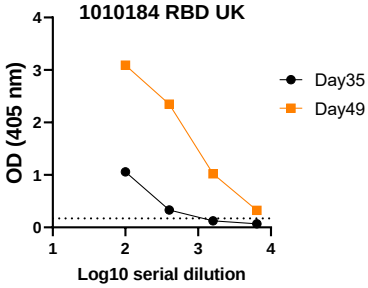
	Day35	Day49	Day90
Total Area	474.2	1094	544.7



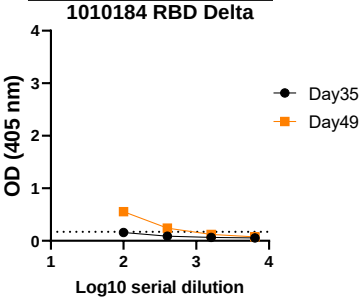
	Day35	Day49
Total Area	1341	5064



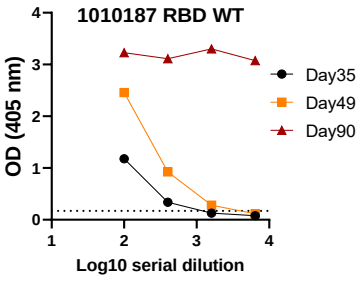
	Day35	Day49
Total Area	951.5	6066



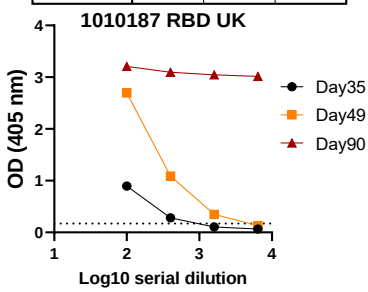
	Day35	Day49
Total Area	413.0	810.2



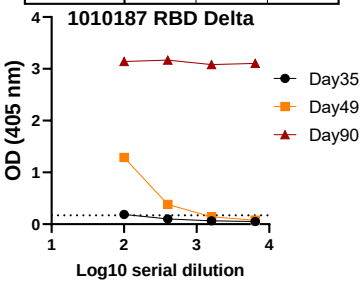
	Day35	Day49	Day90
Total Area	1002	2177	20104



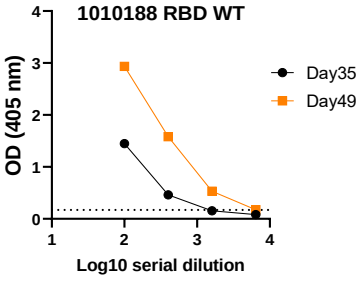
	Day35	Day49	Day90
Total Area	816.0	2585	19177



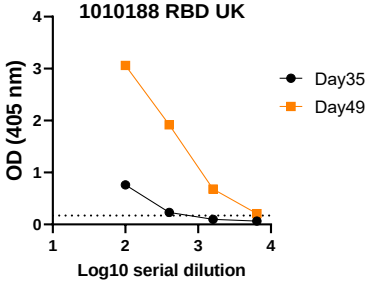
	Day35	Day49	Day90
Total Area	422.3	1086	19544



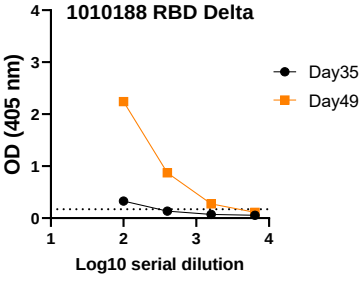
	Day35	Day49
Total Area	1221	3645



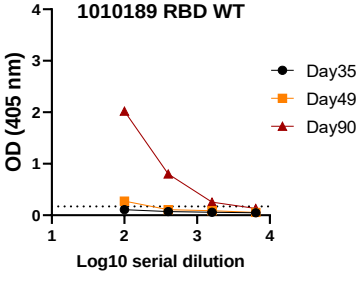
	Day35	Day49
Total Area	741.3	4436



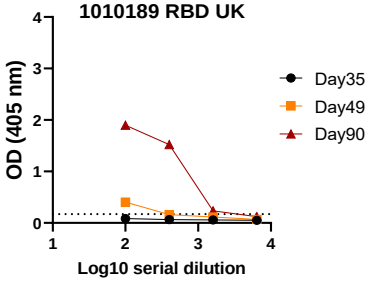
	Day35	Day49
Total Area	500.9	2086



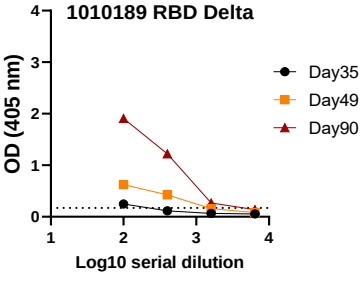
	Day35	Day49	Day90
Total Area	362.4	514.7	1988



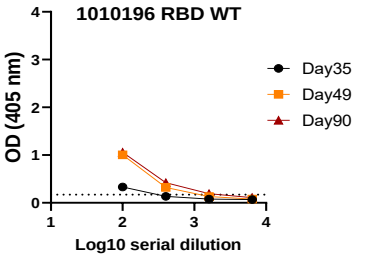
	Day35	Day49	Day90
Total Area	366.6	687.3	2425



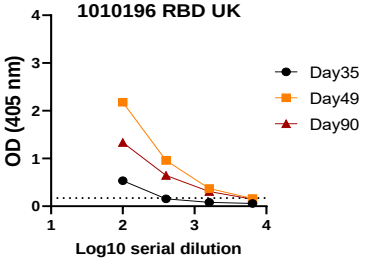
	Day35	Day49	Day90
Total Area	450.2	1085	2336



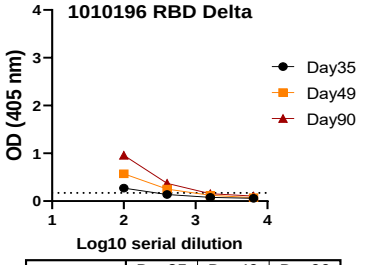
	Day35	Day49	Day90
Total Area	553.8	972.6	1313



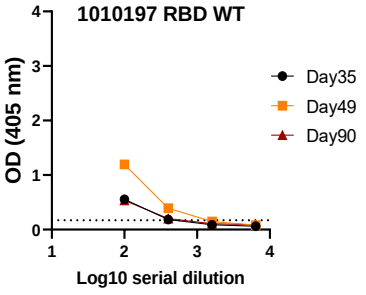
	Day35	Day49	Day90
Total Area	582.8	2552	1969



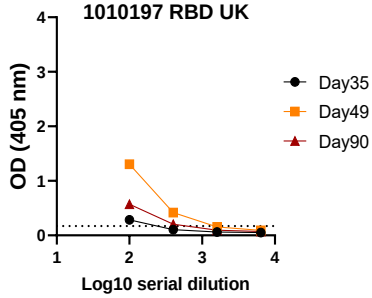
	Day35	Day49	Day90
Total Area	515.9	814.4	1146



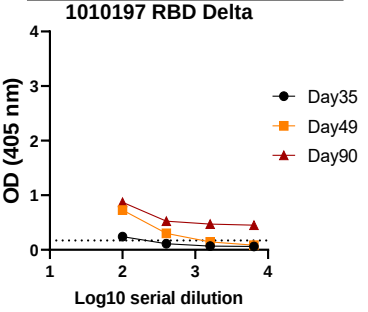
	Day35	Day49	Day90
Total Area	635.0	1113	768.0



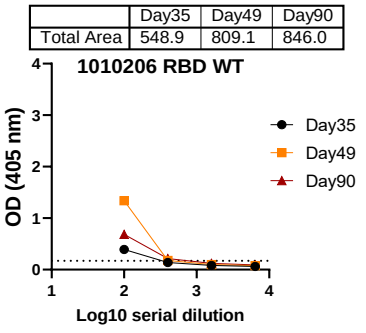
	Day35	Day49	Day90
Total Area	436.2	1194	695.0



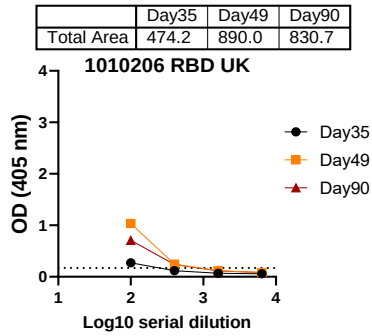
	Day35	Day49	Day90
Total Area	472.4	973.4	3024



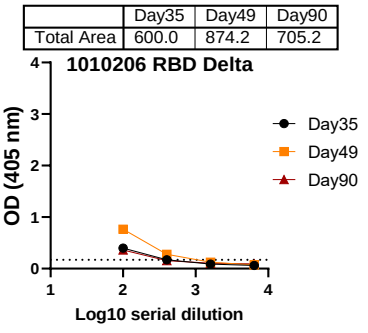
	Day35	Day49	Day90
Total Area	548.9	809.1	846.0



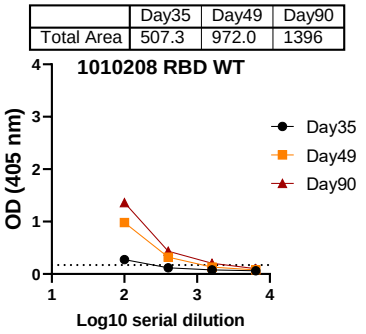
	Day35	Day49	Day90
Total Area	474.2	890.0	830.7



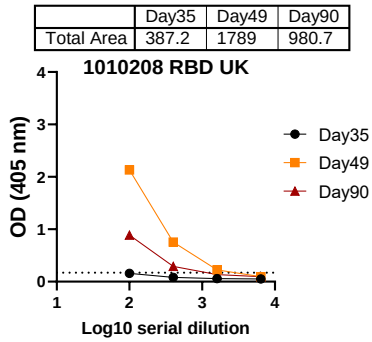
	Day35	Day49	Day90
Total Area	600.0	874.2	705.2



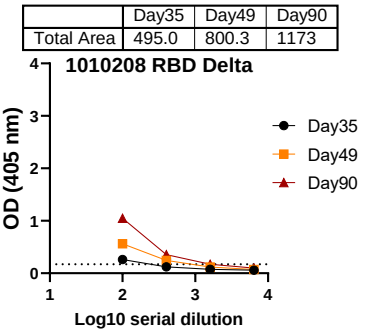
	Day35	Day49	Day90
Total Area	507.3	972.0	1396



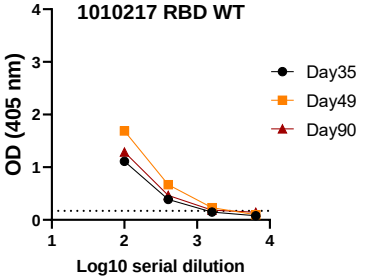
	Day35	Day49	Day90
Total Area	387.2	1789	980.7



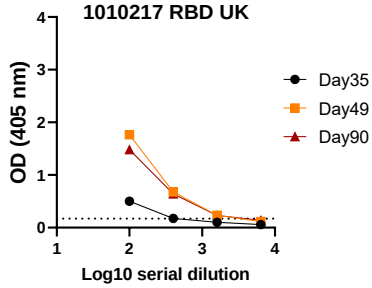
	Day35	Day49	Day90
Total Area	495.0	800.3	1173



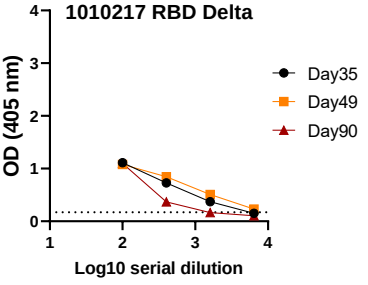
	Day35	Day49	Day90
Total Area	1087	1691	1449



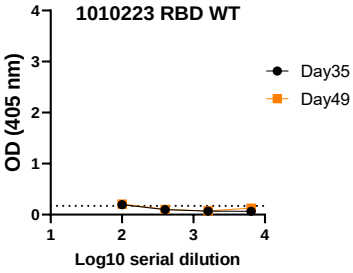
	Day35	Day49	Day90
Total Area	656.4	1755	1730



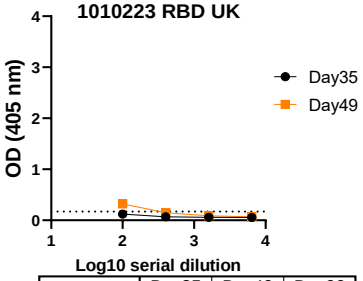
	Day35	Day49	Day90
Total Area	2191	2879	1190



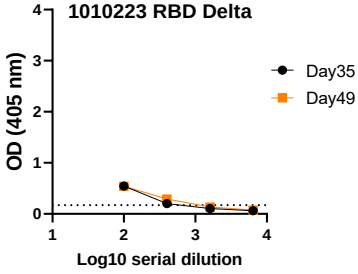
	Day35	Day49
Total Area	464.6	633.8



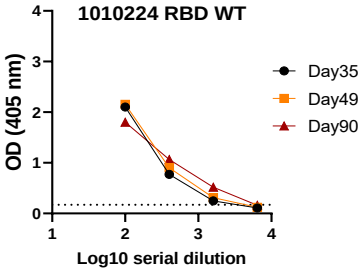
	Day35	Day49
Total Area	380.6	594.2



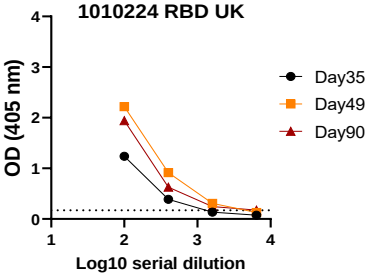
	Day35	Day49
Total Area	693.0	890.7



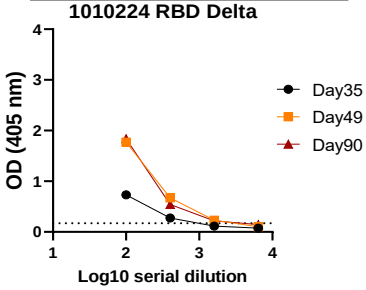
	Day35	Day49	Day90
Total Area	1904	2229	3011



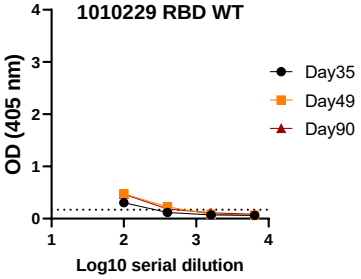
	Day35	Day49	Day90
Total Area	1065	2249	1918



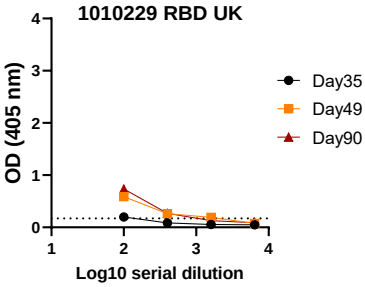
	Day35	Day49	Day90
Total Area	843.2	1708	1680



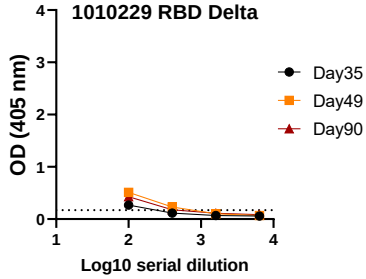
	Day35	Day49	Day90
Total Area	493.5	658.8	748.4



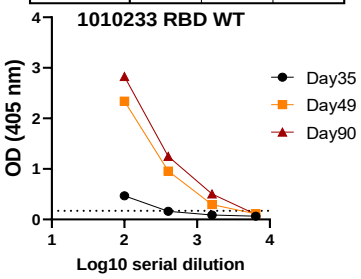
	Day35	Day49	Day90
Total Area	374.0	1041	906.6



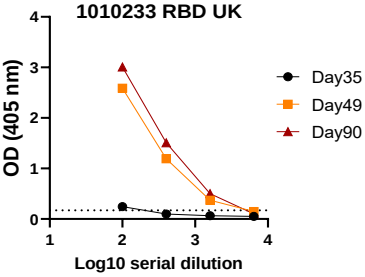
	Day35	Day49	Day90
Total Area	472.2	719.6	737.1



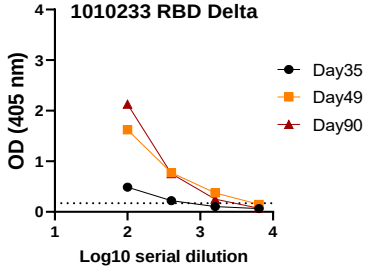
	Day35	Day49	Day90
Total Area	613.5	2228	3112



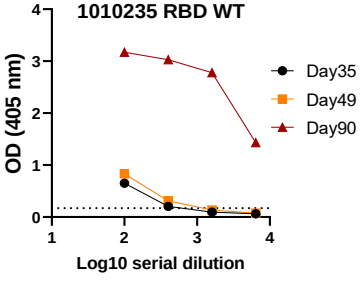
	Day35	Day49	Day90
Total Area	424.8	2753	3326



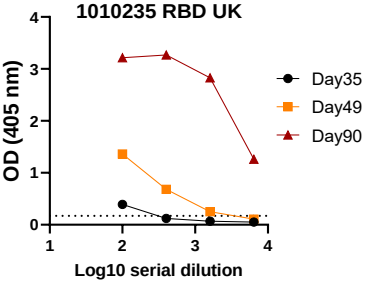
	Day35	Day49	Day90
Total Area	715.4	2307	1812



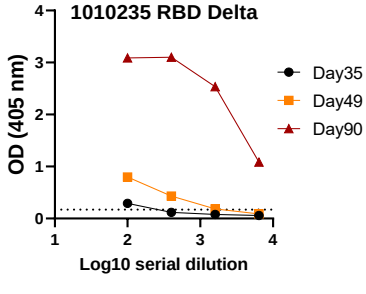
	Day35	Day49	Day90
Total Area	684.5	942.2	14512



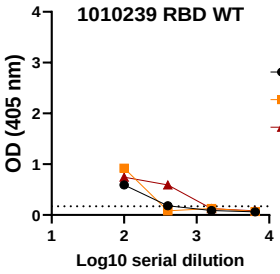
	Day35	Day49	Day90
Total Area	484.5	1727	14449



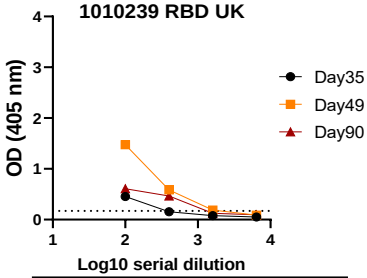
	Day35	Day49	Day90
Total Area	509.9	1208	13001



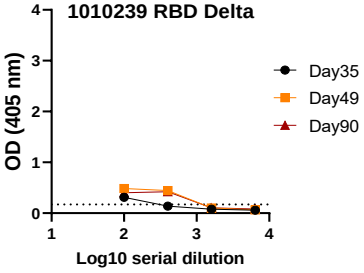
	Day35	Day49	Day90
Total Area	633.5	741.8	1125



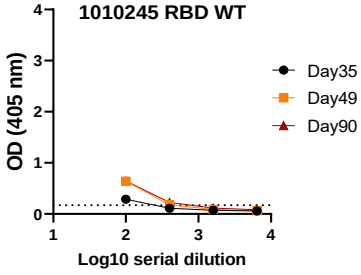
	Day35	Day49	Day90
Total Area	539.4	1441	1043



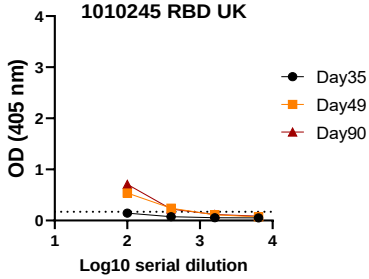
	Day35	Day49	Day90
Total Area	525.0	864.0	883.2



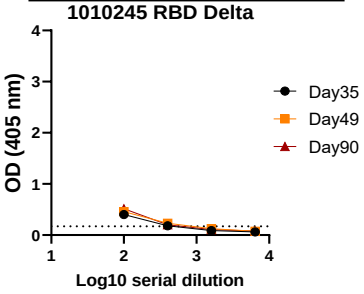
	Day35	Day49	Day90
Total Area	478.1	646.2	804.3



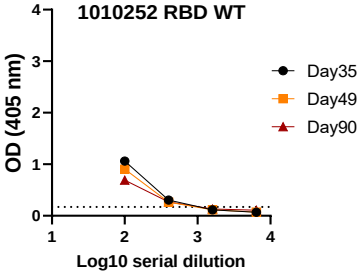
	Day35	Day49	Day90
Total Area	366.0	759.6	835.2



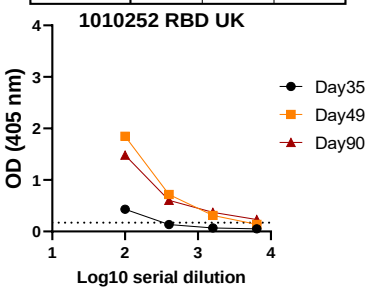
	Day35	Day49	Day90
Total Area	618.0	795.2	738.6



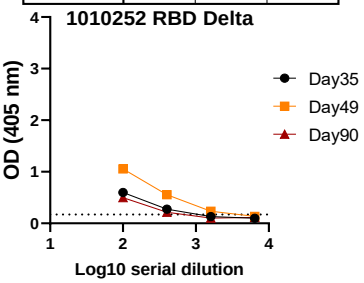
	Day35	Day49	Day90
Total Area	902.6	847.8	955.8



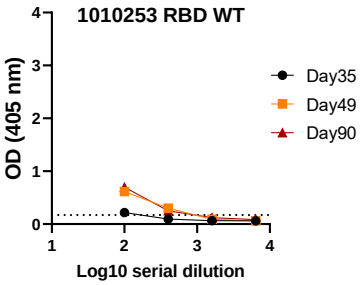
	Day35	Day49	Day90
Total Area	495.2	2083	2346



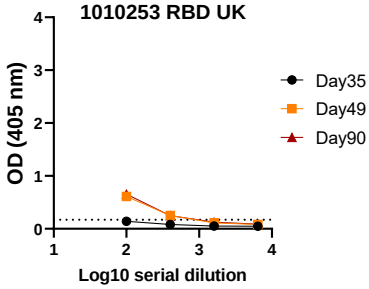
	Day35	Day49	Day90
Total Area	921.8	1604	815.4



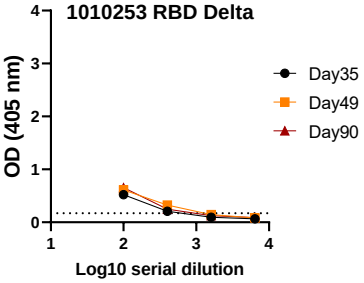
	Day35	Day49	Day90
Total Area	451.5	746.9	859.8



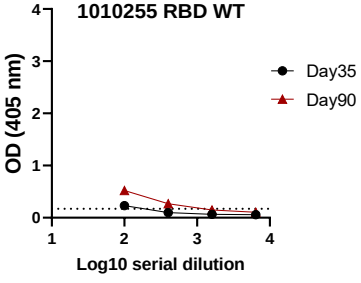
	Day35	Day49	Day90
Total Area	357.2	816.8	867.6



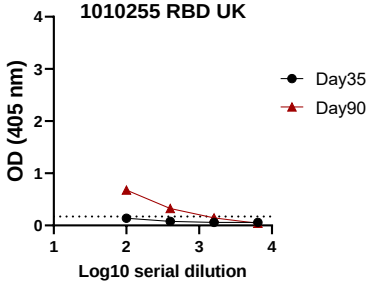
	Day35	Day49	Day90
Total Area	671.4	967.8	867.6



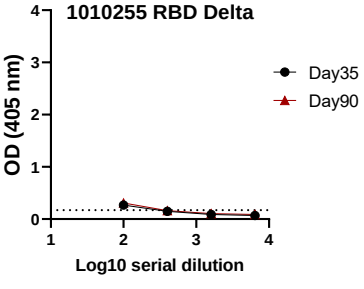
	Day35	Day90
Total Area	451.1	971.6



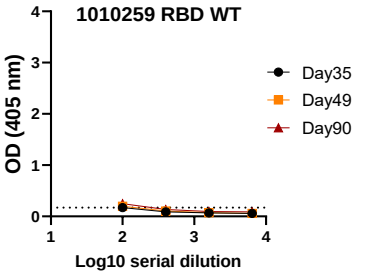
	Day35	Day90
Total Area	396.0	873.6



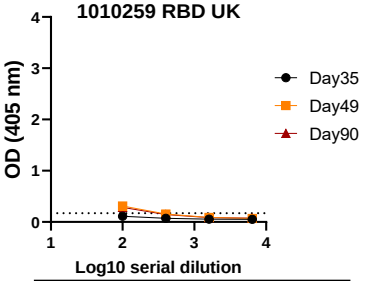
	Day35	Day90
Total Area	575.3	688.5



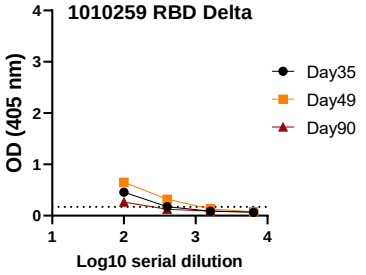
	Day35	Day49	Day90
Total Area	441.3	461.7	640.2



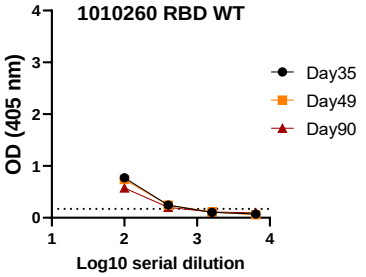
	Day35	Day49	Day90
Total Area	362.6	593.0	587.9



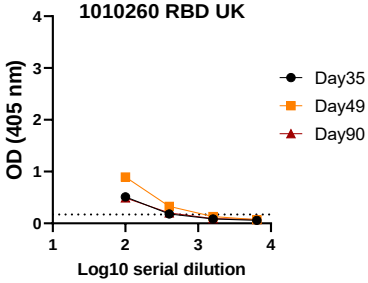
	Day35	Day49	Day90
Total Area	619.8	910.5	594.2



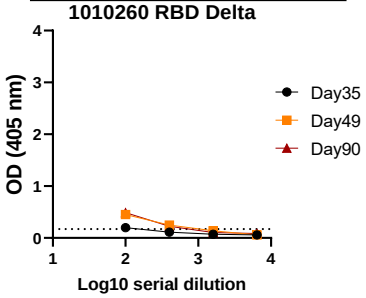
	Day35	Day49	Day90
Total Area	787.8	772.1	802.8



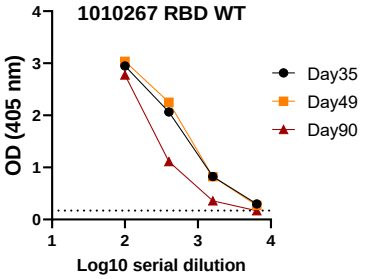
	Day35	Day49	Day90
Total Area	613.8	943.2	679.1



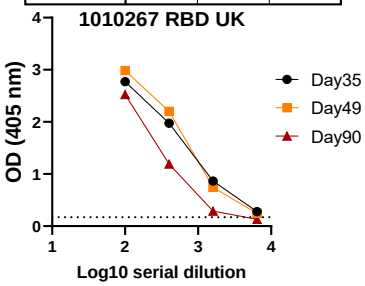
	Day35	Day49	Day90
Total Area	461.9	809.3	754.8



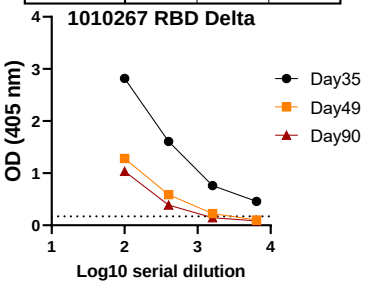
	Day35	Day49	Day90
Total Area	5182	5264	2736



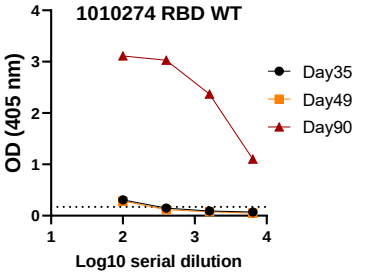
	Day35	Day49	Day90
Total Area	5165	4919	2446



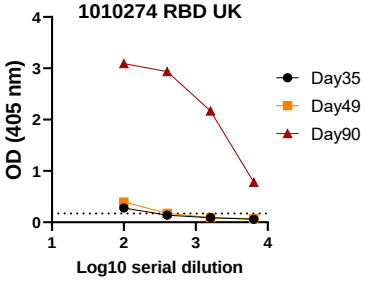
	Day35	Day49	Day90
Total Area	5013	1549	1088



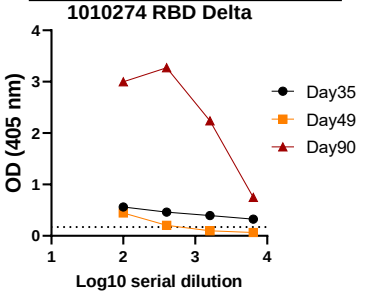
	Day35	Day49	Day90
Total Area	601.4	487.4	12479



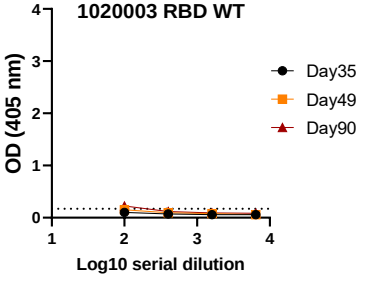
	Day35	Day49	Day90
Total Area	551.7	641.9	11033



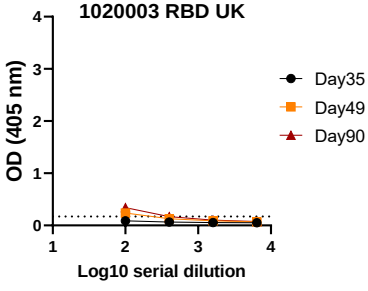
	Day35	Day49	Day90
Total Area	2394	668.1	11413



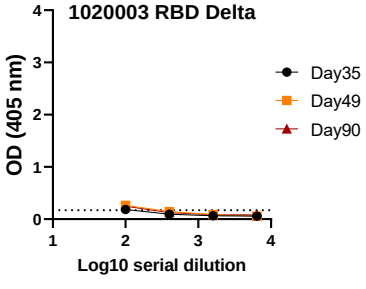
	Day35	Day49	Day90
Total Area	387.0	466.7	603.0



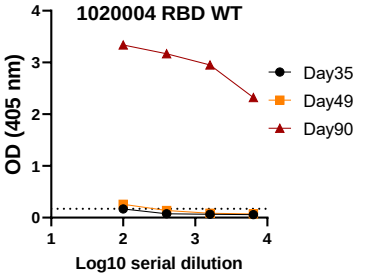
	Day35	Day49	Day90
Total Area	346.4	554.1	666.2



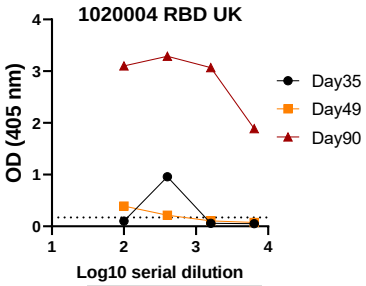
	Day35	Day49	Day90
Total Area	431.0	553.7	580.8



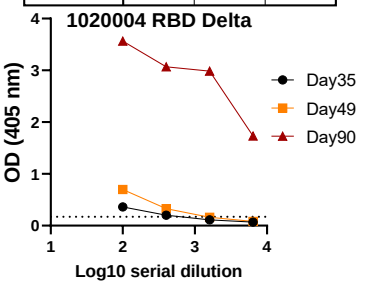
	Day35	Day49	Day90
Total Area	410.9	569.0	17305



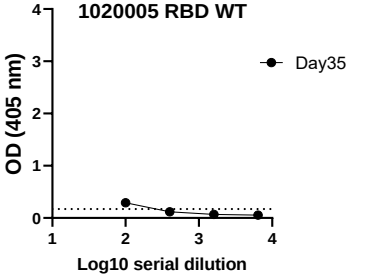
	Day35	Day49	Day90
Total Area	1033	714.8	16661



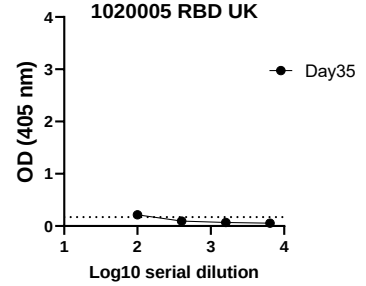
	Day35	Day49	Day90
Total Area	703.7	1028	15944



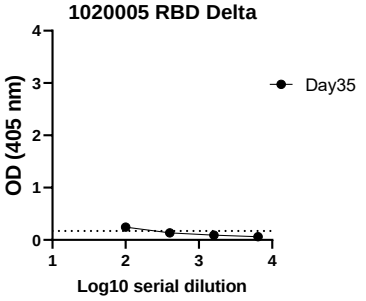
	Day35
Total Area	468.0



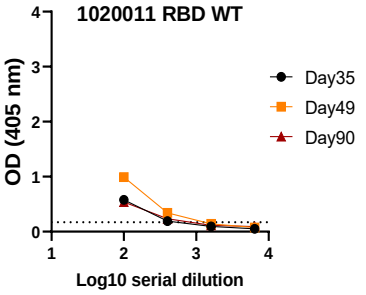
	Day35
Total Area	434.7



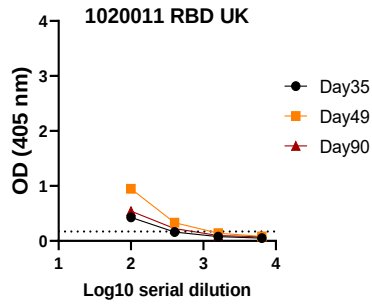
	Day35
Total Area	563.1



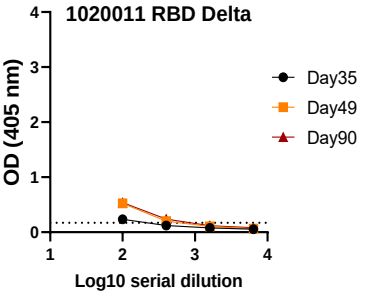
	Day35	Day49	Day90
Total Area	639.0	1009	822.8



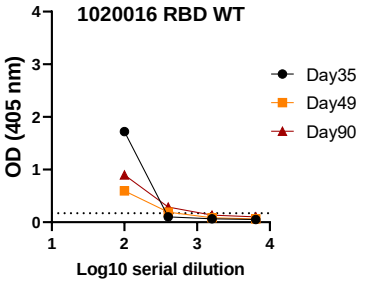
	Day35	Day49	Day90
Total Area	546.6	1008	726.3



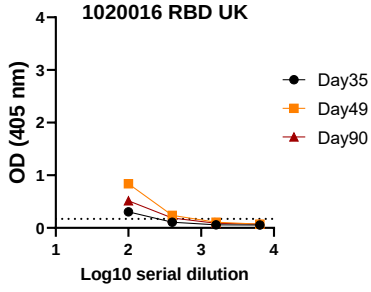
	Day35	Day49	Day90
Total Area	486.5	698.3	808.5



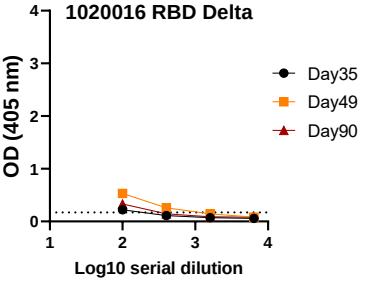
	Day35	Day49	Day90
Total Area	651.9	635.6	997.5



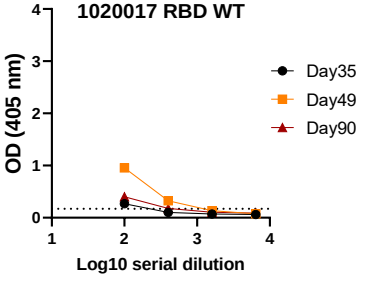
	Day35	Day49	Day90
Total Area	429.5	797.0	653.9



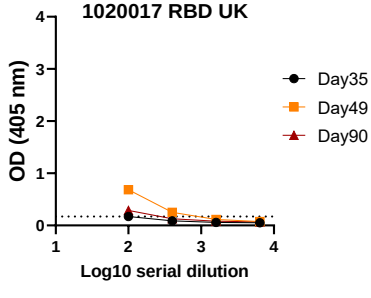
	Day35	Day49	Day90
Total Area	471.3	906.6	616.5



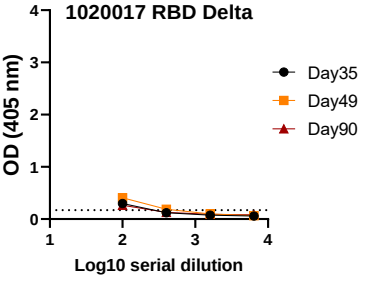
	Day35	Day49	Day90
Total Area	480.6	972.6	721.4



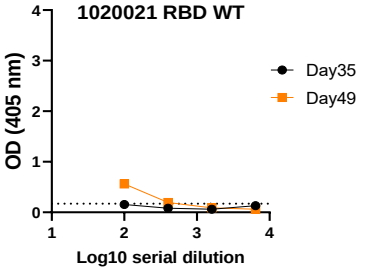
	Day35	Day49	Day90
Total Area	396.6	809.7	551.4



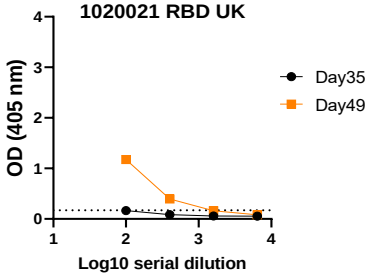
	Day35	Day49	Day90
Total Area	505.4	657.8	602.4



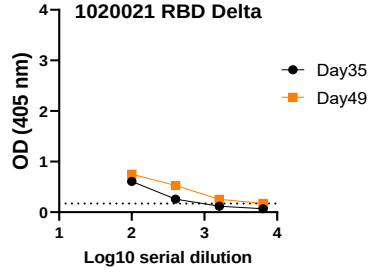
	Day35	Day49
Total Area	582.2	651.8



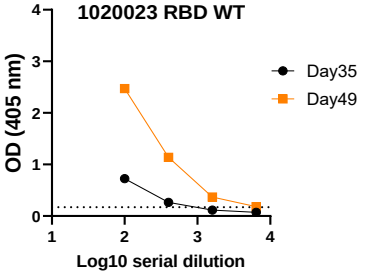
	Day35	Day49
Total Area	397.5	1149



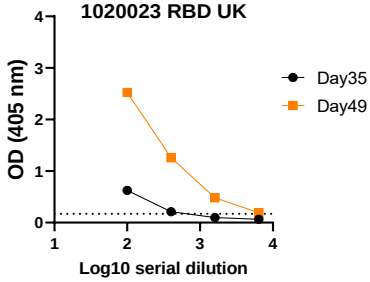
	Day35	Day49
Total Area	804.9	1693



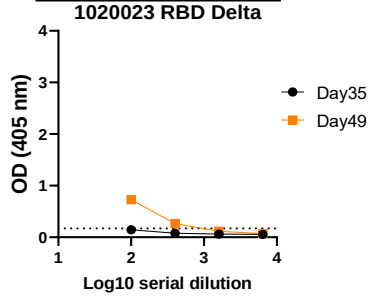
	Day35	Day49
Total Area	817.7	2769



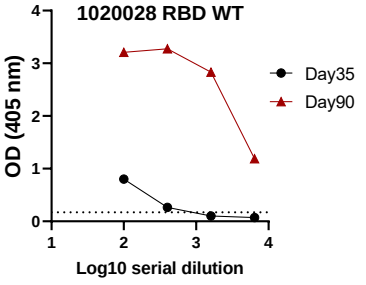
	Day35	Day49
Total Area	703.5	3229



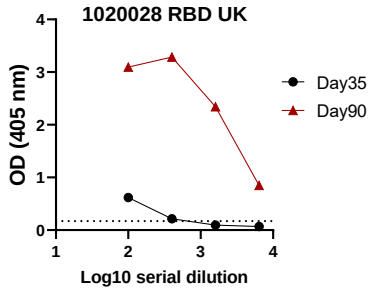
	Day35	Day49
Total Area	395.3	820.7



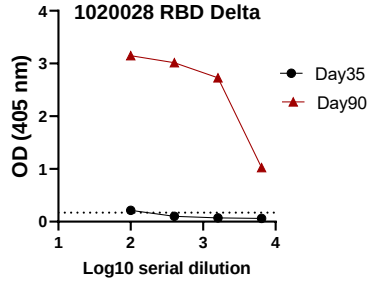
	Day35	Day90
Total Area	795.3	14287



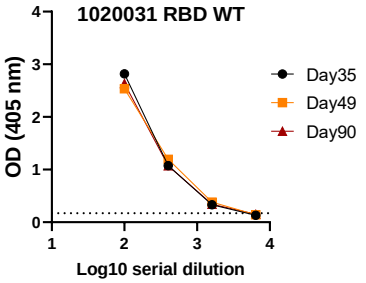
	Day35	Day90
Total Area	707.6	11988



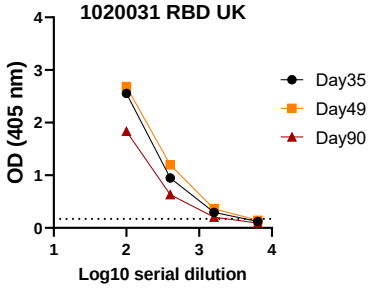
	Day35	Day90
Total Area	479.6	13377



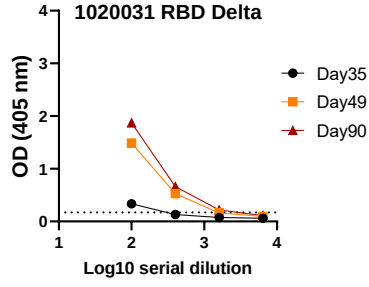
	Day35	Day49	Day90
Total Area	2533	2767	2595



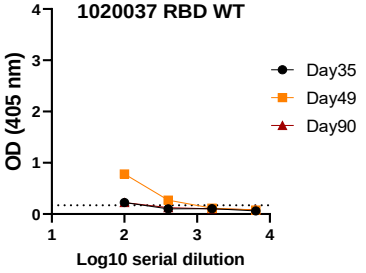
	Day35	Day49	Day90
Total Area	2274	2734	1582



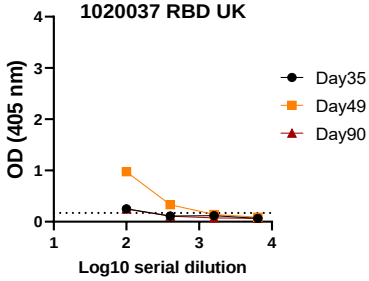
	Day35	Day49	Day90
Total Area	520.1	1337	1704



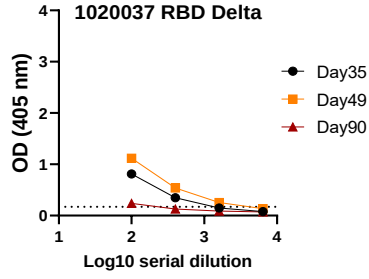
	Day35	Day49	Day90
Total Area	573.5	854.4	641.3



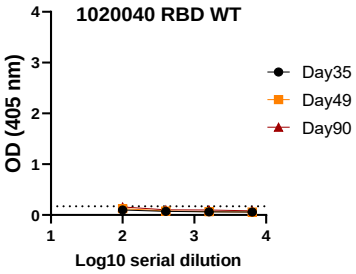
	Day35	Day49	Day90
Total Area	632.7	1028	499.8



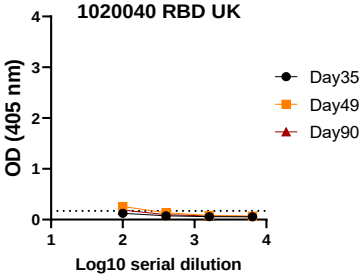
	Day35	Day49	Day90
Total Area	1021	1658	563.3



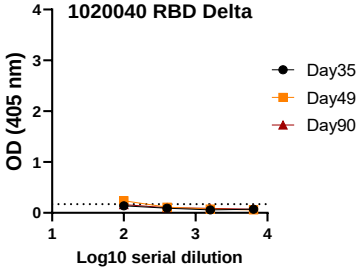
	Day35	Day49	Day90
Total Area	396.3	413.0	590.6



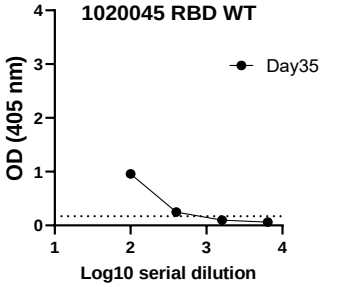
	Day35	Day49	Day90
Total Area	387.3	550.5	460.5



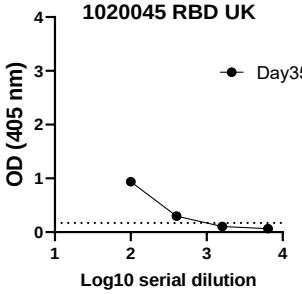
	Day35	Day49	Day90
Total Area	436.8	491.1	543.5



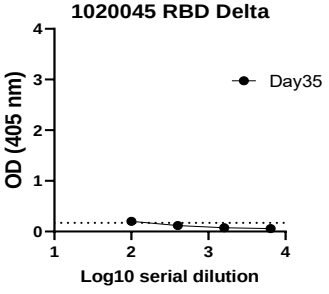
	Day35
Total Area	771.8



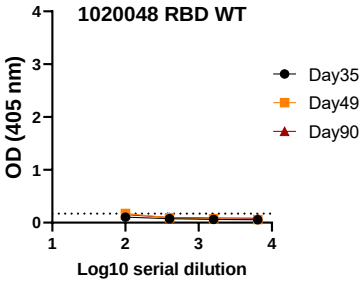
	Day35
Total Area	835.4



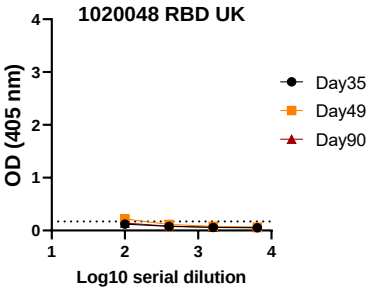
	Day35
Total Area	478.4



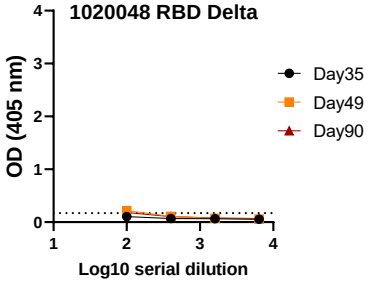
	Day35	Day49	Day90
Total Area	392.1	453.6	564.9



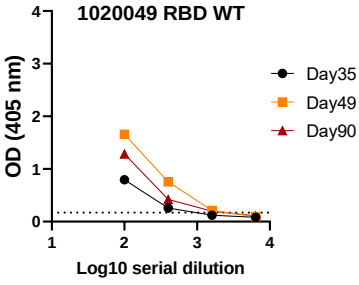
	Day35	Day49	Day90
Total Area	381.0	509.4	420.0



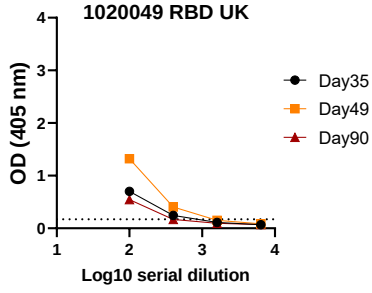
	Day35	Day49	Day90
Total Area	398.6	462.9	503.3



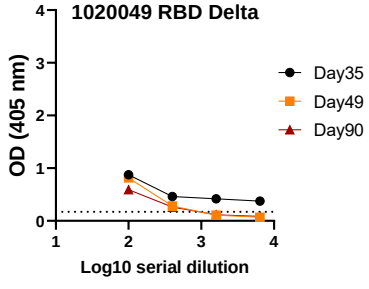
	Day35	Day49	Day90
Total Area	873.0	1678	1359



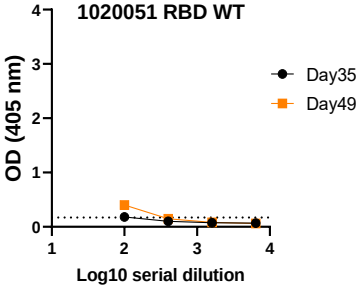
	Day35	Day49	Day90
Total Area	782.3	1157	661.4



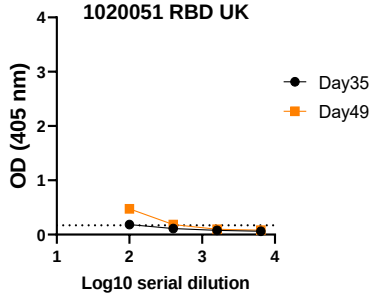
	Day35	Day49	Day90
Total Area	2629	822.6	836.0



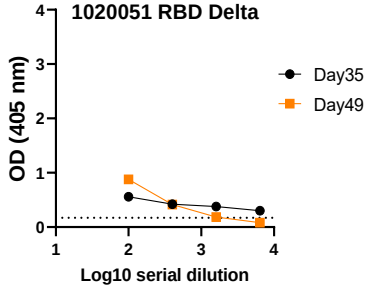
	Day35	Day49
Total Area	495.3	572.9



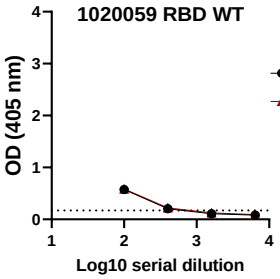
	Day35	Day49
Total Area	491.7	700.5



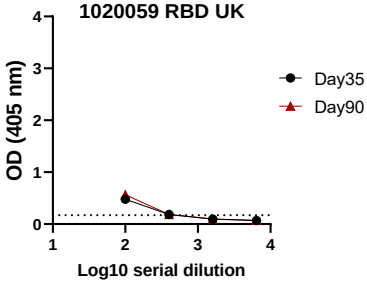
	Day35	Day49
Total Area	2253	1201



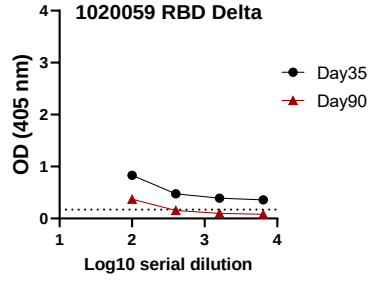
	Day35	Day90
Total Area	761.7	849.9



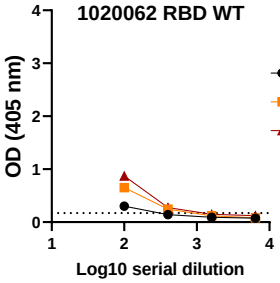
	Day35	Day90
Total Area	655.1	693.3



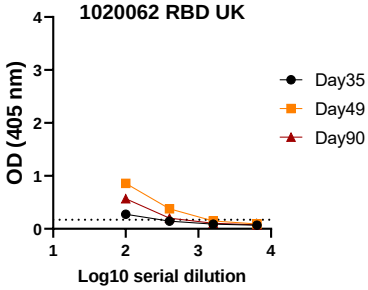
	Day35	Day90
Total Area	2516	658.8



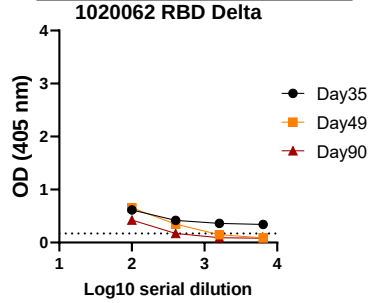
	Day35	Day49	Day90
Total Area	613.2	834.8	1072



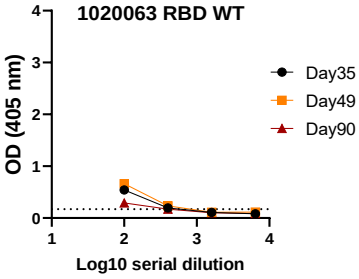
	Day35	Day49	Day90
Total Area	584.7	1080	733.2



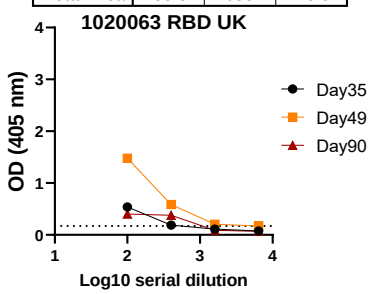
	Day35	Day49	Day90
Total Area	2313	1022	662.7



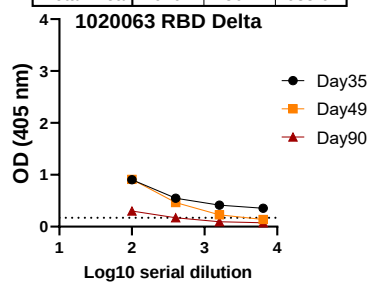
	Day35	Day49	Day90
Total Area	746.7	882.9	686.1



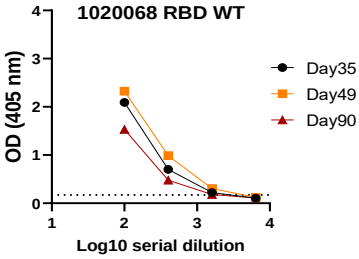
	Day35	Day49	Day90
Total Area	735.3	1683	775.5



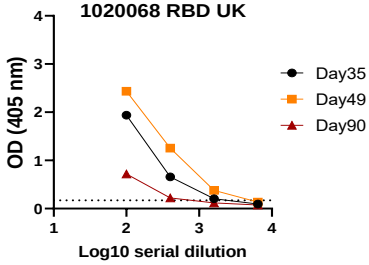
	Day35	Day49	Day90
Total Area	2640	1504	635.0



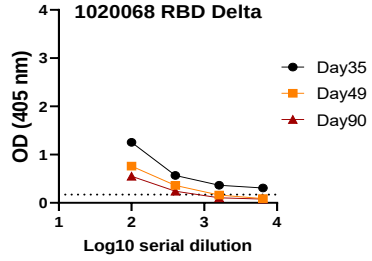
	Day35	Day49	Day90
Total Area	1752	2294	1394



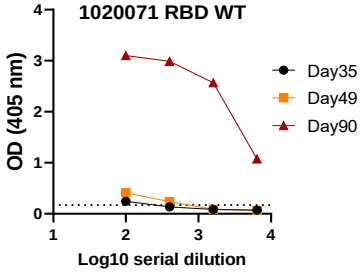
	Day35	Day49	Day90
Total Area	1632	2764	805.2



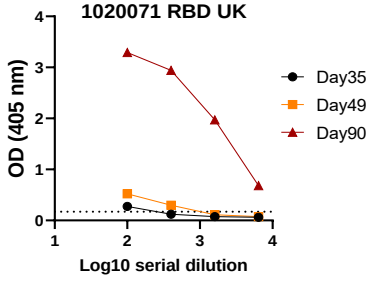
	Day35	Day49	Day90
Total Area	2448	1084	766.1



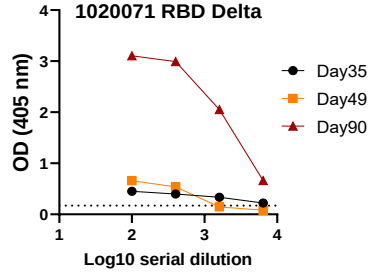
	Day35	Day49	Day90
Total Area	568.2	675.3	12989



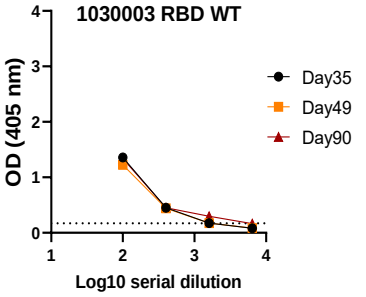
	Day35	Day49	Day90
Total Area	502.1	816.9	10258



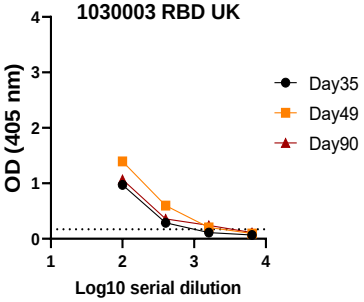
	Day35	Day49	Day90
Total Area	1904	1131	10450



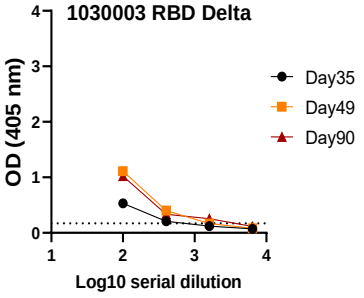
	Day35	Day49	Day90
Total Area	1263	1242	1835



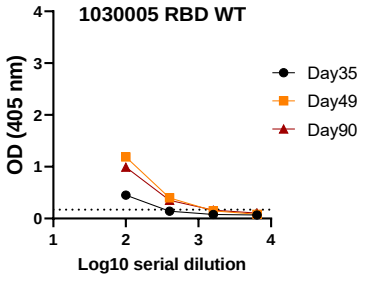
	Day35	Day49	Day90
Total Area	864.9	1497	1419



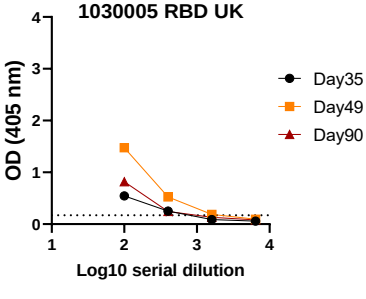
	Day35	Day49	Day90
Total Area	773.3	1173	1448



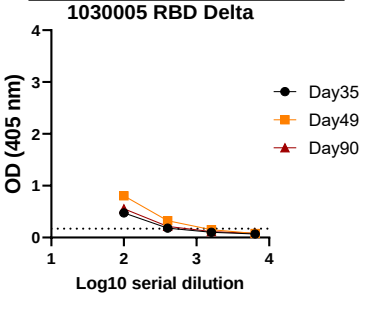
	Day35	Day49	Day90
Total Area	569.0	1119	1149



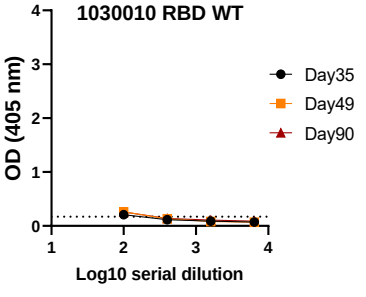
	Day35	Day49	Day90
Total Area	674.3	1412	895.7



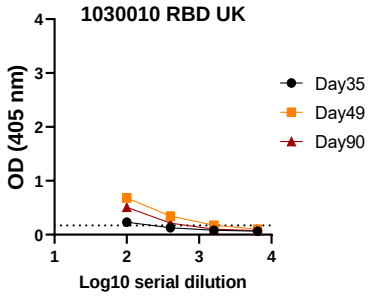
	Day35	Day49	Day90
Total Area	675.3	1012	789.2



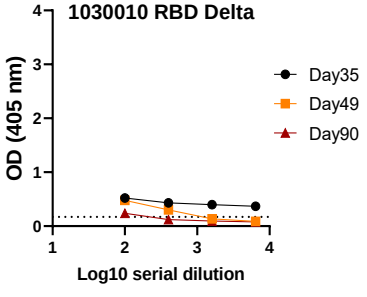
	Day35	Day49	Day90
Total Area	554.4	548.3	671.9



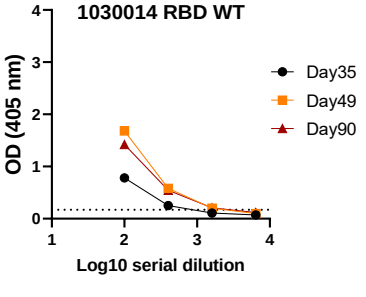
	Day35	Day49	Day90
Total Area	534.9	1130	720.2



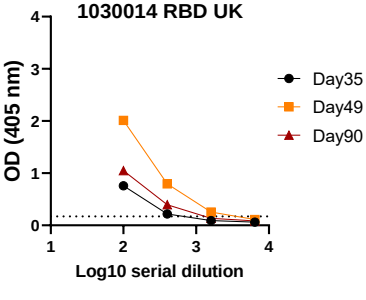
	Day35	Day49	Day90
Total Area	2481	914.4	598.2



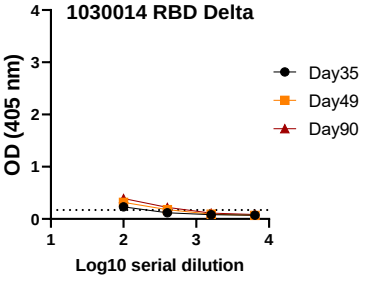
	Day35	Day49	Day90
Total Area	802.2	1527	1533



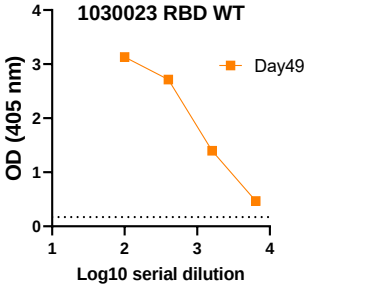
	Day35	Day49	Day90
Total Area	704.9	1930	1062



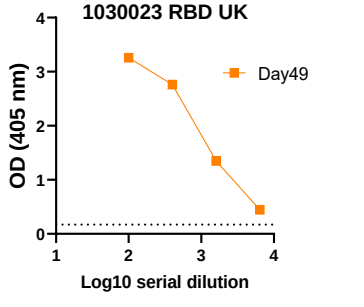
	Day35	Day49	Day90
Total Area	540.6	618.6	758.7



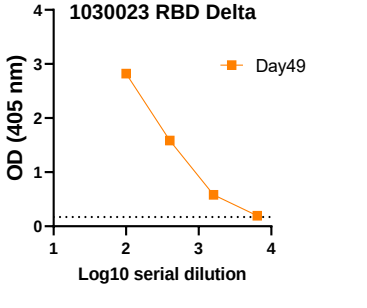
	Day49
Total Area	7820



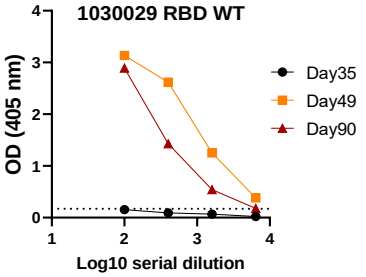
	Day49
Total Area	7675



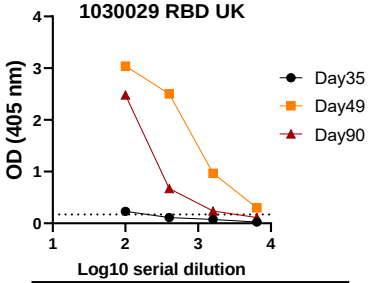
	Day49
Total Area	3826



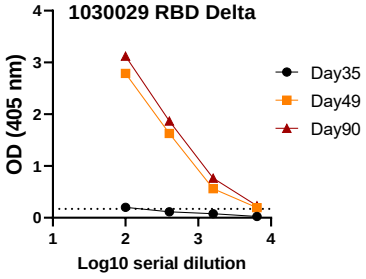
	Day35	Day49	Day90
Total Area	342.0	7102	3551



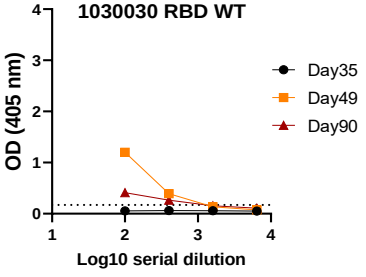
	Day35	Day49	Day90
Total Area	400.8	5950	1856



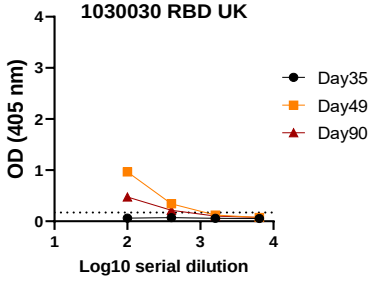
	Day35	Day49	Day90
Total Area	409.8	3791	4720



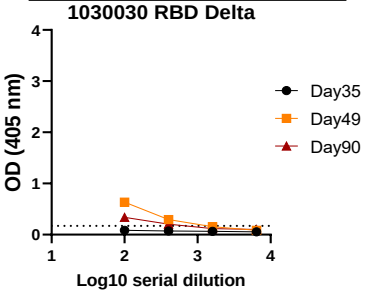
	Day35	Day49	Day90
Total Area	356.7	1061	979.4



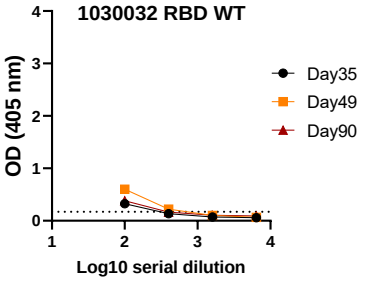
	Day35	Day49	Day90
Total Area	374.0	951.0	715.7



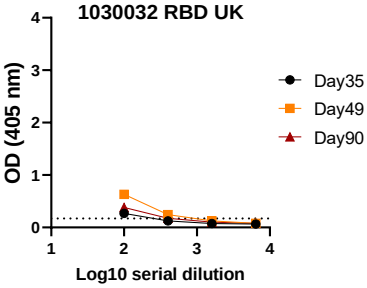
	Day35	Day49	Day90
Total Area	396.2	980.3	795.3



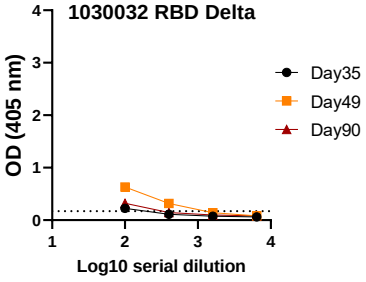
	Day35	Day49	Day90
Total Area	512.3	722.6	718.2



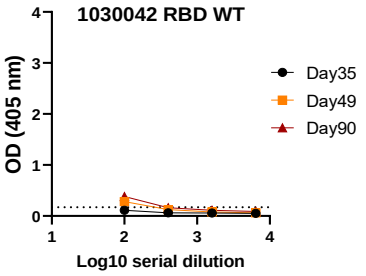
	Day35	Day49	Day90
Total Area	515.4	840.5	688.1



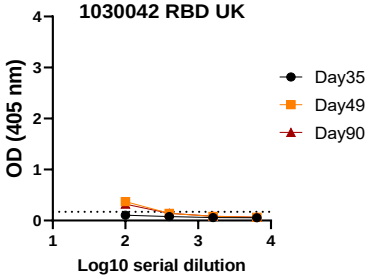
	Day35	Day49	Day90
Total Area	489.5	954.3	651.8



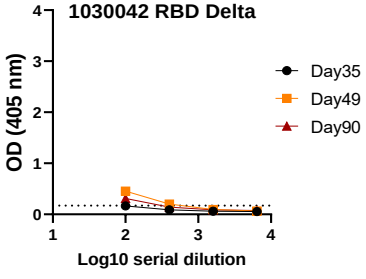
	Day35	Day49	Day90
Total Area	368.1	516.6	731.4



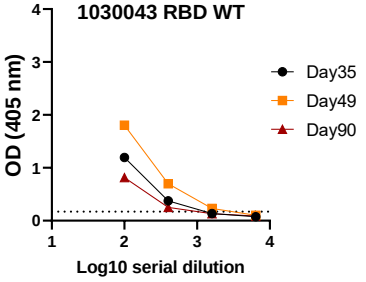
	Day35	Day49	Day90
Total Area	377.1	564.2	563.9



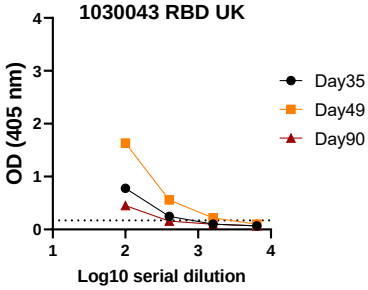
	Day35	Day49	Day90
Total Area	412.8	659.4	603.2



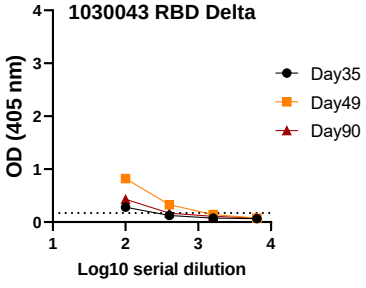
	Day35	Day49	Day90
Total Area	1047	1730	919.2



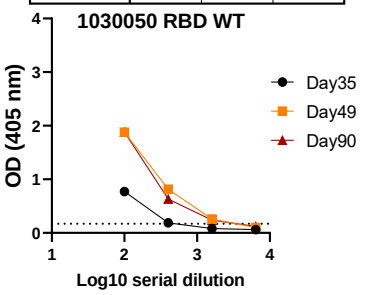
	Day35	Day49	Day90
Total Area	768.8	1557	646.1



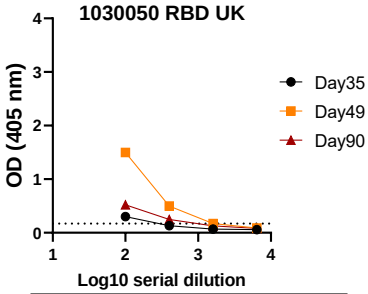
	Day35	Day49	Day90
Total Area	523.1	968.7	698.6



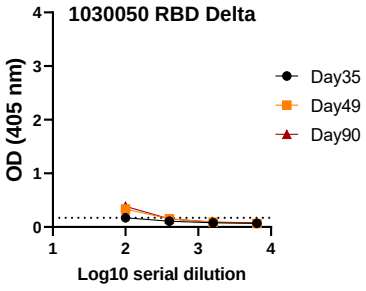
	Day35	Day49	Day90
Total Area	647.1	1899	1759



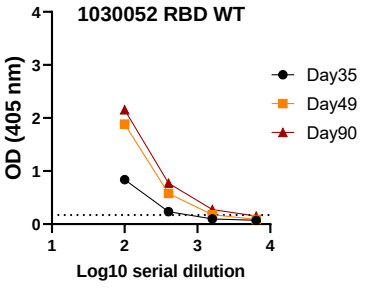
	Day35	Day49	Day90
Total Area	489.2	1323	844.5



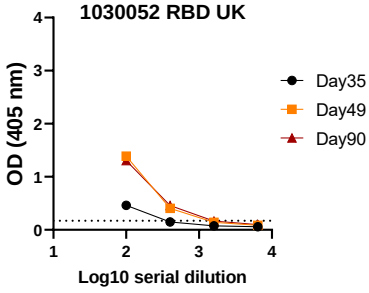
	Day35	Day49	Day90
Total Area	504.0	579.5	632.9



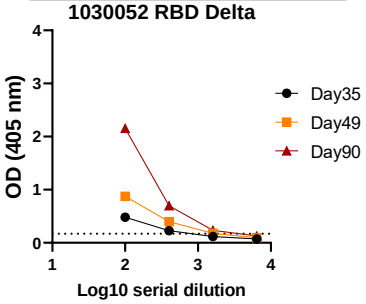
	Day35	Day49	Day90
Total Area	767.0	1468	2089



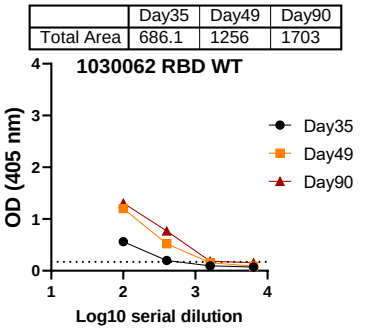
	Day35	Day49	Day90
Total Area	544.7	1143	1269



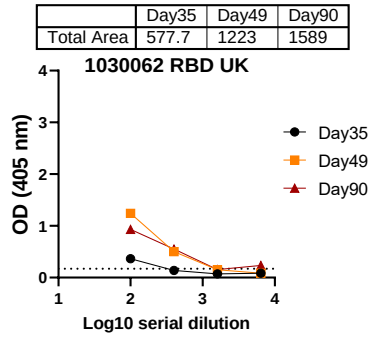
	Day35	Day49	Day90
Total Area	770.6	1193	1858



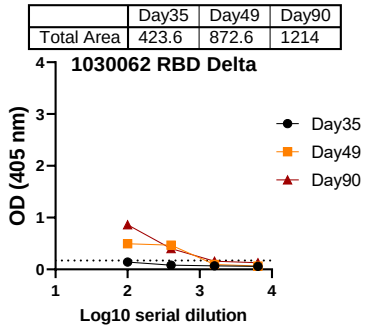
	Day35	Day49	Day90
Total Area	686.1	1256	1703



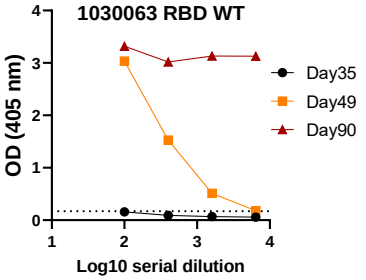
	Day35	Day49	Day90
Total Area	577.7	1223	1589



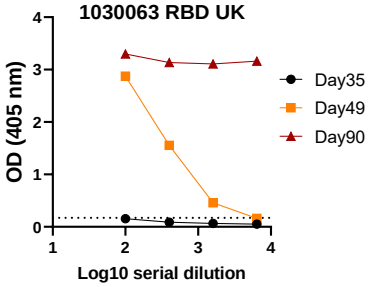
	Day35	Day49	Day90
Total Area	423.6	872.6	1214



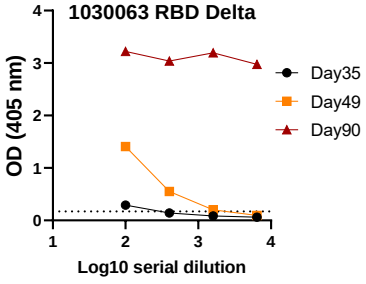
	Day35	Day49	Day90
Total Area	444.5	3580	19665



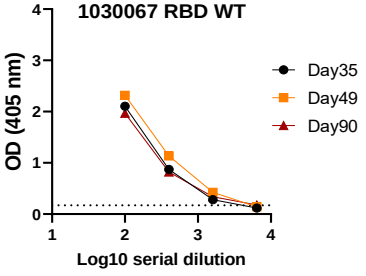
	Day35	Day49	Day90
Total Area	403.1	3352	19765



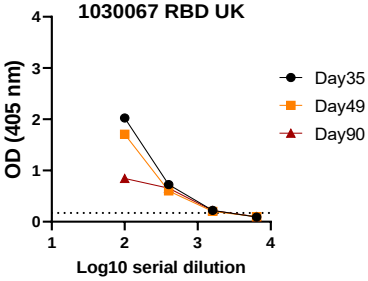
	Day35	Day49	Day90
Total Area	549.5	1457	19487



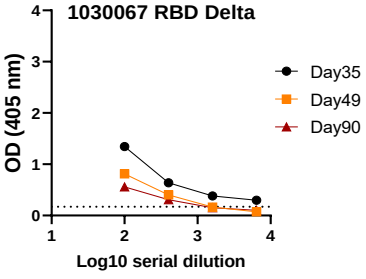
	Day35	Day49	Day90
Total Area	2107	2816	2349



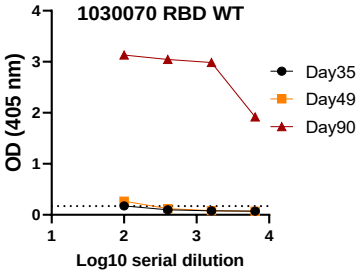
	Day35	Day49	Day90
Total Area	1730	1548	1503



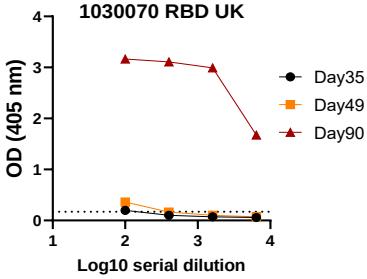
	Day35	Day49	Day90
Total Area	2535	1087	1019



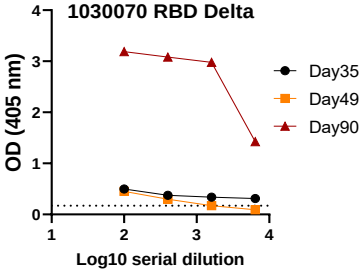
	Day35	Day49	Day90
Total Area	505.4	548.6	16317



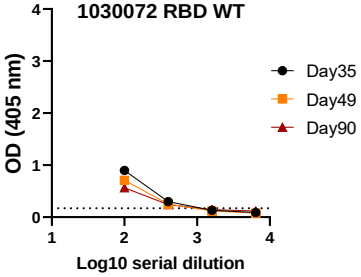
	Day35	Day49	Day90
Total Area	459.6	645.2	15798



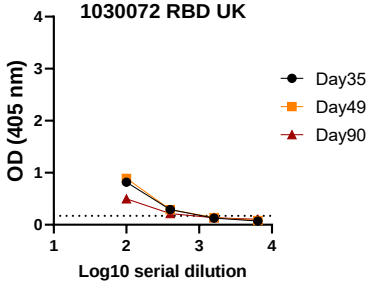
	Day35	Day49	Day90
Total Area	2114	1020	15153



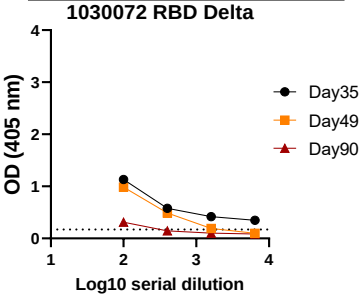
	Day35	Day49	Day90
Total Area	966.6	833.9	987.6



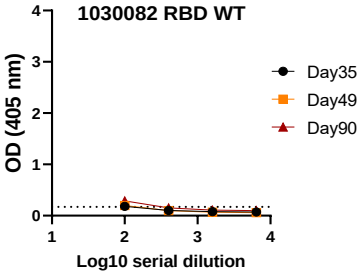
	Day35	Day49	Day90
Total Area	899.0	963.3	896.1



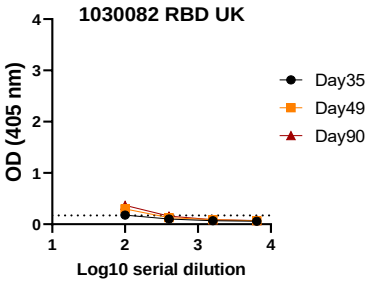
	Day35	Day49	Day90
Total Area	2692	1319	660.8



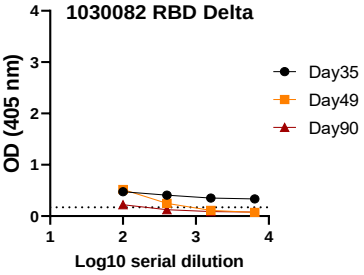
	Day35	Day49	Day90
Total Area	509.7	453.6	716.3



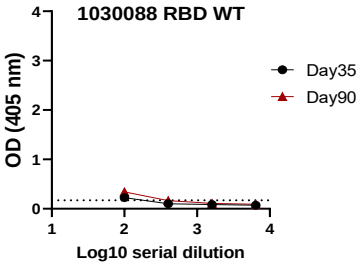
	Day35	Day49	Day90
Total Area	451.8	571.1	609.5



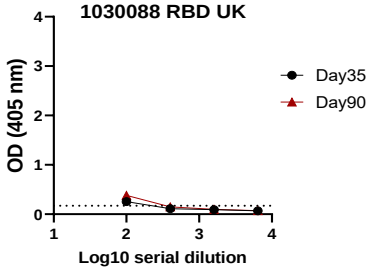
	Day35	Day49	Day90
Total Area	2236	769.7	584.7



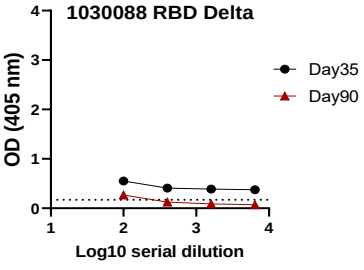
	Day35	Day90
Total Area	533.6	722.0



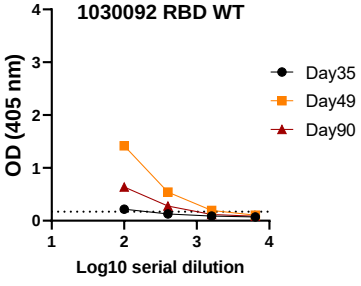
	Day35	Day90
Total Area	554.6	635.3



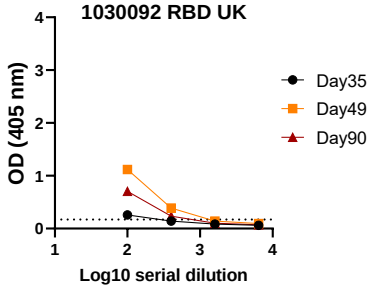
	Day35	Day90
Total Area	2460	567.5



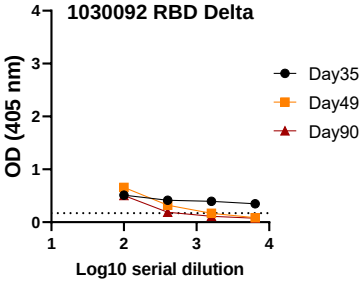
	Day35	Day49	Day90
Total Area	563.1	1452	862.2



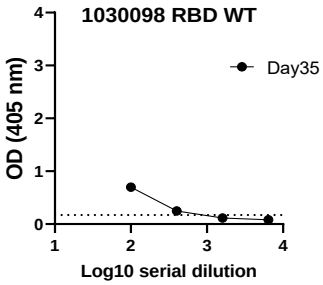
	Day35	Day49	Day90
Total Area	547.5	1106	752.3



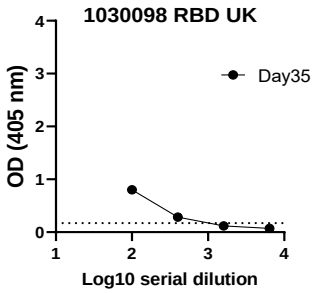
	Day35	Day49	Day90
Total Area	2410	1053	729.9



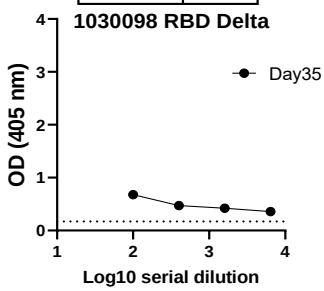
	Day35
Total Area	829.2



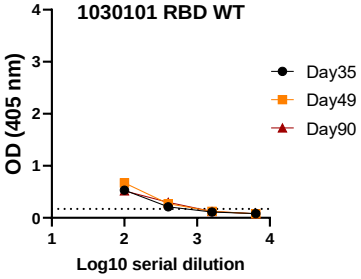
	Day35
Total Area	869.0



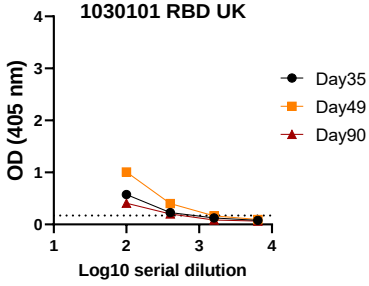
	Day35
Total Area	2580



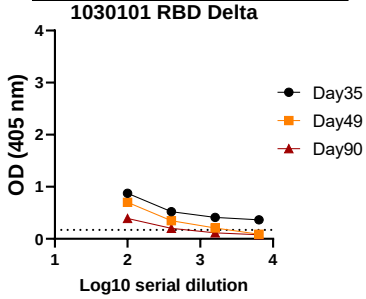
	Day35	Day49	Day90
Total Area	768.8	867.9	856.4



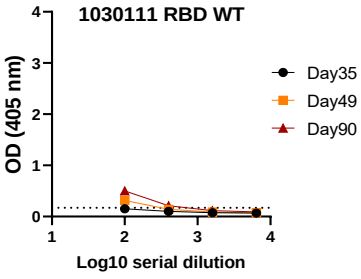
	Day35	Day49	Day90
Total Area	822.8	1173	619.4



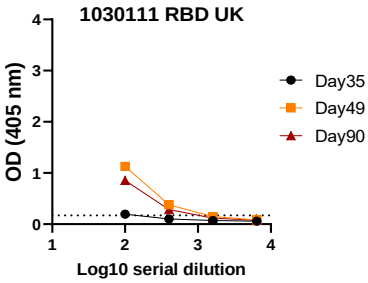
	Day35	Day49	Day90
Total Area	2632	1208	740.6



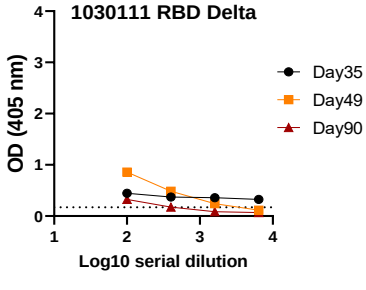
	Day35	Day49	Day90
Total Area	489.9	594.3	801.6



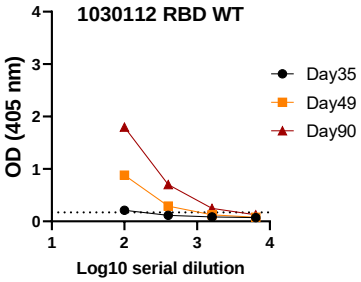
	Day35	Day49	Day90
Total Area	467.4	1094	876.8



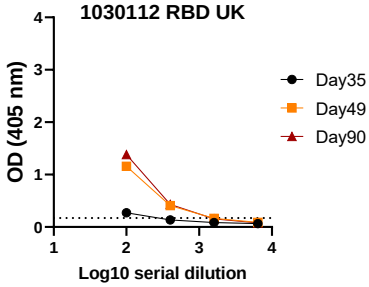
	Day35	Day49	Day90
Total Area	2200	1488	600.3



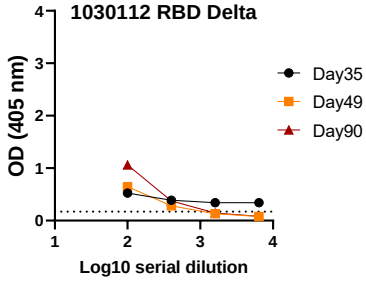
	Day35	Day49	Day90
Total Area	548.7	914.1	1847



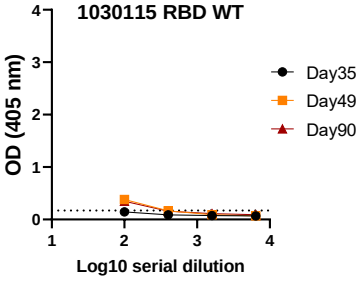
	Day35	Day49	Day90
Total Area	552.6	1193	1183



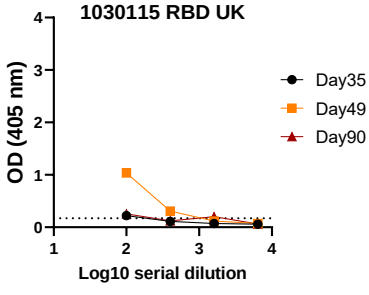
	Day35	Day49	Day90
Total Area	2209	891.9	1068



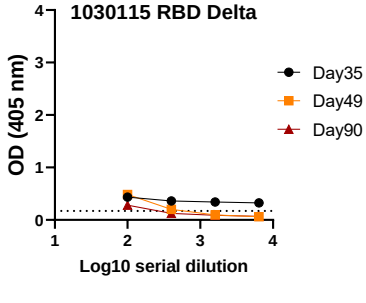
	Day35	Day49	Day90
Total Area	475.8	624.2	730.7



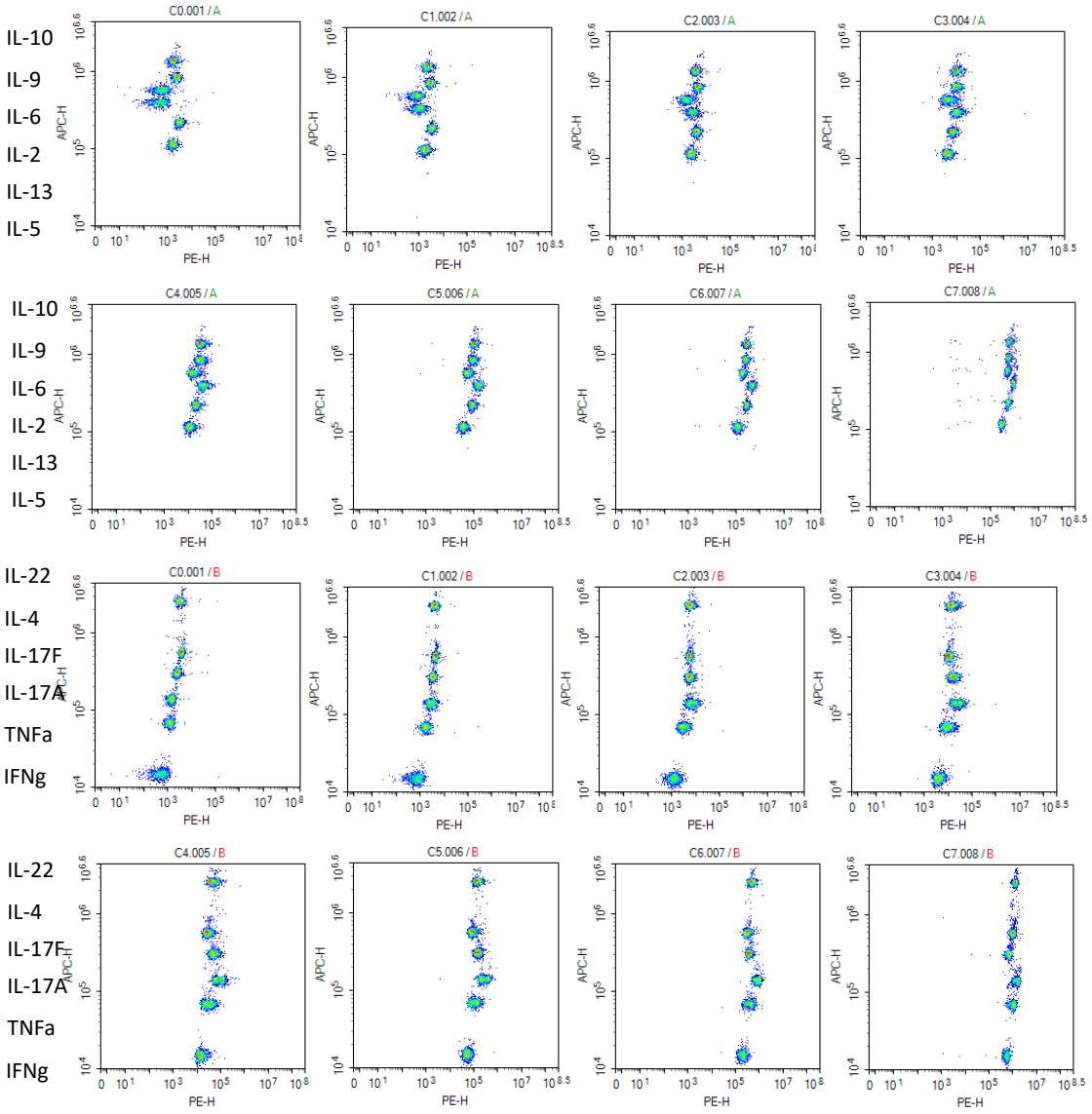
	Day35	Day49	Day90
Total Area	470.7	911.0	885.3



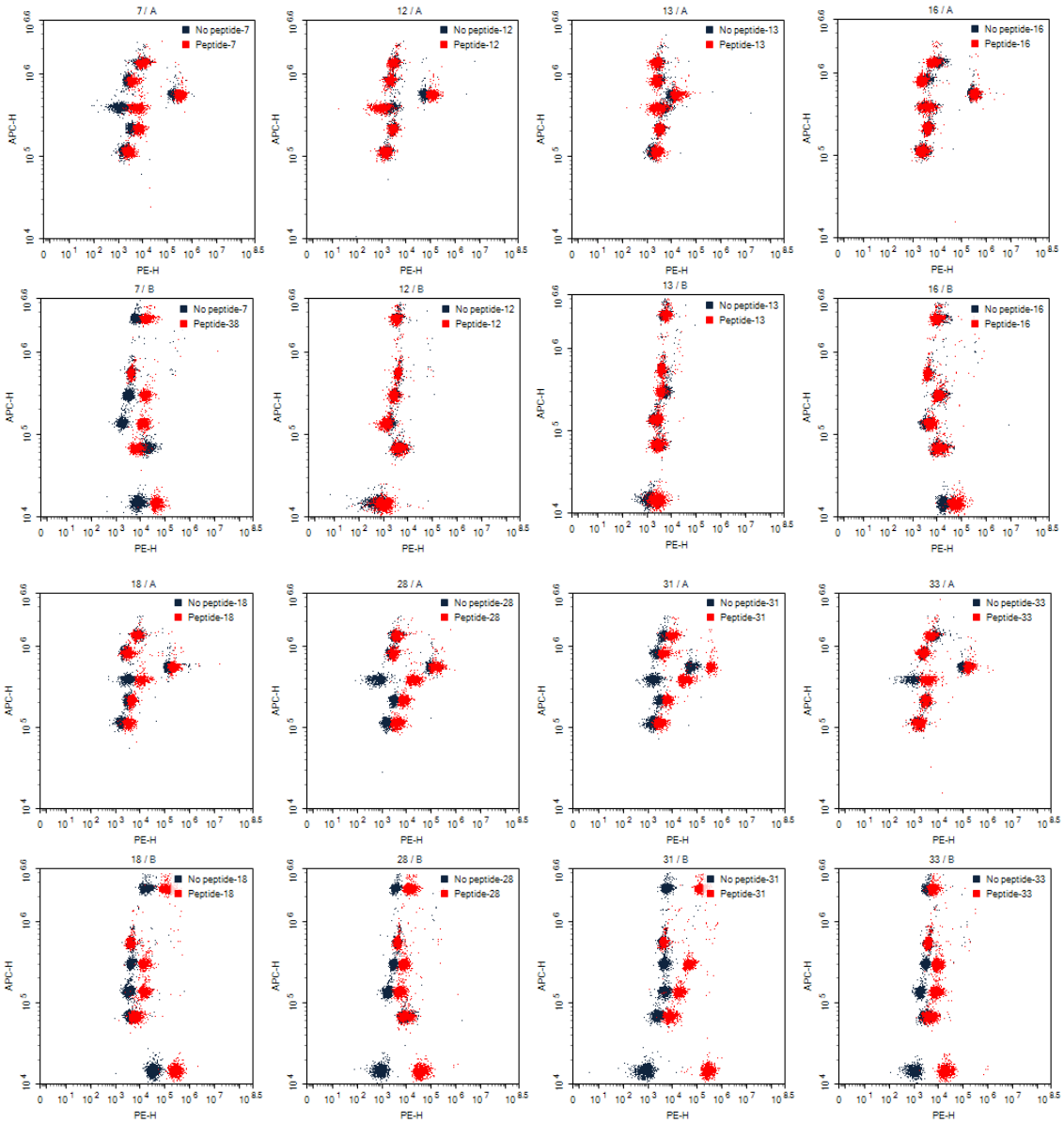
	Day35	Day49	Day90
Total Area	2137	656.1	566.3

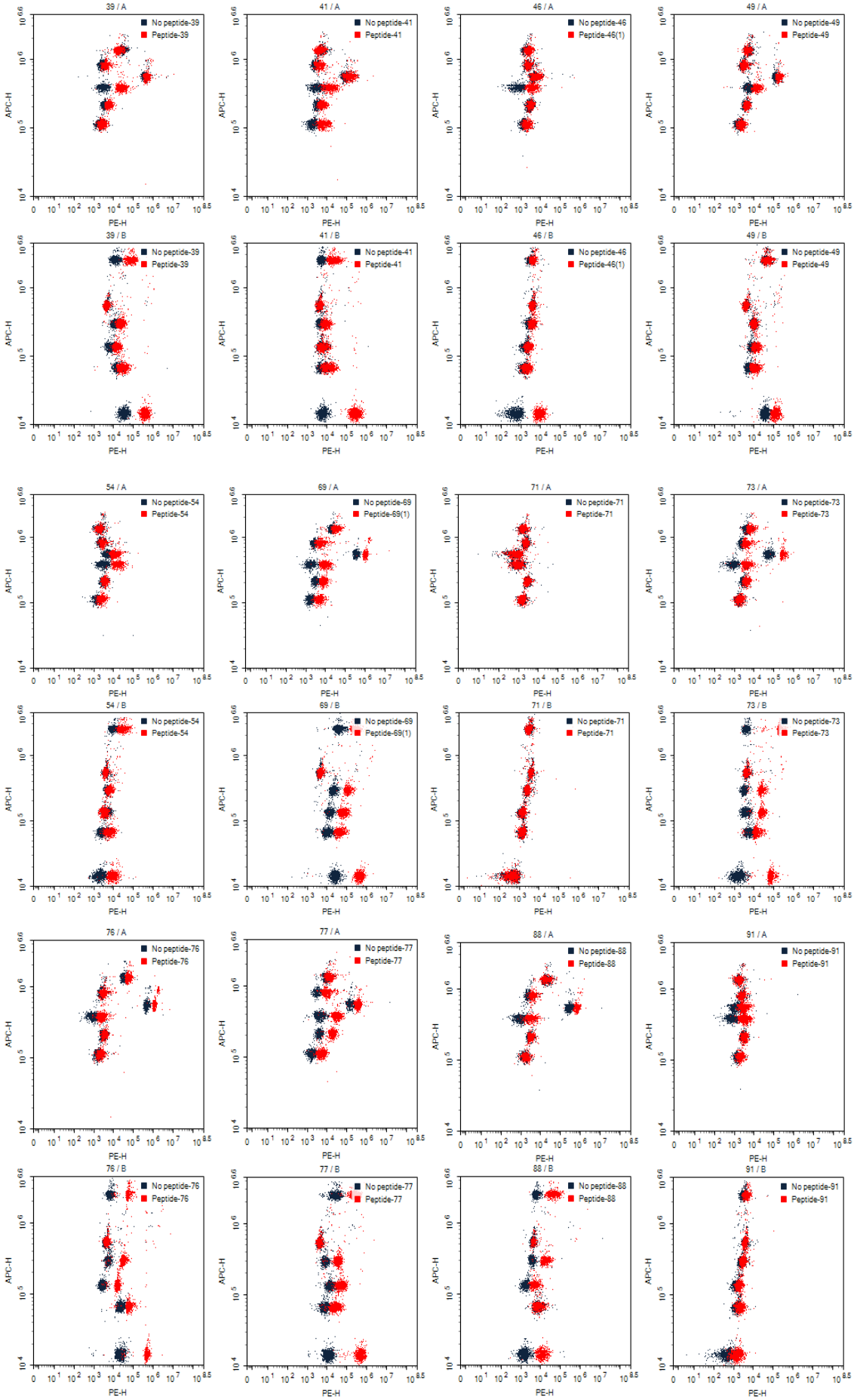


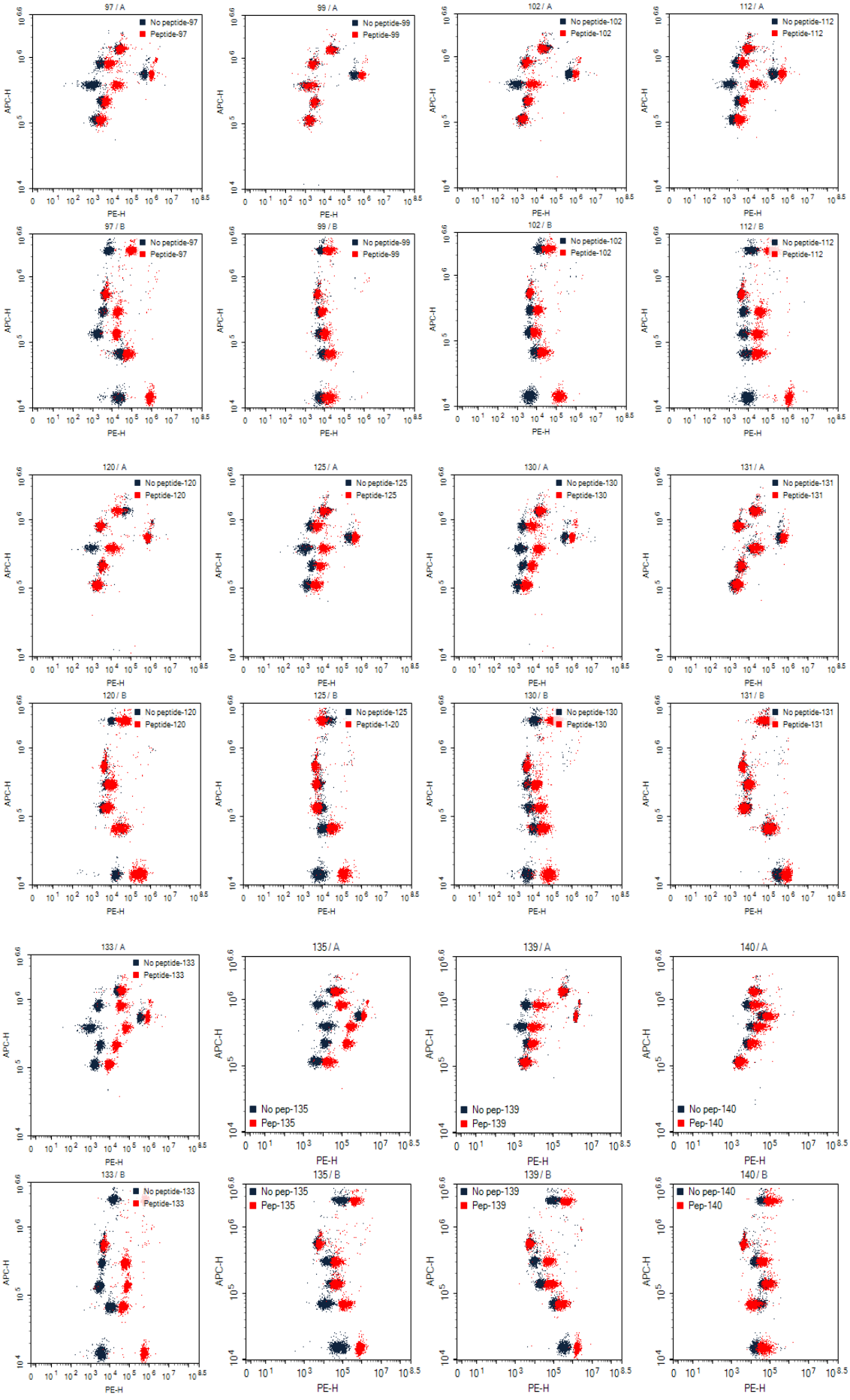
Individual CBA dot plot graphs in this page indicate 8 standards provided by LEGENDplex™ Multi-Analyte Flow Assay Kit (BioLegend, USA) kit (See 2.2.9) and, the cytokines represented on the right site are the match of each cumulative in the graphs from bottom to top. For each dot graph, the same pattern is followed for the next pages which represents CBA overlay do graphs for each phase 2 volunteer.

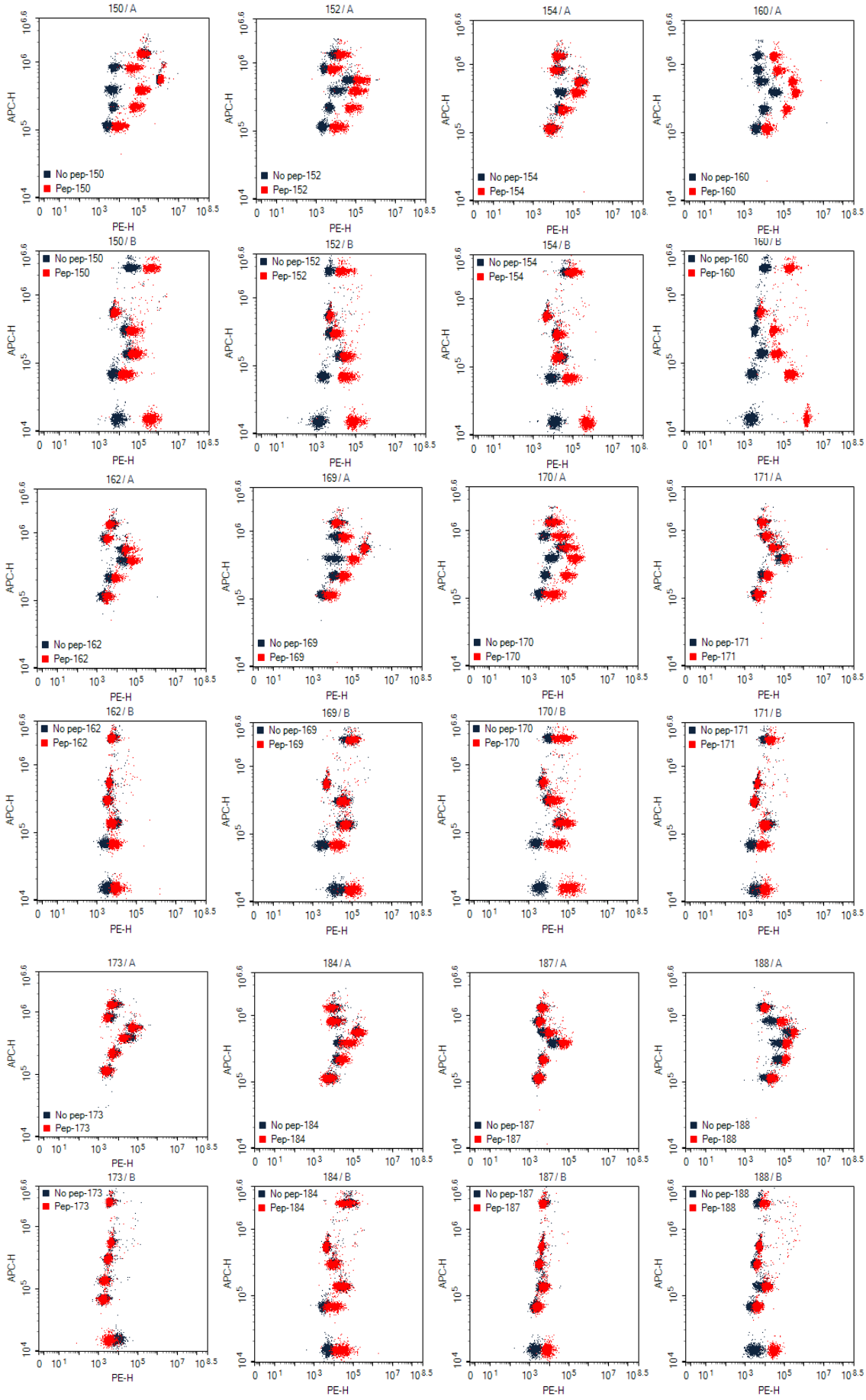


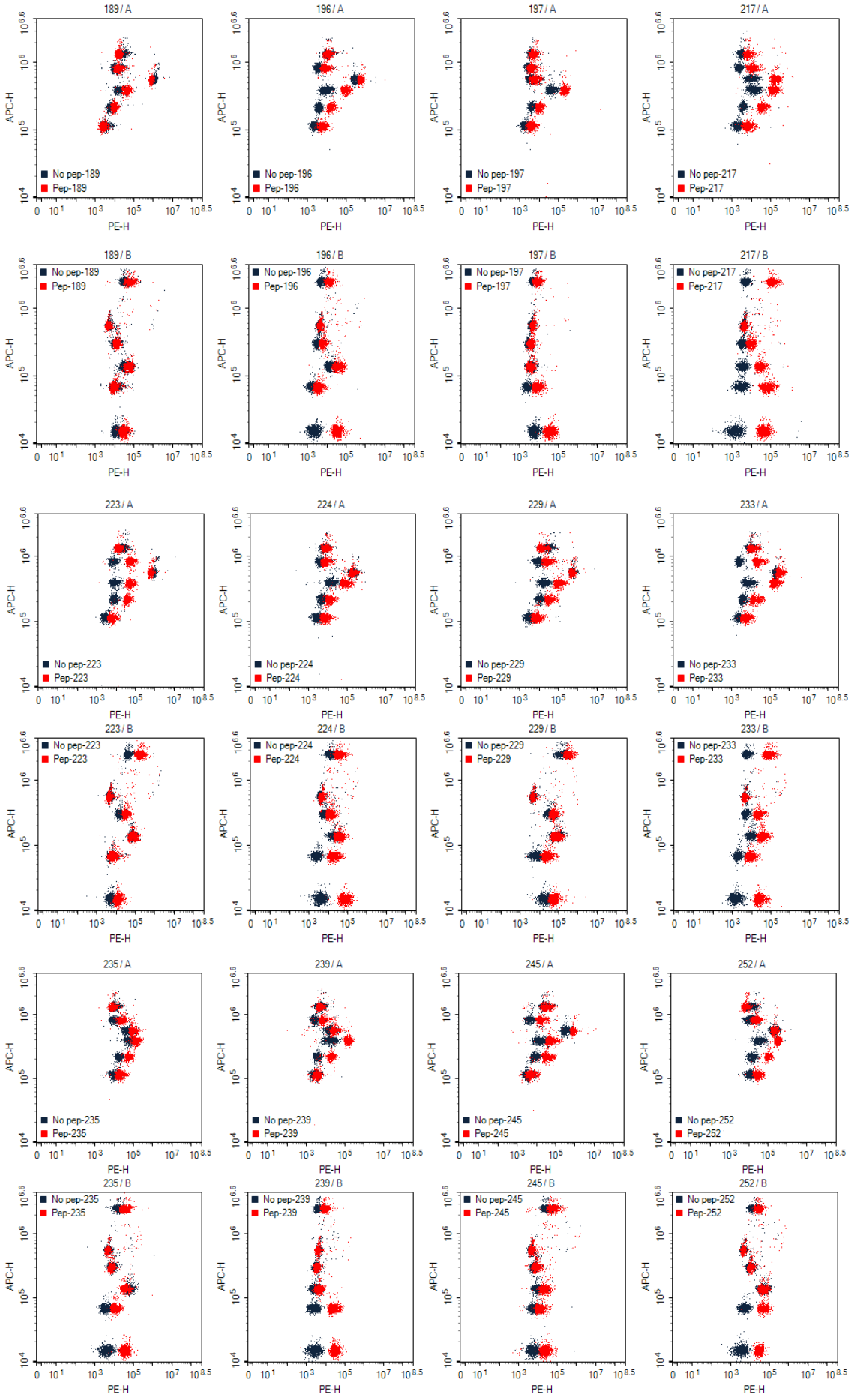
Individual CBA dot plot graphs of Phase2 volunteers to show induction of T cell responses after stimulation with S, N, M and O peptide pools. Stimulated and non-stimulated supernatants were studied according to manufacturer's instructions (LEGENDplex™ HU Th Cytokine Panel (12-plex) w/ VbP kit, Biolegend, USA). The results were analysed with LEGENDplex™ Data Analysis Software (Biolegend, USA). 'Peptide' indicates values after stimulation of PBMCs with SNMO peptide pool and 'No Peptide' indicates values with no stimulation but only resting of PBMCs.

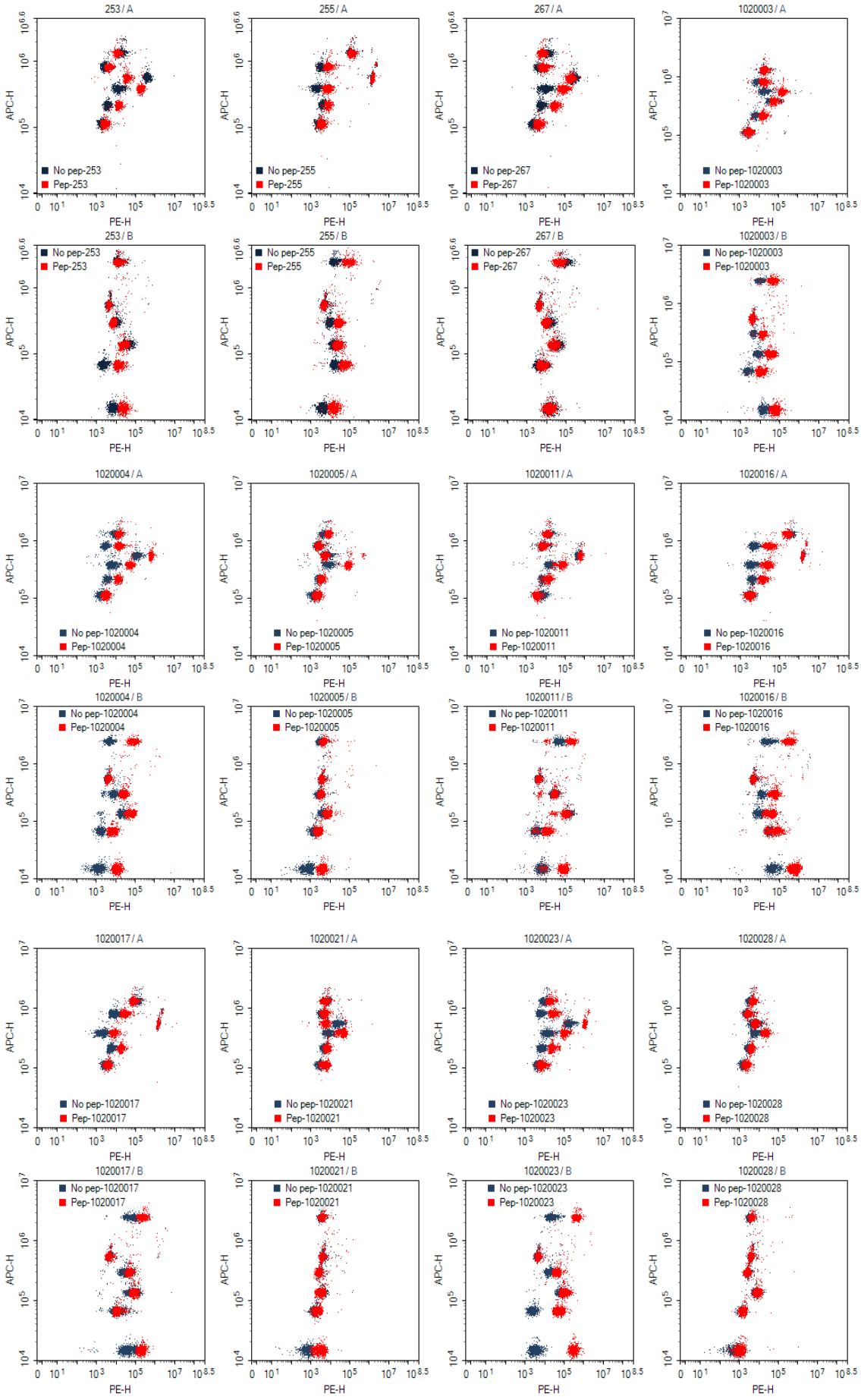


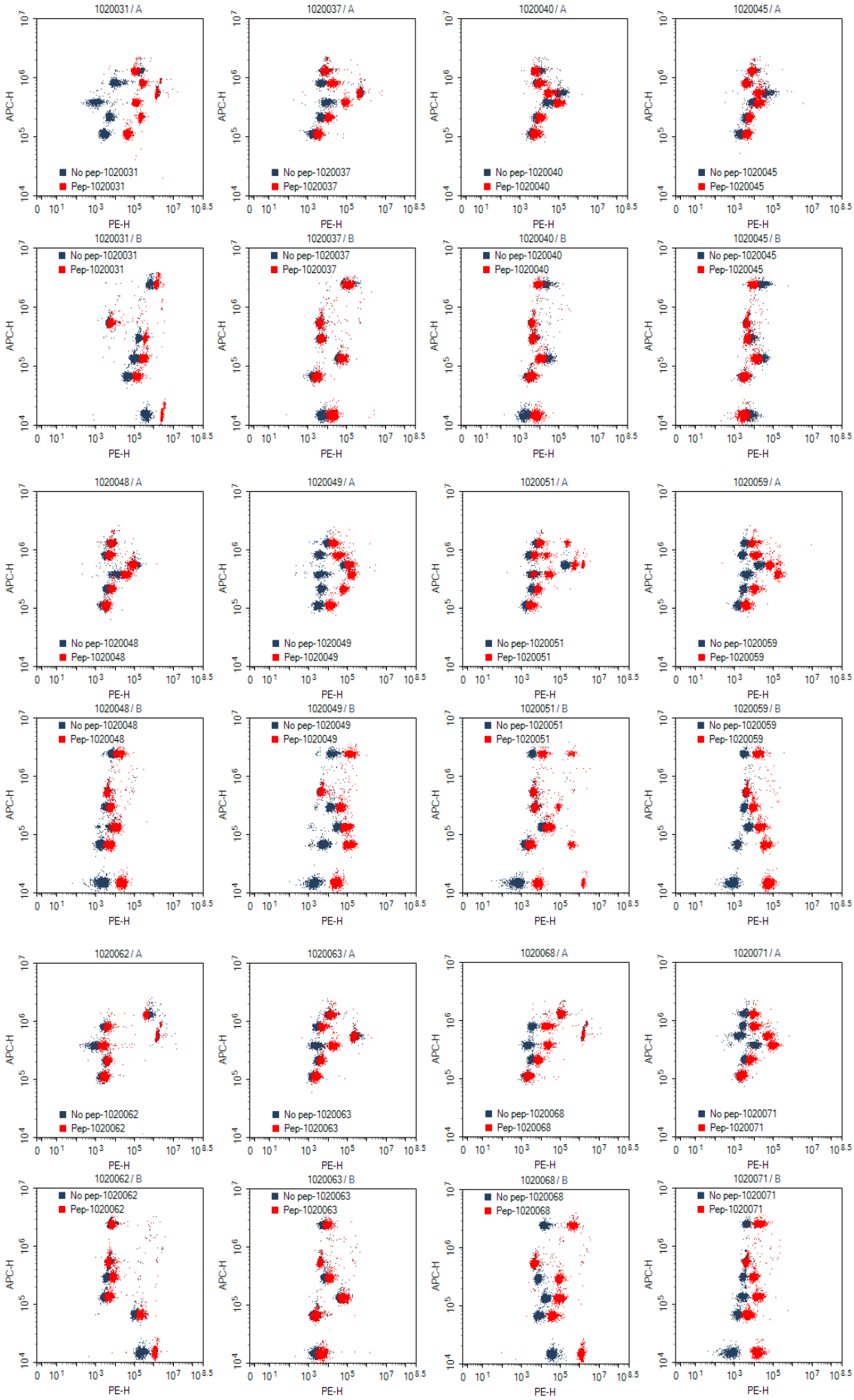

39 / A
No peptide-39
Peptide-39
41 / A
No peptide-41
Peptide-41
46 / A
No peptide-46
Peptide-46(1)
49 / A
No peptide-49
Peptide-49
39 / B
No peptide-39
Peptide-39
41 / B
No peptide-41
Peptide-41
46 / B
No peptide-46
Peptide-46(1)
49 / B
No peptide-49
Peptide-49
54 / A
No peptide-54
Peptide-54
69 / A
No peptide-69
Peptide-69(1)
71 / A
No peptide-71
Peptide-71
73 / A
No peptide-73
Peptide-73
54 / B
No peptide-54
Peptide-54
69 / B
No peptide-69
Peptide-69(1)
71 / B
No peptide-71
Peptide-71
73 / B
No peptide-73
Peptide-73
76 / A
No peptide-76
Peptide-76
77 / A
No peptide-77
Peptide-77
88 / A
No peptide-88
Peptide-88
91 / A
No peptide-91
Peptide-91
76 / B
No peptide-76
Peptide-76
77 / B
No peptide-77
Peptide-77
88 / B
No peptide-88
Peptide-88
91 / B
No peptide-91
Peptide-91
APC-H
PE-H

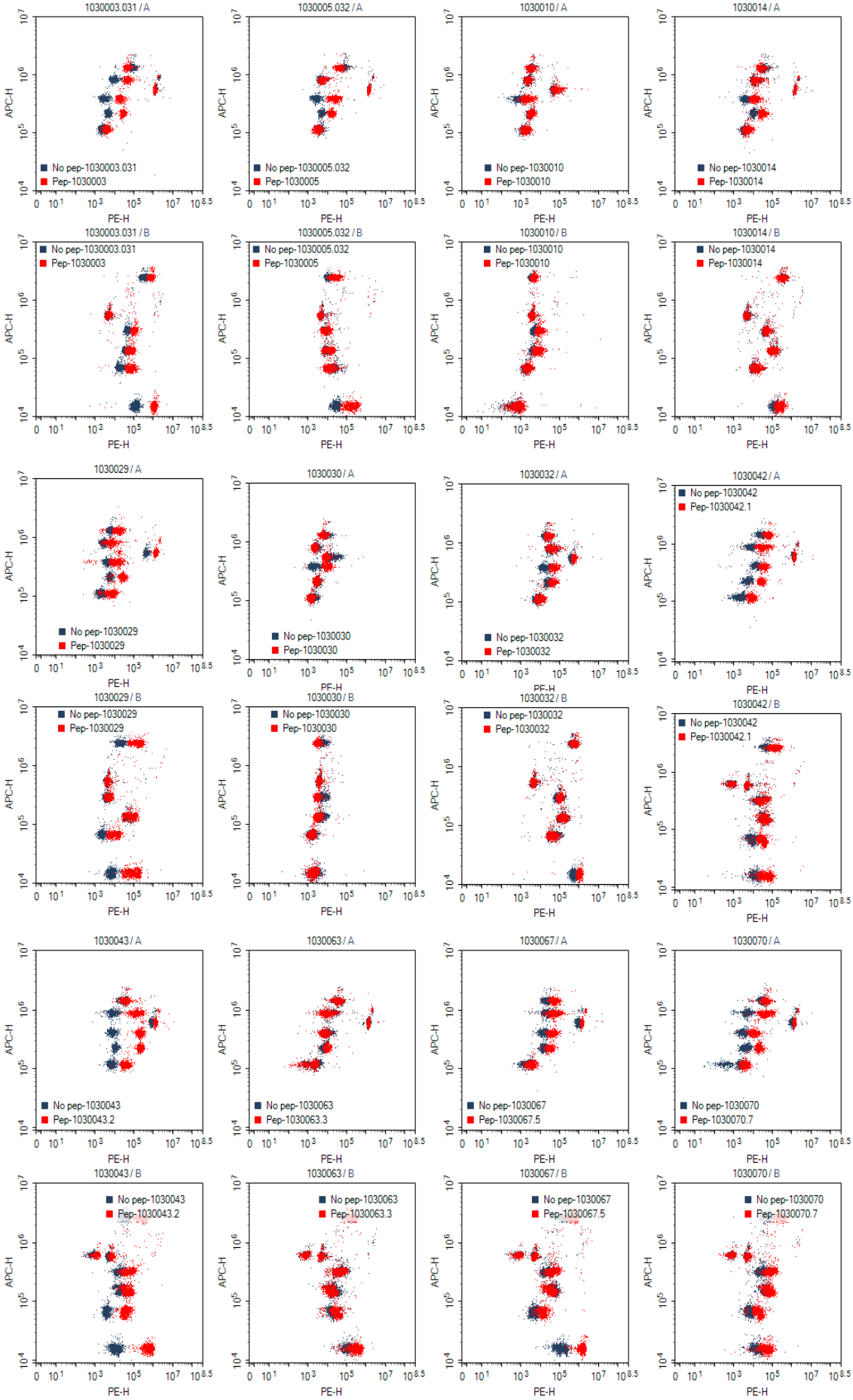

97 / A
No peptide-97
Peptide-97
99 / A
No peptide-99
Peptide-99
102 / A
No peptide-102
Peptide-102
112 / A
No peptide-112
Peptide-112
97 / B
No peptide-97
Peptide-97
99 / B
No peptide-99
Peptide-99
102 / B
No peptide-102
Peptide-102
112 / B
No peptide-112
Peptide-112
120 / A
No peptide-120
Peptide-120
125 / A
No peptide-125
Peptide-125
130 / A
No peptide-130
Peptide-130
131 / A
No peptide-131
Peptide-131
120 / B
No peptide-120
Peptide-120
125 / B
No peptide-125
Peptide-1-20
130 / B
No peptide-130
Peptide-130
131 / B
No peptide-131
Peptide-131
133 / A
No peptide-133
Peptide-133
135 / A
No pep-135
Pep-135
139 / A
No pep-139
Pep-139
140 / A
No pep-140
Pep-140
133 / B
No peptide-133
Peptide-133
135 / B
No pep-135
Pep-135
139 / B
No pep-139
Pep-139
140 / B
No pep-140
Pep-140
APC-H
PE-H

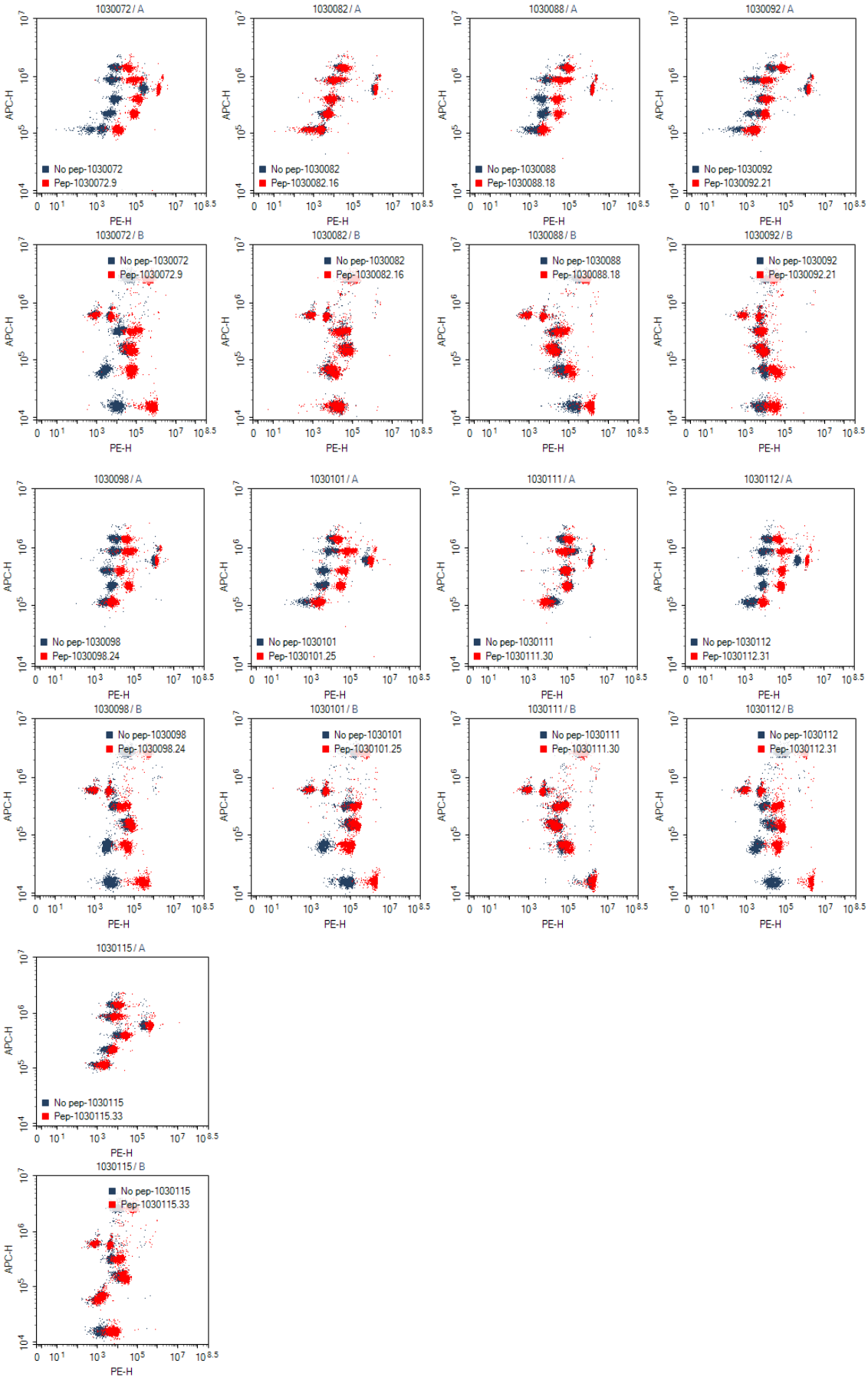

150 / A
No pep-150
Pep-150
152 / A
No pep-152
Pep-152
154 / A
No pep-154
Pep-154
160 / A
No pep-160
Pep-160
150 / B
No pep-150
Pep-150
152 / B
No pep-152
Pep-152
154 / B
No pep-154
Pep-154
160 / B
No pep-160
Pep-160
162 / A
No pep-162
Pep-162
169 / A
No pep-169
Pep-169
170 / A
No pep-170
Pep-170
171 / A
No pep-171
Pep-171
162 / B
No pep-162
Pep-162
169 / B
No pep-169
Pep-169
170 / B
No pep-170
Pep-170
171 / B
No pep-171
Pep-171
173 / A
No pep-173
Pep-173
184 / A
No pep-184
Pep-184
187 / A
No pep-187
Pep-187
188 / A
No pep-188
Pep-188
173 / B
No pep-173
Pep-173
184 / B
No pep-184
Pep-184
187 / B
No pep-187
Pep-187
188 / B
No pep-188
Pep-188
APC-H
PE-H


189 / A
No pep-189
Pep-189
196 / A
No pep-196
Pep-196
197 / A
No pep-197
Pep-197
217 / A
No pep-217
Pep-217
189 / B
No pep-189
Pep-189
196 / B
No pep-196
Pep-196
197 / B
No pep-197
Pep-197
217 / B
No pep-217
Pep-217
223 / A
No pep-223
Pep-223
224 / A
No pep-224
Pep-224
229 / A
No pep-229
Pep-229
233 / A
No pep-233
Pep-233
223 / B
No pep-223
Pep-223
224 / B
No pep-224
Pep-224
229 / B
No pep-229
Pep-229
233 / B
No pep-233
Pep-233
235 / A
No pep-235
Pep-235
239 / A
No pep-239
Pep-239
245 / A
No pep-245
Pep-245
252 / A
No pep-252
Pep-252
235 / B
No pep-235
Pep-235
239 / B
No pep-239
Pep-239
245 / B
No pep-245
Pep-245
252 / B
No pep-252
Pep-252
APC-H
PE-H


253 / A
No pep-253
Pep-253
255 / A
No pep-255
Pep-255
267 / A
No pep-267
Pep-267
1020003 / A
No pep-1020003
Pep-1020003
253 / B
No pep-253
Pep-253
255 / B
No pep-255
Pep-255
267 / B
No pep-267
Pep-267
1020003 / B
No pep-1020003
Pep-1020003
1020004 / A
No pep-1020004
Pep-1020004
1020005 / A
No pep-1020005
Pep-1020005
1020011 / A
No pep-1020011
Pep-1020011
1020016 / A
No pep-1020016
Pep-1020016
1020004 / B
No pep-1020004
Pep-1020004
1020005 / B
No pep-1020005
Pep-1020005
1020011 / B
No pep-1020011
Pep-1020011
1020016 / B
No pep-1020016
Pep-1020016
1020017 / A
No pep-1020017
Pep-1020017
1020021 / A
No pep-1020021
Pep-1020021
1020023 / A
No pep-1020023
Pep-1020023
1020028 / A
No pep-1020028
Pep-1020028
1020017 / B
No pep-1020017
Pep-1020017
1020021 / B
No pep-1020021
Pep-1020021
1020023 / B
No pep-1020023
Pep-1020023
1020028 / B
No pep-1020028
Pep-1020028
APC-H
PE-H


1020031 / A
No pep-1020031
Pep-1020031
1020037 / A
No pep-1020037
Pep-1020037
1020040 / A
No pep-1020040
Pep-1020040
1020045 / A
No pep-1020045
Pep-1020045
1020031 / B
No pep-1020031
Pep-1020031
1020037 / B
No pep-1020037
Pep-1020037
1020040 / B
No pep-1020040
Pep-1020040
1020045 / B
No pep-1020045
Pep-1020045
1020048 / A
No pep-1020048
Pep-1020048
1020049 / A
No pep-1020049
Pep-1020049
1020051 / A
No pep-1020051
Pep-1020051
1020059 / A
No pep-1020059
Pep-1020059
1020048 / B
No pep-1020048
Pep-1020048
1020049 / B
No pep-1020049
Pep-1020049
1020051 / B
No pep-1020051
Pep-1020051
1020059 / B
No pep-1020059
Pep-1020059
1020062 / A
No pep-1020062
Pep-1020062
1020063 / A
No pep-1020063
Pep-1020063
1020068 / A
No pep-1020068
Pep-1020068
1020071 / A
No pep-1020071
Pep-1020071
1020062 / B
No pep-1020062
Pep-1020062
1020063 / B
No pep-1020063
Pep-1020063
1020068 / B
No pep-1020068
Pep-1020068
1020071 / B
No pep-1020071
Pep-1020071
APC-H
PE-H


1030003.031 / A
No pep-1030003.031
Pep-1030003
1030005.032 / A
No pep-1030005.032
Pep-1030005
1030010 / A
No pep-1030010
Pep-1030010
1030014 / A
No pep-1030014
Pep-1030014
1030003.031 / B
No pep-1030003.031
Pep-1030003
1030005.032 / B
No pep-1030005.032
Pep-1030005
1030010 / B
No pep-1030010
Pep-1030010
1030014 / B
No pep-1030014
Pep-1030014
1030029 / A
No pep-1030029
Pep-1030029
1030030 / A
No pep-1030030
Pep-1030030
1030032 / A
No pep-1030032
Pep-1030032
1030042 / A
No pep-1030042
Pep-1030042.1
1030029 / B
No pep-1030029
Pep-1030029
1030030 / B
No pep-1030030
Pep-1030030
1030032 / B
No pep-1030032
Pep-1030032
1030042 / B
No pep-1030042
Pep-1030042.1
1030043 / A
No pep-1030043
Pep-1030043.2
1030063 / A
No pep-1030063
Pep-1030063.3
1030067 / A
No pep-1030067
Pep-1030067.5
1030070 / A
No pep-1030070
Pep-1030070.7
1030043 / B
No pep-1030043
Pep-1030043.2
1030063 / B
No pep-1030063
Pep-1030063.3
1030067 / B
No pep-1030067
Pep-1030067.5
1030070 / B
No pep-1030070
Pep-1030070.7
APC-H
PE-H


1030072 / A
No pep-1030072
Pep-1030072.9
1030082 / A
No pep-1030082
Pep-1030082.16
1030088 / A
No pep-1030088
Pep-1030088.18
1030092 / A
No pep-1030092
Pep-1030092.21
1030072 / B
1030082 / B
1030088 / B
1030092 / B
1030098 / A
No pep-1030098
Pep-1030098.24
1030101 / A
No pep-1030101
Pep-1030101.25
1030111 / A
No pep-1030111
Pep-1030111.30
1030112 / A
No pep-1030112
Pep-1030112.31
1030098 / B
1030101 / B
1030111 / B
1030112 / B
1030115 / A
No pep-1030115
Pep-1030115.33
1030115 / B
APC-H
PE-H

COPYRIGHTS and PERMISSIONS

SPRINGER NATURE LICENSE TERMS AND CONDITIONS

Aug 22, 2022

This Agreement between Ms. Asli Bartan ("You") and Springer Nature ("Springer Nature") consists of your license details and the terms and conditions provided by Springer Nature and Copyright Clearance Center.

License Number	5372431208258
License date	Aug 19, 2022
Licensed Content Publisher	Springer Nature
Licensed Content Publication	Nature Reviews Immunology
Licensed Content Title	Immunotherapeutic uses of CpG oligodeoxynucleotides
Licensed Content Author	Dennis M. Klinman
Licensed Content Date	Apr 1, 2004
Type of Use	Thesis/Dissertation
Requestor type	non-commercial (non-profit)
Format	print and electronic
Portion	figures/tables/illustrations
Number of figures/tables/illustrations	3
High-res required	no
Will you be translating?	no
Circulation/distribution	200 - 499
Author of this Springer Nature content	no
Title	INVESTIGATION OF PRE-CLINICAL AND CLINICAL RESULTS AGAINST SARS-COV-2 WILD-TYPE AND ALPHA VARIANTS COMBINATION OF VLP-58-1023-AL-K3 VACCINE
Institution name	BILKENT UNIVERSITY
Expected presentation date	Aug 2022
Portions	Figures 1,2,3
Requestor Location	Ms. Asli Bartan Ankara Turkey Ankara, other Turkey Attn: Ms. Asli Bartan
Total	**0.00 USD**
Terms and Conditions	

Springer Nature Customer Service Centre GmbH
Terms and Conditions

This agreement sets out the terms and conditions of the licence (the **Licence**) between you and **Springer Nature Customer Service Centre GmbH** (the **Licensor**). By clicking 'accept' and completing the transaction for the material (**Licensed Material**), you also confirm your acceptance of these terms and conditions.

1. Grant of License

1. 1. The Licensor grants you a personal, non-exclusive, non-transferable, world-wide licence to reproduce the Licensed Material for the purpose specified in your order only. Licences are granted for the specific use requested in the order and for no other use, subject to the conditions below.

1. 2. The Licensor warrants that it has, to the best of its knowledge, the rights to license reuse of the Licensed Material. However, you should ensure that the material you are requesting is original to the Licensor and does not carry the copyright of another entity (as credited in the published version).

1. 3. If the credit line on any part of the material you have requested indicates that it was reprinted or adapted with permission from another source, then you should also seek permission from that source to reuse the material.

2. Scope of Licence

2. 1. You may only use the Licensed Content in the manner and to the extent permitted by these Ts&Cs and any applicable laws.

2. 2. A separate licence may be required for any additional use of the Licensed Material, e.g. where a licence has been purchased for print only use, separate permission must be obtained for electronic re-use. Similarly, a licence is only valid in the language selected and does not apply for editions in other languages unless additional translation rights have been granted separately in the licence. Any content owned by third parties are expressly excluded from the licence.

2. 3. Similarly, rights for additional components such as custom editions and derivatives require additional permission and may be subject to an additional fee. Please apply to Journalpermissions@springernature.com/bookpermissions@springernature.com for these rights.

2. 4. Where permission has been granted **free of charge** for material in print, permission may also be granted for any electronic version of that work, provided that the material is incidental to your work as a whole and that the electronic version is essentially equivalent to, or substitutes for, the print version.

2. 5. An alternative scope of licence may apply to signatories of the STM Permissions Guidelines, as amended from time to time.

3. Duration of Licence

3. 1. A licence for is valid from the date of purchase ('Licence Date') at the end of the relevant period in the below table:

Scope of Licence	Duration of Licence
Post on a website	12 months
Presentations	12 months
Books and journals	Lifetime of the edition in the language purchased

4. Acknowledgement

4. 1. The Licensor's permission must be acknowledged next to the Licenced Material in print. In electronic form, this acknowledgement must be visible at the same time as the figures/tables/illustrations or abstract, and must be hyperlinked to the journal/book's homepage. Our required acknowledgement format is in the Appendix below.

5. Restrictions on use

5. 1. Use of the Licensed Material may be permitted for incidental promotional use and minor editing privileges e.g. minor adaptations of single figures, changes of format, colour and/or style where the adaptation is credited as set out in Appendix 1 below. Any other changes including but not limited to, cropping, adapting, omitting material that affect the meaning, intention or moral rights of the author are strictly prohibited.

5. 2. You must not use any Licensed Material as part of any design or trademark.

5. 3. Licensed Material may be used in Open Access Publications (OAP) before publication by Springer Nature, but any Licensed Material must be removed from OAP sites prior to final publication.

6. Ownership of Rights

6. 1. Licensed Material remains the property of either Licensor or the relevant third party and any rights not explicitly granted herein are expressly reserved.

7. Warranty

IN NO EVENT SHALL LICENSOR BE LIABLE TO YOU OR ANY OTHER PARTY OR ANY OTHER PERSON OR FOR ANY SPECIAL, CONSEQUENTIAL, INCIDENTAL OR INDIRECT DAMAGES, HOWEVER CAUSED, ARISING OUT OF OR IN CONNECTION WITH THE DOWNLOADING, VIEWING OR USE OF THE MATERIALS REGARDLESS OF THE FORM OF ACTION, WHETHER FOR BREACH OF CONTRACT, BREACH OF WARRANTY, TORT, NEGLIGENCE, INFRINGEMENT OR OTHERWISE (INCLUDING, WITHOUT LIMITATION, DAMAGES BASED ON LOSS OF PROFITS, DATA, FILES, USE, BUSINESS OPPORTUNITY OR CLAIMS OF THIRD PARTIES), AND
WHETHER OR NOT THE PARTY HAS BEEN ADVISED OF THE POSSIBILITY OF SUCH DAMAGES. THIS LIMITATION SHALL APPLY NOTWITHSTANDING ANY FAILURE OF ESSENTIAL PURPOSE OF ANY LIMITED REMEDY PROVIDED HEREIN.

8. Limitations

8. 1. ***BOOKS ONLY:***Where **'reuse in a dissertation/thesis'** has been selected the following terms apply: Print rights of the final author's accepted manuscript (for clarity, NOT the published version) for up to 100 copies, electronic rights for use only on a personal website or institutional repository as defined by the Sherpa guideline (www.sherpa.ac.uk/romeo/).

8. 2. For content reuse requests that qualify for permission under the STM Permissions Guidelines, which may be updated from time to time, the STM Permissions Guidelines supersede the terms and conditions contained in this licence.

9. Termination and Cancellation

9. 1. Licences will expire after the period shown in Clause 3 (above).

9. 2. Licensee reserves the right to terminate the Licence in the event that payment is not received in full or if there has been a breach of this agreement by you.

Appendix 1 — Acknowledgements:

For Journal Content:
Reprinted by permission from **[the Licensor]**: [**Journal Publisher** (e.g. Nature/Springer/Palgrave)] **[JOURNAL NAME] [REFERENCE CITATION** (Article name, Author(s) Name), [**COPYRIGHT**] (year of publication)

For **Advance Online Publication papers:**
Reprinted by permission from **[the Licensor]**: [**Journal Publisher** (e.g. Nature/Springer/Palgrave)] **[JOURNAL NAME] [REFERENCE CITATION** (Article name, Author(s) Name), [**COPYRIGHT**] (year of publication), advance online publication, day month year (doi: 10.1038/sj.[JOURNAL ACRONYM].)

For Adaptations/Translations:
Adapted/Translated by permission from [**the Licensor**]: [**Journal Publisher** (e.g. Nature/Springer/Palgrave)] [**JOURNAL NAME**] [**REFERENCE CITATION** (Article name, Author(s) Name), [**COPYRIGHT**] (year of publication)

Note: For any republication from the British Journal of Cancer, the following credit line style applies:

Reprinted/adapted/translated by permission from [**the Licensor**]: on behalf of Cancer Research UK: : [**Journal Publisher** (e.g. Nature/Springer/Palgrave)] [**JOURNAL NAME**] [**REFERENCE CITATION** (Article name, Author(s) Name), [**COPYRIGHT]** (year of publication)

For **Advance Online Publication** papers:
Reprinted by permission from The [**the Licensor**]: on behalf of Cancer Research UK: [**Journal Publisher** (e.g. Nature/Springer/Palgrave)] [**JOURNAL NAME**] [**REFERENCE CITATION** (Article name, Author(s) Name), [**COPYRIGHT**] (year of publication), advance online publication, day month year (doi: 10.1038/sj.[JOURNAL ACRONYM])

For Book content:
Reprinted/adapted by permission from [**the Licensor**]: [**Book Publisher** (e.g. Palgrave Macmillan, Springer etc) [**Book Title**] by [**Book author**(s)] [**COPYRIGHT**] (year of publication)

Other Conditions:

Version 1.3

Questions? customercare@copyright.com or +1-855-239-3415 (toll free in the US) or +1-978-646-2777.

SPRINGER NATURE LICENSE
TERMS AND CONDITIONS

Aug 22, 2022

This Agreement between Ms. Asli Bartan ("You") and Springer Nature ("Springer Nature") consists of your license details and the terms and conditions provided by Springer Nature and Copyright Clearance Center.

License Number	5372430990304
License date	Aug 19, 2022
Licensed Content Publisher	Springer Nature
Licensed Content Publication	Springer eBook
Licensed Content Title	Aluminum-Based Nano-adjuvants
Licensed Content Author	Bingbing Sun, Zhaoxia Ji, Tian Xia
Licensed Content Date	Jan 1, 2016
Type of Use	Thesis/Dissertation
Requestor type	non-commercial (non-profit)
Format	print and electronic
Portion	figures/tables/illustrations
Number of figures/tables/illustrations	1
Will you be translating?	no
Circulation/distribution	200 - 499
Author of this Springer Nature content	no
Title	INVESTIGATION OF PRE-CLINICAL AND CLINICAL RESULTS AGAINST SARS-COV-2 WILD-TYPE AND ALPHA VARIANTS COMBINATION OF VLP-58-1023-AL-K3 VACCINE
Institution name	BILKENT UNIVERSITY
Expected presentation date	Aug 2022
Portions	Figure 1
Requestor Location	Ms. Asli Bartan Ankara Turkey Ankara, other Turkey Attn: Ms. Asli Bartan
Total	**0.00 USD**
Terms and Conditions	

Springer Nature Customer Service Centre GmbH
Terms and Conditions

This agreement sets out the terms and conditions of the licence (the **Licence**) between you and **Springer Nature Customer Service Centre GmbH** (the **Licensor**). By clicking 'accept' and completing the transaction for the material (**Licensed Material**), you also confirm your acceptance of these terms and conditions.

1. Grant of License

1. 1. The Licensor grants you a personal, non-exclusive, non-transferable, world-wide licence to reproduce the Licensed Material for the purpose specified in your order only. Licences are granted for the specific use requested in the order and for no other use, subject to the conditions below.

1. 2. The Licensor warrants that it has, to the best of its knowledge, the rights to license reuse of the Licensed Material. However, you should ensure that the material you are requesting is original to the Licensor and does not carry the

copyright of another entity (as credited in the published version).

1. 3. If the credit line on any part of the material you have requested indicates that it was reprinted or adapted with permission from another source, then you should also seek permission from that source to reuse the material.

2. Scope of Licence

2. 1. You may only use the Licensed Content in the manner and to the extent permitted by these Ts&Cs and any applicable laws.

2. 2. A separate licence may be required for any additional use of the Licensed Material, e.g. where a licence has been purchased for print only use, separate permission must be obtained for electronic re-use. Similarly, a licence is only valid in the language selected and does not apply for editions in other languages unless additional translation rights have been granted separately in the licence. Any content owned by third parties are expressly excluded from the licence.

2. 3. Similarly, rights for additional components such as custom editions and derivatives require additional permission and may be subject to an additional fee. Please apply to Journalpermissions@springernature.com/bookpermissions@springernature.com for these rights.

2. 4. Where permission has been granted **free of charge** for material in print, permission may also be granted for any electronic version of that work, provided that the material is incidental to your work as a whole and that the electronic version is essentially equivalent to, or substitutes for, the print version.

2. 5. An alternative scope of licence may apply to signatories of the STM Permissions Guidelines, as amended from time to time.

3. Duration of Licence

3. 1. A licence for is valid from the date of purchase ('Licence Date') at the end of the relevant period in the below table:

Scope of Licence	Duration of Licence
Post on a website	12 months
Presentations	12 months
Books and journals	Lifetime of the edition in the language purchased

4. Acknowledgement

4. 1. The Licensor's permission must be acknowledged next to the Licenced Material in print. In electronic form, this acknowledgement must be visible at the same time as the figures/tables/illustrations or abstract, and must be hyperlinked to the journal/book's homepage. Our required acknowledgement format is in the Appendix below.

5. Restrictions on use

5. 1. Use of the Licensed Material may be permitted for incidental promotional use and minor editing privileges e.g. minor adaptations of single figures, changes of format, colour and/or style where the adaptation is credited as set out in Appendix 1 below. Any other changes including but not limited to, cropping, adapting, omitting material that affect the meaning, intention or moral rights of the author are strictly prohibited.

5. 2. You must not use any Licensed Material as part of any design or trademark.

5. 3. Licensed Material may be used in Open Access Publications (OAP) before publication by Springer Nature, but any Licensed Material must be removed from OAP sites prior to final publication.

6. Ownership of Rights

6. 1. Licensed Material remains the property of either Licensor or the relevant third party and any rights not explicitly granted herein are expressly reserved.

7. Warranty

IN NO EVENT SHALL LICENSOR BE LIABLE TO YOU OR ANY OTHER PARTY OR ANY OTHER PERSON OR FOR ANY SPECIAL, CONSEQUENTIAL, INCIDENTAL OR INDIRECT DAMAGES, HOWEVER CAUSED, ARISING OUT OF OR IN CONNECTION WITH THE DOWNLOADING, VIEWING OR USE OF THE MATERIALS REGARDLESS OF THE FORM OF ACTION, WHETHER FOR BREACH OF CONTRACT, BREACH OF WARRANTY, TORT, NEGLIGENCE, INFRINGEMENT OR OTHERWISE (INCLUDING, WITHOUT LIMITATION, DAMAGES BASED ON LOSS OF PROFITS, DATA, FILES, USE, BUSINESS OPPORTUNITY OR CLAIMS OF THIRD PARTIES), AND
WHETHER OR NOT THE PARTY HAS BEEN ADVISED OF THE POSSIBILITY OF SUCH DAMAGES. THIS LIMITATION SHALL APPLY NOTWITHSTANDING ANY FAILURE OF ESSENTIAL PURPOSE OF ANY LIMITED REMEDY PROVIDED HEREIN.

8. Limitations

8. 1. ***BOOKS ONLY:***Where **'reuse in a dissertation/thesis'** has been selected the following terms apply: Print rights of the final author's accepted manuscript (for clarity, NOT the published version) for up to 100 copies, electronic rights for use only on a personal website or institutional repository as defined by the Sherpa guideline (www.sherpa.ac.uk/romeo/).

8. 2. For content reuse requests that qualify for permission under the STM Permissions Guidelines, which may be updated from time to time, the STM Permissions Guidelines supersede the terms and conditions contained in this licence.

9. Termination and Cancellation

9. 1. Licences will expire after the period shown in Clause 3 (above).

9. 2. Licensee reserves the right to terminate the Licence in the event that payment is not received in full or if there has been a breach of this agreement by you.

Appendix 1 — Acknowledgements:

For Journal Content:
Reprinted by permission from **[the Licensor]**: [**Journal Publisher** (e.g. Nature/Springer/Palgrave)] **[JOURNAL NAME] [REFERENCE CITATION** (Article name, Author(s) Name), [**COPYRIGHT**] (year of publication)

For **Advance Online Publication papers:**
Reprinted by permission from **[the Licensor]**: [**Journal Publisher** (e.g. Nature/Springer/Palgrave)] **[JOURNAL NAME] [REFERENCE CITATION** (Article name, Author(s) Name), [**COPYRIGHT**] (year of publication), advance online publication, day month year (doi: 10.1038/sj.[JOURNAL ACRONYM].)

For Adaptations/Translations:
Adapted/Translated by permission from [**the Licensor**]: [**Journal Publisher** (e.g. Nature/Springer/Palgrave)] [**JOURNAL NAME**] [**REFERENCE CITATION** (Article name, Author(s) Name), [**COPYRIGHT**] (year of publication)

Note: For any republication from the British Journal of Cancer, the following credit line style applies:

Reprinted/adapted/translated by permission from [**the Licensor**]: on behalf of Cancer Research UK: : [**Journal Publisher** (e.g. Nature/Springer/Palgrave)] **[JOURNAL NAME]** [**REFERENCE CITATION** (Article name, Author(s) Name), **[COPYRIGHT]** (year of publication)

For **Advance Online Publication** papers:
Reprinted by permission from The [**the Licensor**]: on behalf of Cancer Research UK: [**Journal Publisher** (e.g. Nature/Springer/Palgrave)] [**JOURNAL NAME**] [**REFERENCE CITATION** (Article name, Author(s) Name), [**COPYRIGHT**] (year of publication), advance online publication, day month year (doi: 10.1038/sj.[JOURNAL ACRONYM])

For Book content:
Reprinted/adapted by permission from [**the Licensor**]: [**Book Publisher** (e.g. Palgrave Macmillan, Springer etc) [**Book Title**] by [**Book author**(s)] [**COPYRIGHT**] (year of publication)

Other Conditions:

Version 1.3

Questions? customercare@copyright.com or +1-855-239-3415 (toll free in the US) or +1-978-646-2777.

SPRINGER NATURE LICENSE
TERMS AND CONDITIONS

Aug 22, 2022

This Agreement between Ms. Asli Bartan ("You") and Springer Nature ("Springer Nature") consists of your license details and the terms and conditions provided by Springer Nature and Copyright Clearance Center.

License Number	5372430696493
License date	Aug 19, 2022
Licensed Content Publisher	Springer Nature
Licensed Content Publication	Nature Reviews Immunology
Licensed Content Title	The trinity of COVID-19: immunity, inflammation and intervention
Licensed Content Author	Matthew Zirui Tay et al
Licensed Content Date	Apr 28, 2020
Type of Use	Thesis/Dissertation
Requestor type	non-commercial (non-profit)
Format	print and electronic
Portion	figures/tables/illustrations
Number of figures/tables/illustrations	1
High-res required	no
Will you be translating?	no
Circulation/distribution	200 - 499
Author of this Springer Nature content	no
Title	INVESTIGATION OF PRE-CLINICAL AND CLINICAL RESULTS AGAINST SARS-COV-2 WILD-TYPE AND ALPHA VARIANTS COMBINATION OF VLP-58-1023-AL-K3 VACCINE
Institution name	BILKENT UNIVERSITY
Expected presentation date	Aug 2022
Portions	Figure 1
Requestor Location	Ms. Asli Bartan Ankara Turkey Ankara, other Turkey Attn: Ms. Asli Bartan
Total	**0.00 USD**
Terms and Conditions	

Springer Nature Customer Service Centre GmbH
Terms and Conditions

This agreement sets out the terms and conditions of the licence (the **Licence**) between you and **Springer Nature Customer Service Centre GmbH** (the **Licensor**). By clicking 'accept' and completing the transaction for the material (**Licensed Material**), you also confirm your acceptance of these terms and conditions.

1. Grant of License

1. 1. The Licensor grants you a personal, non-exclusive, non-transferable, world-wide licence to reproduce the Licensed Material for the purpose specified in your order only. Licences are granted for the specific use requested in the order and for no other use, subject to the conditions below.

1. 2. The Licensor warrants that it has, to the best of its knowledge, the rights to license reuse of the Licensed Material. However, you should ensure that the material you are requesting is original to the Licensor and does not carry the copyright of another entity (as credited in the published version).

1. 3. If the credit line on any part of the material you have requested indicates that it was reprinted or adapted with permission from another source, then you should also seek permission from that source to reuse the material.

2. Scope of Licence

2. 1. You may only use the Licensed Content in the manner and to the extent permitted by these Ts&Cs and any applicable laws.

2. 2. A separate licence may be required for any additional use of the Licensed Material, e.g. where a licence has been purchased for print only use, separate permission must be obtained for electronic re-use. Similarly, a licence is only valid in the language selected and does not apply for editions in other languages unless additional translation rights have been granted separately in the licence. Any content owned by third parties are expressly excluded from the licence.

2. 3. Similarly, rights for additional components such as custom editions and derivatives require additional permission and may be subject to an additional fee. Please apply to Journalpermissions@springernature.com/bookpermissions@springernature.com for these rights.

2. 4. Where permission has been granted **free of charge** for material in print, permission may also be granted for any electronic version of that work, provided that the material is incidental to your work as a whole and that the electronic version is essentially equivalent to, or substitutes for, the print version.

2. 5. An alternative scope of licence may apply to signatories of the STM Permissions Guidelines, as amended from time to time.

3. Duration of Licence

3. 1. A licence for is valid from the date of purchase ('Licence Date') at the end of the relevant period in the below table:

Scope of Licence	Duration of Licence
Post on a website	12 months
Presentations	12 months
Books and journals	Lifetime of the edition in the language purchased

4. Acknowledgement

4. 1. The Licensor's permission must be acknowledged next to the Licenced Material in print. In electronic form, this acknowledgement must be visible at the same time as the figures/tables/illustrations or abstract, and must be hyperlinked to the journal/book's homepage. Our required acknowledgement format is in the Appendix below.

5. Restrictions on use

5. 1. Use of the Licensed Material may be permitted for incidental promotional use and minor editing privileges e.g. minor adaptations of single figures, changes of format, colour and/or style where the adaptation is credited as set out in Appendix 1 below. Any other changes including but not limited to, cropping, adapting, omitting material that affect the meaning, intention or moral rights of the author are strictly prohibited.

5. 2. You must not use any Licensed Material as part of any design or trademark.

5. 3. Licensed Material may be used in Open Access Publications (OAP) before publication by Springer Nature, but any Licensed Material must be removed from OAP sites prior to final publication.

6. Ownership of Rights

6. 1. Licensed Material remains the property of either Licensor or the relevant third party and any rights not explicitly granted herein are expressly reserved.

7. Warranty

IN NO EVENT SHALL LICENSOR BE LIABLE TO YOU OR ANY OTHER PARTY OR ANY OTHER PERSON OR FOR ANY SPECIAL, CONSEQUENTIAL, INCIDENTAL OR INDIRECT DAMAGES, HOWEVER CAUSED, ARISING OUT OF OR IN CONNECTION WITH THE DOWNLOADING, VIEWING OR USE OF THE MATERIALS REGARDLESS OF THE FORM OF ACTION, WHETHER FOR BREACH OF CONTRACT, BREACH OF WARRANTY, TORT, NEGLIGENCE, INFRINGEMENT OR OTHERWISE (INCLUDING, WITHOUT LIMITATION, DAMAGES BASED ON LOSS OF PROFITS, DATA, FILES, USE, BUSINESS OPPORTUNITY OR CLAIMS OF THIRD PARTIES), AND
WHETHER OR NOT THE PARTY HAS BEEN ADVISED OF THE POSSIBILITY OF SUCH DAMAGES. THIS LIMITATION SHALL APPLY NOTWITHSTANDING ANY FAILURE OF ESSENTIAL PURPOSE OF ANY LIMITED REMEDY PROVIDED HEREIN.

8. Limitations

8. 1. ***BOOKS ONLY:***Where **'reuse in a dissertation/thesis'** has been selected the following terms apply: Print rights of the final author's accepted manuscript (for clarity, NOT the published version) for up to 100 copies, electronic rights for use only on a personal website or institutional repository as defined by the Sherpa guideline (www.sherpa.ac.uk/romeo/).

8. 2. For content reuse requests that qualify for permission under the STM Permissions Guidelines, which may be updated from time to time, the STM Permissions Guidelines supersede the terms and conditions contained in this licence.

9. Termination and Cancellation

9. 1. Licences will expire after the period shown in Clause 3 (above).

9. 2. Licensee reserves the right to terminate the Licence in the event that payment is not received in full or if there has been a breach of this agreement by you.

Appendix 1 — Acknowledgements:

For Journal Content:
Reprinted by permission from **[the Licensor]**: [**Journal Publisher** (e.g. Nature/Springer/Palgrave)] **[JOURNAL NAME] [REFERENCE CITATION** (Article name, Author(s) Name), [**COPYRIGHT**] (year of publication)

For **Advance Online Publication papers:**
Reprinted by permission from **[the Licensor]**: [**Journal Publisher** (e.g. Nature/Springer/Palgrave)] **[JOURNAL NAME] [REFERENCE CITATION** (Article name, Author(s) Name), [**COPYRIGHT**] (year of publication), advance online publication, day month year (doi: 10.1038/sj.[JOURNAL ACRONYM].)

For Adaptations/Translations:
Adapted/Translated by permission from [**the Licensor**]: [**Journal Publisher** (e.g. Nature/Springer/Palgrave)] [**JOURNAL NAME**] [**REFERENCE CITATION** (Article name, Author(s) Name), [**COPYRIGHT**] (year of publication)

Note: For any republication from the British Journal of Cancer, the following credit line style applies:

Reprinted/adapted/translated by permission from [**the Licensor**]: on behalf of Cancer Research UK: : [**Journal Publisher** (e.g. Nature/Springer/Palgrave)] [**JOURNAL NAME**] [**REFERENCE CITATION** (Article name, Author(s) Name), [**COPYRIGHT]** (year of publication)

For **Advance Online Publication** papers:
Reprinted by permission from The [**the Licensor**]: on behalf of Cancer Research UK: [**Journal Publisher** (e.g. Nature/Springer/Palgrave)] [**JOURNAL NAME**] [**REFERENCE CITATION** (Article name, Author(s) Name), [**COPYRIGHT**] (year of publication), advance online publication, day month year (doi: 10.1038/sj.[JOURNAL ACRONYM])

For Book content:
Reprinted/adapted by permission from [**the Licensor**]: [**Book Publisher** (e.g. Palgrave Macmillan, Springer etc) [**Book Title**] by [**Book author**(s)] [**COPYRIGHT**] (year of publication)

Other Conditions:

Version 1.3

Questions? customercare@copyright.com or +1-855-239-3415 (toll free in the US) or +1-978-646-2777.

SPRINGER NATURE LICENSE
TERMS AND CONDITIONS

Aug 22, 2022

This Agreement between Ms. Asli Bartan ("You") and Springer Nature ("Springer Nature") consists of your license details and the terms and conditions provided by Springer Nature and Copyright Clearance Center.

License Number	5372430501094
License date	Aug 19, 2022
Licensed Content Publisher	Springer Nature
Licensed Content Publication	Nature Nanotechnology
Licensed Content Title	Immune-mediated approaches against COVID-19
Licensed Content Author	Helena F. Florindo et al
Licensed Content Date	Jul 13, 2020
Type of Use	Thesis/Dissertation
Requestor type	non-commercial (non-profit)
Format	print and electronic
Portion	figures/tables/illustrations
Number of figures/tables/illustrations	1
High-res required	no
Will you be translating?	no
Circulation/distribution	200 - 499
Author of this Springer Nature content	no
Title	INVESTIGATION OF PRE-CLINICAL AND CLINICAL RESULTS AGAINST SARS-COV-2 WILD-TYPE AND ALPHA VARIANTS COMBINATION OF VLP-58-1023-AL-K3 VACCINE
Institution name	BILKENT UNIVERSITY
Expected presentation date	Aug 2022
Portions	Figure 1
Requestor Location	Ms. Asli Bartan Ankara Turkey Ankara, other Turkey Attn: Ms. Asli Bartan
Total	**0.00 USD**
Terms and Conditions	

Springer Nature Customer Service Centre GmbH
Terms and Conditions

This agreement sets out the terms and conditions of the licence (the **Licence**) between you and **Springer Nature Customer Service Centre GmbH** (the **Licensor**). By clicking 'accept' and completing the transaction for the material (**Licensed Material**), you also confirm your acceptance of these terms and conditions.

1. Grant of License

1. 1. The Licensor grants you a personal, non-exclusive, non-transferable, world-wide licence to reproduce the Licensed Material for the purpose specified in your order only. Licences are granted for the specific use requested in the order and for no other use, subject to the conditions below.

1. 2. The Licensor warrants that it has, to the best of its knowledge, the rights to license reuse of the Licensed Material. However, you should ensure that the material you are requesting is original to the Licensor and does not carry the copyright of another entity (as credited in the published version).

1. 3. If the credit line on any part of the material you have requested indicates that it was reprinted or adapted with permission from another source, then you should also seek permission from that source to reuse the material.

2. Scope of Licence

2. 1. You may only use the Licensed Content in the manner and to the extent permitted by these Ts&Cs and any applicable laws.

2. 2. A separate licence may be required for any additional use of the Licensed Material, e.g. where a licence has been purchased for print only use, separate permission must be obtained for electronic re-use. Similarly, a licence is only valid in the language selected and does not apply for editions in other languages unless additional translation rights have been granted separately in the licence. Any content owned by third parties are expressly excluded from the licence.

2. 3. Similarly, rights for additional components such as custom editions and derivatives require additional permission and may be subject to an additional fee. Please apply to Journalpermissions@springernature.com/bookpermissions@springernature.com for these rights.

2. 4. Where permission has been granted **free of charge** for material in print, permission may also be granted for any electronic version of that work, provided that the material is incidental to your work as a whole and that the electronic version is essentially equivalent to, or substitutes for, the print version.

2. 5. An alternative scope of licence may apply to signatories of the STM Permissions Guidelines, as amended from time to time.

3. Duration of Licence

3. 1. A licence for is valid from the date of purchase ('Licence Date') at the end of the relevant period in the below table:

Scope of Licence	Duration of Licence
Post on a website	12 months
Presentations	12 months
Books and journals	Lifetime of the edition in the language purchased

4. Acknowledgement

4. 1. The Licensor's permission must be acknowledged next to the Licenced Material in print. In electronic form, this acknowledgement must be visible at the same time as the figures/tables/illustrations or abstract, and must be hyperlinked to the journal/book's homepage. Our required acknowledgement format is in the Appendix below.

5. Restrictions on use

5. 1. Use of the Licensed Material may be permitted for incidental promotional use and minor editing privileges e.g. minor adaptations of single figures, changes of format, colour and/or style where the adaptation is credited as set out in Appendix 1 below. Any other changes including but not limited to, cropping, adapting, omitting material that affect the meaning, intention or moral rights of the author are strictly prohibited.

5. 2. You must not use any Licensed Material as part of any design or trademark.

5. 3. Licensed Material may be used in Open Access Publications (OAP) before publication by Springer Nature, but any Licensed Material must be removed from OAP sites prior to final publication.

6. Ownership of Rights

6. 1. Licensed Material remains the property of either Licensor or the relevant third party and any rights not explicitly granted herein are expressly reserved.

7. Warranty

IN NO EVENT SHALL LICENSOR BE LIABLE TO YOU OR ANY OTHER PARTY OR ANY OTHER PERSON OR FOR ANY SPECIAL, CONSEQUENTIAL, INCIDENTAL OR INDIRECT DAMAGES, HOWEVER CAUSED, ARISING OUT OF OR IN CONNECTION WITH THE DOWNLOADING, VIEWING OR USE OF THE MATERIALS REGARDLESS OF THE FORM OF ACTION, WHETHER FOR BREACH OF CONTRACT, BREACH OF WARRANTY, TORT, NEGLIGENCE, INFRINGEMENT OR OTHERWISE (INCLUDING, WITHOUT LIMITATION, DAMAGES BASED ON LOSS OF PROFITS, DATA, FILES, USE, BUSINESS OPPORTUNITY OR CLAIMS OF THIRD PARTIES), AND
WHETHER OR NOT THE PARTY HAS BEEN ADVISED OF THE POSSIBILITY OF SUCH DAMAGES. THIS LIMITATION SHALL APPLY NOTWITHSTANDING ANY FAILURE OF ESSENTIAL PURPOSE OF ANY LIMITED REMEDY PROVIDED HEREIN.

8. Limitations

8. 1. ***BOOKS ONLY:***Where **'reuse in a dissertation/thesis'** has been selected the following terms apply: Print rights of the final author's accepted manuscript (for clarity, NOT the published version) for up to 100 copies, electronic rights for use only on a personal website or institutional repository as defined by the Sherpa guideline (www.sherpa.ac.uk/romeo/).

8. 2. For content reuse requests that qualify for permission under the STM Permissions Guidelines, which may be updated from time to time, the STM Permissions Guidelines supersede the terms and conditions contained in this licence.

9. Termination and Cancellation

9. 1. Licences will expire after the period shown in Clause 3 (above).

9. 2. Licensee reserves the right to terminate the Licence in the event that payment is not received in full or if there has been a breach of this agreement by you.

Appendix 1 — Acknowledgements:

For Journal Content:
Reprinted by permission from **[the Licensor]**: [**Journal Publisher** (e.g. Nature/Springer/Palgrave)] **[JOURNAL NAME] [REFERENCE CITATION** (Article name, Author(s) Name), [**COPYRIGHT**] (year of publication)

For **Advance Online Publication papers:**
Reprinted by permission from **[the Licensor]**: [**Journal Publisher** (e.g. Nature/Springer/Palgrave)] **[JOURNAL NAME] [REFERENCE CITATION** (Article name, Author(s) Name), [**COPYRIGHT**] (year of publication), advance online publication, day month year (doi: 10.1038/sj.[JOURNAL ACRONYM].)

For Adaptations/Translations:
Adapted/Translated by permission from [**the Licensor**]: [**Journal Publisher** (e.g. Nature/Springer/Palgrave)] [**JOURNAL NAME**] [**REFERENCE CITATION** (Article name, Author(s) Name), [**COPYRIGHT**] (year of publication)

Note: For any republication from the British Journal of Cancer, the following credit line style applies:

Reprinted/adapted/translated by permission from [**the Licensor**]: on behalf of Cancer Research UK: : [**Journal Publisher** (e.g. Nature/Springer/Palgrave)] [**JOURNAL NAME**] [**REFERENCE CITATION** (Article name, Author(s) Name), [**COPYRIGHT]** (year of publication)

For **Advance Online Publication** papers:
Reprinted by permission from The [**the Licensor**]: on behalf of Cancer Research UK: [**Journal Publisher** (e.g. Nature/Springer/Palgrave)] [**JOURNAL NAME**] [**REFERENCE CITATION** (Article name, Author(s) Name), [**COPYRIGHT**] (year of publication), advance online publication, day month year (doi: 10.1038/sj.[JOURNAL ACRONYM])

For Book content:
Reprinted/adapted by permission from [**the Licensor**]: [**Book Publisher** (e.g. Palgrave Macmillan, Springer etc) [**Book Title**] by [**Book author**(s)] [**COPYRIGHT**] (year of publication)

Other Conditions:

Version 1.3

Questions? customercare@copyright.com or +1-855-239-3415 (toll free in the US) or +1-978-646-2777.